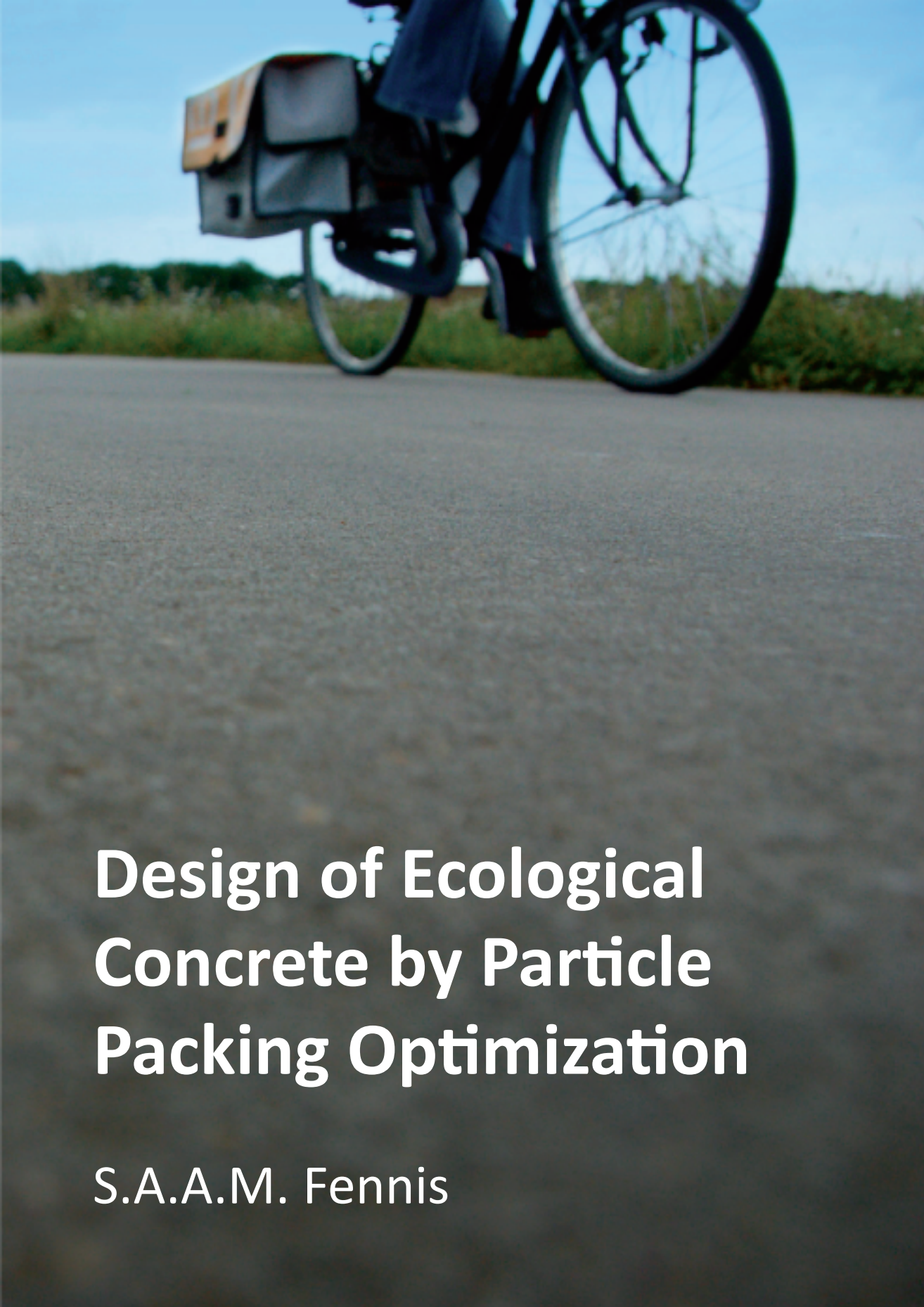

Design of Ecological Concrete by Particle Packing Optimization

S.A.A.M. Fennis

Design of Ecological Concrete by Particle Packing Optimization

S.A.A.M. Fennis

Design of Ecological Concrete by Particle Packing Optimization

Proefschrift

Ter verkrijging van de graad van doctor
aan de Technische Universiteit Delft,
op gezag van de Rector Magnificus prof. ir. K.C.A.M. Luyben,
voorzitter van het College voor Promoties
in het openbaar te verdedigen

op maandag 17 januari 2011 om 15:00 uur
door

Sebastiana Antonia Adriana Maria FENNIS-HUIJBEN

Civiel ingenieur
geboren te Amersfoort

Dit proefschrift is goedgekeurd door de promotor:

Prof. dr. ir. Dr.-Ing. e.h. J.C. Walraven

Samenstelling promotiecommissie:

Rector Magnificus,	Voorzitter
Prof. dr. ir. Dr.-Ing. e.h. J.C. Walraven	Technische Universiteit Delft, promotor
Univ.-Prof. Dr.-Ing. habil. M. Schmidt	Universität Kassel, Duitsland
Prof. dr. ir. H.J.H. Brouwers	Technische Universiteit Eindhoven
Prof. dr. ir. E.M. Haas	Technische Universiteit Delft
Prof. dr. R.B. Polder	Technische Universiteit Delft
Dr. F. de Larrard	Laboratoire Central des Ponts et Chaussées, Frankrijk
Ir. J.A. den Uijl	Technische Universiteit Delft

This research is supported by the Dutch Technology Foundation STW, which is the applied science division of NWO, and the Technology Programme of the Ministry of Economic Affairs (project number 06922).

ISBN 978-94-6108-109-4
Printed by Gildeprint, the Netherlands.
Cover: Hemaalpad Rosmalen, the Netherlands.
Coverdesign: Peter van Limbeek (Gildeprint) and Yuguang Yang.

© 2010 S.A.A.M. Fennis-Huijben. All rights reserved. No part of the material protected by this copyright notice may be reproduced or utilized in any form or by any means, electronic or mechanical, including photocopying, recording or by any information storage and retrieval system, without permission from the author.

Summary

Design of Ecological Concrete by Particle Packing Optimization

In a concrete mixture the cement is responsible for more than 50% of the CO_2-emission. Energy consumption and CO_2-emission of concrete can be reduced when cement is replaced by secondary materials such as residual products from other industries. To replace cement in concrete in a safe way, the main question answered in this research project was how particle packing models can be used to predict the mechanical properties of ecological concrete from its basic components. First a literature survey on ecological concrete was carried out with emphasis on the use of fillers and binders and the influence of replacing cement on the material properties of concrete. Furthermore, various particle size distribution optimization methods were evaluated with regard to their advantages and disadvantages concerning ecological concrete mixture optimization.

Influences on the packing density such as particle characteristics, particle structure and interparticle forces were investigated. Analytical particle packing models can predict a packing density based on the particle characteristics. The particle packing models evaluated in this thesis were: the Furnas model, the Toufar and modified Toufar model, the Dewar model, the Linear Packing Density Model, the Compressible Packing Model, the Schwanda model and the Linear-Mixture Packing Model. The Compressible Packing Model was judged to be the most accurate model with the largest potential for modification to include additional interactions.

Preliminary investigations showed that it is possible to optimize the concrete composition with packing density models in order to lower the cement content, meanwhile retaining satisfactory mechanical properties. Testing of compressive strength, tensile strength, modulus of elasticity, shrinkage and creep of ecological mixtures showed that the compressive strength can be used as a governing design parameter. The packing density of the fine particles and binders should be included in the optimization. For that reason, first packing density measurement techniques were evaluated. The mixing energy test was chosen for the experiments on quartz powder for the development and calibration of a new packing density model.

The Compressible Packing Model was extended to the Compaction-Interaction Packing Model. This was done with the help of discrete element modelling, which was used to investigate the influence of interparticle forces on the particle packing density, wall effect and loosening effect. A new contact model based on Van der Waals forces and

electrostatic forces was implemented in the *HADES* program. Then simulations were performed to compare effects of agglomerating and non-agglomerating particles. The effects were implemented in the Compaction-Interaction Packing Model after adjusting the interaction formulas in such a way that scaling of the interaction was made possible. The increased loosening effect and decreased wall effect for particle groups smaller than 25 µm were implemented by combining interaction with compaction.

Cement pastes and mortar experiments showed that cement can be replaced by very fine fillers, while simultaneously decreasing the water/cement ratio. The suitability of the fillers can be tested by evaluating the packing density and water demand of stable particle structures. More than hundred mortar mixtures were tested on rheological properties and compressive strength. Furthermore, from the mixtures containing quartz powder also the cement pastes were tested on viscosity and heat generation. The water demand and flow value of these mixtures is related to the packing density via the relative water volume or relative amount of excess water. No direct relation between maximum packing density and the heat generation of the cement or the strength was found. A good relation was found between strength and the volumetric distance between the cement particles expressed as the cement spacing factor. The cement spacing factor takes into account the water demand and packing density of a mixture to predict the strength of the concrete. This prediction is used in the cyclic design method for ecological concrete. In this method water demand and strength of concrete mixtures are predicted based on the calculated packing densities by the Compaction-Interaction Packing Model. The cyclic design enables mixture composition adjustment based on material requirements, which makes the method also suitable for defined performance concrete design.

The cyclic design method was used to design ecological concrete mixtures containing fly ash, quartz powder and ground incinerator bottom ash. Experiments on compressive strength, tensile strength, modulus of elasticity, shrinkage and creep showed that the strength relations correspond to those for normal concrete. Demonstration projects and durability tests were carried out which emphasized the need to pay attention to the early strength gain in relation to the applied curing. Electrical resistance testing and compressive strength development in time showed that the cyclic design method improved mixture compositions without any trial and error testing. More than 50% cement could be saved and the CO_2-emission could be reduced with 25%, while at the same time the concrete mixtures still satisfied the demands for appropriate use.

Samenvatting

Ontwerpen van Ecologisch Beton door Korrelpakkingoptimalisatie

In beton is het cement verantwoordelijk voor meer dan 50% van de CO_2-emissie. Het energieverbruik en de CO_2 uitstoot van beton kunnen worden verminderd als het cement wordt vervangen door rest- of bijproducten van andere industrieën. De onderzoeksvraag was hoe korrelpakkingmodellen gebruikt kunnen worden voor het voorspellen van de mechanische eigenschappen van ecologisch beton op basis van de gebruikte grondstoffen, zodat het cement op een veilige manier vervangen kan worden. De literatuurstudie naar ecologisch beton richtte zich op het gebruik van vulstoffen en de invloed van deze cement-vervangende materialen op de eigenschappen van het beton. Tevens zijn verschillende optimalisatiemethoden voor het bepalen van korrelgrootteverdelingen geëvalueerd op hun voor- en nadelen met betrekking tot de optimalisatie van ecologische betonmengsels.

Invloeden op de pakkingdichtheid zoals korreleigenschappen, korrelstructuren en krachten tussen de korrels onderling zijn onderzocht. Analytische korrelpakking-modellen kunnen de pakkingdichtheid voorspellen op basis van korreleigenschappen. De korrelpakkingmodellen die geëvalueerd zijn in dit proefschrift zijn: het Furnas model, het Toufar en aangepaste Toufar model, het Linear Packing Density Model, het Compressible Packing Model, het Schwanda model en het Linear-Mixture Packing Model. Het Compressible Packing Model is beoordeeld als het meest precieze model, met de grootste potentie om aanvullende interacties te kunnen implementeren.

De vooronderzoeken hebben aangetoond dat het mogelijk is om betonsamenstellingen te optimaliseren met behulp van korrelpakkingmodellen, op een zodanige wijze dat het cementgehalte verlaagd kan worden, terwijl de mechanische eigenschappen behouden blijven. De druksterkte-, treksterkte-, elasticiteitsmodulus-, krimp- en kruipmetingen op ecologische betonmengsels hebben aangetoond dat de druksterkte gebruikt kan worden als maatgevende ontwerpparameter. De pakkingdichtheid van de vulstoffen en bindmiddelen moet worden meegenomen in de optimalisatie. Om die reden zijn eerst verschillende meettechnieken voor het bepalen van de pakkingdichtheid geëvalueerd. Het meten van de mengenergie is gekozen voor de vervolgexperimenten met kwartsmeel voor de ontwikkeling en kalibratie van het nieuwe korrelpakkingmodel.

Het Compressible Packing Model is verder uitgebreid tot het Compaction-Interaction Packing Model. Dit is gedaan met behulp van een discrete-elementen model, wat gebruikt is voor het onderzoeken van de onderlinge krachten tussen de korrels, het wandeffect en

het uit-elkaar-drukeffect. Hiervoor is een nieuw contactmodel, gebaseerd op vanderwaalskrachten en elektrostatische krachten, geïmplementeerd in het programma *HADES*. Vervolgens zijn met behulp van simulaties de effecten van geagglomereerde en niet geagglomereerde korrels met elkaar vergeleken. Deze effecten zijn geïmplementeerd in het Compaction-Interaction Packing Model nadat de interactieformules op zodanige wijze waren aangepast dat vergroten en verkleinen van de interactie-effecten mogelijk is. Het vergrote uit-elkaar-drukeffect en verkleinde wandeffect voor korrelgroepen kleiner dan 25 µm zijn gerealiseerd door interactie te combineren met verdichting.

Experimenten op cementpasta's en mortels hebben aangetoond dat cement vervangen kan worden door zeer fijne vulstof, terwijl tegelijkertijd de water-cementfactor kleiner wordt. De mate van geschiktheid van een vulstof kan worden bepaald door het evalueren van de pakkingdichtheid en waterbehoefte van een stabiele korrelstructuur. Meer dan honderd mortels werden getest op rheologische eigenschappen en druksterkte. Tevens werd van de mengsels met kwartsmeel de viscositeit en de warmteontwikkeling van de cementpasta gemeten. De waterbehoefte en de vloeimaat van deze mortels is gerelateerd aan de pakkingdichtheid via het relatieve watervolume of via het relatieve overschot aan water. Geen directe relatie werd gevonden tussen de maximale korrelpakking en de warmteontwikkeling of de sterkte. Er bestaat wel een goede relatie tussen de sterkte en de volumetrische afstand tussen twee cementkorrels uitgedrukt als de 'cement spacing factor'. Deze factor houdt rekening met de waterbehoefte en de sterkte van betonmengsels zoals voorspeld op basis van de berekende pakkingdichtheid. Het cyclische ontwerp maakt het mogelijk mengselsamenstellingen te wijzigen op basis van eisen aan het beton, waardoor deze methode ook geschikt is voor prestatiegericht ontwerpen.

De cyclische ontwerpmethode is gebruikt voor het ontwerpen van ecologisch beton met vliegas, kwartsmeel en gemalen bodemas uit een afvalverbrandingsinstallatie. De geteste druksterkte, treksterkte, elasticiteitsmodulus, krimp en kruip hebben aangetoond dat de sterkterelaties overeenkomen met die van normaal beton. Demonstratieprojecten en duurzaamheidtests zijn uitgevoerd en benadrukten dat aandacht besteed moet worden aan de sterkteontwikkeling in de eerste dagen en aan het toepassen van een goede nabehandeling. Metingen van de elektrische weerstand en de druksterkteontwikkeling hebben aangetoond dat de cyclische ontwerpmethode de mengselsamenstellingen verbeterde zonder dat extra proeftesten nodig waren. Meer dan 50% van het cement kon worden uitgespaard en de CO_2-emissie kon met 25% worden verminderd, terwijl de ecologische betonmengsels nog steeds voldeden aan de gebruikseisen.

Table of contents

Summary **V**
Samenvatting **VII**
Notations and symbols **XIII**

1 Introduction **1**
1.1 General 2
1.2 Research objective 3
1.3 Research strategy and outline 4

2 Ecological concrete design: a survey of literature **9**
2.1 Introduction 10
2.2 Replacing cement 12
2.2.1 Cement replacing materials 12
2.2.2 Influences of fillers on workability 15
2.2.3 Influence of fillers on strength 17
2.2.4 Influence of fillers on mechanical properties and durability 19
2.2.5 Influence of binders 20
2.3 Ecological concrete design 22
2.3.1 Green concrete, Denmark 22
2.3.2 High volume fly ash concrete, Ecosmart concrete Canada 25
2.3.3 Green concrete, Dundee, Scotland 26
2.3.4 Ultrafine particles in concrete, Sweden 27
2.4 Particle size optimization methods 28
2.4.1 Overview 28
2.4.2 Optimization curves 30
2.4.3 Particle packing models 32
2.4.4 Discrete element models 34
2.5 Concluding remarks 36

3 Evaluation of particle packing models **39**
3.1 Particle packing 40
3.1.1 Packing density 40
3.1.2 Particle characteristics 41
3.1.3 Particle forces 44
3.1.4 Particle structure 46
3.2 The Furnas model 49

3.3 The Toufar and modified Toufar model 51
3.4 The Dewar model 54
3.5 Linear Packing Density Model 56
3.6 Compressible Packing Model 59
3.7 The Schwanda model 61
3.8 Linear-Mixture Packing Model 63
3.9 Concluding remarks 65

4 Preliminary experimental investigations: particle packing of ecological mixtures 67
4.1 Ecological concrete mixtures 68
4.1.1 Set-up 68
4.1.2 Results 71
4.1.3 Discussion 76
4.2 Packing density measurements 77
4.2.1 Test methods for measuring particle packing 77
4.2.2 Particle packing and agglomeration 79
4.2.3 Particle packing results 82
4.2.4 Discussion 86
4.3 Concluding remarks 88

5 Compaction-Interaction Packing Model 89
5.1 Geometrical interaction 90
5.2 Interaction by surface forces 93
5.2.1 DLVO-theory 93
5.2.2 HADES simulations 95
5.2.3 Interaction forces in the Compaction-Interaction Packing Model 100
5.3 Compaction 103
5.3.1 Theory on deformation of the particle structure through compaction 103
5.3.2 Implementation 104
5.3.3 Influence of compaction values 106
5.4 Compaction-Interaction Packing Model: user information 108
5.4.1 From experiments to modelling 108
5.4.2 Input 111
5.4.3 Compaction-interaction values 112
5.5 Concluding remarks 113

6 Cement paste and mortar experiments 115
6.1 Experiments 116
6.1.1 Introduction 116
6.1.2 Mortar mixtures with cement 116
6.1.3 Mixtures including quartz powder 117
6.2 Packing density 119
6.2.1 Packing density measurements 119
6.2.2 Packing density evaluation CIPM 120
6.2.3 Suitability analysis of fillers 121
6.3 Packing density and water demand 125
6.3.1 Viscosity measurements of pastes 125
6.3.2 Flow value measurements of mortars 128
6.3.3 Water layer analysis 128
6.4 Packing density and strength 135
6.4.1 Isothermal calorimetry measurements 135
6.4.2 Strength measurements 138
6.4.3 Particle distance analysis 140
6.5 Concluding remarks 144

7 Design method for ecological concrete 147
7.1 Cyclic design procedure 148
7.1.1 Input parameters and design steps 149
7.2 Particle packing 151
7.3 Water demand 153
7.4 Strength 155
7.5 Mixture adjustment 159
7.5.1 Mixture composition restrictions 159
7.5.2 Defined performance concrete 160
7.6 Example of ecological concrete design 161
7.7 Concluding remarks 165

8 Application of ecological concrete mixtures 167
8.1 Ecological mixture design 168
8.1.1 Introduction 168
8.1.2 Mixtures 168
8.1.3 Ecological impact 171
8.2 Performance of ecological mixtures 173

8.3 Durability aspects 178
8.3.1 Drying out during hardening process 179
8.3.2 Electrical resistance 181
8.3.3 Polarizing and fluorescent microscopy 184
8.4 Demonstration projects 188
8.4.1 Industrial pavement Werf Heijmans Rosmalen 188
8.4.2 Cycling path Hemaalpad Rosmalen 192
8.4.3 Self-compacting concrete Heembeton 193
8.5 Concluding remarks 197

9 Conclusions and recommendations 199
9.1 Conclusions 200
9.2 Recommendations 206

References 209
Appendix A Material properties 219
Appendix B Measuring water demand or packing density of micro powders - comparison of methods 225
Appendix C Packing profiles CPM 237
Appendix D Packing profiles CIPM 242
Appendix E Cement pastes and mortar mixtures 247
Acknowledgements 253
Curriculum vitae 255

Notations and symbols

Greek

α	packing density of a mixture [-]
$\alpha_{aggregate}$	packing density of the aggregate [-]
α_c	packing density of the cement particles [-]
$\alpha_{\exp}$	experimentally determined packing density of a mixture [-]
α_i	packing density of dominant size class i [-]
α_j	packing density of size class j [-]
α_{ij}	assisting variable for packing density in the Toufar model [-]
α_t	calculated packing density of a mixture [-]
$\alpha_{wbr=c}$	packing density at constant water/binder ratio [-]
$\alpha_{wcr=c}$	packing density at constant water/cement ratio [-]
β	virtual packing density of a mixture [-]
β_{hl}	interaction formula in the Linear-Mixture Packing Model [-]
β_i	virtual packing density of size class i [-]
β_j	virtual packing density of size class j [-]
β_t	calculated virtual packing density of a mixture [-]
β_{ti}	calculated virtual packing density of a mixture when size class i is dominant [-]
ε	voids content or porosity of a mixture [-]
$\varepsilon_{cd,0}$	basic drying shrinkage strain of concrete [mm/m]
$\varepsilon_{cd}(t)$	drying shrinkage of concrete [mm/m]
ε_{large}	porosity of the large size class in the Schwanda model [-]
ε_{small}	porosity of the small size class in the Schwanda model [-]
$\varphi(t,t_0)$	creep coefficient, defining creep between times t and t_0, related to elastic deformation at 28 days [-]
φ_0	the notional creep coefficient according to Eurocode 2, depending on relative humidity, concrete strength, concrete age at loading and h_o [-]
φ_c	experimentally determined creep coefficient of concrete [-]
φ_{cem}	the partial volume occupied by the cement in a stable particle structure [-]
φ^*_{cem}	maximum partial volume that the cement may occupy given the presence of other particles [-]
φ_i	partial volume: the volume occupied by size class i in a unit volume [-]

φ_i^*	maximum partial volume that size class i may occupy given the presence of the other particles [-]
φ_j	partial volume: the volume occupied by size class j in a unit volume [-]
φ_{large}	volume occupied by the large size class in a unit volume in the Schwanda model [-]
φ_{mix}	partial volume of all the particles of a mixture in a unit volume [-]
φ_{small}	volume occupied by the small size class in a unit volume in the Schwanda model [-]
γ_{hl}	interaction formula in the Linear-Mixture Packing Model [-]
ρ_b	density of a binder [kg/m^3]
ρ_{bulk}	bulk density of a material [kg/m^3]
ρ_c	density of cement [kg/m^3]
ρ_p	particle density [kg/m^3]
ρ_w	density of water [kg/m^3]
υ	overall specific volume of a mixture, defined as the apparent volume occupied by a unit volume of particles $(\upsilon = 1/\alpha)$ in the Linear-Mixture Packing model [-]
υ_i	initial specific volume of the *i*th component [-]
υ_i^{mix}	partial specific volume of the controlling mixture corresponding to the *i*th component [-]
υ_i^T	calculated specific volume under the assumption that the controlling mixture corresponding to the component of size class d_{pi} is the controlling component [-]
$\upsilon_{filling}^s$	contribution of small particles as filling component [-]
$\upsilon_{additive}^l$	contribution of large particles as additive component [-]

Roman

a_{ij}	factor which describes the loosening effect caused by the particles in size class j on the packing density of the particles in size class i [-]
$a_{ij,c}$	factor which describes the loosening effect caused by the particles in class j on the packing of the particles in class i to determine φ_i^* [-]
$a_{i,j}$	particle interaction factor in the Schwanda model [-]

A_0	Hamaker constant = 1.6E-20 [Nm]
A_c	concrete cross-sectional area [mm^2]
A_p	surface area of (a group of) particles [m^2/kg]
$A(s)$	Hamaker factor [Nm]
aircontent	volume of air in a concrete mixture [%]
b_{ij}	factor which describes the wall effect caused by the particles in class j on the packing of the particles in class i [-]
$b_{ij,c}$	factor which describes the wall effect caused by the particles in class j on the packing of the particles in class i to determine φ_i^* [-]
C_a	compaction-interaction constant within the loosening effect $a_{ij,c}$ [-]
C_b	compaction-interaction constant within the wall effect $b_{ij,c}$ [-]
C_i	constant, specified by its index number i
CJ	cohesion factor in the Dewar model [-]
CSF	cement spacing factor [-]
d	particle diameter [m]
d_{ci}	cut-off diameter in the CIPM below which compaction-interaction is taken into account [m]
d_i	diameter of dominant size class i [m]
d_j	diameter of particle class j ($j=1$ for the largest diameter in the Furnas model, LPDM, CPM, Linear-Mixture Packing Model and CIPM, $j=1$ for the smallest diameter in the Toufar model and the Dewar model) [m]
d_{large}	diameter of size class consisting of large particles [m]
$d_{\min}$	minimum particle diameter in a mixture [m]
$d_{\max}$	maximum particle diameter in a mixture [m]
d_{pi}	equivalent packing diameter of the *i*th component [m]
d_{small}	diameter of size class consisting of small particles [m]
d_w	particle diameter of a small size class which starts to exert interaction on size class i in the Schwanda model [m]
d_{50}	median particle diameter of a group of particles for which 50% [m^3/m^3] of the particles is larger and 50% [m^3/m^3] of the particles is smaller [m]
E_{cm}	secant modulus of elasticity of concrete [N/mm^2]
$f_{ck,cube}$	characteristic cube compressive strength [N/mm^2]
$f_{cm(n)}$	mean value of cube compressive strength after n days of hardening [N/mm^2]
f_{cm}	mean value of concrete compressive strength [N/mm^2]

$f_{ct,sp}$	mean value of concrete tensile splitting strength [N/mm^2]
$f(i,j)$	interaction formula – loosening effect of size class j on dominant size particle class i [-]
$f(d_1,d_2)$	factor/formula based on the particle sizes d_1 and d_2 [-]
$f_{\text{int}}(d_i,d_j)$	interaction formula based on the particle sizes d_i and d_j [-]
$f_{\text{int},a}(d_j)$	interaction formula describing the loosening effect based on the particle size d_j [-]
$f_{int,b}(d_i)$	interaction formula describing the wall effect based on the particle size d_i [-]
f_{shape}	interaction formula based on particle shape [-]
F_{total}	the total cohesive force working on a particle in *HADES* [N]
F_{el}	electrostatic force [N]
F_{vdw}	Van der Waals force [N]
$g(j,i)$	interaction formula - wall effect of size class j on dominant small size class i [-]
h	integer, assisting variable in the Linear-Mixture Packing Model
h	thickness of a layer which has to be lifted in order to overcome the interlock and enable shear deformation [m]
h_0	the notional size of the cross-section $h_0 = \frac{2A_c}{u}$ [mm]
i	integer denoting the dominant size class in a mixture
j	integer denoting a size class in a mixture
J	empirical adjustment factor in the Dewar model [-]
k	efficiency factor for binders [-]
K	compaction index [-]
K_b	the sum of all K_i values representing the size classes of the binder [-]
K_{cem}	the sum of all K_i values representing the size classes of the cement [-]
k_d	diameter ratio of two size classes in the Toufar model [-]
K_{exp}	experimental compaction index of a mixture [-]
K_{fa}	the sum of all K_i values representing the size classes of the fly ash [-]
k_{fa}	efficiency factor of fly ash [-]
k_h	coefficient for drying shrinkage depending on h_0 [-]
K_i	partial compaction index of size class i within CIPM [-]
k_s	factor in the Toufar model, section 3.3 [-]
K_t	compaction index of a mixture within CIPM [-]

k_1	factor for calculating scatter in tensile splitting strength from mean compressive strength [-]
l	integer, assisting variable in the Linear-Mixture Packing Model
L_a	compaction-interaction constant within the loosening effect a_{ij} [-]
L_b	compaction-interaction constant within the wall effect b_{ij} [-]
m	spacing factor in the Dewar model, representing the additional space necessary to add small particles in voids between large particles [-]
m_c	mass of the cement in a mixture [kg]
m_{fa}	mass of the fly ash in a mixture [kg]
m_p	mass of the particles in a mixture [kg]
m_w	mass of water in a mixture [kg]
n	number of size classes in a mixture
N_n	normative strength of cement after n days [N/mm^2]
$P(d)$	size cumulative distribution function [-]
q	particle interference factor in the Dewar model [-]
q	exponent in the models by Andreasen and Andersen, Funk and Dinger [-]
r_b	volume fraction of binder in a mixture [-]
r_c	volume fraction of the cement in a mixture [-]
r_{fa}	volume fraction of the fly ash in a mixture [-]
r_i	volume fraction of size class i, by definition $r_i = \varphi_i \Big/ \sum_{i=1}^{n} \varphi_i$ and $\sum_{i=1}^{n} r_i = 1$ [-]
r_{ij}	assisting variable Toufar model [-]
r_{i-j}	assisting variable Toufar model [-]
r_j	volume fraction of size class j [-]
r_{j-i}	assisting variable Toufar model [-]
r_{small}	volume fraction of the small particles in the Schwanda model [-]
r_X^{mix}	volume fraction of particle class X in a controlling mixture consists of Y to Z components $(1 \le Y \le i \le Z \le n)$, by definition $r_X^{mix} = r_X \Big/ \sum_{h=Y}^{Z} r_h$ [-]
s	distance between two particles [m]
s_0	cut-off value of s [m]
t	thickness of a layer [m]
t	time being considered [day]
t_0	the age of concrete at the time of loading [day]
t_{ep}	thickness of the excess paste layer [m]
t_{ew}	thickness of the excess water layer [m]

t_s	the age of the concrete at the beginning of drying shrinkage [day]
u	perimeter of that part of a cross section which is exposed to drying [mm]
U	voids ratio of a mixture [-]
U_{case1}	voids ratio of a mixture when the large particles are the dominant size class in the Schwanda model [-]
U_{case2}	voids ratio of a mixture when the small particles are the dominant size class in the Schwanda model [-]
U_i	voids ratio of the dominant particle class i [-]
U_{large}	voids ratio of the small particles in the Schwanda model [-]
$U_{\max}$	maximum voids ratio as calculated by the Schwanda model [-]
U_{small}	voids ratio of the small particles in the Schwanda model [-]
V	volume [m^3]
$V_{aggregate}$	volume of the aggregate [m^3]
V_b	bulk volume [m^3]
V_c	volume of cement particles [m^3]
$V_{container}$	container volume [m^3]
V_{cp}	volume of cement paste [m^3]
V_{ep}	volume of excess paste [m^3]
V_{ew}	volume of excess water [m^3]
V_i	volume of particles in size group i [m^3]
V_{mix}	total volume of the mixture [m^3]
V_p	volume of all the particles in a mixture [m^3]
V_{vw}	volume of water exactly filling all the voids between the particles [m^3]
V_w	volume of the water in a mixture [m^3]
w	particle interaction range [-]
wbr	water/binder ratio [kg/kg]
wcr	water/cement ratio [kg/kg]
w_0	maximum range of particle interaction [-]
$w_{0,a}$	maximum range of loosening effect [-]
$w_{0,b}$	maximum range of wall effect [-]
w_a	constant denoting the maximum range of loosening effect [-]
w_b	constant denoting the maximum range of wall effect [-]
W_{rv}	relative water volume [-]
x	representative length of a void between particles in the Dewar model [m]

x	assisting variable in the Toufar model [-]
X	integer, assisting variable in the Linear-Mixture Packing model
Y	integer, assisting variable denoting the largest size class in a dominant mixture in the Linear-Mixture Packing model
Z	integer, assisting variable denoting the smallest size class in a dominant mixture in the Linear-Mixture Packing model

Abbreviations

CPM	Compressible Packing Model
CIPM	Compaction-interaction Packing Model
CSF	Cement Spacing Factor
LPDM	Linear Packing Density Model
PFM	Polarizing and Fluorescent Microscopy
RH	Relative Humidity
wbr	water/binder ratio
wcr	water/cement ratio
wpr	water/powder ratio

1 Introduction

This chapter explains in section 1.1 the reason why this research project was carried out. The main research question of this project and the most important research restrictions are presented in section 1.2. Section 1.3 describes the outline of this thesis on the basis of the research strategy.

1.1 General

Nowadays environmentally friendly building is one of the main focuses of attention in the concrete industry. Though concrete is a structural material of which the total environmental impact per cubic meter is limited compared to similar types of building materials, the CO_2-emission resulting from cement production is large, because of the vast amount of cement and concrete produced yearly. In the Netherlands alone, already about 40 million tons of concrete are produced each year. Replacing concrete by other building materials would not solve the environmental problem. Therefore, the solution should be found in reducing the environmental impact of the concrete itself. In a concrete mixture the cement is responsible for more than 50% of the CO_2-emission. Energy consumption and CO_2-emission of concrete can be reduced when cement is replaced by secondary materials such as residual products from other industries. By this strategy not only the emissions are reduced but also residual products are reused. Therefore, fewer products are dumped as landfill and more natural resources are spared. Many of the residual products from industries, like silica fume, fly ash or blast furnace slag, have characteristics that can positively influence concrete properties. However, regulations in the Netherlands do not permit the use of large amounts of cement replacing materials. This is because Dutch regulations prescribe a minimum amount of cement in reinforced concrete of 260 kg/m^3, to make sure that concrete properties such as strength and durability are at a sufficient level.

To design new concrete compositions and to ensure that these new concretes have good material properties and satisfy the requirements, nowadays lots of experiments have to be performed. These tests need to prove equivalent performance of the new type of concrete. This process can be accelerated when the material properties of concrete can be predicted by a performance-based design procedure. Since ecological concrete can be defined in many different ways by various users, a general mixture optimisation method based on defined performance would be a great contribution. In ecological concrete design, particle packing models can help to compose mixtures with the most ideal packing of environmentally friendly materials. In this way an optimal mixture composition can be designed for any application, fulfilling different requirements each time. For instance, when high strength is not required but low shrinkage is, Portland cement can be replaced by fly ash, thus sparing natural resources and favourably using industrial by-products.

Performance-based design of concrete will always deliver the most economical and environmentally friendly solution for each application.

In concrete technology new particle packing models and underlying theories make it possible to design new types of concrete, such as high strength concrete and self compacting concrete. However, in about 75% of the applications these specific performances are not required and concrete with an average strength is better suitable for the application. When particle packing models can be used to design concrete with a reduced cement content, a more ecologically friendly material could be produced. However, particle packing models are often used in such a way that the maximum packing density of the aggregate structure (≥125 µm) for various combinations of fractions is predicted. After that, the optimal aggregate structure is combined with a sufficient amount of flowable and stable cement paste to create good concrete. Some models can take into account particle packing of cement and fillers (<125 µm) as well, but research in this area is far from finished. Experimental optimization of the cement paste is necessary, whereas the optimal cement paste does not guarantee the best mixture for concrete. Time and money can be saved in this design phase when particle packing models can predict concrete properties from all its basic components including the fine powders and cement replacing materials. Still, knowledge of the resulting mechanical behaviour and durability aspects is essential in order to reliably design environmentally friendly concrete with this method. This is because not every cement replacing material will influence each material property of concrete in the same way.

1.2 Research objective

To reduce the environmental impact of concrete, optimal mixture compositions for ecological concrete should be designed. However, it is important that when environmentally friendly concrete is designed and applied, the material properties of that concrete satisfy the demands. Therefore the main question of this research project is:

How can particle packing models be used to predict the mechanical properties of ecological concrete from its basic components?

Important subjects in this respect are the design of ecological concrete and the development of a design method based on particle packing models for predicting mechanical properties of ecological concrete. In this thesis concrete is considered to be ecologic when the cement content is reduced compared to a regular concrete mixture, while at the same time the concrete still satisfies the demands for appropriate use. It is conceded that this is not the only solution to design concrete with lower CO_2-emissions or lower environmental impact. Lots of factors will influence the environmental impact, for instance the origin of the basic materials, grinding, mixing, compaction and transportation of the materials and concrete. However, cement is considered to be the basic component with the highest environmental impact with regard to CO_2-emissions and energy consumption. In this way, optimization of ecological concrete mixtures is situated in the field of concrete technology and can directly be related to designing concrete from its basic components by making use of particle packing models.

1.3 Research strategy and outline

The research aims at predicting the mechanical properties of ecological concrete based on the packing density of its particle structure. This particle structure consists of aggregates (≥125 µm), fillers, binders and cement particles. To be able to model its packing density an important part of this research project focuses on defining particle characteristics and describing and measuring particle structures. The influence of different types of superplasticizers on the packing density of concrete is not investigated. This is because combining various types and amounts of superplasticizer with the various types of cement replacing materials which were used in this research project, would lead to an impractical amount of design variables to be investigated. Therefore, the use of a fixed amount of a certain superplasticizer is taken as a constant research parameter. Information on the packing density model is recorded in the chapters 3, 4, and 5. This part includes the particle characteristics which influence the packing density, the measuring of the packing density of fine particles <125 µm and the modelling of the packing density including these fine particles.

Furthermore, the particle structure and its packing density serve as the starting-point in the design procedure for ecological concrete. The procedure is created on the basis of relations between particle packing, water demand and concrete strength resulting from

experimental research. The chapters 5, 6, 7 and 8 focus on the design of ecological concrete mixtures. In this part of thesis packing density predictions are combined with experimental results in order to create a design procedure for ecological concrete which is then used to design ecological concrete mixtures. The outline of the thesis is presented in Figure 1.1.

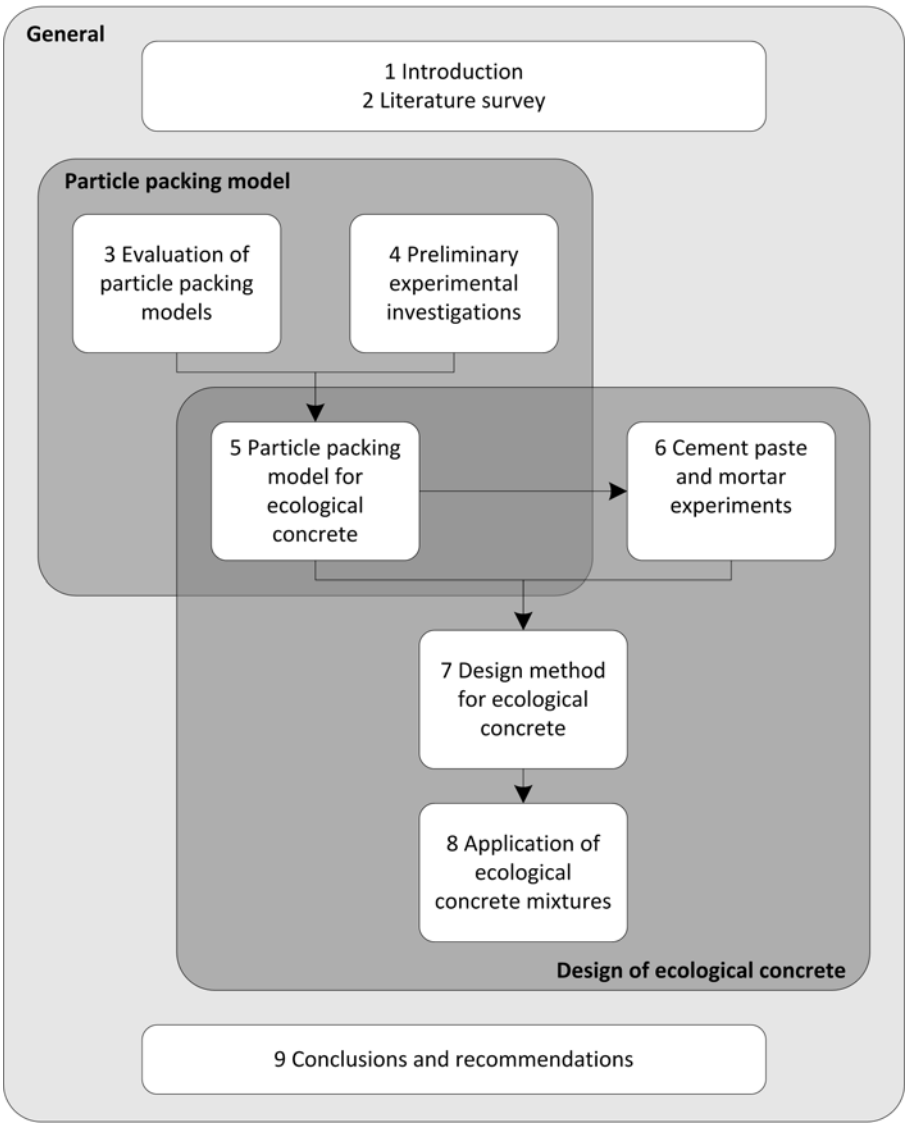

Figure 1.1 Outline of the thesis.

Chapter 2 is a literature survey on ecological concrete and cement replacement. Emphasis is put on the use of fillers and binders and the influence of replacing cement on the material properties of concrete. Furthermore, this chapter points out important factors in the design of ecological concrete based on particle packing density. The advantages and disadvantages of the different particle packing optimization methods are summarized.

Chapter 3 describes particle characteristics influencing packing density as well as influences such as interaction and compaction on the resulting particle structure. Several particle size distribution optimization models are evaluated. Input parameters and user friendliness are important as well as the practicability of the output. However, to meet new requirements from ecological concrete mixture design, the mathematical basis and adaptability with regard to particle characteristics, interaction and compaction are relevant as well.

The fourth chapter contains the results of the preliminary experimental investigations. These experiments are conducted to evaluate the suitability of current packing density models for the design of ecological concrete, to record the major factors influencing the material properties of ecological concrete and to determine particle packing of basic components of ecological mixtures. The influence of a low cement content in concrete on the mechanical properties is investigated to check the validity of existing relationships between compressive strength of concrete and other mechanical properties for ecological concrete.

Knowledge from the previous chapters is used to develop an optimised particle packing model in chapter 5. The improved model includes the major factors influencing packing density as registered in the chapters 2, 3 and 4. Discrete element modelling is used to investigate the influence of interparticle forces on the packing density. Interaction formulas are adjusted to implement changes in the loosening effect and wall effect for the fine particles (<125 µm).

In chapter 6 the results of the experimental investigations are presented. The experiments aim at relating particle packing, water demand and strength of ecological mixtures. These experiments demonstrate the suitability of fillers to replace cement. Relations between packing density and water demand, for instance expressed as water layer thickness or void filling water, are used to predict strength as one step in the design method. Based on measurements of heat generation and strength, relations between packing density and strength are derived.

Chapter 7 describes the procedure to design ecological concrete on the basis of particle packing. Depending on the relationships found in chapter 6, a design method is developed in which particle packing densities as calculated by the new particle packing model (chapter 5) are related to ecological concrete mixture optimization.

To show how the design procedure from chapter 7 can be applied to optimize ecological concrete mixtures, in chapter 8 ecological concrete mixtures are discussed. A number of optimized ecological concrete mixtures are tested on strength development, modulus of elasticity, shrinkage and creep. The demonstration projects provide insight into the applicability of ecological concrete mixtures for practical purposes.

In chapter 9 the conclusions are summarized. Recommendations for applying ecological concrete are given with special attention to the areas in which ecological concrete and its design deviates from normal concrete.

2 Ecological concrete design: a survey of literature

Chapter 2 gives a literature survey on particle packing and cement replacement in ecological concrete. This chapter points out the most important factors in the design of ecological concrete based on particle packing. Most mixture designs aim at reducing the cement content by replacing cement by fillers or binders. The use of fillers and binders and the influence of replacing cement on the material properties of concrete are described in section 2.2. Interesting projects in the field of ecological concrete are described in section 2.3. In this thesis ecological concrete is designed using particle packing methods. Therefore, section 2.4 describes different particle size distribution optimization methods and their advantages and disadvantages with regard to ecological concrete mixture optimization. The concluding remarks in section 2.5 contain some aspects to be taken into consideration when designing ecological concrete based on particle packing. Chapter 3 focuses on the use of particle packing models for the design of ecological concrete in more detail.

2.1 Introduction

Ecological concrete or 'green' concrete is designed all over the world; however, the definition of the material differs a lot. For example, in some countries concrete is defined as ecological when the CO_2-emissions resulting from the production of the material are lower than those resulting from the production of conventional concrete. This can be reached by for instance using waste materials or changing the production process. Also recycling of concrete and the total life cycle of the concrete are often regarded in ecological design. In this research project the focus is on concrete mixture proportioning. For that reason, life cycle analysis and environmental impact of the production process are not taken into account. The aim is to design ecological concrete with a reduced cement content compared to regular concrete mixtures. Cement is considered to be the basic component with the highest environmental impact with regard to CO_2-emission and energy consumption. Therefore, reducing the cement content while retaining the concrete properties, will result in a more ecological concrete.

Estimations of the contribution of cement and concrete on the worldwide CO_2-emission vary from 3 to 7%. According to Mehta (2001), the world's yearly cement production of 1.6 billion tons accounts for about 7% of the global loading of carbon dioxide into the atmosphere. Also in 2001, Worrell et al. presented that the cement industry contributes about 5% to the global CO_2-emission. Boden (2009) presents that in 2006 the total CO_2-emission from cement production is estimated at 348 million metric ton of the total 8230 million metric ton CO_2-emission world wide. According to Glavind and Munch-Petersen (2002), worldwide about 12.6 billion tons of concrete are produced. For each ton of concrete, the CO_2-emission related to concrete production and primarily to cement production, is between 0.1 and 0.2 metric ton per ton of produced concrete. These figures were used for a first estimation of the possible reduction of CO_2-emission by making use of ecological concrete. Reducing the average cement content in concrete from 300 kg/m^3 to 225 kg/m^3 would lead to a decrease of the global CO_2-emission of at least 1%.

In the Netherlands, concrete contains on average about 300-330 kg/m^3 cement. Mixtures with these amounts of cement often reach a strength class C28/35 or higher. However, for most applications this strength is not necessary. In applications such as residential building walls, industrial floors and underwater concrete stresses are low, so that often mass or density of the concrete becomes the governing structural design parameter. Also other

concrete structures which are permanently wet, such as foundations under water, or permanently dry do not require high strength for durability reasons. However, Dutch regulations only allow strength class C12/15 for concrete without risk of rebar corrosion. In other countries also lower strength classes are allowed, for instance for the so called Controlled Low-Strength Materials (Adaska, 1997; Trejo, et al., 2004), but relations between compressive strength, tensile strength and durability differ from normal concrete (Weng and Vipulanandan, 1999). For reinforced concrete strength class C20/25 or higher should be applied according to the Dutch standards. These regulations also prescribe a minimum water/cement ratio and a minimum cement content ranging from 260 to 360 kg cement per cubic meter concrete (NEN-EN 206-1:2001). Fillers are allowed to be used, but only fly ash and silica fume are accepted as cement replacing material. The use of silica fume is not taken into account in this research project. Equations 2.1 to 2.3 present how and to what extent fly ash can be used as binder in 1 m^3 concrete, while still fulfilling the minimum prescribed cement content in kg/m^3. The maximum allowed water/binder ratio wbr depends on the mass of the water m_w [kg/m^3], mass of cement m_c [kg/m^3] and mass of fly ash m_{fa} [kg/m^3] present in a mixture (NEN-EN 206-1:2001).

$$\frac{m_{fa}}{m_c} \leq 0.33 \tag{2.1}$$

$$wbr = \frac{m_w}{\left(m_c + k_{fa} m_{fa}\right)} \tag{2.2}$$

$$m_c \geq \text{minimum cement content} - k_{fa} * \left(\text{minimum cement content} - 200\right) \quad \text{and}$$

$$m_{fa} \geq \text{minimum cement content} - m_c \tag{2.3}$$

For Dutch Portland cement in strength class 42.5 and higher the efficiency factor of fly ash $k_{fa} = 0.4$. This leads for a minimum cement content of 260 kg/m^3 per cubic meter of concrete to a minimum amount of 236 kg/m^3 cement when combined with at least 24 kg/m^3 fly ash.

The main focus in this research project is to design ecological concrete with a low cement content. This comprehends all structural concretes with a cement or binder content lower than the prescribed 260 kg/m^3 in the Dutch standards. Furthermore, to comply with the Dutch standard (NEN-EN 206-1:2001) for reinforced concrete with regard to the allowed strength classes it is chosen to limit the concrete mixture design to strength class C20/25

or higher. The water/cement ratio is chosen to be a free design parameter. This is because some fillers might also show binding properties which would make it possible to design a good and durable concrete with a higher water/cement ratio than the minimum as prescribed in (NEN-EN 206-1:2001). However, since this research is based on physically improving the concrete mixture design by increasing the packing density, research is limited to cement types including Portland clinker which are replaced by (a combination of) fillers or binders. This means that any chemical activation of fillers and binders other than by the Portland cement present in the mixture is not applied.

2.2 Replacing cement

Portland cement or clinker can be replaced in two different ways. Firstly the Portland clinker can be replaced by other materials such as blast furnace slag or fly ash in the cement factory. Because these materials are mixed or sometimes even co-grinded together in the factory the resulting product has constant and good properties. This combined product is called cement and it is composed in such a way that when it is used in concrete it will be just as strong as ordinary Portland cement at 28 days. This can be done by, for example, grinding until higher fineness is reached. Increased fineness causes slowly reacting particles to react faster due to increased surface area.

A second possibility to replace cement is to interchange it with another binder or fine filler in the fresh concrete mixture. In this way any type of cement can be replaced by fine materials such as fly ash, granulated blast furnace slag, lime stone powder, or inert mineral powders like quartz powder.

This research aims at lowering the amount of cement by optimizing the mixture design of ecological concrete. Therefore cements created in the first way will be taken into account as basic materials, but the cement content will be lowered by interchanging cement with fillers or binders.

2.2.1 Cement replacing materials

Binders

Binders are defined as reactive particles which actively create a binding structure between the aggregates or inert particles. Their reaction products make up the cement gel or

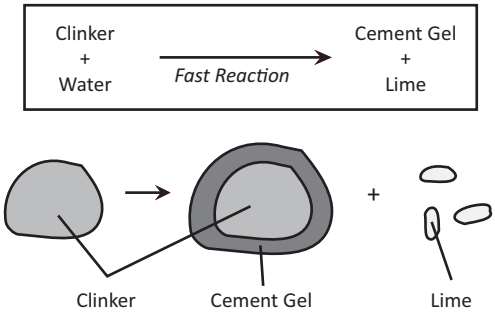

Figure 2.1 The reaction of clinker particles with water. After (Bakker, 1999).

so-called glue which bonds the aggregates. Besides their binding ability these fine particles often improve the material properties of concrete by improving particle packing density and reducing the water demand (filler effect). The binders can be divided into three groups. The first group consists of the hydraulic particles, which react with water to form an insoluble substance. In this way Portland cement clinker reacts to form cement gel, as shown in Figure 2.1. With this reaction calcium hydroxide is released.

Secondly, latent hydraulic particles also react with water to form cement gel, but this reaction is very slow and needs to be activated to be useful, Figure 2.2. Granulated blast furnace slag is one of these slowly reacting materials, which need to be activated. Possible activators are alkalis or sulfates. Calcium hydroxide resulting from Portland cement reaction creates a strong alkaline environment, which can act as an activator for blast furnace slag. In this research project granulated blast furnace slag is not taken into account as a separate binder; however, in some experimental series blast furnace slag cement CEM III/B 42.5 N is used in addition to Portland cement.

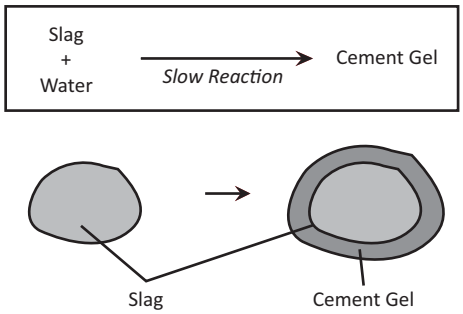

Figure 2.2 The reaction of blast furnace slag particles with water. After (Bakker, 1999)

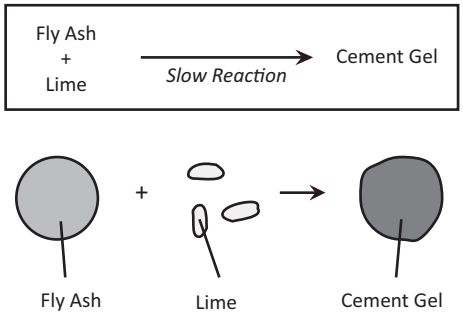

Figure 2.3 The reaction of fly ash particles with lime. After (Bakker, 1999).

Pozzolanic materials make up the third group. These materials, such as fly ash and silica fume, can also form a gel structure. However, the particles do not react with water, but with a calcium hydroxide solution, Figure 2.3. Reaction speed depends on the particle fineness and the alkalinity of the environment. For example silica fume reacts faster than fly ash because of its fineness. The maximum degree of pozzolanic material reacting depends on the amount of calcium hydroxide in the water, usually resulting from Portland cement clinker reaction.

Depending on the type of binder used, the chemical composition and internal structure of the cement gel can differ. Therefore the material properties of the concrete can vary distinctively when different types of binders are used.
(Bakker, 1999; Reinhardt, 2002; Souwerbren C., 1998)

Fillers

In this thesis fillers are defined as inert fine particles which do not actively form cement gel. Even though fillers defined in this way are not reactive, they do have a positive influence on concrete properties. This is because they fill up the open spaces between larger aggregate particles. As fine particles they not only increase particle packing density and decrease water demand, but they also create a better bond between cement gel and the aggregate. The reason for this is that fine fillers influence formation and orientation of large crystals in the cement gel. The fine particles act as nucleation sites on which cement gel can settle. Especially in the interface zone around larger particles this will lead to a stronger cement matrix. It is conceded that cement replacing materials used in concrete

as filler material often also have a tendency to form some chemical phases, such as for instance carbo-aluminate phase. Materials with a substantial chemical binding effect are regarded as binders in this thesis. (Gopalan, 1993; Kadri, et al., 2009; Poppe and Schutter, 2005)

From subsection 2.2.1 it follows that fillers and binders influence the internal structure of the concrete. The next subsections summarize research reporting on the influence of the changed internal structure on the properties of concrete.

2.2.2 Influences of fillers on workability

The workability of concrete is influenced when fine particles are used in a concrete mixture. Various types of methods are used to measure this workability and depending on the method various properties are used to describe it, such as yield stress, plastic viscosity, slump, flow value or flow time. Furthermore, the effect of adding fillers on the workability a concrete mixture depends very much on the original composition and properties of that mixture. Nevertheless, in these paragraphs it is tried to summarize some general effects and theories on the workability of concrete in relation to the use of fillers.

In general two theories to predict the workability of a concrete mixture are adopted, the water layer theory and the packing theory. The water layer theory assumes that the water demand of a mixture depends on the surface area of the particles in that mixture, Figure 2.4. Increasing the surface area by adding small particles will increase the water requirement (Fraaij and Rooij, 2008; Hunger and Brouwers, 2009; Maeyama, et al., 1998; Midorikawa, et al., 2001; Teichmann, 2008). Packing theory assumes that adding fine particles to a particle structure helps filling up the voids in the particle structure leaving only minimum space for water, Figure 2.4. In this way adding fine particles will reduce the water requirement (Kronlöf, 1997; Larrard F. de, 1999; Wong and Kwan, 2008b). The theories seem contradicting, but also models supporting both theories exist. These are often based on a system in which the water fills the voids between particles and an excess amount of water surrounds the particles as a layer. The fact that both theories are still supported might be explained by differences in filler types, filler sizes and or the usage of superplasticizer in research projects all over the world. For instance, Kronlöf (1997) stated that the workability of concrete with fine fillers varies to a great extent due to the

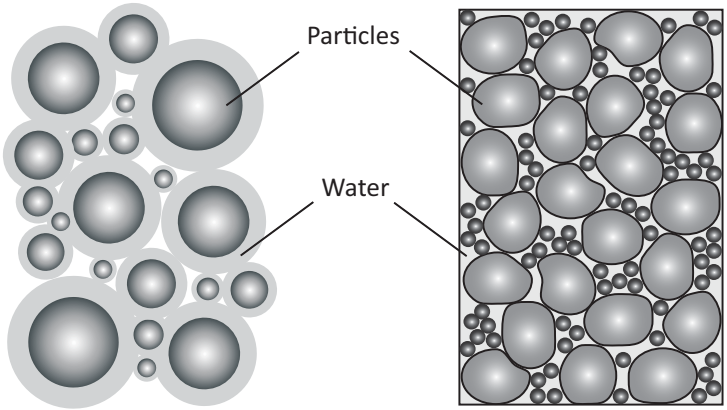

Figure 2.4 Water layer theory with layers of water surrounding each particle (left hand side) and particle packing theory in which water fills the voids in between the particles (right hand side).

flocculation of small particles. In mixtures without superplasticizer, fine particles are flocculated and cannot fill spaces of their own size class,which explains why they often require more water. The first condition that must be met for applying the packing theory is the use of a superplasticizer to break flocculation. Kronlöf also postulated that particle packing models are able to give a rough water requirement of a compact mix, but do not estimate the water volume fraction needed to convert a mix from compact to workable. This extra water volume was found to vary depending on the actual mixture composition and consistency requirement, and is larger the closer the mixture composition is to the highest packing density (Kronlöf, 1997). Also Nehdi (2000) stated that the superplasticizer in combination with the fineness of the filler reduces the water demand according to the particle packing theory. The author suggested that fine fillers complement the deficiency in fine particles of the cement's particle size distribution, improve the flowability and stability of fresh concrete and at later age they obstruct the capillary pores. With increasing fineness of the filler, he reported a rapid loss of workability in time for some types of carbonate filler. This loss of workability probably depends on the efficiency of the superplasticizer, which depends on the mineral composition of the filler (Nehdi, 2000). Bigas and Gallias (2002) showed that besides the fineness of the particles morphological characteristics, shape and especially texture, influence the water requirement and consequently the packing density.

Furthermore, most researchers supporting the particle packing theory also report the need of an excess amount of water or cement paste to provide workability. Reschke (2000) stated that cement paste should not only fill the voids between the aggregates but surround all particles with a thin layer of paste to fulfill workability requirements. The required amount of paste for this layer depends on the specific surface area of the particles. The larger the surface area of the particles, the smaller the thickness of the surrounding paste layer and the larger the available surface for cement matrix–aggregate bond (Reschke, 2000). Also Kwan and Mora (2001) reported that maximum particle packing density does not necessarily guarantee a workable concrete mixture. They found that a very dense particle structure that consists of too many fine particles produces a harsh concrete mixture.

The capability of fly ash to improve workability is not disputed among researchers. It is often regarded as the ball-bearing effect, though different terms have been used to describe it (builditgreen.org; Crouch, et al., 2007; fhwa.dot.gov; flyash.com; Naik, et al., 2009). However, it should be stated that the ball-bearing effect of fine rounded particles such as fly ash is supported by both an increased packing density in the packing theory and by the low specific surface area of spheres in the water layer theory.

Some general conclusions on the use of fine particles in mortar in agreement with this section come from (Westerholm, et al., 2008). They concluded that rheological properties and water demand of mortars strongly depend on the properties of the fine aggregate. Yield stress is believed to increase due to high amounts of fines. Plastic viscosity increases due to a particle shape effect and increased interparticle friction. The effects can be eliminated or reduced by increasing the paste volume of the mortar or concrete or by the use of an effective superplasticizer (Westerholm, et al., 2008).

2.2.3 Influence of fillers on strength

In spite of the disagreement on the influence of fillers on the water demand of concrete, most researchers agree that adding fillers to cement will improve strength. Nehdi (2000) shows that some limestone filler can accelerate the setting. Furthermore, Bornemann (2005), Kaufmann and Winnefeld (2002) and Lagerblad and Vogt (2004) stated that adding particles smaller than the cement particles will improve early strength gain. This complies with the theory that (early) strength is increased when an increased amount of nucleation

sites is present for hydration products to precipitate (Cyr, et al., 2005; Kadri and Duval, 2002; Moosberg-Bustnes, et al., 2004; Nijland, et al., 2007). Also Reschke (2000) found that the strength increases when the aggregate surface increases due to the increased available surface for the cement matrix-aggregate bond and the decreased thickness of the cement paste surrounding the particles. Lange et al. (1997) postulated that hydration is quickened and compressive strength becomes higher when using fillers.

In general, adding fine particles results in stronger concrete. This can be caused by a reduced water requirement, but that is not always the case as argued before. In (Kaufmann and Winnefeld, 2002) high strengths were found to be achieved due to a reduced water/cement ratio and the filling effect of the fine particles. Other causes for strength increase were presented by Lagerblad and Vogt (2004), who investigated the effect of very fine fillers on concrete strength. Adding the filler increases strength or similar strength is obtained with replacement ratios up to 40%. The main effect seems to occur due to the fact that ultrafine particles become an integrated part of the cement matrix, and increase the homogeneity of the interfacial zone. Also cement hydration is accelerated by ultrafine particles (Lagerblad and Vogt, 2004).

If cement is replaced by fine particles the cement matrix usually becomes less dense causing concrete strength to reduce; however this can depend on the fineness of the filler. For instance, Reschke stated that with a narrower sieve distribution of inert filler, the packing density of the cement matrix decreases. The increased volume of the cement matrix causes a small (non significant) strength reduction. When cement is replaced by inert filler, strength decreases with increasing amount of filler. This is because the voids between the particles will not be filled completely with cement gel, when the cement amount is decreased. The result is a less strong cement matrix with a higher porosity (Reschke, 2000). Bentz (2005) has shown that replacing all coarse cement particles above 30 µm by an inert lime stone filler (from which the particles smaller than 30 µm were removed) slightly decreased the seven day strength. However, at 56 days the strength development of the blended mixture caught up to the reference.

Other influences on the strength development of concrete including fine fillers which were found in literature were coming from the aggregate structure and the use of superplasticizers. Kronlöf (1997) found, based on experiments with plasticized mixtures, that using a filler reduced the water requirement and increased strength, especially in mixtures with crushed aggregates. Also Reschke (2002) takes into account the amount and type of aggregate. He stated that concrete strength is defined by the aggregate content,

the properties of the cement matrix (depending on composition of binders and fillers, water/binder ratio, reactivity etc.), the properties of the aggregates and the bond between cement matrix and the aggregates. In general the aggregates are stronger than the cement matrix. This means that when the cement matrix content is decreased a stronger concrete is expected as long as all voids between the aggregates are filled (Reschke, 2000). With regard to the use of superplasticizer it should be stated that in literature about the influence of fine particles on concrete strength most researchers used superplasticizer, but did not investigate different amounts or types of superplasticizer. It is evident that a reduced water demand and increased strength can only be achieved in properly dispersed mixtures. The other way around, Reschke (2000) states that without superplasticizer, the fineness of the filler has almost no influence on concrete strength.

2.2.4 Influence of fillers on mechanical properties and durability

General results on the influence of fillers on mechanical properties such as shrinkage or creep and on durability are difficult to obtain, because of the influence of the chemical composition of the fillers. Therefore the next statements, to qualify the influence of the fillers on the mechanical properties of concrete, are more generally based on cement content and packing density of the particle/aggregate structure.

A strong aggregate structure with a high packing density will restrain the amount of shrinkage and creep that can actually be realized. Furthermore, a lower water/cement ratio reduces shrinkage, because of the reduced amount of evaporable water in the cement paste (Neville, 1995). Similarly, Kwan and Mora (2001) reason that a higher packing density leads to a smaller void ratio and thus a smaller amount of cement paste is needed. The heat of hydration and the drying shrinkage are reduced, since both are roughly proportional to the volume of cement paste in the concrete (Kwan and Mora, 2001). Dhir et al. (2005) demonstrated that changes in the performance of other engineering properties when using particle packing techniques, different cement types and lower water and cement contents, are proportional to the changes in cube strength.

With regard to durability, some of the results presented for concrete strength are also valid for the density of the microstructure. Adding filler increases the density of the microstructure when water demand is reduced. Lange et al. (1997) found that the packing density of the paste increases when about 15% of filler is added, leading to a decreased porosity and a more homogeneous and dense microstructure. However, replacing cement

by a fine filler often leads to a less dense microstructure, because of the lowered amount of cement and higher water/cement ratio. Apart from that, durability of mixtures with binders or fillers strongly depends on the density and pore structure of the cement matrix. Since these properties depend on the type of fine materials used and their size distribution, durability properties of concrete are not fixed unambiguously and therefore they have to be considered for each concrete mixture individually. Water/cement ratio or water/binder ratio will in that case be a directive parameter. Kronlöf (1997) has shown that when packing density is optimized by adding inert filler, the carbonation rate is lower and freeze-thaw resistance higher, because of the water reduction.

2.2.5 Influence of binders

Since binders can influence the resulting concrete properties by their chemical, mineralogical, morphological and physical properties, it is difficult to make general remarks about their influence on concrete properties. Binders could be regarded as a special kind of filler, showing general filling effects as described in the previous paragraph and additional chemical binding effects. However, in research on binders it is even harder to separate these two effects. For instance, Erdoğdu and Türker (1998) and Liu and Xie (2005) investigated the effect of the fineness of fly ash on concrete, but they discovered that fly ash does not have the same properties for every size fraction. Therefore the following research results coming from research on fly ash should be interpreted with caution. The only other binder which is allowed to be used in the Netherlands is silica fume and is not included in this research project.

Fineness of fly ash

The influence on flowability, setting time, non-evaporable water content and strength of normal graded fly ash and ultrafine fly ash in paste and mortars is investigated by Liu and Xie (2005). Fly ash increases flowability of low water/binder ratio pastes. Ultra fine fly ash increases paste flowability more, and with lower fly ash contents (as from 10%), than normal fly ash. Normal fly ash improves workability most at 30% cement replacement. For mortars with 20% or less ultra fine and normal fly ash, the effect of the fly ash on workability is the same. At higher amounts of fly ash, however, ultrafine particles further improve workability while coarser fly ash particles do not. Setting time increases when

Table 2.1 The effect of particle size of fly ash on the compressive strength of mortars (Erdoğdu and Türker, 1998).

		Compressive strength [N/mm^2]			
	Size fly ash	**2-day**	**7-day**	**28-day**	**90-day**
100% CEM I 32.5	-	38	44.4	51.6	58.2
75% CEM I 32.5 + 25% LOW FA	> 125 µm	17.9	24.4	26.7	29.9
	90-125 µm	21.6	29.2	32	37.1
	63-90 µm	22.6	29.6	34.9	40.6
	45-63 µm	23.8	33.5	37.4	46.8
	< 45 µm	26.6	37.3	43.4	57.2

increasing amounts of cement are replaced by fly ash, for both types of fly ashes. From the non-evaporable water content measurements, it is concluded that the fineness has little influence on the hydration of fly ash. The highest 28-day hydration rates are found with a 20% fly ash content for both types of fly ashes. Increasing fly ash content decreases the early strength of pastes and mortars. The fineness of fly ash is an important factor influencing the strength at low water/binder ratios (Liu and Xie, 2005).

Erdoğdu and Türker (1998) could observe the effect of particle size on the compressive strength of mortars since the low lime content fly ash fractions (LOW FA) they used did not show any considerable difference in chemical and mineralogical composition. Table 2.1 shows a 48% strength increase after 2 days up to a 91% strength increase after 90 days when fly ash particles smaller than 45 µm are used instead of particles larger than 125 µm in mixtures containing 25% of fly ash and 75% Portland cement. Similar results of fineness of fly ash were found by Slanička (1991). Gopalan (1993) showed that the strength contribution of fly ash up to 28 days can be broadly attributed to the nucleation effect and after 28 days to the pozzolanic reaction, while the onset of the pozzolanic reaction was delayed even more for higher fly ash-cementitious ratios.

2.3 Ecological concrete design

This section summarizes recent investigations which contributed significantly to the field of ecological concrete mixture design.

2.3.1 Green concrete, Denmark

The green concrete project, by the concrete centre from the Danish Technological Institute, aimed at reducing the environmental impact of concrete and developing a technical solution to implement green concrete in the building market. Concrete was defined to be green, when the production process and/or the mixture composition resulted in at least a 30% reduction of the CO_2-emission or when residual products were used for cement replacement or aggregate replacement. Especially the part on mixture optimization to reduce the cement content or to replace cement by residual products interrelates to this thesis. After trial testing, 14 green mixtures were tested in an extensive

Table 2.2 Green concrete mixture compositions for exposure class XC1, Denmark (Glavind and Munch-Petersen, 2002).

	Mixtures					
	PR	**P2**	**P3**	**P5**	**P6**	**P7**
Composition	Reference	50% FA + 10% KD	17% SSIA	Concrete Slurry	100% stone dust	30% FA bio fuels
Cement [kg/m^3]	143	90	137	141	267	191
FA [kg/m^3]	51	128	15	52	-	-
SF [kg/m^3]	10	14	10	10	-	-
SPT [kg/m^3]	-	1.1	3.2	-	1.8	1.9
Equiv. w/c [-]	0.73	0.66	0.78	0.77	0.72	0.69
Compr. strength						
28-day [N/mm^2]	-	26	21	23	29	28
56-day [N/mm^2)	-	34	31	27	33	32
56-day [% of ref.]	-	100	93	80	97	94

SSIA: Sewage sludge incineration ash, FA: Fly ash, SF: Silica fume, KD: Kiln dust,

SPT: Superplasticizer, CREP: Cement with reduced environmental impact

Table 2.3 Green concrete mixture compositions for exposure classes XD or XF, Denmark (Glavind and Munch-Petersen, 2002).

	Mixtures					
	AR	**A0**	**A1**	**A3**	**A5**	**A6**
Composition	Reference	CREP	40% FA + CREP	10% SSIA + CREP	Concrete Slurry	50% stone dust
Cement [kg/m^3]	288	287	189	227	398	397
FA [kg/m^3]	34	32	137	-	-	-
SF [kg/m^3]	17	17	18	17	-	-
SPT [kg/m^3]	-	-	3.4	3.2	4	6.8
Equiv. w/c [-]	0.45	0.47	0.46	0.45	0.38	0.37
Compr. strength						
28-day [N/mm^2]	-	51	58	58	64	62
56-day [N/mm^2)	-	58	61	68	68	63
56-day [% of ref.]	-	112	117	130	130	121

SSIA: Sewage sludge incineration ash, FA: Fly ash, SF: Silica fume, KD: Kiln dust,
SPT: Superplasticizer, CREP: Cement with reduced environmental impact

research program on workability, changes in workability after 30 minutes, air content, compressive strength development, modulus of elasticity, heat development, homogeneity, bleeding, setting time, density and pumpability. Promising mixtures were tested on loss of workability, sensitivity for compaction, curing time, tensile splitting strength, shrinkage, creep, carbonation, chloride ingress, freeze-thaw resistance, fire resistance, moisture transport, rebar anchorage and structural resistance to bending, shear and instability.

The research on rheological properties of green concrete demonstrated that some mixtures showed a faster loss of workability, were stickier or demanded longer resting time before finishing could begin than the reference mixtures. Rheological properties are expected to improve with mixture optimization. The mechanical properties of the green concrete do not differ significantly from the mechanical properties in the reference mixtures. Mixture P2 in Table 2.2 reaches a 28-day strength of 26 N/mm^2 with only 90

kg/m^3 Portland cement and mixture A1 (Table 2.3) reaches a 28-day strength of 58 N/mm^2 with 189 kg/m^3 Portland cement. These amounts of cements are considerably lower than prescribed in Dutch regulations; however, the silica fume in these mixtures will also contribute to the strength and durability. Furthermore, the durability tests performed on mixture A1 to A6 (Table 2.3) showed that only mixture A1 and A6 do not fulfill the requirements of the Danish standards with regard to respectively freeze-thaw resistance and chloride-ingress.
(Glavind and Munch-Petersen, 2002; gronbeton.dk; Jepsen, et al., 2001; Tange Hasholt and Mathiesen, 2002)

Table 2.4 Mixture compositions strength class C20/25 (EBA, 2004).

		Fly ash		
Composition		**25%**	**35%**	**45%**
water	[kg/m^3]	164	158	158
cement	[kg/m^3]	225	195	165
fly ash	[kg/m^3]	75	105	135
20-5 mm coarse aggregate	[kg/m^3]	980	985	987
sand	[kg/m^3]	1013	1010	1000
polyheed 997	[mL/100kg powder]	650	650	550
wpr	[-]	0.547	0.527	0.527
density	[kg/m^3]	2457	2453	2444
slump	[mm]	80	80	70
air content	[%]	2	2	1,8
measured density	[kg/m^3]	2485	2504	2496
Compressive strength *				
3 – day	[N/mm^2]	22.2	18.8	13.1
7 – day	[N/mm^2]	29	26.9	24.7
14 – day	[N/mm^2]	36.4	32.8	32.1
28 – day	[N/mm^2]	43.4	38.7	36.4
56 – day	[N/mm^2]	45.7	44.9	44.2

* *average of two 150 mm diameter test cylinders*

2.3.2 High volume fly ash concrete, Ecosmart concrete Canada

The Ecosmart steering committee supports research on the use of fine fillers and cement replacing materials. On the basis of demonstration projects, CO_2-emissions are reduced by stimulating the use of high volumes of cement replacing materials. Although the project aims at using different types of cement replacing materials such as waste incineration ash, metakaolin, natural pozzolans, rice husk ash, silica fume or blast furnace slag, it mainly focuses on fly ash. Fly ash is the most common and best available filler in Canada and therefore they are very confident in using it in concrete. With high volume fly ash concrete (45%) it is possible to produce concrete in strength class C20/25 with a cement content of only 165 Kg/m^3, Table 2.4.

Using fly ash in concrete generally reduces permeability, and so chloride ingress and sulfate resistance. Furthermore, the water demand is reduced due to improvement of the plasticity and workability of the fresh concrete. However, a low water/binder ratio is required to guarantee the durability and also curing periods might have to be extended. Especially, freeze-thaw resistance and carbonation are sensitive to these aspects.

The Ecosmart project has contributed to an increase in the average fly ash percentage in concrete from 15% in 1999 to 25% in 2002 in Canada. Demonstration projects have shown that 50% cement replacement by fly ash is profitable with regard to costs, execution and performance. However, it was also concluded that still political, technical and economical barriers remain. For the concrete, increased setting time, slower strength development, curing and uncertainties about freeze-thaw resistance are obstacles. Furthermore, the varying quality of the fly ash, the extra costs for transportation and storage, the colour of concrete surfaces and the lack of guidelines and standards might resist commercialization of high volume fly ash concrete.
(Bilodeau and Malhotra, 2000; Bilodeau, et al., 2001; Bouzoubaâ and Fournier, 2002; EBA, 2004; Joshi and Lohtia, 1997)

2.3.3 Green concrete, Dundee, Scotland

The green concrete project from the Concrete Technology Unit of the University of Dundee aimed at increasing the use of recycled materials and industrial by-products in concrete. Research was carried out to exploit the use of fly ash, conditioned fly ash, recycled concrete aggregate, incinerator ashes, recycled glass or granulated rubber in concrete. Research included testing of fresh concrete properties, strength development, modulus of elasticity, shrinkage, creep, chloride ingress, carbonation, sulfate resistance, freeze-thaw resistance, abrasion resistance and case studies. The project provided a route for increasing the level of confidence and awareness of these materials within the construction industry; however, it was also concluded that, currently, the percentage use of the recycled materials and by-products in concrete is not at a desired or sustainable level.

The main results from Dhir (2005) in relation to this thesis are on the cement reduction by using particle packing techniques. Models by Dewar (1999) and Larrard (1999) were used to minimize void contents. Cement contents were minimized by using fillers, cement additions attained from industrial by-products, and by using high range water-reducing admixtures. Table 2.5 shows mixture A6D with 175 kg/m^3 cement and 75 kg/m^3 fly ash reaching a 28-day characteristic cube compressive strength of 27 N/mm^2. Packing optimization improves strength, especially for mixtures with a low cement content as shown by reference series AR 1-4 compared to the optimized series AM 1-4. The tests prove that in concretes with a given water/cement ratio the cement content can be lowered while retaining similar strength. This is done by particle packing optimization and including filler and superplasticizer to retain the fines content and workability. For example, exchanging 50 kg/m^3 cement by filler at a water/cement ratio of 0.40, reduced the water content from 160 to 140 l/m^3 and cube compressive strength retained about 60 N/mm^2 for mixture A4R compared to mixture A3M. Furthermore, changes in the performance of other engineering properties when using particle packing techniques, different cement types and lower water and cement contents, are proportional to the changes in cube compressive strength. Accepted and assumed relations between engineering properties and compressive strength as used in most design codes are therefore valid.

(Dhir, et al., 2002; 2005)

Table 2.5 Mixture compositions [kg/m^3] and characteristic cube compressive strength $f_{ck,cube}$, with $k_{fa} = 1$ (Dhir, et al., 2005).

Mixture	Portland cement	lime stone filler	fly ash	aggregate sand	aggregate 5-10 mm	aggregate 10-20 mm	free water	*wbr* [-]	$f_{ck,cube}$ [N/mm^2]
A1R	250	-	-	835	390	785	160	0.64	34.5
A2R	300	-	-	755	400	805	160	0.53	46.5
A3R	350	-	-	705	400	800	160	0.46	49.0
A4R	400	-	-	670	395	795	160	0.40	59.0
A1M	250	55	-	655	435	870	140	0.56	48.0
A2M	300	25	-	630	440	880	140	0.47	52.0
A3M	350	25	-	545	455	905	140	0.40	61.5
A4M	400	35	-	440	475	950	140	0.35	65.5
A6D	175	30	75	590	355	1000	145	0.58	27.0

2.3.4 Ultrafine particles in concrete, Sweden

Ultrafine particles (< 10µm) were investigated to act as a cement replacing material by Lagerblad and Vogt (2004, 2006, 2010). Due to effective superplasticizers, it is possible to include large amounts of these fine particles in concrete and increase the strength. The ultrafine particles are presented to have an efficiency factor of 1, which means that the concrete does not loose strength when the cement is replaced (kg/kg) by ultrafine particles. Since different minerals have different influence on hydration properties the effect of various types of ultrafine particles on hydration, paste structure, shrinkage and strength has been investigated, such as silica fume, quartz, wollastonite and nepheline syenite rock. The incorporation of ultrafine particles accelerates the cement hydration. The effect increases with the fineness. The ultrafine particles become an integrated part of the hydrated cement paste and improve the homogeneity of the interfacial zone. A finer pore system is measured by mercury intrusion tests.

Table 2.6 28-day compressive strength of concrete mixtures with low cement contents including ultrafine particles. SF: silica fume, SP: PCE superplasticizer, dry content, M300 and M6000: quartz powder. (Vogt and Lagerblad, 2006).

Mixture	filler type	cement [kg/m^3]	water [kg/m^3]	filler [kg/m^3]	SF [kg/m^3]	aggregate [kg/m^3]	SP [kg/m^3]	*wcr* [-]	*wpr* [-]	strength [N/mm^2]
LCC1	M300+M6000	150	114	200	30	2009	5	0.76	0.3	70
LCC2	Quartz slurry	150	114	200	30	2010	5	0.76	0.3	60
LCC3	Quartz slurry	150	118	200	45	2010	7.8	0.79	0.3	68
LCC4	Quartz slurry	100	126	300	20	1855	4.2	1.26	0.3	38
LCC5	M300+M6000	60	150	350	60	1679	12.5	2.5	0.32	40
LCC6	M300+M6000	150	112	230	-	1976	5	0.76	0.29	60
LCC7	Quartz slurry	315	140	400	35	1576	9	0.44	0.25	102

Table 2.6 shows that mixture LCC6 with only 150 kg of cement per m^3 and no silica fume reaches a 28-day strength of 60 N/mm^2. The water/cement ratio is 0.76, which indicates that the traditional relationship between water/cement ratio and strength is no longer valid. With the optimized recipes it is possible to replace more than 40% of the cement and still obtain similar strength. The best effect is achieved, when the cement is replaced but the water/cement ratio is kept constant.
(Lagerblad and Vogt, 2004; Moosberg-Bustnes, et al., 2004; Vogt, 2010; Vogt and Lagerblad, 2006; Westerholm, et al., 2008)

2.4 Particle size optimization methods

For the design of ecological concrete various design methods are used. This section presents a general overview of design methods for concrete which aim at optimizing the particle size distribution.

2.4.1 Overview

The field of particle packing covers the selection of the right sizes and amounts of various particles. The particles should be selected to fill up the voids between large particles with

smaller particles and so on. In the history of concrete the concept of packing of aggregates already received interest in the 19th century. One of the first articles on the subject of particle packing for concrete production was published by Feret in 1892 (Feret, 1892). Most of the early researchers, working on packing of aggregates, proposed methods to design an ideal aggregate size distribution curve, like (Fuller and Thompson, 1907) and (Andreasen and Andersen, 1930). In that time also the first analytical packing models were designed to predict the voids ratio of a mixture of two particle groups (Furnas, 1929). In these two-component models interaction between particle groups was not yet taken into account. Extensive research by (Powers, 1968) on the interaction between different components in concrete mixtures contributed to particle packing knowledge. In that period, two-component models with interaction were formulated, such as the model by (Ben Aïm and Le Goff, 1967). The next development in the packing models was the extension to multi-component packing models including interaction, which are the models that are still used today, such as the model by (Larrard F. de, 1999). Since the introduction of the computer, several computer programs and modified models based on these analytical packing models have been released: *Europack* (Idorn, 1995), *RENÉ-LCPC* (lcpc.fr) and *4C-Packing* (dti.dk).

In the meantime, the availability of computers also started a new development in the field of particle size optimization: discrete element modelling. These simulation models started with placing particles or particle groups in a 2D area; however, computation speed increased explosively, which created all sorts of new possibilities such as 3D packing structures of non-spherical particles or simulations of flowing concrete.

Despite the development of these packing density models, concrete remains to be a conventional material and people producing concrete usually rely on practical experience and guidelines. For example, in most European standards aggregate distribution is determined by optimizing the mixture towards an ideal grading curve or within a given grading area, which has proven to deliver good concrete mixtures. For that reason the Fuller curve is still famous and various researchers still use the same concept when designing concrete mixtures. This does not mean the optimization curve has not changed over the last hundred years. The most important development was the implementation of the minimum particle size by Funk and Dinger in 1980 (Funk, et al., 1980). Furthermore, several researchers proposed different values for the exponent in the equation in order to adjust the curve for self compacting concrete or high performance concrete.

Especially the last decade, particle size optimization has gained new interest since the introduction of new types of superplasticizers for the design of high performance concrete and other concrete types with high amounts of fillers. Also for ecological concrete particle size optimization is very important, because the highest particle packing density of the aggregates will lead to the lowest amount of voids to be filled with cement paste. In this way a lean cement mixture can still achieve sufficient strength (Johansen and Andersen, 1991). The particle size optimization methods can be divided into three groups:

- *Optimization curves*. Particle groups are combined in such a way that the total particle size distribution of the mixture is closest to the optimum curve. (Section 2.4.2)
- *Particle packing models*. These models are analytical models which calculate the overall packing density of a mixture based on the geometry of the combined particle groups. (Section 2.4.3)
- *Discrete element models*. This type of computer models generate a 'virtual' particle structure from a given particle size distribution. (Section 2.4.4)

2.4.2 Optimization curves

Since Feret in 1892 put forward that the choice of aggregates influences concrete strength, many researchers tried to find the ideal grading curve. In this area the best known researcher is Fuller with his famous Fuller curve (Fuller and Thompson, 1907). Mix design calculations based on his curve are still used today. The Fuller curve is described by (Talbot and Richart, 1923) as Equation 2.4 with $q = 0.5$. See also Figure 2.5.

Some researchers tried to improve this curve, like (Andreasen and Andersen, 1930). They proposed the use of an exponent q in the range of 0.33 – 0.50, Equation 2.4. This adjustment factor q had to be determined experimentally and therefore can differ depending on the characteristics of the particles. With angular coarse particles the ideal curve would be best prescribed with a lower q or in other words more fine particles should be added to fill the voids between the coarse particles (Kumar and Santhanam, 2003).

$$P(d) = \left(\frac{d}{d_{\max}} \right)^q \tag{2.4}$$

In 1980 Funk and Dinger recognized that any real size distribution must have a finite lower size limit $d_{\min}$ (Funk and Dinger, 1994). So in contrast to the Fuller curve their ideal size distribution not only pays attention to the largest grain but also to the smallest used grain. For that reason the fine range is better represented. Andreasen's equation was modified into in Equation 2.5. They proposed an adjustment factor of $q = 0.37$ for optimum packing.

$$P(d) = \frac{d^q - d_{\min}{}^q}{d_{\max}{}^q - d_{\min}{}^q} \tag{2.5}$$

The curves presented should lead to the mixture with the highest packing density when optimal amounts of differently sized particles are combined. However, these curves are based on the fact that if a wider range of particles is used, this would lead to a higher packing density without taking into account the particle shape. Particle shape greatly influences the resulting packing density, especially, when particles of several size classes, with varying particle characteristics, are used (Walker, 2003; Zheng, et al., 1990). For that reason, Zheng et al. tried to solve this problem by determining q as the average of all q -values for each size class with varying particle shape. (Peronius and Sweeting, 1985) presented an equation for calculating the porosity of mixtures, depending on the,

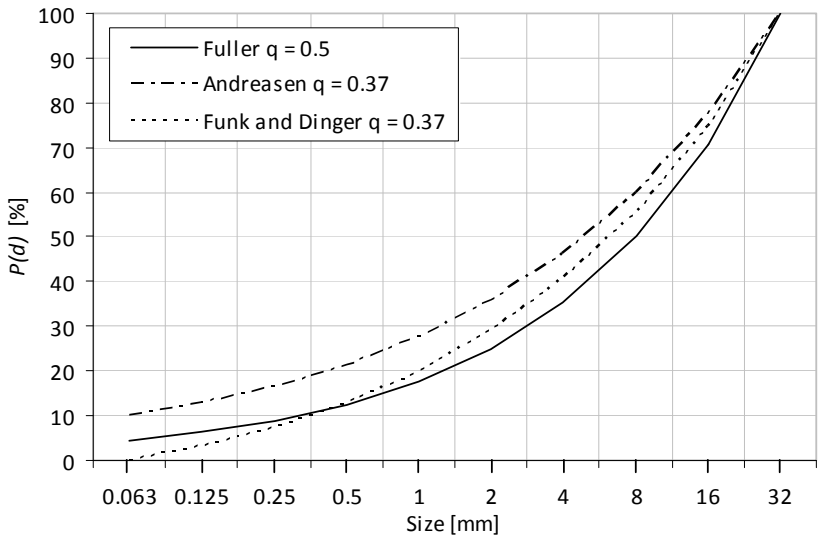

Figure 2.5 Ideal packing curves according to Fuller, Andreasen and Funk and Dinger for a maximum particle diameter of 32 mm and a minimum particle diameter of 63 µm.

roundness of the particles and the deviation from the Fuller curve. Other researchers, such as (Brouwers and Radix, 2005; Garas and Kurtis, 2008; Hunger, 2010; Kumar and Santhanam, 2003; Vogt and Lagerblad, 2006) used the model by Funk and Dinger to optimize their concrete mixtures by adjusting the q -value based on their experimental results or the required workability.

Optimizing to a curve is easy to use and requires only a limited amount of input parameters. When the q factor is fixed, only the particle size distributions of the available materials are necessary to optimize a concrete mixture. Commercial computer programs such as *EMMA* (concrete.elkem.com) are available. However, particle characteristics like shape or packing density are not taken into account. The output of the model is an optimized particle size distribution, which is not inevitably the mixture with the highest packing density. For instance, Palm and Wolter (2009) and Stroeven et al. (2003) show that the application of gap graded mixtures can lead to higher packing densities.

Optimization curves are continuous particle size distributions based on geometrical considerations. Andreasen and Andersen (1930) started with the assumption of a similarity condition which has to be fulfilled as the particles and their environments increase in size. In this way a change of size scale should not affect the packing density of the system. Funk and Dinger (1994) demonstrated that this concept for continuous particle size distributions corresponds closely to the packing of multiple monosized particle groups as described by Furnas (1931). However, they were not convinced the two methods are actually related (Funk and Dinger, 1994, pp 76). In 2006 Brouwers demonstrated that the theories on discrete (section 2.4.3) and continuous (section 2.4.2) packings are related mathematically and are actually complementary for packings consisting of multiple particle groups with the same monsized packing density (Brouwers, 2006).

2.4.3 Particle packing models

Particle packing models are based on mathematical equations prescribing how particles of different size interact geometrically. The models calculate the theoretical packing density of a mixture based on its particle size distribution and the packing density of the particle groups. The basic mathematical equations of almost all particle packing models are the same and purely based on the geometry of the particles. The equations prescribing the

packing density were first introduced by Furnas (1929). They are valid for two monosized groups of particles without interaction between the particles. Either the large particles are dominant and small particles fit in their voids or the small particles are dominant and large particles are embedded in a matrix of small particles.

Since the equations depend on the particle packing and amount of particles of the monosized groups, they are valid for any type of particle and automatically include particle characteristics such as shape and texture, as long as the particles preserve their shape during packing. However, the equations do not take into account interaction between the particle groups. Westman and Hugill (1930) developed an algorithm that used discrete theory of packing, which could already be used for multiple particle groups without interaction. Particle interaction was acknowledged, but the model did not yet take into account interaction between particle groups. In 1931 Furnas published a method to calculate maximum packing density of multiple particle groups as well as an equation to describe the effect of interaction between two different size classes on the maximum packing density (Furnas, 1931). Ben Aïm and Le Goff (1967) implemented the interaction of large particles on the packing density of small particles into the Furnas model. Later this particle interaction effect became more generally known as the wall effect. On the other hand, Reschke (2000) presented in his thesis the model by Schwanda (1966) which already incorporates both interaction of large particles on small particles and interaction of small particles on large particles.

The next step in improving particle packing models was the extension to multiple particle groups. Toufar et al. (1976), Stovall et al. (1986) and Yu and Standish (1987) combined the basic equations from Furnas, while Dewar (1999) came up with a concept where smaller particles are packed in the voids of larger particles and so on. This way, the particle packing models are suitable to calculate the packing density of concrete based on a particle size distribution. The input parameters are the packing density and particle size distribution of the particle groups used in a concrete mixture. The output of a packing model is the theoretical packing density of the mixture. For mixture optimization, the packing density of several mixture compositions has to be determined until the maximum packing density is found. A more detailed review of analytical multi component particle packing models is presented in chapter 3. A suggestion for further reading on particle packing models is to start with the overviews by (Funk and Dinger, 1994; Goltermann, et al., 1997; Johansen and Andersen, 1991; Kumar and Santhanam, 2003). For further information on packing density modelling or the use of packing density models reference

is made to (Abdel-Jawad and Salman Abdullah, 2002; Ball, 1998; Bonneau, et al., 2000; Fedors and Landel, 1979; Hoffmann and Finkers, 1995; Hwang and Tsai, 2005; Lee, 1970; Lees, 1970; Mahmoodi Baram, 2005; McGeary, 1961; Miyajima, et al., 2000).

2.4.4 Discrete element models

Discrete element models generate a 'virtual' particle structure from a given particle size distribution. In the earliest models, once a particle was placed, its position would not change anymore. In these static simulations usually particles are randomly positioned in a defined space, starting with the largest particles. The result is a three dimensional space filled with particles of different sizes, which usually do not have contact with each other. Because of this, the result is officially not a packing or packing structure. Examples of models using static simulations are the hymostruc model (citg.tudelft.nl) or the model used by Zheng and Stroeven (1999) with which e.g. the distribution shown in Figure 2.6, left hand side, was generated.

With increasing computational speed, the models evolved to dynamic models in which all particles can move. Particles are generated and move because of forces acting on the particles. For instance, particles fall due to gravitation, but are stopped or bounce back as soon as they meet a boundary or another particle. In this way, the resulting packing

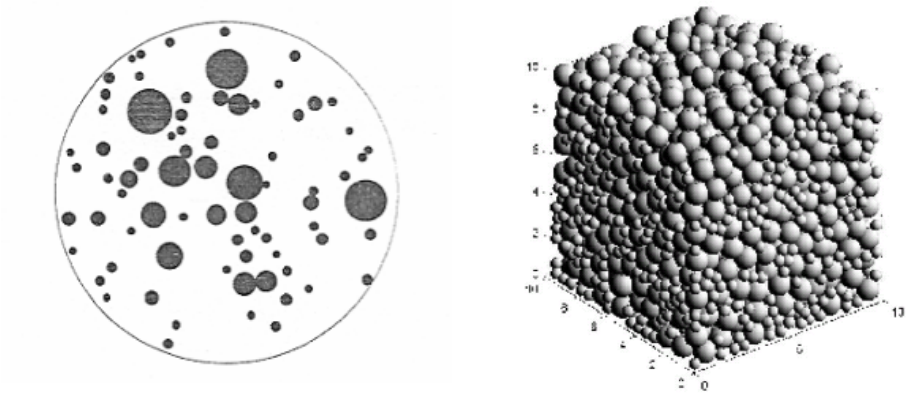

Figure 2.6 Discrete element models creating a particle structure without particles touching each other (left hand side (Zheng and Stroeven, 1999)) or a stable particle structure (right hand side (Fu and Dekelbab, 2003).

corresponds to a random loose packing. A disadvantage of this simulation type is, that the resulting packing structure does not have the highest possible packing density that can be achieved with the given particle size distribution (Fu and Dekelbab, 2003). To solve this, some models generate particles in a container and than decrease the container volume (Stroeven and Stroeven, 1999). Other models allow particles to overlap initially and then rearrange the particles while enlarging the container size until no particles overlap (Kolonko, et al., 2008).

The result of each simulation is a virtual particle structure in which the size, the shape and the location of all particles are known, see also Figure 2.6 right hand side. In this way, the virtual structure can be used to assess random particle packing. Packing density can be calculated from the total occupied volume in the container; however, the particle structure contains much more information. It can be used to evaluate for instance the resistance to external loads (Snoeijer, et al., 2003) or the number of contacts between particles. Also it is possible to simulate flowing concrete such as in a slump flow measurement (Gram and Silfwerbrand, 2007; Roussel, et al., 2007).

To find the mixture composition with the highest packing density, several mixture compositions should be simulated, which is very time consuming. Especially with broader particle size distributions, computational time increases with hours, because of the high amount of small particles in the mixture. Some researchers like (Kolonko, et al., 2008) solve this problem by making use of a stepwise approach in which small particles are packed and then serve as a matrix between larger particles. However, this leads to an increase of the input parameters, which already consist of not only particle size distribution, container size and/or the amount of particles, but also include several model parameters such as gravity, density, damping, elasticity, shear, friction and particle contact.

The differences between the several discrete element models are not further elaborated in this thesis. For further information on discrete element modelling and the use of discrete element models to similute concrete behaviour reference is made to (Chu and Machida, 1998; Jiao, et al., 2008; Mechtcherine and Shyshko, 2007; Puri and Uomoto, 1999; Stroeven, et al., 2006; wikipedia.org; Wouterse, 2008).

2.5 Concluding remarks

Ecological concrete, as defined in this research project, comprehends all concrete mixtures containing a cement content below 260 kg/m^3 and within strength class C20/25. The mixtures should be based on either a Portland cement or a binder activated by Portland cement combined with fillers. Here, silica fume is not taken into account. Research results regarding the use of fillers in concrete show large variations, probably caused by varying research parameters such as testing of cement paste, mortar or concrete or the type and amount of superplasticizer used. In general, the literature study shows that adding inert fillers or binders to concrete will lead to improved workability due to a decreased water demand. Also when the water/cement ratio is decreased, fast hydration and dense microstructures are reported, for fillers as well as for binders. This leads to higher strength and durability. However, when cement is replaced by fillers also loss of workability is reported and in concretes with increased water/cement ratio the cement matrix becomes less dense. Therefore, replacing cement requires attention on the filler type and amount but also on the production process, by for instance increasing the curing time. The filler should be suitable with regard to water demand and workability. Especially size, but also shape and texture are demonstrated to be important for workability as well as for strength. Furthermore, some results or theories valid for self-compacting concrete, such as the water layer theory, might not be valid in ecological concrete with low amounts of paste and increased particle friction. While at the same time it is even more important to control the water demand of the ecological mixtures, because the low cement content might otherwise lead to very high water/cement ratios.

Ecological concrete projects from all over the world have shown that it is possible to design strong and durable concrete with cement contents below 260 kg/m^3. With ultrafine filler a mixture with only 150 kg/m^3 cement can even reach a strength of 60 N/mm^2 in 28 days. In most projects particle size optimization techniques are used. However, since aggregates and fillers differ from country to country also a lot of trial and error mixing remains. One of the reasons for that might be the utilization of optimization curves. The ideal particle size distribution depends on the particle type, wherefore it varies with each type of concrete. For instance, when rounded sand is combined with coarse recycled aggregates, the optimal particle size distribution will differ from one of a mixture with angular sand and rounded coarse aggregates. Therefore, an ideal optimization curve does

not inevitably lead to the mixture with the highest packing density. For ecological concrete this high packing density is important to reduce the cement paste and water content. Particle packing models and discrete element models can calculate the maximum packing density of concrete mixtures; however, due to limitations in computational speed discrete element models are not yet suitable for concrete mixture optimization. This is because the simulation of one mixture with a broad particle size distribution requires several hours while numerous mixtures have to be evaluated to find the optimal composition. Therefore, at this moment analytical particle packing models provide the best solution for ecological concrete mixture optimization. Chapter 3 will focus on particle packing and the differences between the existing particle packing models. Since ecological mixtures differ depending on the available components like filler and aggregates, a design method based on particle packing density is beneficial for all ecological concrete design.

3 Evaluation of particle packing models

In this chapter different particle packing models are analysed mathematically. Section 3.1 first gives background information on particle packing density and the influence of particle characteristics on the packing density and particle structure. This information is used to evaluate particle packing models for the design of ecological concrete. In sections 3.2 to 3.8 particle packing models currently used in research projects or commercially available programs are described. Each model or method is evaluated with regard to input parameters, user friendliness and practicability of the output, especially in relation to the main factors for ecological concrete design as found in chapter 2. Furthermore, the mathematical basis and adaptability with regard to particle characteristics, interaction and compaction are important, especially when new requirements from ecological concrete design (resulting from chapter 4) have to be implemented. In section 3.9 one of the models is chosen for further development in chapter 5.

3.1 Particle packing

3.1.1 Packing density

Particle packing describes to what degree a unit volume is filled up with particles. It is usually measured in terms of packing density α [-], which is defined as the ratio of the solid volume of the particles V_p to the bulk volume occupied by the particles V_b, Equation 3.1.

$$\alpha = \frac{V_p}{V_b} = \frac{\rho_{bulk}}{\rho_p} \tag{3.1}$$

Voids content or porosity ε is the volume of voids between the particles divided by the bulk volume occupied by those particles. From the packing density α the voids content ε may be obtained by Equation 3.2.

$$\varepsilon = 1 - \alpha \tag{3.2}$$

The dry packing density of particles can be measured by filling a container with particles, subjecting the particles to prescribed compaction and weighing the mass of the particles m_p [kg] in the container as prescribed in (NEN-EN 1097-3:1998), Equation 3.3.

$$\alpha = \frac{m_p}{\rho_p V_{container}} \tag{3.3}$$

The packing density of the particles in ecological concrete is important because a lower voids content of the aggregates will lead to a smaller amount of cement paste and a lower voids content of the particles will reduce the water demand. In concrete the packing density of the aggregates may vary from 0.55 to 0.80. In the hardened state the cement paste fills up the spaces in the aggregate structure to ‘glue’ the constituents of concrete together.

Filling up the voids by small particles improves the packing density and contributes considerably to the interparticle friction of the mixture. The mixture becomes stronger and stiffer, which is good for the concrete properties in the hardened state, but workability may suffer. Therefore, in the fresh state, the cement paste not only needs to

fill up the voids between the particles, but an excess amount of cement paste is needed to lubricate the concrete mix and give the mix sufficient workability. If there is no excess amount of paste, fillers would only fill the voids between the large particles, thereby decreasing the space available for passage and increasing interparticle friction, thus decreasing workability. Therefore, concrete producers and engineers have been and still are trying to improve the particle packing and particle size distribution of concrete.

3.1.2 Particle characteristics

This subsection describes the influence of various particle characteristics on the packing density and the packing structure. Chemical, mineralogical, morphological and physical properties are influenced by the origin of a particle. Furthermore, chemical or mineralogical properties influence the morphological properties, for instance when the surface texture or shape is changed by abrasion. This means the origin and composition of a particle have a significant but indirect influence on the packing density. Only the characteristics directly influencing packing density are presented in this subsection. The influence of interparticle forces, caused by chemical and mineralogical properties, is described in the next subsection.

Density

Generally, the density of a material has no significant influence on its packing density. Particles of an equal size and shape will pack to the same packing density in spite of varying theoretical densities (German, 1989). However, when two or more materials with different densities are packed together, segregation can occur due to the difference in density. Density of materials can be measured by e.g. (NEN-EN 1097-6:2000). Attention should be paid to the particle porosity, since open pores will decrease packing density and increase water demand by water absorption. Closed pores will only lead to a lower particle density.

Particle size and size distribution

For a packing composed of large particles, the absolute particle size is not important for the packing density. However, for smaller particles, below approximately 100 µm, packing

density decreases due to an increase in the surface area, a lower particle mass, and a greater significance of short-range, weak forces (German, 1989). In general, packing density is improved if smaller particles fill the voids between larger particles. For this reason, packing density of a uniform distribution increases if the distribution becomes wider (German, 1989). But not only the size range of a distribution influences the optimal packing, so does the distribution itself. For instance too much small particles or particles too large to fill voids will push larger particles away from each other, thus influencing packing density, Figure 3.1. Packing density of a uniform distribution will increase most by adding some large particles. This is because the space occupied by the larger particle does not contain voids anymore and therefore in total more volume is occupied by particles. Adding small particles to a uniform distribution can either increase or decrease packing density. Since angular particles can pack less dense than round particles, the optimal size distribution for the highest packing density always depends on the characteristics of the different fractions used. (Peronius and Sweeting, 1985)

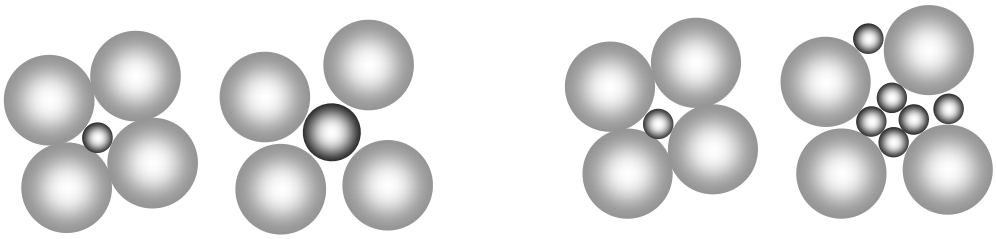

Figure 3.1 Relative size and relative amount of particles influence packing density.

Shape

Shape can be expressed by three properties: overall shape, roundness and surface texture (Barret, 1980). Overall shape relates to particles with varying sizes in one, two or three dimensions, like elongated, flat or spherical particles. Packing density decreases when more particles deviate from spherical to flat or elongated. Roundness is usually expressed as rounded, sub-rounded, sub-angular or angular. Roundness or sharpness of the corners is important when considering the abrasive and crushing resistance of particles, while convexity is more important when considering the interlocking ability and packing density of the particles. The third property surface texture is described as very rough, rough,

smooth or polished. These three properties are geometrically independent, although there may be natural correlation between them because of the common physical factors affecting them (Kwan and Mora, 2001).

During particle mixing, more irregular particle shapes will interfere with the mixing, but will also help to maintain a homogenous mixture by complicating segregation. In the same way polished spherical shapes minimize interparticle friction, thereby increasing packing density. High packing is achieved because the rounded particles produce a more workable mix, which requires less compaction energy to achieve its maximum packing density. Angular rough particles contribute to a stronger and more stable particle structure with a lower packing density. In concrete the surface texture relates also to the adhesion of cement matrix to the aggregate. The bond between the cement matrix and natural rough particles is very good, while polished particles and the cement matrix have a weak connection. With a mixture of spherical and irregular particles, the packing density of the spheres is not significantly degraded by the irregular particles until the mixture contains approximately 10% of irregular particles. Thus, the addition of irregular particles may not harm packing density for spheres, yet may improve compact strength by providing more interparticle friction (German, 1989).

Stability

The particle packing density is influenced by the ability of the particles to preserve their shape. Factors influencing a constant shape are elasticity or resilience, thermal properties and durability properties. When particles change shape during packing operations or throughout the lifespan of the packing structure, this influences packing density. Highly elastic particles pack closer because they can deform but the resulting packing structure is less stiff. Furthermore, resilience, which is the ability of a particle to rebound at impact, can cause higher or lower packing density depending on the way of deposition. Volume changes of the particles due to temperature variation can demolish the packing structure.
Particle durability is the ability to resist for instance crushing, degradation, disintegration or damage from freeze-thaw cycle. Particles damaged by one of these mechanisms change the intended packing density because in time more fine particles appear.

Wettability and adhesion

Wettability and adhesion influence the packing density and strength of a particle structure in moist and wet conditions, especially for smaller particles. Wettability refers to the affinity of the particles for a liquid. It depends on the absence of a bond-breaker on the surface of the particle, like pollution or clay, and on the electro-chemical compatibility of liquid and particle. The electro-chemical wettability depends on the surface energy of the particle and thus on its chemical composition. This can be shown by the variety in the contact angle of a drop of water on the surface of different particles. Also surface polarity can influence wettability. Surfaces of granites are usually negatively charged.

Furthermore, adhesion plays an important role in the combined packing structure of particles and a liquid. Adhesion refers to the mechanical and chemical bond of the liquid to an individual particle. The chemical bond can result from the basic minerals of the particles reacting with minerals present in the liquid. The mechanical bond is related to surface texture, porosity, particle size and surface area of the particle (Creegan and Monismith, 1996). High amounts of open pores and the related rougher surface texture increase liquid demand, but result in a stronger bond between the liquid and the particles (Reschke, 2000).

3.1.3 Particle forces

Packing density in concrete is usually dominated by gravitation and shear forces between the particles, which are in turn dependent of particle characteristics like shape, size and density. Furthermore, the deposition and applied compaction energy, interparticle forces and the use of water and superplasticizer influence the packing density.

The effective compaction energy depends on the way the particles get packed. The achieved packing density depends on whether particles are only placed or also mixed and vibrated. Softly pouring will deliver loose bulk density with a high amount of voids. The packing density can be increased by adding energy. When a loose packing structure is vibrated, it will pack closer together under its own weight. Vibrating causes voids to open up and surrounding particles fill up these opened voids because of gravitational forces working on them. When a packing structure is not only vibrated but also subjected to an external load helping gravitation, the packing density will become even closer.

For small particles the surface forces become increasingly important. These are traditionally not considered in packing programs because for coarse particles external

forces like gravity and mechanical impact surpass the surface forces in effect (Yu, et al., 2003). However, for small particles the surface area to volume ratio is higher, which makes the attractive surface-related forces between particles dominant over the volume related gravitation per particle. Therefore, surface forces begin to play a part for particles smaller than 1 mm (Reschke, 2000). The most important surface forces influencing packing density are the van der Waals force, electrical double layer force and steric forces. When polymers adsorb on a small particle, the adsorbed layer induces a steric hindrance of the particles to approach each other. Depending on the size of the adsorbed layer, the particles will be partly or fully stabilized by the polymers, as a result of which agglomeration will be prevented. The van der Waals force is always attractive between materials that are alike. It arises from the interaction of atomic and molecular electric dipoles (Kjeldsen, 2007). The van der Waals force is significant for particles below 0.05 µm in size (German, 1989; Gray, 1968). An electrical double layer can be formed with particles in a solution: electrostatic charged particles form, with surrounded ions of the opposite sign, an electrical double layer in which the charge is being balanced. This creates a repulsive force in the solution around the particle. The summed-up attractive surface forces can cause particles to agglomerate. The solution to this problem is to modify the surface forces by, for example, adding surface active agents.

In concrete the use of water and superplasticizer influences the surface forces between the particles. The presence of a liquid between coarse particles influences especially the interparticle friction. However, for smaller particles this interaction becomes increasingly complex, due to the increased role of the surface forces. For example, water not only reduces interparticle friction, it can cause an increase in surface stickiness. This surface stickiness will decrease the packing density of small particles since gravity has relatively little impact compared to the 'sticky' surface forces. Packing density is therefore influenced by the wettability and adhesion of the particles, but also by the amount of water present in the mixture. When particles are wetted slowly, liquid or condensed vapor gather at the particle contacts and form bonds between particles, Figure 3.2a. The strength of the pendular bond increases with the liquid-vapor surface energy and depends inversely on the square of the particle diameter. At less than total saturation, the strength of the bond between the particles increases with the amount of liquid and the surface energy of the liquid, Figure 3.2b. The absence of internal liquid vapor surfaces at 100% saturation causes the strength between the particles to suddenly decrease at this point,

Figure 3.2c. In most concrete mixtures voids are fully saturated and capillary forces are negligible.

Optionally, superplasticizers can be used to reduce interparticle friction, for instance by lubricating surfaces via short range repulsive forces, which improves the flow and packing of particles. The level of improvement depends on the molecular size of the additive, its polar character, the layers of coverage, the particle surface condition, the particle size and the temperature (German, 1989).

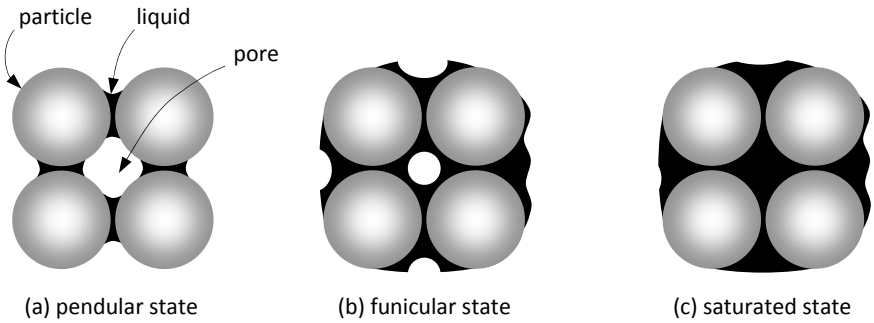

Figure 3.2 The states associated with agglomeration of powders due to a wetting liquid: (a) pendular state with capillary bridges localized at particle contacts, (b) funicular state in which pendular bonds merge, but pores are not completely filled with liquid (There is a connected path between both the liquid phase and the pores.), and (c) saturated state in which the pores are fully filled with water. After (German, 1989).

3.1.4 Particle structure

Due to the combination of forces working on the particles as discussed in the previous section, particles move away from each other or stick to each other, thus forming a particle structure. This means that within a randomly packed structure several effects can occur which influence the packing density over a distance larger than one or two particle diameters.

Wall effect

Close to a container wall a random packing is forced to some kind of ordered packing. Depending on the packing structure and container shape, it takes from one to ten particle diameters from the wall to establish truly random packing. Since the container wall can be seen as a very large particle, its characteristics influence packing in the same way as the particle characteristics described in 3.1.2. The wall effect is larger at higher packing densities and with smoother, flatter or monosized spherical particles, giving local regions of oscillating high and low porosity in the first few particle layers near the wall, Figure 3.3.

Agglomeration

Agglomeration is caused by the cohesive forces between the particles. With small particles these cohesive forces such as van der Waals attraction, electrostatic charges and chemical bonding can be larger than the forces breaking up the agglomerates such as gravitation and shear. This causes small particles to cluster. The agglomerate size depends on the size and size distribution of the particles, the shape and surface roughness, the wettability of the particles and the viscosity and distribution of the liquid as presented in Figure 3.2 (Schaafsma, et al., 1998). Agglomeration makes mixing and compacting more difficult and

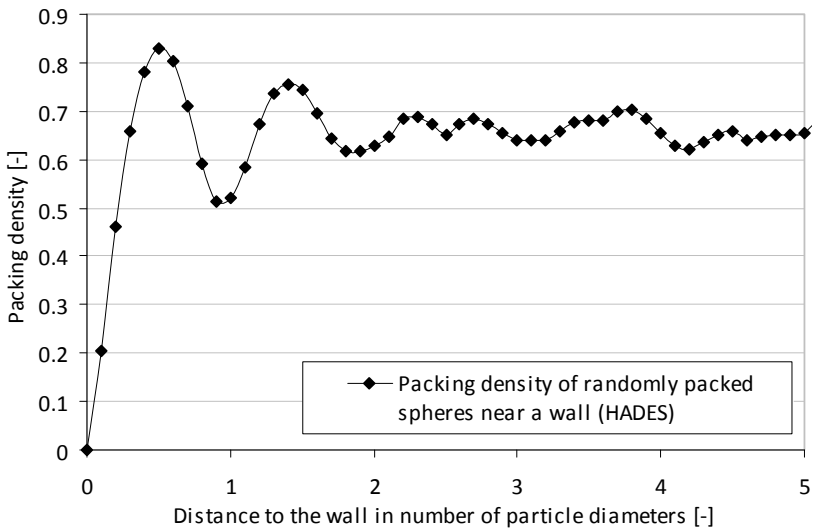

Figure 3.3 Wall effect of randomly packed monosized spheres, simulated with HADES.

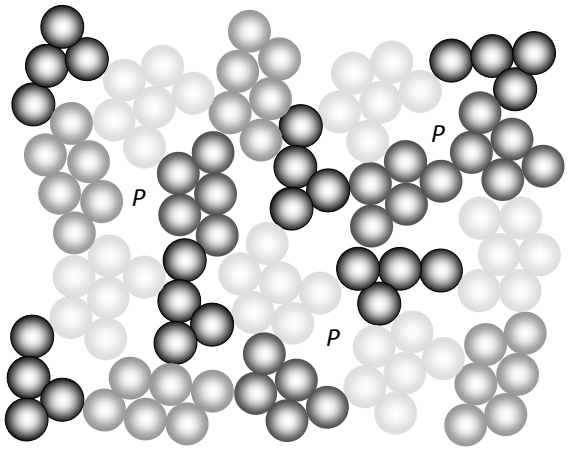

Figure 3.4 Agglomeration of particles decreases packing density, because of high porosity regions (P) between the agglomerates.

lowers packing density. This is because the particles cluster into agglomerates with a high amount of particle contacts. However, the agglomerates themselves are separated by high porosity regions, Figure 3.4. Agglomerates can be (partly) broken by applying sufficient mixing or compaction energy or by using effective superplasticizers. A thin coating of polar molecules creates surface repulsive forces, which reduces the interparticle friction between cohesive particles.

Segregation

Segregation is caused by variations in particle sizes, densities and shapes. Larger, heavier particles are subjected to higher gravitational forces, which can lead to a disharmoneus packing structure. Furthermore, size segregation can be caused by vibration. Through vibration local voids between particles open up, making it more likely for the small particles to fall by gravitation into these voids. Irregular particle shapes and high interparticle friction (small cohesive particles) decrease the tendency of a mixture to segregate.

An irregular particle shape will prevent size segregation and less segregation occurs with smaller particle sizes because of the greater interparticle friction. Segregation leads to point to point variations in the packing density and a decreased overall packing density.

Arch building

Arch building is the creation of an arch by a number of particles. These arches can create large pores in the region underneath the arch and thus lower packing density. Non-spherical particles, especially angular shapes, will increase the tendency of a powder to build arches. Furthermore, arch building increases with smaller particles and sticky or cohesive surfaces. It is also more likely to occur near the container wall. Large pores underneath an arch can be eliminated by vibration.

3.2 The Furnas model

The Furnas model (Furnas, 1929) is only valid for two groups of monosized particles without interaction between the particles ($d_1 \gg d_2$). However, since most current models are based on this model, the mathematical equations are presented in this section.

By definition the volume of each monosized particle class can be expressed in its partial volume φ_i , which is the volume occupied by size class i in a unit volume. Furthermore, the relative volume of each size class can be expressed as its volume fraction r_i, Equations 3.4 and 3.5.

$$r_i = \varphi_i \Big/ \sum_{i=1}^{n} \varphi_i \tag{3.4}$$

$$\sum_{i=1}^{n} r_i = 1 \tag{3.5}$$

With only one size class $r_1 = 1$ and the partial volume of this size class (φ_1) is equal to the total occupied volume or total packing density α_t. When there are two size classes present, the following two cases can be distinguished.

Case 1: The volume fraction r of the large particles is much larger than the volume fraction of the small particles ($r_1 \gg r_2$).

Small particles (diameter d_2) can be added to a container filled with large particles (diameter d_1). By adding the small particles into the voids between the large particles, the voids are filled and thus the total occupied volume and the packing density

increase. The total volume occupied by particles in a container is expressed by Equation 3.6. In this case the total packing density equals the volume of the large particles (which is restricted by the maximum packing density of the large particles) plus the volume of the small particles, in a unit volume.

$$\alpha_t = \varphi_1 + \varphi_2 = \alpha_1 + \varphi_2 \quad \rightarrow \quad \alpha_t = \frac{\alpha_1}{1 - r_2} = \frac{\alpha_1}{r_1} \tag{3.6}$$

Case 2: The volume fraction of the small particles is much larger than the volume fraction of the large particles ($r_2 \gg r_1$).

Large particles can be added to a container filled with a matrix of small particles. By adding some large particles into a matrix of small particles, the large particles fill up the volume they occupy by 100%. Their contribution to the packing density is therefore equal to their partial volume φ_1. The small particles can fill up the rest of the unit volume ($1 - \varphi_1$) with their maximum packing density as expressed in Equation 3.7. In this case the total packing density equals the volume of the large particles plus the remaining volume filled with the maximum amount of small particles (which is restricted by the maximum packing density of the small particles), in a unit volume.

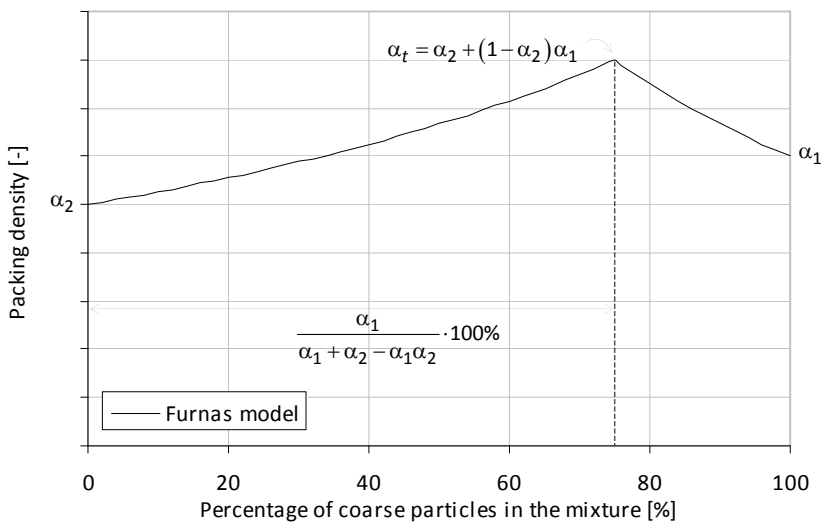

Figure 3.5 Packing profile of two monosized particle classes ($d_1 \gg d_2$).

$$\alpha_t = \varphi_1 + \varphi_2 = \varphi_1 + \alpha_2 (1 - \varphi_1) \quad \rightarrow \quad \alpha_t = \frac{1}{r_1 + (r_2/\alpha_2)} \tag{3.7}$$

The maximum packing density can directly be derived from the equations as presented in Figure 3.5.

3.3 The Toufar and modified Toufar model

Toufar et al. (1976) described a model to calculate the packing of binary mixtures for diameter ratios 0.22 < d_1/d_2 < 1.0. The concept of the model is that for diameter ratios > 0.22 the smaller particles with diameter d_1 will actually be too large to be situated within the interstices between the larger particles with diameter d_2. Therefore, the packing density should depend on the diameter ratio of the two particle classes, as expressed by the factor k_d. Furthermore, Toufar et al. considered the statistical probability of the number of interstices between the coarser particles that are free from smaller particles. It was assumed that each of the fine particles is placed between exactly four of the coarse particles, which led to the factor k_s. The total packing density is described by Equations 3.8-3.11 (Goltermann, et al., 1997).

$$\alpha_t = \frac{1}{\frac{r_1}{\alpha_1} + \frac{r_2}{\alpha_2} - r_2\left(\frac{1}{\alpha_2} - 1\right) k_d k_s} \tag{3.8}$$

$$k_d = \left(\frac{d_2 - d_1}{d_1 + d_2}\right) \tag{3.9}$$

$$k_s = 1 - \frac{1 + 4x}{(1 + x)^4} \tag{3.10}$$

$$x = \frac{r_1}{r_2} \frac{\alpha_2}{\alpha_1 (1 - \alpha_2)} \tag{3.11}$$

Without interaction $k_d = 1$ and the packing density corresponds to the Furnas model for $r_1 \gg r_2$ and $r_1 \ll r_2$. However, later comparisons with tests show that this model predicts that the packing density of a sample of coarse particles does not increase when a small

amount of fine particles is added to the coarse particles. This is due to the assumption that each fine particle is placed in a space, which is limited by four of the coarse particles. This unrealistic behavior was corrected by introducing a modification in the k_s -expression as presented in Equations 3.12 and 3.13.

$$k_s = \frac{0.3881x}{0.4753} \qquad \text{for } x < 0.4753 \tag{3.12}$$

$$k_s = 1 - \frac{1+4x}{(1+x)^4} \qquad \text{for } x \geq 0.4753 \tag{3.13}$$

Both the original Toufar model and the modified model can be used for estimating the packing of a multicomponent system by Equations 3.14-3.17 (Johansen and Andersen, 1991).

$$r_{i-j} = \frac{r_i r_j}{1 - r_i} \tag{3.14}$$

$$r_{ij} = r_{i-j} + r_{j-i} \tag{3.15}$$

$$\alpha_{ij} = \frac{1}{\dfrac{\left(r_{i-j}/r_{ij}\right)}{\alpha_i} + \dfrac{\left(r_{j-i}/r_{ij}\right)}{\alpha_j} - \left(r_{j-i}/r_{ij}\right)\left(\dfrac{1}{\alpha_j} - 1\right) k_{d(ij)} k_{s(ij)}} \tag{3.16}$$

$$\alpha_t = \frac{1}{\sum_{j=2}^{n} \sum_{i=1}^{j-1} \dfrac{r_{ij}}{\alpha_{ij}}} \tag{3.17}$$

However, calculating the packing density of multi-component mixtures according to this procedure tends to underestimate the packing density. The deviation from the expected packing density increases with the number of size classes. This is best shown by comparing a two-component mixture with the same mixture but then split up into more size classes. Table 3.1 shows that a mixture divided into more size classes leads to a lower predicted packing density by the Toufar model, though the mixture physically remains the same.

Table 3.1 Comparison of packing density calculations with the Toufar model for one mixture split up in two or more size classes with $\alpha_i = 0.6$.

volume r_i	size d_i
0.5	1
0.5	2

2 classes:

$\alpha_t =$ **0.640**

volume r_i	size d_i
0.25	1
0.25	1
0.5	2

3 classes:

$\alpha_t =$ **0.636**

volume r_i	size d_i
0.25	1
0.25	1
0.25	2
0.25	2

4 classes:

$\alpha_t =$ **0.626**

In the *Europack* computer program (Idorn, 1995) this problem is solved by a stepwise calculation procedure. The program uses Equations 3.8-3.13 to calculate binary packing densities. For three size classes, first, the two classes with the highest d_1/d_2 ratio are combined. Their mutual packing density is calculated together with their new average diameter. This results in a new particle group which then is used to combine with the third size class in the next calculation step. However, this procedure results in diverging packing densities for mixtures with constant aspect ratios d_1/d_2 when α_t is calculated as a mixture of two large size classes combined with one fine size class or as a mixture of two small size classes combined with one large size class.

The Toufar model can predict the packing density of a mixture consisting of two monosized particle classes. The calculation includes the size and amounts of particles in the mixture. Shape effects are indirectly taken into account via the packing density of the size classes and Equation 3.13. However, the calculation procedures are not suitable to extend to a high amount of size classes as is required for the design of ecological concrete including fine fillers.

3.4 The Dewar model

The concept behind Dewar's particle packing model (Dewar, 1999) is that when two particle groups are mixed, the smaller particles will fill the voids between the larger particles, while the entire particle structure is influenced by particle interference. This will result in a particle structure with a voids ratio *U*. The voids ratio is related to the porosity ε and the packing density α as presented in Equation 3.18.

$$U = \frac{\varepsilon}{\alpha} = \frac{1-\alpha}{\alpha} \tag{3.18}$$

The overall packing density of mixtures of *n* size classes can be determined by making use of the characteristic (average) diameters d_i, with d_1 being the diameter of the smallest size class, and the voids ratios U_i. Each time two classes are packed together, starting with the smallest two. After calculating the new voids ratio and the new characteristic diameter of this two-component mixture, it can be combined with a third larger size class and so on. The equations are based on the increase of the void space between the large particles due to the increased amount of smaller particles. The large particles, schematized as cubes, occupy a volume α_2 in a unit space, Equation 3.19 and Figure 3.6.

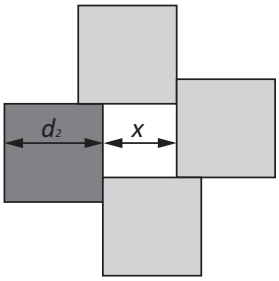

Figure 3.6 Three-dimensional model of a cubical particle with edge length d_i, the associated void with length x, and the related particles. (Dewar, 1999)

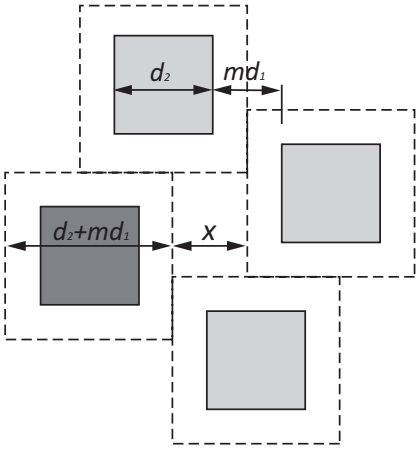

Figure 3.7 Three-dimensional model of the dilated structure of large particles in a mixture containing small particles. (Dewar, 1999)

$$\alpha_2 = \frac{d_2^{\,3}}{d_2^{\,3} + x^3} \tag{3.19}$$

The space between the large particles, represented as *x*, is increased when small particles are added. The large particles are pushed away from each other by *m* times d_1, which makes the spacing factor *m* dependent on the size-ratio d_2/d_1 and the amount of fine particles present, Figure 3.7. The new packing density $\alpha_{2,new}$ of the large particles is presented in Equation 3.20.

$$\alpha_{2,new} = \frac{d_2^{\,3}}{x^3 + \left(d_2 + m d_1\right)^3} \tag{3.20}$$

$$\alpha = \alpha_{2,new} + q\alpha_1 \tag{3.21}$$

The total packing density α is calculated by Equation 3.21, in which q is a factor taking into account the particle interference. The factor adjusts the bulk particle packing of the small particles due to the wall effect of the large particles.

For every two size classes, six possible mixtures are calculated. Each of these mixtures is then combined with the third size class in order to find the optimal composition for the highest packing density. This procedure can be expanded for more than three size classes but will result in the calculation of the packing density of $6^{(n-1)}$ mixtures for *n* particle classes. Furthermore, to predict the real packing density the calculated packing density has to be adjusted with a cohesion factor *CJ* (based on experiments) and an empirical adjustment factor *J*. *MixSim* is a commercially available concrete mix design program based on the Dewar model. (Dewar, 1999; Jones, et al., 2002; mixsim.net; Schuitemaker, 2002)

The Dewar model predicts packing density from the mean size and amount of two or more monosized particle classes. The packing and interaction equations are based on cubical particles, but applied to real voids ratios, thus indirectly including particle shape and surface texture to some extent. The model can calculate the packing density of concrete mixtures; however, the model becomes progressively slower with more size classes. Also, just as the *Europack* model, using an average diameter and packing density of two combined size classes, might underestimate the interaction of this 'new' size class with the

larger particles of the next size class. Therefore, with a higher number of size classes, decreasing accuracy of the particle packing prediction is expected. This in combination with the use of the adjustment factors CJ and J makes the model less suitable to extend for varying particle shapes or particle interaction due to surface forces.

3.5 Linear Packing Density Model

In the Linear Packing Density Model (Larrard F. de, 1999; Stovall, et al., 1986) the Furnas model is improved in two major respects. The two-component model by Furnas was extended in such way that it combined the use of multi-components with geometrical interaction between the particles.

For a binary mixture, the packing density is always the smallest of the two α_t calculated by the Furnas model. This is because of the physical meaning of the expressions. When $r_2 >> r_1$ (much more small particles) the larger particles cannot be fully packed, for the simple reason that if they would be, there would be not enough space to place all the fine particles in their voids. Vice versa, when $r_1 >> r_2$ (much more large particles) the smaller particles cannot be fully packed simply because there are not enough particles to fully fill up the space in-between the large particles. For this reason the packing density is always the minimum of α_t and the size class with the lowest α_t is called the dominant size class.

Stovall et al. (1986) proved that this relation is also true for multi-component mixtures. A system which is fully packed has at least one packed class, which is called the dominant size class i. The packing density is determined according to Equation 3.22 in which $i = 1$ always denotes the largest particle.

$$\alpha_t = \underset{i=1}{\overset{n}{Minimum}} \left\{ \frac{\alpha_i}{1-(1-\alpha_i)\sum_{j=1}^{i-1} r_j - \sum_{j=i+1}^{n} r_j} \right\} \tag{3.22}$$

This model is valid only when $d_i \gg d_{i+1}$. If this condition is not fulfilled, the packing density of the binary mixture will also depend on the diameter ratios of the size classes. The reason for this is the interaction between the particles described by the wall effect and the loosening effect.

Wall effect: Small particles close to a larger particle (or the wall of a container) cannot be packed as dense as the maximum bulk packing density of the small particles.

Loosening effect: The smaller particles are too large to be situated within the interstices of the larger particles and will therefore disturb the packing of the large particles.

Geometrical interaction is implemented in the model as the influence of a single size class onto the dominant size class *i*. When small particles perturb the packing density of the larger dominant size class *i*, the local expansion of the packing of the larger particles due to the introduction of the smaller ones (loosening effect) is expressed via function $f(i,j)$. The other way around, when small particles are fully packed, the packing density of the dominant small particles i will be lower close to a large particle due to the wall effect, as expressed with the help of $g(j,i)$. The total packing density results in Equation 3.23.

$$\alpha_t = \underset{i=1}{\overset{n}{Minimum}} \left\{ \frac{\alpha_i}{1-(1-\alpha_i)\sum_{j=1}^{i-1} g(j,i) r_j - \sum_{j=i+1}^{n} f(i,j) r_j} \right\} \tag{3.23}$$

This is a mathematical solution to model interaction under the assumption that interactions between the not fully packed size classes (j) in the system may be neglected. It is expected that the calculation becomes less accurate when the partial volume of a not fully packed size class approaches its maximum possible compaction (Stovall, et al., 1986). Without interaction $f(i,j)$ and $g(j,i)$ become one and Equation 3.22 is fulfilled. Stovall (1986) presents a description for $f(i,j)$ and $g(j,i)$ in the case of spherical particles.

The Linear Packing Density Model (LPDM) can be used to optimize the grading curve of a concrete mixture. In Figure 3.8 the optimal grading curve is constructed for a distribution consisting of fifteen size classes, each with a packing density $\alpha_i = 0.6$. Without interaction

the LPDM is comparable to the Funk and Dinger optimization curve for $q = 0.44$. Due to interaction the optimal grading curve changes, so each mixture has its own optimal composition. For instance, when rounded sand is combined with coarse angular aggregates, the optimal particle-size distribution will differ from the one of a mixture with sand from crushed rock and rounded coarse aggregates. To determine this optimal composition a computer program such as *4C-Packing* (dti.dk; Glavind, et al., 1999) can be used.

The Linear Packing Density Model can predict the packing density for several particle classes, which makes the model suitable for real concrete mixtures. The particle size distribution of the mixture and packing densities of each size class are taken into account. Furthermore, the influence of particle shape and surface texture is implemented indirectly via α. The accuracy of the model depends on the interaction formulas $f(i,j)$ and $g(j,i)$, which are relations derived from the packing density of two-component mixtures. This corresponds to the assumption that interactions between the not fully packed size classes in the system may be neglected. The setup of the model and the equations used make the model mathematically consistent and robust. The use of the interaction formulas creates possibilities to adapt the model for the use of ecological concrete, including particle interaction due to surface forces.

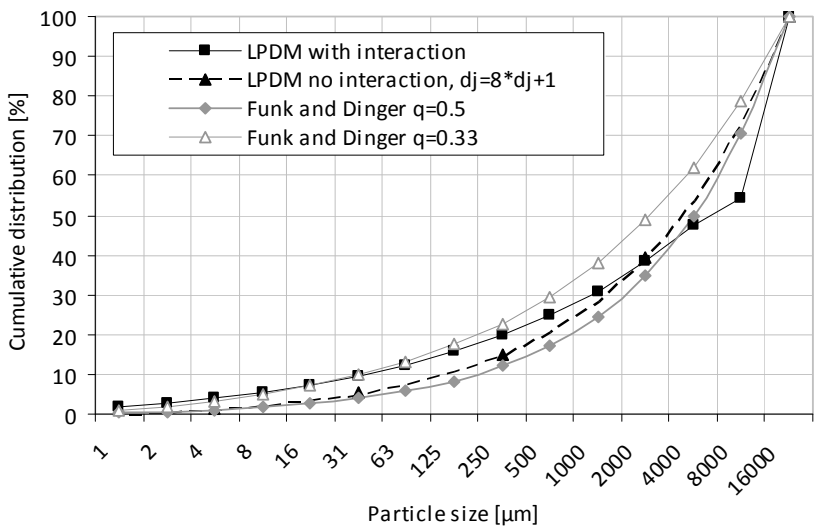

Figure 3.8 Optimal particle size distributions for LPDM in relation to the Funk and Dinger optimization curve. $a_i = 0.6$ *and for LPDM without interaction* d_j *is 8 times larger than* d_{j+1}.

3.6 Compressible Packing Model

The Compressible Packing Model (Larrard, 1999) includes the compaction of a mixture via the virtual compactness β. β is defined as the maximum potential packing density of a mixture if the particles would have been placed one by one in such a way that they use the minimum amount of space. For example, for a regular stacking consisting of monosized spheres β is 0.74. If the same particles were combined to from a randomly ordered structure, the packing density is in the range of 0.60 to 0.64.

The general model equation, which represents the virtual packing density of a mixture containing *n* size classes with category i being dominant, is expressed as Equation 3.24.

$$\beta_{ti} = \frac{\beta_i}{1 - \sum_{j=1}^{i-1} [1 - \beta_i + b_{ij}\beta_i \left(1 - 1/\beta_j\right)] r_j - \sum_{j=i+1}^{n} [1 - a_{ij}\beta_i/\beta_j] r_j} \tag{3.24}$$

For a monosized particle class β_j can be determined by Equation 3.25 from the experimentally determined packing density α_j. The coefficients a_{ij} and b_{ij} represent the loosening and wall effect. In Larrard (1999) binary granular mixtures were evaluated with the Compressible Packing Model (CPM) to determine Equations 3.26 and 3.27.

$$\alpha_j = \beta_j \Big/ \left(1 + \frac{1}{K}\right) \tag{3.25}$$

$$a_{ij} = \sqrt{1 - \left(1 - d_j/d_i\right)^{1.02}} \tag{3.26}$$

$$b_{ij} = 1 - \left(1 - d_i/d_j\right)^{1.50} \tag{3.27}$$

The virtual packing density is higher than the real packing density, which depends on the applied compaction energy. To determine the real packing density a scalar (i.e. the compaction index K) is introduced, which is defined to depend on the applied compaction only. As K tends to infinity, the real packing density α_t tends to the virtual packing density β_t. The packing density α_t is determined indirectly from Equation 3.28.

$$K = \sum_{i=1}^{n} K_i = \sum_{i=1}^{n} \frac{r_i/\beta_i}{1/\alpha_t - 1/\beta_{ti}} \tag{3.28}$$

The value of index K depends on the compaction energy applied to the mixture and should therefore be determined for each compacting process. Table 3.2 presents K values for various packing processes. If, for each size class, the packing densities and their accompanying K values are determined experimentally, the CPM can predict the packing density of any mixture composition. Commercially available computer programs can be used, such as *RENE LCPC* to determine the maximum packing density or *BETONLABPRO* to determine an optimal mixture composition (lcpc.fr).

The Compressible Packing Model is an extension of the Linear Packing Density Model including compaction energy. It predicts the packing density of a mixture from the particle size distribution and the packing densities of each monosized particle class. The influence of particle shape and surface texture is indirectly taken into account via α. The accuracy of the model depends on the interaction formulas a_{ij} and b_{ij} and the utilization of the K value concept. Particle fractions which cover multiple size classes lead to various input possibilities, therefore more user experience is required. In exchange, the implementation of compaction energy in the model increases the accuracy of the packing predictions compared to the Linaer Packing Density Model. The setup of the model and the used equations make the model mathematically consistent and robust. The use of the interaction formulas creates possibilities to adapt the model for the use of ecological concrete, including particle interaction due to surface forces. However, in that case the distribution of compaction energy over the size classes might change and lead to changes in the K value concept.

Table 3.2 K values for different packing processes (Larrard, 1999).

Packing process		K value
dry	pouring	4.1
	sticking with a rod	4.5
	vibration	4.75
	vibration + compression 10 kPa	9
wet	smooth thick paste (Sedran and Larrard, 2000)	6.7
	Proctor test (Pouliot, et al., 2001)	12
virtual	-	∞

3.7 The Schwanda model

Schwanda's particle packing model calculates the maximum voids ratio U, which corresponds to the minimum voids content ε and maximum packing density α according to Equation 3.29.

$$U = \frac{\varepsilon}{\alpha} \tag{3.29}$$

Each size class is combined with all the other size classes, and the voids ratio U of the combined multi-component mixture is calculated. To calculate U, three cases are considered. Case 1 and Case 2 can directly be derived from the Furnas model (Furnas, 1929).

Case 1: The small particles fill up the voids in between the large particles. The large particles are dominant and the voids ratio U is described by Equation 3.30. φ is the volume occupied by one size class in a unit volume and r_{small} is the volume fraction of the small particles.

$$\begin{aligned} U_{case1} &= \frac{\varepsilon_{large} - \varphi_{small}}{\varphi_{large} + \varphi_{small}} \\ U_{case1} &= U_{large} - \left(U_{large} + 1\right) r_{small} \end{aligned} \tag{3.30}$$

Case 2: There are more fine particles than there are voids in between the large particles. The large particles 'float' in a packing of small particles. The voids ratio U can be determined according to Equation 3.31 when the small particles are dominant.

$$\begin{aligned} U_{case2} &= \frac{\varepsilon_{small}}{\varphi_{large} + \varphi_{small}} \\ U_{case2} &= U_{small} - U_{small} r_{small} \end{aligned} \tag{3.31}$$

Case 3 occurs in the transition zone, when small and large particles influence each others particle packing density. When the small particles are too large to fit in between the large particles, due to particle interaction the total volume is enlarged. The resulting increase in

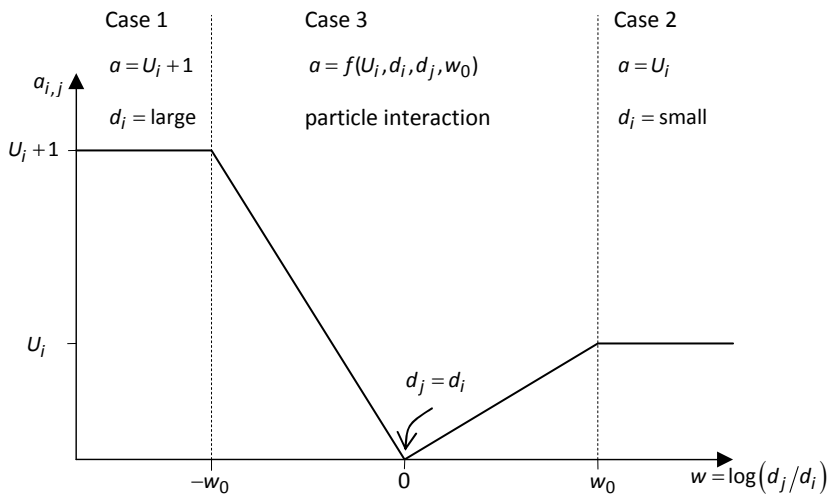

Figure 3.9 Factor $a_{i,j}$ describing the particle interaction depending on a fixed range of particle interaction w_0 and the size-ratio d_j/d_i, where U_i is the voids ratio U of the dominant size class i.

the voids ratio can be expressed in a factor $a_{i,j}$ (see Figure 3.9) which is influenced over a range *w*. *w* depends on the size-ratio of d_i and d_w, where d_w is the particle diameter of a small size class which starts to exert interaction on size class *i*, Equation 3.32 and Figure 3.9.

$$w = \log\left(\frac{d_i}{d_w}\right) \qquad \left\{-w \le \log\left(\frac{d_i}{d_j}\right) \le +w\right\} \tag{3.32}$$

Based on the relations between the three cases the voids ratio *U* is examined for every size class j as dominant size class i with Equation 3.33 (Reschke, 2000).

$$U = U_i - \sum_{j=1}^{n} a_{i,j} r_j \tag{3.33}$$

$a_{i,j}$ depends on the size-ratio of the classes according to Figure 3.9. U_i is the voids ratio of the dominant size class *i*, and U is the total voids ratio of the multi-component mixture when *i* is dominant.

The final packing density is calculated by Equation 3.34 from the maximum voids ratio $U_{\max}$ resulting from Equation 3.33 for each dominant size class *i*.

$$\alpha = \frac{1}{1 + U_{\max}} \tag{3.34}$$

The Schwanda model as described by Reschke (2000) can be used for fillers or aggregates, but also for combined fillers and aggregates. Next to the particle size distribution, the influence of particle shape and surface texture is taken into account indirectly via U or α. Particle interaction is directly based on the particle size of each class via parameter w and $a_{i,j}$. The existing model is easy to use and depends only on the (chosen) value for w_0 ($w_0 = 0.9$ is recommended), the packing densities and the size distributions of the particle groups. The model can be used for two size classes, but it can also be extended to any desired amount of size classes (Geisenhanslüke, 2008). Additional particle interactions due to surface forces as well as packing structure are not taken into account; however, the set-up of the model creates possibilities to implement additional interaction effects within $a_{i,j}$.

When using the model attention should be paid to particle mixtures consisting of classes with varying packing density. In that case the choice of the dominating size class *i* according to Equation 3.34 might lead to a discontinuity in the packing density profile of two size classes. The same problem causes that the calculated packing density of a mixture of two equally sized classes (total interaction) is equal to the lowest packing density of the two classes. In other words: adding particles with a higher packing density to a particle class with low packing density does not increase the calculated packing density.

3.8 Linear-Mixture Packing Model

Yu and Standish (1991) developed a model which draws a distinction between filling or additive components and occupying or mixing components. Very small particles can be added to a packing of large particles without disturbing the packing structure of the larger particles. In that case the small particles are regarded as the filling or additive component. When the small particles are too large to fit in the voids of the packing of the larger

particles, the packing of the larger particles is disturbed and the small and large particles together form a new packing structure. All components or size classes dominating the new packing structure are occupying or mixing components. The transition is at the critical ratio of entrance defined as $d_j/d_i = 0.154$. For smaller size-ratios, packing density is calculated by the Linear Packing Density Model (Stovall, et al., 1986) in which the dominating size class i can now be a group of size classes consisting of the mixing components. The packing density of the mixing components is determined according to a mixture packing model (Yu and Standish, 1988), in which the controlling mixture consists of Y to Z components $(1 \le Y \le i \le Z \le n)$. The diameters are ordered so that $(d_1 \ge d_2 \ge d_3 \ge \ldots \ge d_n)$. The overall specific volume υ is defined as the apparent volume occupied by a unit volume of particles, which is the reciprocal of the packing density α. To determine the packing density of a mixture Equations 3.35-3.39 are solved.

$$\upsilon = \max\left(\upsilon_1^T, \upsilon_2^T, \upsilon_3^T, \ldots, \upsilon_n^T\right) \tag{3.35}$$

$$\upsilon_i^T = \upsilon_i^{mix} \sum_{j=Y}^{Z} r_j + \upsilon_{filling}^s + \upsilon_{additive}^l \qquad i = 1,2,\ldots,n \tag{3.36}$$

$$\upsilon_i^{mix} = \sum_{X=Y}^{Z} r_X^{mix} \upsilon_X + \frac{\sum_{h=Y}^{Z-1} \sum_{l=h+1}^{Z} \beta_{hl} r_h r_l}{\left(\sum_{j=y}^{z} r_j\right)^2} + \frac{\sum_{h=Y}^{Z-1} \sum_{l=h+1}^{Z} \gamma_{hl} r_h r_l \left(r_h - r_l\right)}{\left(\sum_{j=y}^{z} r_j\right)^3} \tag{3.37}$$

$$\upsilon_{additive}^l = \begin{cases} 0 & y = 1 \\ \sum_{j=1}^{Y-1} \left[\upsilon_i^{mix} - \left(\upsilon_i^{mix} - 1\right) g(j,i)\right] r_j & y \ge 2 \end{cases} \tag{3.38}$$

$$\upsilon_{filling}^s = \begin{cases} 0 & Z = n \\ \sum_{j=Z+1}^{n} \upsilon_i^{mix} \left[1 - f(i,j)\right] r_j & Z \le n-1 \end{cases} \tag{3.39}$$

Y and Z are determined according to Equations 3.40 and 3.41 for each i.

$$Y = \begin{cases} X & d_X \ge d_i/0.154 > d_{X+1} \\ 1 & d_i/0.154 > d_1 \end{cases} \qquad X = 1,2,\ldots,i \tag{3.40}$$

$$Z = \begin{cases} X & d_{X-1} \ge 0.154 d_i > d_X \\ n & 0.154 d_i < d_n \end{cases} \qquad X = i, i+1, \ldots, n \tag{3.41}$$

The model is developed for predicting the packing density of mixtures consisting of spherical particles. This is included in the interaction formulas β_{hl}, γ_{hl}, $f(i,j)$ and $g(j,i)$ (Yu and Standish, 1991). However, these equations were originally based on the increase in packing density due to mixing in relation to the original packing density of each size class α_i. This causes that the model can not be used for mixtures with varying initial monosized packing densities, which is often the case for angular particles or very fine agglomerating particles (Yu and Standish, 1993). Therefore, the Linear-Mixture Packing Model was modified by Yu et al. (1996) to include new interaction functions $f(i,j)$ and $g(j,i)$. The Linear Packing Density Model (LPDM (Stovall, et al., 1986), section 3.5) is seen as a special case of the Linear-Mixture Packing Model in which there is only one component in the controlling mixture, so that $Y = Z = i$ and $\upsilon_i^{mix} = \upsilon_i$. Using the Linear-Mixture Packing Model in this way solves one of the physical inadequacies of this model with regard to the transition between mixing and filling effect. In the model the transition is determined by size-ratio only, while in reality mixing and filling is affected by volume amounts too.

The Linear-Mixture Packing Model is an extension to the LPDM including an additional set of equations to calculate the mixing effect. It predicts the packing density of a mixture from the particle sizes and the packing densities of each monosized particle class. However, shape and varying monosized packing densities can not be taken into account. The model was modified to the Modified Linear Packing Model to include these factors, which basically led to a variant of the LPDM with different interaction formulas. Though the Linear-Mixture Packing Model is not suitable to predict the packing density of a real concrete mixture, acknowledging the concept of mixing and filling was a major step in the field of particle packing optimization.

3.9 Concluding remarks

The packing density of the particles in ecological concrete is important because a lower voids ratio of the particles will lead to a reduced water demand. This means less cement can be used while retaining a constant water/cement ratio. Adding small particles contributes to the interparticle friction of the mixture, which is good for the concrete properties in the hardened state. However, when the small particles agglomerate, this can lead to bad workability or high water demands. Therefore, a good model to predict the packing density of mixtures containing small fillers is required. The models evaluated in this chapter have proven to be able to predict the packing density of randomly ordered

particle structures consisting of coarse particles. They take into account the most important material factors for coarse particles such as size distribution and shape. However, at some points the Toufar model and the Schwanda model are mathematically inconsistent with regard to the calculated packing density because of the way the size classes get grouped. The Dewar model becomes less accurate and increasingly time consuming with an increased number of size classes due to the stepwise approach. The Linear-Mixture Packing Model can not be used for ecological concrete with varying monosized packing densities of the components.

In ecological concrete not only the packing density of the coarse particles is important, but especially the packing of the fine fillers replacing the cement. These small particles have a different packing structure and increased particle interaction. The models do not yet take into account particle forces and the resulting packing structure directly. It is partly implemented via the packing density of the employed monosized particle classes, but the models assume random packing structure. This is accurate for coarse particles (>1 mm) because in that case surface forces are negligible compared to the shear and gravitational forces resulting from the size distribution and shape of the particles. However, for smaller particles the models will increasingly deviate, due to the increasing interparticle forces.

From section 3.1 it follows that when smaller particles are included also water and superplasticizer should be taken into account. In the models, the packing density for coarse particles can be considered to be equal for wet and dry mixtures. However, for small particles the models should be able to include wet packing densities. The LPDM and Linear-Mixture Packing Model are robust and due to the direct calculation procedure easier to extent than the CPM. On the other hand, CPM is the most accurate model because it includes compaction and can therefore directly be used for wet and dry packing densities. In chapter 5 the CPM is modified for ecological concrete by implementing additional equations for small particles. An important aspect in this respect is the mutual influence of compaction and interaction on the particle structure.

4 Preliminary experimental investigations: particle packing of ecological mixtures

Chapter 4 contains the results of the preliminary experimental investigations. These experiments were conducted to serve as input for particle packing models and to evaluate the suitability of existing particle packing models to design ecological concrete. In section 4.1 ecological concrete is designed with existing particle packing models to record major factors influencing the material properties. The particle packing of the fine powders is found to be an important factor to control the water demand and concrete strength. In section 4.2 particle packing measurements of powders are presented in combination with packing results of aggregates. Section 4.3 discusses which factors influencing the particle packing of ecological concrete should be taken into account in the design method for ecological concrete as presented in the next chapters.

4.1 Ecological concrete mixtures

4.1.1 Set-up

Ecological concrete mixtures were tested in order to investigate the major factors influencing the material properties of ecological concrete. The tests were used to evaluate the suitability of existing particle packing models to design ecological concrete. The mixtures were designed to gain insight in the question to what extent the cement content can be minimized in a concrete in strength class C20/25. Since the existing particle packing models can only take into account small particles as if they were large particles, mixtures are optimized in two steps. In series A the particle size distribution of all the aggregates larger than 125 micrometer is optimized. In series B the optimal aggregate distribution is then combined with various paste compositions.

The tests were conducted with Portland cement CEM I 32.5 R, blast furnace slag cement CEM III/B 42.5 N and fly ash combined with rounded river sand and gravel, see Appendix A. All dry powders were combined with the aggregates and mixed during one minute. Then water and superplasticizer Cugla Cretoplast SL-01 con. 35% were added and mixing was continued for three more minutes. The particle size distribution of the sand and

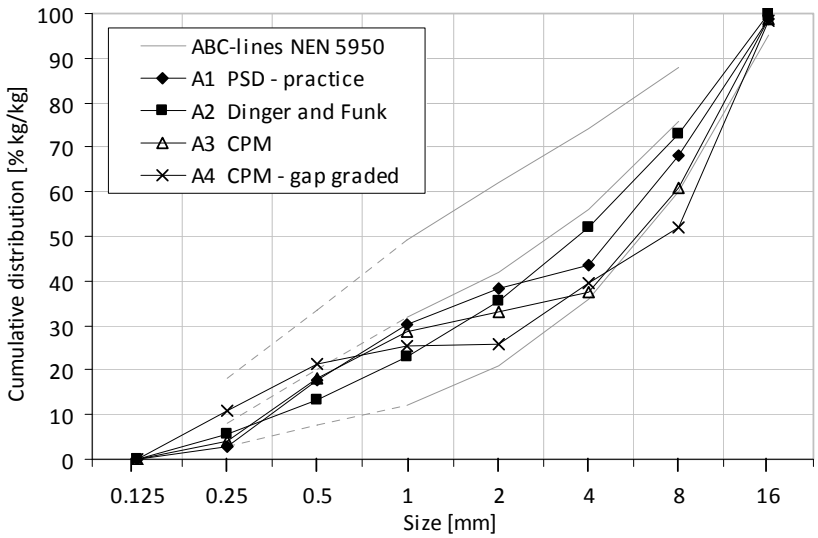

Figure 4.1 Particle size distributions of aggregates, series A.

gravel was optimized by different optimization methods to comply with the limits set by (NEN 5950:1995 nl) for a good workability of mixtures, see Figure 4.1. When concrete is considered to be a two phase material consisting of aggregates and cement paste, the highest particle packing density of the aggregates will lead to the lowest amount of cement paste necessary to fill up the voids in the aggregate structure. The optimized aggregate structure was combined with a sufficient amount of paste to achieve a slump of 50-100 mm. Following this design approach two series were tested, each with a constant water/powder ratio.

Series A: Optimization of particle size distribution by existing models.
The particle size distribution of the aggregates is optimized and then combined with a constant amount and composition of cement paste. The mixtures were tested on cube compressive strength development at 3, 7, 14 and 28-days and on modulus of elasticity and tensile splitting strength at 28 days.

Series B: Optimization of the paste composition.
The optimal particle size distribution (CPM) from series A is combined with varying paste compositions in which 30, 50, 70% [kg/kg] cement is replaced by fly ash. These mixtures are tested on compressive and tensile strength development and 28-day modulus of elasticity. Three mixtures were tested on shrinkage and creep and evaluated on durability by water ingress, electrical resistance and microscopy measurements.

The mixture compositions are presented in Table 4.1. Existing particle packing methods as presented in chapter 3 were used to design the aggregate structure. Mixture A1 was designed with a particle size distribution as used in practice in the Netherlands. In mixture A2 the particle size distribution is optimized by the Dinger and Funk optimization method. Mixture A3 and A4 were optimized by CPM to obtain maximum particle packing density of the aggregate. The gap-graded aggregate structure of mixture A4, with a very low amount of 0.5 to 2 mm particles, was the only one not complying to (NEN 5950:1995 nl). The particle size distributions of the aggregates of mixtures A1-A4 are presented in Figure 4.1. Aggregate packing densities of A3 and A4 (0.839) were only slightly higher than A1 (0.834) and A2 (0.836).

Table 4.1 Mixture compositions [kg/m^3] and the measured rheological and mechanical properties of series A and B

		Mixtures									
Composition		**A1**	**A2**	**A3**	**A4**	**B1**	**B2**	**B3**	**B4**	**B5**	**B6**
CEM I 32.5 R	[kg/m^3]	250	250	250	250	175	-	125	-	75	-
CEM III/B 42.5	[kg/m^3]	-	-	-	-	-	175	-	125	-	75
Fly ash SMZ	[kg/m^3]	-	-	-	-	75	75	125	125	175	175
Aggregates 4-16	[kg/m^3]	1126	929	1243	1186	1269	1264	1261	1256	1251	1248
Sand 0-4	[kg/m^3]	867	1063	748	802	749	745	744	741	738	736
Cugla Cretoplast SL-01 con. 35	[%]	1.3	1.3	1.3	1.3	2	1.3	0.85	1.3	0.85	0.85
Effective amount of water	[kg/m^3]	158	158	158	158	119	119	119	119	119	119
Water cement ratio	[-]	0.63	0.63	0.63	0.63	0.68	0.68	0.95	0.95	1.59	1.59
Water powder ratio	[-]	0.63	0.63	0.63	0.63	0.48	0.48	0.48	0.48	0.48	0.48
estimated density (1% air)	[kg/m^3]	2374	2374	2374	2373	2406	2397	2391	2384	2375	2371
Optimization of aggregate structure		PSD Practice	Dinger Funk	CPM	CPM gap graded	CPM	CPM	CPM	CPM	CPM	CPM
Rheological											
Slump	[cm]	12	12	14	3	17	7	7	14	3	3
Air content	[%]	1.7	1.7	1.4	1.3	1.4	1.5	1.3	0.8	1.1	1.0
Density	[kg/m^3]	2361	2371	2371	2359	2389	2404	2404	2395	2388	2379
Mechanical											
3-day cube compressive strength	[N/mm^2]	13.4*	17.7	17.6	19.1	-	-	-	-	-	-
7-day cube compressive strength	[N/mm^2]	21.5	23.5	22.11*	23.2	25.1	23.1	15.8	11.9	5.7	4.3
14-day cube compressive strength	[N/mm^2]	26.1	27.6	27.6	28.7	-	-	-	-	-	-
28-day cube compressive strength	[N/mm^2]	31.8	31.0	31.8	31.7	39.4	33.4	26.3	21.4	9.0	10.6
56-day cube compressive strength	[N/mm^2]	-	-	-	-	47.0	36.2	30.6	25.0	12.5	14.6
90-day cube compressive strength	[N/mm^2]	-	-	-	-	49.3	38.7	38.1	28.7	14.4	16.1
365-day cube compressive strength	[N/mm^2]	-	-	-	-	69.4	45.3	59.2	36.7	43.5	23.7
28-day splitting tensile strength	[N/mm^2]	2.6	2.7	2.7	1.2	3.0	3.1	2.1	2.1	1.0	1.1
28-day prism compressive strength	[N/mm^2]	23.6	23.8	23.6	25.8	27.3	28.1	19.5	16.1	8.0	8.2
28-day modulus of elasticity	[N/mm^2]	31500	31500	32000	31500	32500	32500	30000	29500	22000	23000

* measurement was one day earlier, at 2 days or 6 days

For series B, the composition of the paste was varied by replacing cement with fly ash. Combining cement with fly ash can increase the packing density, depending on the packing densities of the cement and the fly ash and their particle size distributions. By this approach the strength loss caused by the decreased amount of cement can be balanced by an increased packing density and the pozzolanic reaction of the fly ash.

4.1.2 Results

Evaluation of the fresh state of the ecological concrete mixtures showed that all mixtures in series A and B were homogeneous and stable. Slump measurements (NEN-EN 12350-2:2009), air content (NEN-EN 12350-7:2009) and density (NEN-EN 12350-6:2009) are presented in Table 4.1. All the mixtures had sufficient workability for casting and vibration. Only mixture A4 was judged as difficult to compact. Including fly ash improved the workability in such a way that the water content was decreased in mixtures B1 to B6 compared to mixture A3.

The cube compressive strength developments of series A and B are presented in Table 4.1 and Figures 4.2 and 4.3. Within series A there are no significant differences in 28-day cube compressive strength and modulus of elasticity. However, the tensile splitting strength of gap graded mixture A4 is much lower than expected (see also Figure 4.4). Possibly, this is the result of the bad workability and compactability of this mixture.

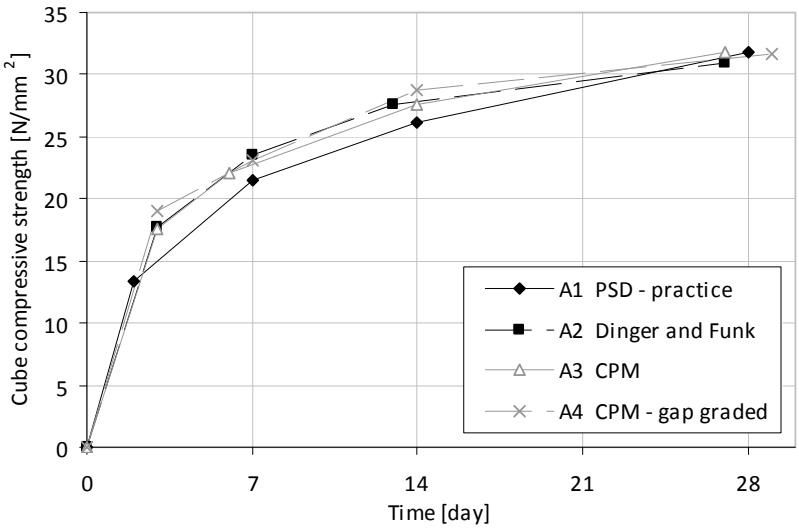

Figure 4.2 Cube compressive strength development of series A during the first 28 days.

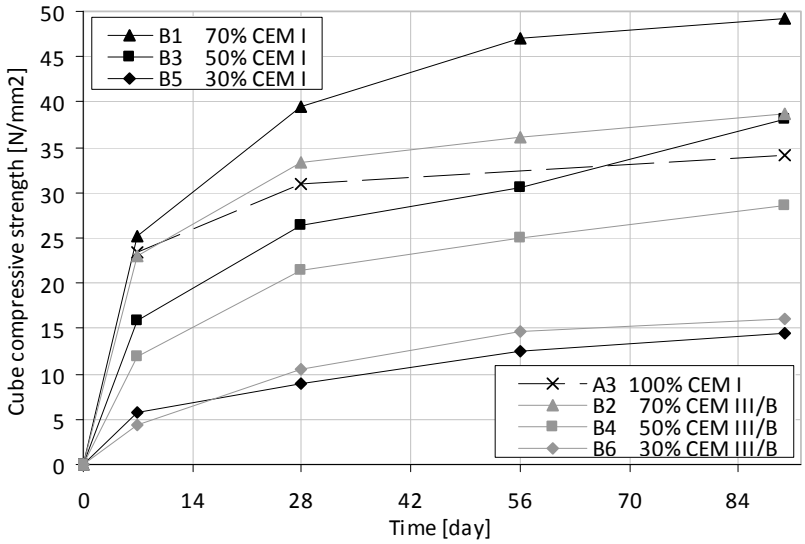

Figure 4.3 Cube compressive strength development of series B during the first 90 days. Reference mixture A3 has a higher water/cement ratio because the mixtures were designed for constant workability.

Mixtures B1 and B2 are within strength class C20/25 after 28 days, whereas mixture B3 reaches that order of magnitude after 90 days. When fly ash is combined with Portland cement there is an additional strength gain from the fly ash in the long-term. This is visible in the strength development of B3 and B5 after 56 days, compared to the strength development of the blast furnace slag mixtures B4 and B6. B5 reaches a strength of 43.5 N/mm^2 after 365 days. B6 reaches only 23.7 N/mm^2. In mixture B6 the fly ash does not seem to contribute much to strength development, which could be explained by the low amount of calcium hydroxide in the mixture (see also section 2.2). Blast furnace slag as well as fly ash continue to contribute to the long-term strength development, which makes it difficult to determine the influence of the fly ash on the long-term strength in mixtures with blast furnace slag cement. Short term strength development due to pozzolanic reaction of the fly ash was not observed (see also subsection 8.3.3).

The relationship between the average cube compressive strength and the tensile splitting strength of the ecological mixtures is the same as for normal concrete, as shown in Figure 4.4. The correlation given by Eurocode 2, as well as the allowed scatter as applied in the

Netherlands for normal concrete (k_1=1) are presented by Equations 4.1-4.3 (CUR Rapport 94-12, 1994; NEN-EN 1992-1-1:2005).

$$f_{ct,sp} = \frac{0.3\left(f_{cm} - 8\right)^{2/3}}{0.9} \tag{4.1}$$

$$f_{ct,sp-\min} = 0{,}22 k_1 f_{cm}{}^{2/3} \tag{4.2}$$

$$f_{ct,sp-\max} = 0{,}33 k_1 f_{cm}{}^{2/3} \tag{4.3}$$

$$E_{cm} = 22000\left(\frac{f_{cm}}{10}\right)^{0.3} \tag{4.4}$$

The measured moduli of elasticity of the ecological mixtures comply with the relation for compressive strength versus modulus of elasticity as described in Eurocode 2 for normal concrete, Equation 4.4. The deviance is always less than 1000 N/mm^2 except for mixture B4 which has a relative high modulus of elasticity compared to its strength.

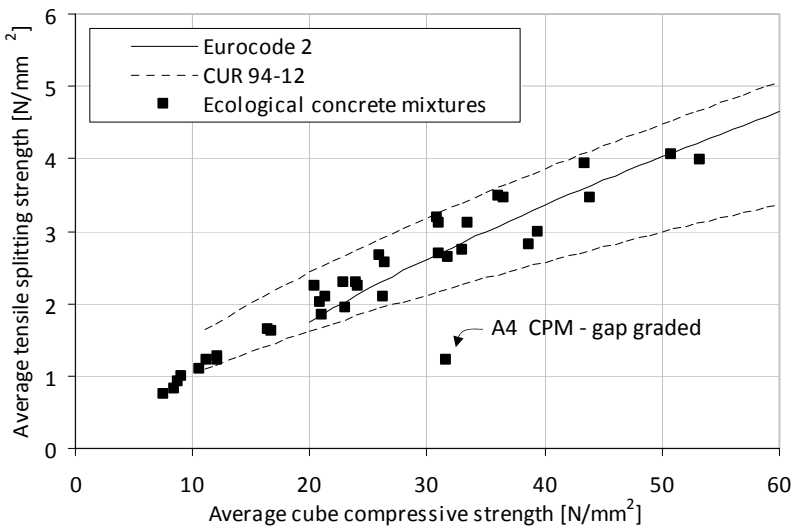

Figure 4.4 Correlation between the average cube compressive strength and the tensile splitting strength of ecological mixtures compared to Eurocode 2 (NEN-EN 1992-1-1:2005).

The drying shrinkage and creep of the ecological mixtures B1, B2 and B3 were measured on 100×100×400 mm concrete prisms in the longitudinal direction over a distance of 200 mm. Shrinkage testing started after 7 days of hardening at 20°C, 95% RH. Creep measurement started after 28 days, with 7 days of hardening at 20°C, 95% RH and 21 days at 20°C, 50% RH. For the creep measurement a force of 0.33 times the prism compressive strength was applied. The prism compressive strength is determined on similar specimens hardened under the same conditions. The shrinkage and creep tests were conducted for 90 days at 20°C and 50% RH.

In Figures 4.5 and 4.6 the shrinkage and creep measurements are compared with the standards. Creep measurements are presented as the creep coefficient according to Equation 4.5 in which ε is the measured creep deformation in mm/m.

$$\varphi_c = \frac{\varepsilon_{cc}}{\varepsilon_{cc,t=0}} - 1 \tag{4.5}$$

By presenting the creep measurements as creep coefficients, they can be compared to the creep values given by Eurocode 2 for concrete in strength class C20/25. The drying shrinkage $\varepsilon_{cd}(t)$ according to Eurocode 2 is determined by Equation 4.6 with the notional size of the cross-section $h_0 = 50$ mm, factor $k_h = 1$ and basic drying shrinkage strain $\varepsilon_{cd,0} = 0.51$ ‰ for concrete at 50% RH. The shrinkage on time t depends on the age of the concrete at the beginning of drying shrinkage denoted by t_s .

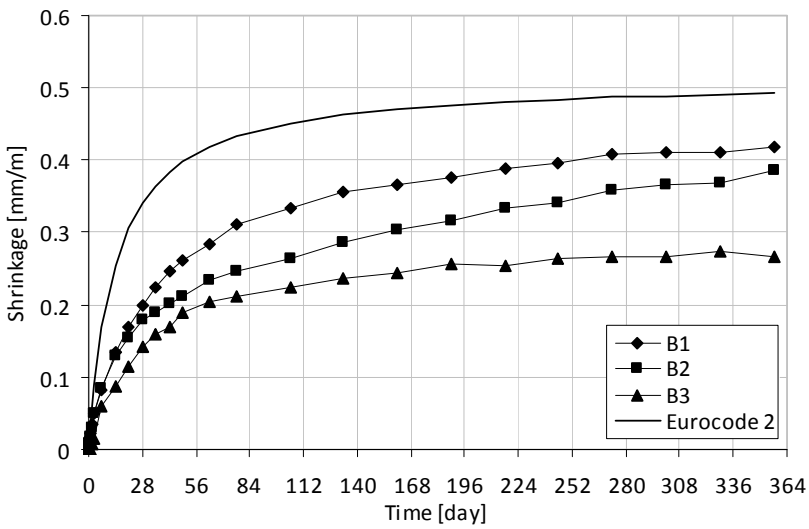

Figure 4.5 Shrinkage measurements of mixtures B1, B2 and B3 compared to Eurocode 2.

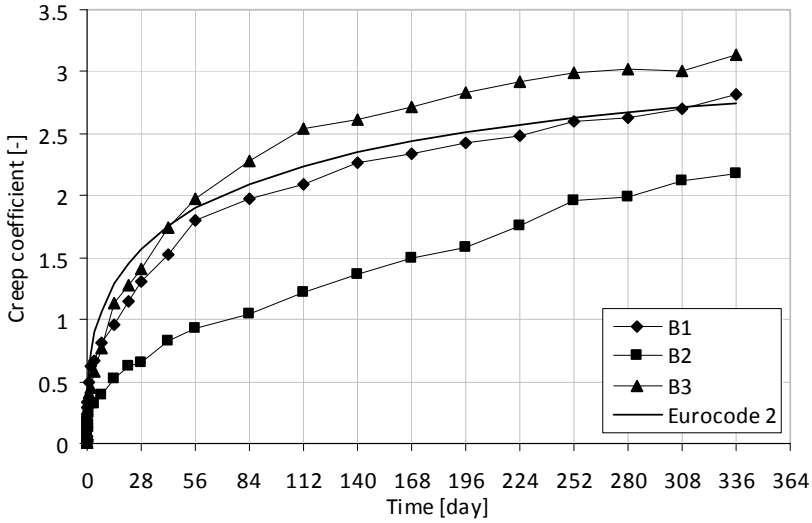

Figure 4.6 Creep measurements of mixtures B1, B2 and B3 expressed as creep coefficients and compared to the value given by Eurocode 2.

The standard creep coefficient $\varphi(t,t_0)$ is determined by Equation 4.7, in which the notional creep coefficient $\varphi_0 = 3.37$ for compressive concrete strength $f_{cm} = 33$ N/mm^2. The creep coefficient depends on the considered moment in time t and the age of the concrete at the time of loading t_0.

$$\varepsilon_{cd}(t) = \frac{(t - t_s)}{(t - t_s) + 0.04\sqrt{h_0^3}} k_h \varepsilon_{cd,0} \tag{4.6}$$

$$\varphi(t,t_0) = \varphi_0 \left(\frac{(t - t_0)}{(325 + t - t_0)} \right)^{0.3} \tag{4.7}$$

The measured shrinkage and creep values of the ecological mixtures are relatively low compared to the values from the standard, Figure 4.5. Their low shrinkage is in contrast to the high shrinkage and creep values normally predicted for concrete in the lower strength classes. The results can be explained by the relatively low cement content, the standard modulus of elasticity and the high packing density of the aggregate structure, which provides resistance against deformation of the cement matrix. Mixture B3 has a relatively higher creep coefficient than the presented creep coefficient of Eurocode 2. This is

because this mixture has a relatively lower strength than the mean compressive strength of $f_{cm} = 33$ N/mm^2 which was used to calculate the creep coefficient according to Eurocode 2.

4.1.3 Discussion

Ecological concrete with a low cement content complies with strength class C20/25. Series A shows that optimization of the aggregates does not lead to significant strength differences. Further strength gain of the ecological mixtures by optimizing the aggregate structure alone is not expected. Still, applying particle packing models to aggregates can be a useful tool when evaluating new types of aggregate and to determine the optimal aggregate distribution with these aggregates. Furthermore, large differences in workability were found. The use of a packing density model does not necessarily lead to a workable mixture. Mixing procedures and especially the grading curve have a large influence on the workability. Since for most concrete mixtures workability is one of the leading design factors, this explains the popularity of grading curves optimization techniques such as the Andreasen and Andersen model (Andreasen and Andersen, 1930). For ecological concrete, using the CPM is advantageous with regard to controlling the water or paste content in the mixture, in particular because ecological mixtures have a low powder content.

The cement content in relation to the filler content as investigated with series B significantly influences concrete strength. The mixtures including fly ash have a lower water demand than the mixtures of series A for a constant workability. Because of the low amount of water in the mixtures strength class C20/25 can be reached with only 125 kg/m^3 cement. These large strength differences emphasize the importance to include the small particles in the packing density model to avoid time consuming trial and error testing. Including the small particles in the model should also lead to a better prediction of the water demand of mixtures.

Mechanical testing of tensile strength, modulus of elasticity, shrinkage and creep showed that for these mixtures the compressive strength can be used as the governing design criterion for these properties. For ecological concrete with low powder contents the relationship between the cube compressive strength and tensile splitting strength and between cube compressive strength and modulus of elasticity are the same as for normal concrete. Shrinkage and creep deformation were even smaller than the values prescribed

by the Dutch standards. This can be explained by the concrete composition, which is characterised by a relatively low cement content, a normal modulus of elasticity and a high packing density of the aggregate structure. Lower cement contents lead to decreased shrinkage and creep. From these findings it can be concluded that, when the cement content is decreased and the amount of cement is sufficient to reach the required strength, the other mechanical properties will be at least as good as normal concrete properties. However, it was also found that it is challenging to control the water demand and workability of concrete mixtures with low powder contents. Small changes in the amount of water and the workability possibly lead to a larger scatter in the material properties. Because of the importance of this with regard to safety, extra attention is being paid to workability and curing in chapter 8.

4.2 Packing density measurements

The experimental investigations on the ecological mixtures (section 4.1) showed that the paste composition and thus the amount of powders in the paste has a large influence on concrete strength. Therefore, it is important to include the powders in the particle packing model and design method for ecological concrete. To implement particle packing of fine powders in the packing model, information on their packing behavior is investigated experimentally in section 4.2 and by packing simulations in subsection 5.2.2.

4.2.1 Test methods for measuring particle packing

The maximum packing density of dry particles can be determined according to NEN-EN 1097-3:1998 for loose bulk density. The particles are weighed in a container with a known volume. Packing density is calculated by dividing the weight of the particles in a unit volume by the specific gravity of the particles. The method can be extended to determine the maximum packing density at a certain compaction level by applying external loads such as vibration or top-weight. This method is suitable for particles larger than one millimeter, where gravitational forces and shear forces between the particles are dominant. However, with finer particles, the interparticle forces (subsection 3.1.3) become increasingly important. These interparticle forces can cause, for instance, agglomeration of particles, thus lowering the packing density. Since the interparticle

forces depend on the conditions (dry, wet) of the packing structure, also packing density is influenced by this. Therefore, it is important that the maximum packing density of the particles is measured under the same conditions as under which the particles would be used in concrete and in the particle packing model. For concrete, this means that particles are conditioned in water with or without admixtures during mixing, casting and compaction.

To determine the maximum packing density of wet particles (<125 µm) no single method is generally accepted and therefore various test methods are used to determine packing density or water demand of fine particles. In this research project the next methods to determine packing density or water demand were evaluated.

1. Water demand - France (Larrard, 1999; Sedran and Larrard, 2000)
2. Water demand - Germany (Puntke, 2002)
3. Water demand by determining mixing energy (Marquardt, 2002)
4. Proctor test (NEN-EN 13286-2:2004; Wong and Kwan, 2008a)
5. Centrifugal consolidation (Kjeldsen, 2007; Miller, et al., 1996)
6. Water demand - Japan (Okamura and Ozawa, 1995)
7. Rheology measurements Krieger and Dougherty (Mansoutre, et al., 1999)

A description of each method is presented in Appendix B. Most methods determine the minimum amount of water necessary to fill the voids between particles in a packing. In this basic principle, maximum packing density is achieved when all voids are just filled with water, but no excess amount of water is available to form a layer surrounding the particles. However, none of the methods proves that maximum packing density is achieved or no excess amount of water is surrounding the particles.

The methods 1-3 determine the minimum water demand directly by mixing a paste with a very low water/powder ratio (water, powder and superplasticizer) and subsequently adding water until reaching the point were all voids are filled. The methods are fast, but depend on the homogeneity of the mixture. Therefore, the method described by Puntke is less accurate than the other two. Determining water demand by measuring the mixing energy is found to have the highest reproducibility and is chosen as comparative packing density measurement for this research (Appendix B, Hunger and Brouwers, 2009).

The proctor test and centrifugal consolidation have to be used on a number of mixtures consisting of the powder and a varying water content. This makes the methods accurate, but also time consuming. Furthermore, in these methods the packing density measurements depend on the achievable degree of compaction, which is influenced by e.g. the air content in the mixtures and the compaction energy. This means that, though both methods can be used for comparative measurements of particle packing density, they do not measure the maximum packing density as requested in this research project. Furthermore, the method of centrifugal consolidation can cause various sized particles to segregate (Fennis, et al., 2008), which especially influences the measured packing density of multiple monosized particle groups with a low size-ratio d_{small}/d_{large} .

The Japanese method and the Krieger and Dougherty method determine the minimum water demand of a powder indirectly from measurements on various oversaturated mixtures. These methods strongly depend on the fitting equations. Furthermore, a very high accuracy of the measurement values is necessary in order to make a good fit. These methods were found not suitable to be used for comparative particle packing measurements.

4.2.2 Particle packing and agglomeration

The packing density and size distribution of each particle group are used as input for the particle packing model in chapter 5. For large particles these characteristics are constant for different particle-liquid structures. However, small particles in water tend to agglomerate. Agglomerates will be created or broken depending on the particle characteristics, liquid characteristics, surface active agents and the applied de-agglomeration energy (for instance mixing or ultrasonic dispersion). This means that measuring methods and the applied amount and type of superplasticizer have an influence on the measured packing density and the measured particle size distribution of a certain powder.

The particle size distributions of the powders used in this research project are measured in ethanol (Appendix A). This is done to achieve the best possible dispersion of the particles and to be able to compare the measurements. Particle size distribution measurements of hydraulic powders, such as cement, are not stable in water. A reaction will start as soon as the powder is dissolved in the water. According to Figure 4.7 (Brendle, et al., 2008) the

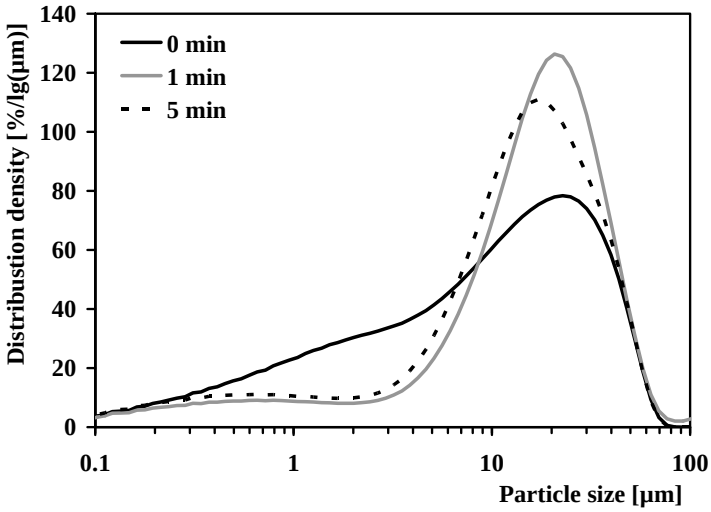

Figure 4.7 Particle size distributions for cement powder and paste according to (Brendle, et al., 2008).

finer fraction up to 4 µm decreases in relation to the coarser fraction. This might be explained by fine particles agglomerating and then being measured as a larger particle in combination with newly formed product layers on the particle surfaces.

Figure 4.8 also shows more fine particles when measuring cement in ethanol, compared to measurements in water. However, due to the cement reaction, the measurement in water was not stable in time and cannot be regarded as accurate. Measuring the changes in the particle size distribution in time is out of the scope of this research project. Therefore, it is recognised that cement and other fine powders in water will agglomerate more than in ethanol and real particle size distribution can differ from the measurements. However, for input for the packing model it is assumed that superplasticizers and an appropriate mixing procedure can break the agglomerates.

Superplasticizers influence the interparticle forces by either changing the characteristics of the solid-liquid interface or by sterical rejection. Depending on the chemical composition of the particles one type of superplasticizer can be more effective than the other. Since different types of powders are used in this investigation a single most effective superplasticizer with regard to de-agglomeration can not be indicated. Superplasticizers used in this project are Cugla Cretoplast SL01 con.35%, which is naphthalene sulphonate based and used in practice in the Netherlands, and Glenium 51 BASF con.35% for the tests

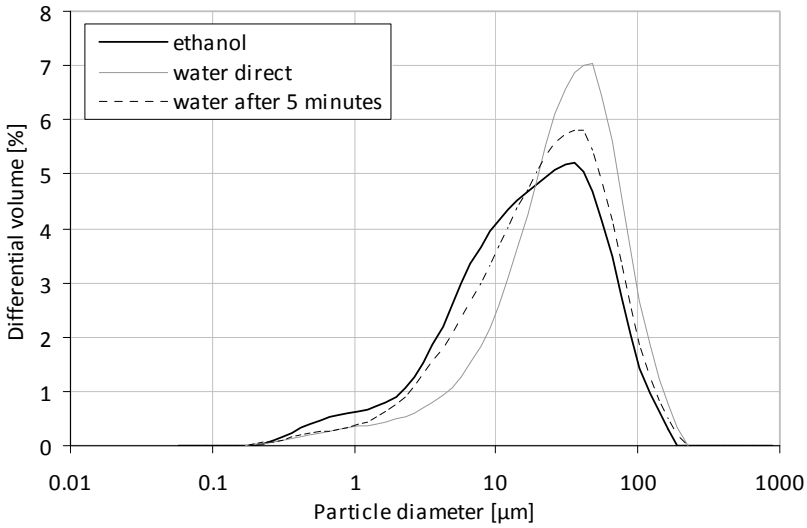

Figure 4.8 Particle size distributions for cement CEM I 42.5 N in water and ethanol (Appendix A).

on fine powders. Glenium 51 is a polycarboxylate ether which disperses very small particles more effectively by sterical rejection. Whenever a superplasticizer is used it is recommended to test the effectiveness of the superplasticizer in combination with the powder. Furthermore, for each type of superplasticizer the dosage should be determined in order to ensure stable mixtures and avoid overdosage. In this research project it is chosen to apply Glenium 51 as 1.2% kg/kg of the powder content of the mixtures as a constant research parameter. The packing density of the powders was tested by measuring the mixing energy following the procedure described in Appendix B. Figure 4.9 shows that applying an appropriate amount of Glenium 51 can increase the packing density of cement by more than 5%.

The Compressible Packing Model calculates packing density for random packing structures without agglomerates. In the next chapters it is assumed that the applied mixing methods in combination with the use of Glenium 51 will provide the same level of particle dispersion as with the particle size measurement in ethanol. If further research shows that particles are not totally dispersed, the model can still be used in the same way and according to the procedures described in this thesis. In that case it is suggested to adjust the input parameters in such a way that an agglomerate of fine particles is represented by a larger particle with a lower packing density.

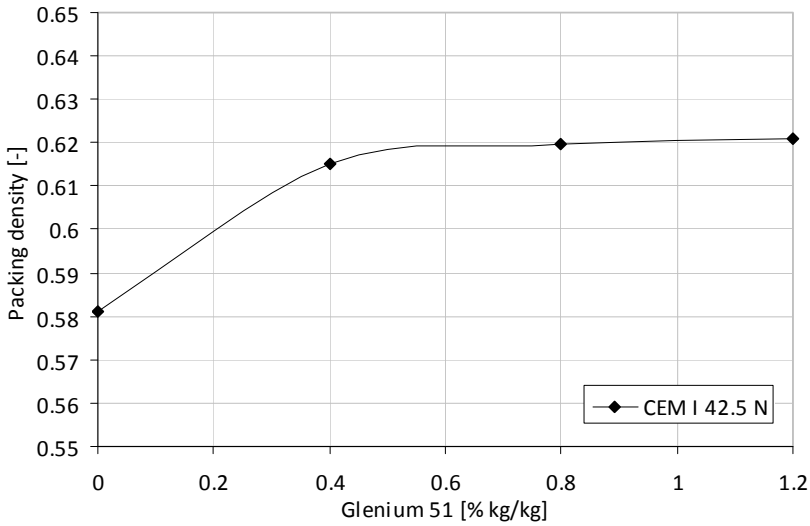

Figure 4.9 Packing density of CEM I 42.5 N in relation to the amount of Glenium 51.

4.2.3 Particle packing results

The packing density of particles larger than 125 µm is measured according to NEN-EN 1097-3:1998. Aggregates in seven different size fractions were measured. (See also Appendix A for material properties). Table 4.2 shows packing densities around 0.57 for larger aggregates and a decreasing packing density for the smallest size fractions. These results can be explained by the origin of the material. To obtain the smallest fractions, Dutch river sand was ground. The angular shape and possible higher interparticle forces of these small particles cause a lower packing density.

Packing profiles can be determined by combining two (or more) fractions with varying amounts. Packing profiles of aggregates consisting of fraction 1-2 mm in combination with other fractions 0.25-0.5, 0.5-1, 2-4, 4-8 mm were determined. Dry particles were poured into a contatiner to from a loose particle structure with $K = 4.1$. The experimental data is evaluated to check the performance of the Compressible Packing Model (see Appendix C). Figure 4.10 demonstrates a good correlation between experiments and CPM. The average error is 0.7% and the maximum 2.3%. For large particles with narrow particle size distributions the compressible packing model corresponds well with the experiments for rounded as well as angular particles. Similar precisions are also reported by Larrard (1999) and Jones et al. (2002).

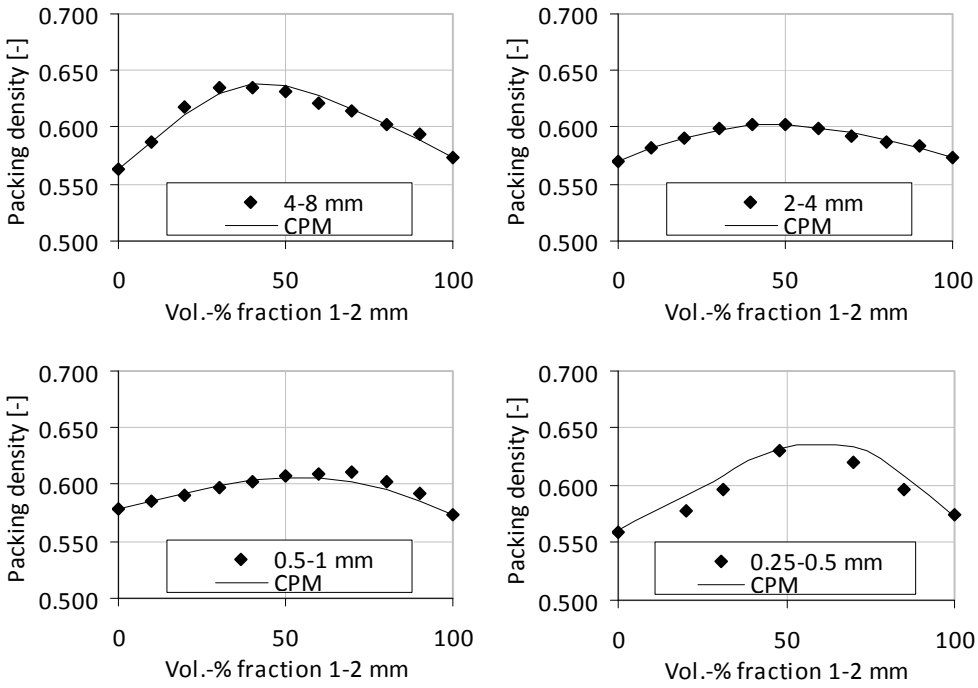

Figure 4.10 Packing profiles of aggregates 1-2 mm combined with fractions 4-8, 2-4, 0.5-1, 0.25-0.5 mm (K = 4.1).

The packing density of particles smaller than 125 µm is measured with the mixing energy test (Appendix B). Each mixture consisted of 1500 grams of powder. The mixing procedure is shown in Figure 4.11 in relation to the power consumption. The procedure started by mixing the dry powders with (an estimated) 95% of the water and the superplasticizer (1.2% kg/kg Glenium 51) in a three litre Hobart mixer for one minute. After two minutes resting and scraping, mixing was continued with a constant water supply of ± 0.3 ml/s until maximum power consumption was reached in about 2 minutes. Tests on each powder type or size fraction are performed at least twice to ensure a packing density precision of 0.002 [-]. The average amount of water in the mixture at maximum power consumption was taken as the void volume between the particles to calculate the packing density.

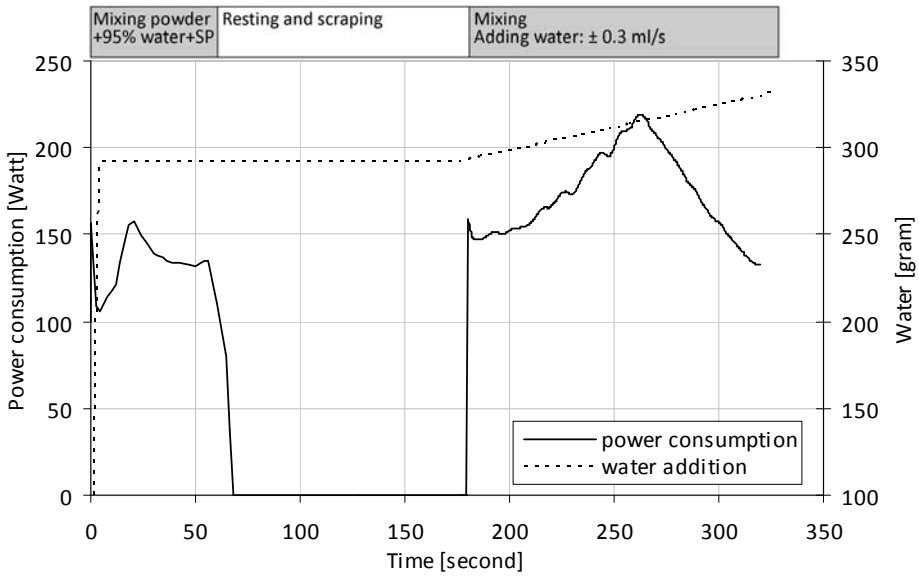

Figure 4.11 Power consumption and water supply during the mixing process.

To investigate the influence of size on particle packing density, quartz powder is chosen as reference material. It is commercially available in various size fractions. Furthermore material properties (Appendix A) are constant and the material is considered to be inert (Kronlöf, 1997). The quartz powder is used in this research project; however, whether it is feasible to be used as filler in concrete with regard to costs and health issues should be investigated. Table 4.3 shows that wet quartz powder with superplasticizer has a higher packing density than dry powder. Furthermore, packing density is lower for smaller particles. For loose dry particle packing density this effect is stronger than for the wet packing density measurements with superplasticizer. Figure 4.12 shows that the ratio between the wet and dry packing density increases with decreasing particle size for very small particles, where interparticle forces become dominant.

Table 4.2 Packing density of aggregates, precision ±0.002.

Fraction [mm]	α_{exp} dry, loose [-]	α_{exp} wet [-]
8-16	0.564	-
4-8	0.563	-
2-4	0.570	-
1-2	0.574	-
0.5-1	0.578	-
0.25-0.5	0.560	0.644
0.125-0.25	0.524	0.596

Table 4.3 Packing density of quartz powder, precision ±0.002.

Fraction	α_{exp} dry, loose [-]	α_{exp} wet [-]
M3	0.472	0.625
M4	0.434	0.618
M6	0.377	0.583
M10	0.340	0.576
M300	0.321	0.542
M400	0.264	0.567
M600	0.226	0.527*

**Due to required high mixing energy, one measurement only*

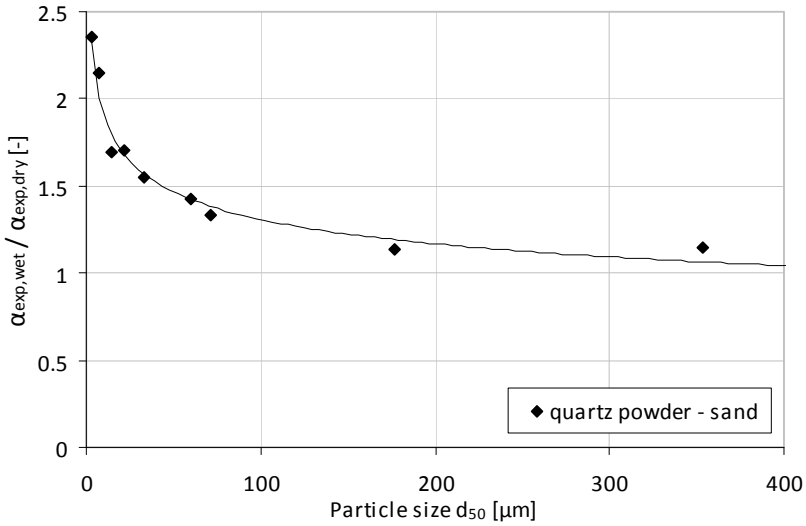

Figure 4.12 Ratio between the wet and dry packing density versus the median particle size d_{50} of that size fraction.

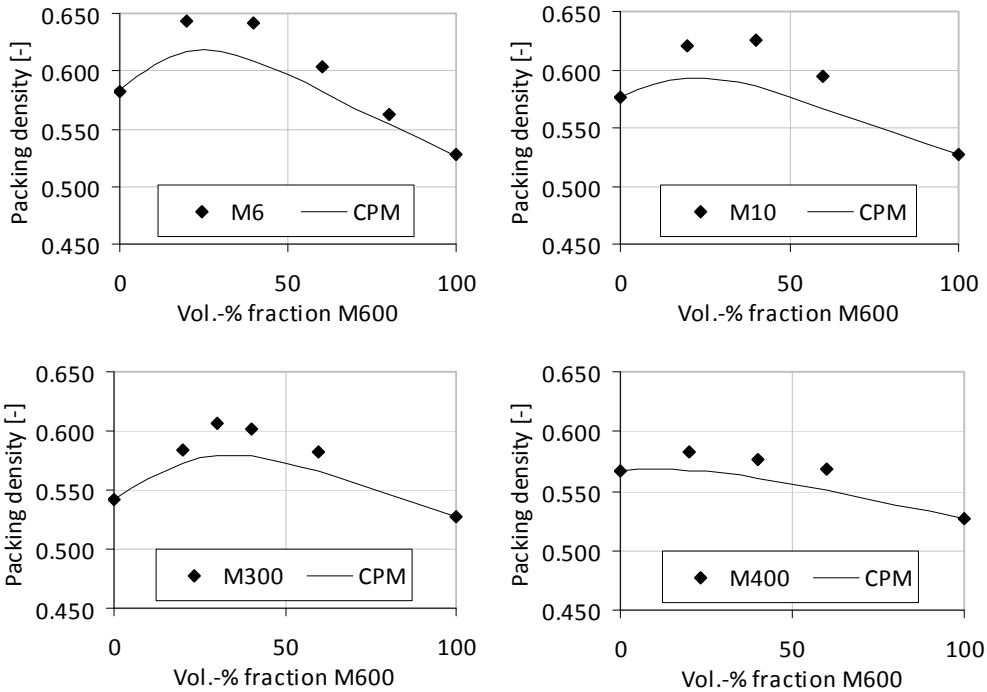

Figure 4.13 Packing profiles of quartz powder M600 combined with M6, M10, M300 and M400.

The packing profiles determined by combining two (or more) fractions serve as input for the modelling in chapter 5. Data from Appendix C is evaluated to check the performance of the Compressible Packing Model. For quartz powder in the size range of cement a good correlation is found with a compaction value $K = 12.2$. The average error is 0.2% and the maximum is 0.8%. However, for fine particles M600 CPM deviates from the experimental data. Figure 4.13 demonstrates an underestimation by the CPM of 3.8% on average and maximum 6.4%. For small quartz powder particles M600 the Compressible Packing Model can not directly be applied in the same way as for coarser particles with the same accuracy.

4.2.4 Discussion

To be able to design ecological concrete including fine particles an accurate model is necessary. The tests performed in section 4.2 have shown that particle packing of powders can not be modeled in the same way as the particle packing of coarse particles. For coarse

particles the geometrical interaction as used in the CPM is dominant, but for particles smaller than 125 µm the interparticle forces become increasingly important. Therefore, the compressible packing model is not as accurate for small particle sizes as it is for larger size fractions. Other causes might be found in the more angular particle shape or the wider particle size distributions, which both would increase interaction; however, no literature was found indicating lower accuracy of the model for angular particles or wider particle size distributions.

Furthermore, tests have shown that it is important to take the compaction level into account. The wet packing density test method based on mixing energy will result in different packing densities than a dry loose packing measurement or pressure vibrated packing density method. For aggregates good agreement was found with the K value concept for monosized particle groups (Larrard, 1999), Equation 4.8.

$$K = \frac{1}{\beta/\alpha_{\exp} - 1} \tag{4.8}$$

K values found for monosized aggregates were 4.1-5.1 for loose packing density, 6.5-7.5 for vibrated packing densities and 9 for vibration under pressure. This corresponds to the values originally presented by de Larrard (1999) of respectively 4.1 and 9 for loose packing and packing vibrated under compression. In a first attempt to apply the K value concept to the wet packing density measurements a K value of 12.2 was found for cement and fly ash. The quartz powder experiments show however that a single K value concept for all size fractions can not be used. A K value of 4.1 for dry loose packing would lead to virtual packing densities lower than the measured wet packing density. Also Larrard et al. (2003) state packing density of dry fine particles should be measured using high compaction techniques. The fact that the concept does not work with small particles can easily be explained when interparticle forces are regarded. To break the agglomerates between small particles more compaction energy is necessary to reach a certain packing density. The other way around, in a loose packing agglomerates are not broken (by gravitation alone) and packing density is smaller.

Because compaction energy influences the packing density of the small particles differently than the packing density of large particles, the CPM should be adjusted to be able to calculate the optimal packing density of ecological concrete containing small fillers.

4.3 Concluding remarks

The preliminary investigations presented in this chapter show that it is possible to optimize the concrete composition with packing density models in order to lower the cement content while retaining satisfactory mechanical properties. The relationship between the average cube compressive strength, the tensile splitting strength and the modulus of elasticity of the ecological mixtures is the same as for normal concrete, while shrinkage and creep are lower than in normal concrete. For low powder content concrete mixtures this means that, when the cement content is decreased and the amount of cement is sufficient to reach the required strength, the other mechanical properties will be at least as good as normal concrete properties. Therefore, compressive strength can be used as the governing design criterion for the mechanical properties. For this research project a strength controlled design method based on particle packing density is therefore adopted.

For other material properties, such as chloride ingress or carbonation, further investigations on the influence of low cement content in concrete are required. Especially with ecological concrete, the microstructure changes due to the low amount of cement and the increased water/cement ratio, but also due to the flowability and the level of compaction. The preliminary investigations have shown that ecological mixtures were susceptible to water demand as well as small changes in water demand. It is difficult to determine the water demand for a desired workability. A solution is to apply an optimized amount of admixtures and a proper mixing procedure. However, to avoid intensive trial and error mixing a particle packing model which predicts the water demand of ecological concrete mixtures is desired.

With ecological concrete mixtures, the packing density of the aggregates and fillers can be increased in order to lower the water demand. For sand and aggregates packing density measurements comply with the K value concept with regard to loose, compacted and virtual packing densities. However, this concept can not directly be applied on fine particles. With fine particles interparticle forces become dominating and are not always neutralized by mixing or compaction. Therefore, implementation of rules on how to use fine particles in analytical particle packing models is desired for the design of ecological concrete.

5 Compaction-Interaction Packing Model

In this chapter an optimised particle packing model for ecological concrete is developed. For the design of ecological concrete with a low cement content especially the fine particles are important, as concluded in chapters 2 and 4. The particle packing models as described in chapter 3 take into account geometrical interaction. However, with particles smaller than 125 µm additional interactions as described in section 3.1.3 are expected. Therefore, in this chapter an extension is made to the geometrical particle packing model as described in section 3.6. Section 5.1 presents the adjustment of the model which enables the implementation of new formulas for interaction and compaction. Sections 5.2 and 5.3 elaborate on the implementation of interaction and compaction. Section 5.4 elaborates on the calculation procedures, to give more insight on how to use the model. Following this calculation procedure the improved particle packing model provides the maximum packing density belonging to a compacted particle structure. In chapters 6 to 8 the maximum packing density is used as input for the design of ecological concrete.

5.1 Geometrical interaction

To implement interaction forces as an additional module into a geometrical particle packing model, first an expression for the geometrical interaction is required. This expression should be able to include the wall effect and the loosening effect. Furthermore, it should be possible to extend this expression enabling to include an additional size-related interaction effect.

Originally in the Compressible Packing Model (CPM) (Larrard F. de, 1999) geometrical interaction is represented by a_{ij} for the loosening effect and b_{ij} for the wall effect in Equation 5.1.

$$\beta_{ti} = \frac{\beta_i}{1 - \sum_{j=1}^{i-1} [1 - \beta_i + b_{ij}\beta_i \left(1 - 1/\beta_j\right)] r_j - \sum_{j=i+1}^{n} [1 - a_{ij}\beta_i/\beta_j] r_j} \tag{5.1}$$

The coefficients a_{ij} and b_{ij}, presented in Equations 5.2 and 5.3, are constant for a given size-ratio, thus fulfilling the requirement that the specific volume varies linearly with the fractional solid volume for any size-ratio. The size-ratio is defined as the diameter of a small size class divided by the diameter of a larger size class. This means that the size-ratio is always a value between 0 and 1. Size classes are by definition ordered from the largest size class with diameter d_1 to the smallest size class with diameter d_n. For a_{ij} describing the loosening effect this means that the size-ratio is d_j/d_i. However, for the wall effect b_{ij} index j (of the larger size class) is always smaller than index i (of the dominating size class), wherefore the size-ratio becomes d_i/d_j.

$$a_{ij} = \sqrt{1 - \left(1 - d_j/d_i\right)^{1.02}} \tag{5.2}$$

$$b_{ij} = 1 - \left(1 - d_i/d_j\right)^{1.50} \tag{5.3}$$

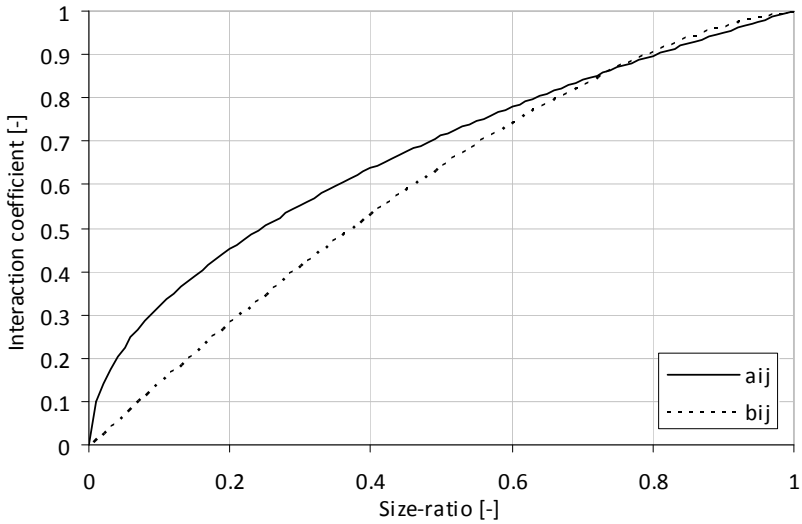

Figure 5.1 Interaction functions a_{ij} and b_{ij} as a function of size-ratio.

As shown in Figure 5.1, the factor a_{ij} describing the loosening effect is larger than b_{ij}, except when the size-ratio is larger than 0.72. In that case, the wall effect exceeds the loosening effect. For a mixture of two size classes with 70% of large particles ($\alpha = 0.6$ and $K = \infty$) this leads to a crossover in the dominating size class i when the size-ratio decreases. For size classes of 9 and 10 mm the small particles are dominant, while for 1 and 10 mm the large particles are dominant. The variance in interaction causes the maximum packing density of the mixture to occur at 69% of the 10 mm particles when combined with 9 mm particles, at 74% of the 10 mm particles when combined with 8 mm particles and at 68% of the 10 mm when combined with 6 mm particles.

When scaling the interaction coefficients to extend the model, these crossover effects are undesired, since such crossovers might lead to unexpected changes in interaction. For that reason, the interaction coefficients a_{ij} and b_{ij} were reprogrammed to enable scaling. The equations should comply with $a_{ij} = b_{ij} = 0$ at zero interaction occurring at small size-ratios and $a_{ij} = b_{ij} = 1$ at full interaction occurring at a size-ratio of 1. The background of the new equations comes from the Schwanda model (section 3.7). The final result of the implementation of the geometrical interaction in a_{ij} and b_{ij} is presented in Equations 5.4 and 5.5.

$$a_{ij} = \begin{cases} 1 - \dfrac{\log\left(d_i/d_j\right)}{w_{0,a}} & \log\left(d_i/d_j\right) < w_{0,a} \\ 0 & \log\left(d_i/d_j\right) \geq w_{0,a} \end{cases} \tag{5.4}$$

$$b_{ij} = \begin{cases} 1 - \dfrac{\log\left(d_j/d_i\right)}{w_{0,b}} & \log\left(d_j/d_i\right) < w_{0,b} \\ 0 & \log\left(d_j/d_i\right) \geq w_{0,b} \end{cases} \tag{5.5}$$

The simplest solution to implement interaction in this way is when $w_{0,a} = w_{0,b} = w_0$ with $w_0 = 0.9$ as in the Schwanda model. In addition to this, $w_{0,a}$ or $w_{0,b}$ can be increased to strengthen the interaction or decreased to weaken the interaction. Figure 5.2 shows the effect of varying $w_{0,a}$ on the interaction coefficient a_{ij}, where lower values of $w_{0,a}$ always lead to lower interaction coefficients for each size-ratio.

The advantage of the new interaction function as presented above is that $w_{0,a}$ and $w_{0,b}$ could also be functions. In this way, possibilities are created to implement additional interaction through surface forces or to change geometrical interaction with varying particle shapes. In that case, $w_{0,a}$ as well as $w_{0,b}$ can be represented by Equation 5.6.

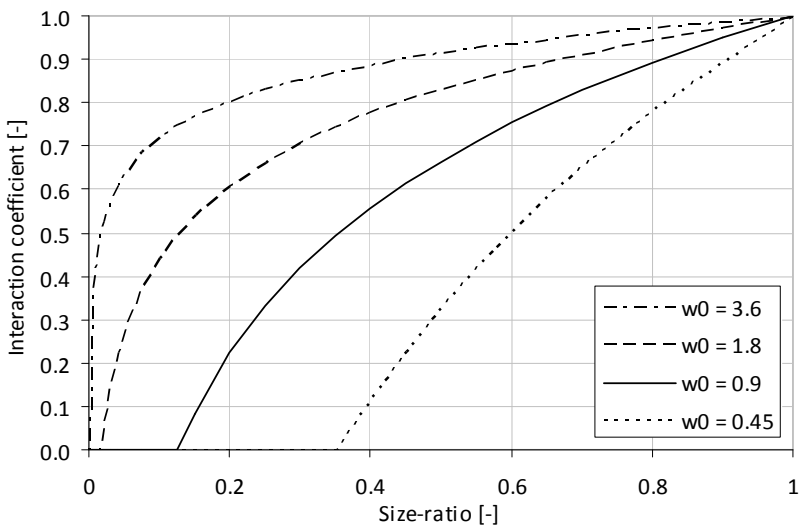

Figure 5.2 Interaction function a_{ij} as a function of the size-ratio for various values of $w_{0,a}$.

$$w_0 = f_{\text{int}}(d_i, d_j) * f_{shape} \quad \text{with} \quad w_0 \geq 0 \tag{5.6}$$

In this equation f_{shape} can be either a shape factor or a function depending on the shape or roughness of size class i in combination with size class j. In this thesis shape is not actively investigated and therefore f_{shape} is fixed at 1, which could be interpreted to represent that all particles in each size class are similarly shaped. In this way shape is only taken into account implicitly trough the packing density of each size class. For information about the influence of particle shape on packing density, reference is made to Stark and Müller (2008). Changes of w_0 due to interaction forces between the particles can be implemented in the function describing the interaction $f_{\text{int}}(d_i, d_j)$. This is elaborated in section 5.2. Furthermore, Equation 5.6 creates possibilities for further extension in the future, for instance to implement the use of superplasticizers.

5.2 Interaction by surface forces

5.2.1 DLVO-theory

As described in section 3.1 for smaller particles the surface-related forces between particles increase in relation to the gravitational volume-related force per particle. Therefore, particles either start to attract or repel each other, depending on the size of the forces. The most commonly used description for particle forces in colloid systems is the DLVO-theory (Derjaguin and Landau, 1941; Verwey and Overbeek, 1948). In the DLVO-theory, repulsive electrostatic double layer forces are compensated by attractive van der Waals forces. In a solution, electrostatic charged particles form, together with surrounding ions of the opposite sign, an electrostatic double layer in which the charge is being balanced. This creates a repulsive force in the solution around the particle. On the other hand, the Van der Waals force is always attractive between materials that are alike. It arises from the interaction of atomic and molecular electric dipoles. Dipole-dipole attraction depends on the atom or molecule type and the distance between the particles. The Van der Waals attraction for micrometer particles in a colloid system can be over one million times stronger than the gravitational force. Therefore, these forces have an important influence on the particle structure and can not be neglected in particle packing modelling of microparticles.

According to the DLVO-theory the stability of a dispersion depends on the attractive van der Waals energy and repulsive electrostatic energy. When particles in a mixture approach each other the double layers of these particles influence each other. The ions in each layer relocate and the free energy in the system increases, which leads to repulsion between the particles. At the same time, the attractive energy increases inversely proportional with the second power of the interparticle distance. Figure 5.4 shows an example of the resulting potential energy curve, which is created by addition of the attractive and repulsive potential curves from Figure 5.3. For small particle distances the attractive energy dominates while at greater distances also the electrostatic energy can dominate. (Kordts, 2005; Stephan, et al., 2008; Tattersall and Banfill, 1983)

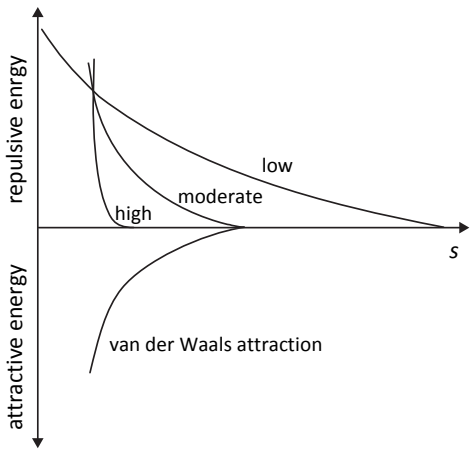

Figure 5.3 Attractive and repulsive energy curves for high, moderate and low ion concentrations in the fluid as a function of interparticle distance s (Tattersall and Banfill, 1983).

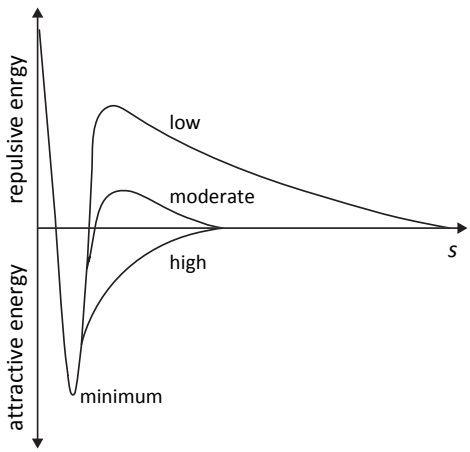

Figure 5.4 Resultant of attractive and repulsive potential energy curves for high, moderate and low ion concentrations (Tattersall and Banfill, 1983).

5.2.2 HADES simulations

Implementation of surface forces

To investigate the influence of the surface-related forces on the packing density and particle structure of a mixture, the discrete element model *HADES* was used. *HADES* works originally with the Hertz contact model (He, 2010; Stroeven, 2006). To be able to simulate agglomerating particles according to the DLVO-theory, a new contact model was added to *HADES*. The contact model calculates whether a cohesive force is working on a particle according to Equation 5.7.

$$F_{total} = F_{el} - F_{vdw} \tag{5.7}$$

The total cohesive force F_{total} working on a particle consists of the repulsive electrostatic force F_{el} and the attractive van der Waals force F_{vdw} [N]. Once a particle comes close to another particle, the forces acting upon both particles are calculated. The Van der Waals forces are described by Equation 5.8.

$$F_{vdw} = A(s)\frac{1}{6}\left(\frac{(d_1 d_2)/(d_1 + d_2)}{2s^2} + \frac{d_1 + d_2}{2d_1 d_2} - \frac{1}{s}\right) \tag{5.8}$$

In which $A(s)$ [Nm] is the Hamaker factor according to Flatt (2004), d is the particle diameter [m] and s is the distance between two particles [m]. The Hamaker factor depends on the material of the particles and the separation distance between the particles. Flatt (2004) investigated the Hamaker factor for silica, quartz, MgO, Alumina and other materials and described it by Equation 5.9.

$$A(s) = A_0\left(C_1 s^2 + C_2 s + C_3\right)\exp\left(-sC_4\right) + C_5 \exp\left(-sC_6\right) \tag{5.9}$$

$A_0 = 1.6E{-}20$

$C_1 = 1.7429E14$ $\quad$ $C_4 = 3.2368E7$

$C_2 = -1.1626E7$ $\quad$ $C_5 = 0.087425$

$C_3 = 0.92551$ $\quad$ $C_6 = 2.7014E6$

The electrostatic force depends on the particle radius, the solvent permeability, the ionic composition and the zeta potential and therefore on the materials and type of fluid used in a mixture. For the implementation in *HADES*, a general equation of the form $1/s^c$ was adopted. In this equation s is the separation distance between particles and always positive. To allow adjustment of the electrostatic force for each material, and thus for each simulation within *HADES*, the general and adjustable Equation 5.10 was implemented.

$$F_{el} = \frac{C_7}{\left(abs\left(s - s_0\right)\right)^{f(d_1,d_2)}} \tag{5.10}$$

The function $f(d_1,d_2)$ can be a constant, but it might also depend on the diameters of the particles approaching each other. This will also lead to a constant value for $f(d_1,d_2)$, but it creates the opportunity to easily adjust the electrostatic force for particles of various sizes. The distance shift s_0 creates the possibility to implement behaviour as caused by superplasticizers by making use of a cut-off value. In a real mixture, the superplasticizer is assumed to stabilize the particles in the fluid and surround them with a thin layer. Over the thickness of this layer (for instance ± 10 nm), particles will not be able to approach each other. In that case a minimum separation distance exists. With Equation 5.10 in *HADES* an impenetrable boundary is created at a distance of s_0 from the particle.

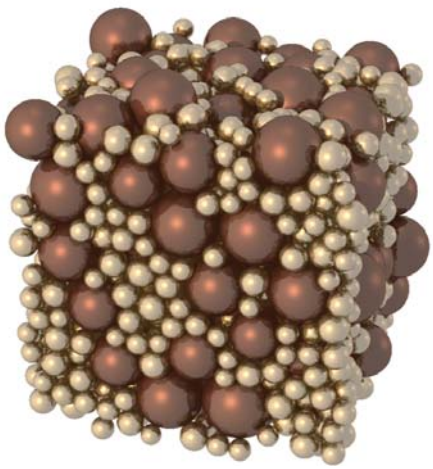

Figure 5.5 HADES simulation of a 3-dimensional container filled with 30% [m^3/m^3] 4 mm spheres and 70% [m^3/m^3] 10 mm particles.

***HADES* simulations coarse particles**

To investigate the influence of agglomerating particles on the packing density and particle structure of a mixture, simulations including the new cohesive contact model are compared to simulations without cohesive contact. This subsection deals with simulations of coarse spheres in the mm range without cohesive contact. In the next subsection the particle structure and packing density of microparticles will be assessed.

In *HADES* a 3-dimensional container is filled with groups of spheres of size d with a uniform distribution [0.8d, 1.2d] in order to create a random particle structure. The average particle diameter d of each group of spheres is varied from 2 to 10 mm in steps of 1 mm. The spheres are compacted by gravitational force only and form a particle structure with a loose packing density. The output of the *HADES* simulation contains all the spheres and their locations. This gives a good view of the real particle structure, such as the particle structure of 4 mm spheres combined with 10 mm spheres as plotted in Figure 5.5. Furthermore, overall packing density as well as local packing density can be studied. The overall packing density is the volume occupied by the particles in a unit volume. The local packing density is defined as the volume occupied by particles in a layer of thickness t within this unit volume. This way a container of 50 mm high can be divided into 50 layers of thickness $t = 1$ mm, creating the possibility to evaluate the wall effect. For instance,

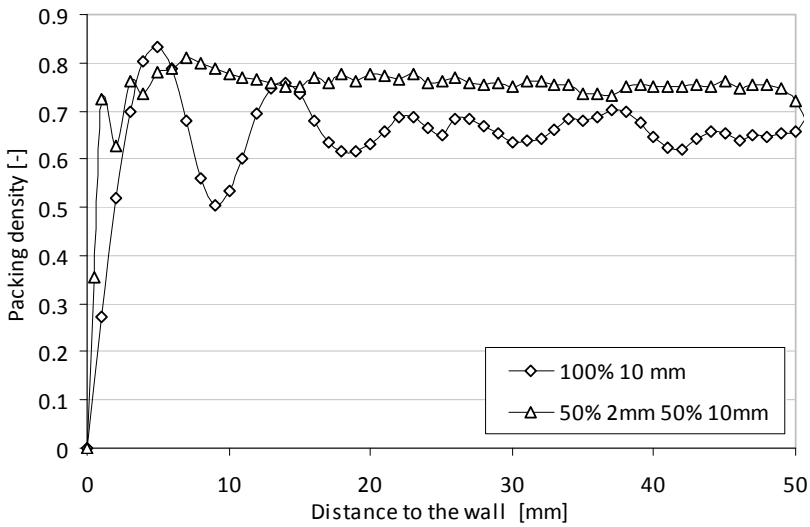

Figure 5.6 Wall effect of a monosized particle mixture with 100% 10 mm spheres compared to a mixture containing 50% 2 mm as well as 50% 10 mm spheres, studied by HADES simulations.

Figure 5.6 shows that the wall effect in a packing of almost uniform spheres influences the packing density over larger distances than in a packing with 50% small spheres and 50% large spheres. Spheres touching the wall are ordered, increasing the local packing density at a distance of 0.5*d* and decreasing the packing density at a distance *d*. This effect remains visible for more than four particle diameters with almost monosized particles. With wider particle size distributions, such as in a mixture with 50% 2 mm spheres and 50% 10 mm spheres, the wall effect reduces.

To minimize the wall effect in the simulations, a sufficiently large container is used, with virtual boundaries. Spheres leaving the container via one of the sidewalls will reappear on the opposite site of the container, thus giving the wall the same 'texture' as the particle structure within the container.

The overall packing density of several mixtures is evaluated and presented in Figure 5.7. In each mixture 10 mm spheres are combined with smaller sized spheres ranging from 2 to 9 mm. The volume distribution is changed in steps of 10% to create particle packing profiles for each size-ratio. Figure 5.7 shows that particle interaction for large size-ratios (d_{small}/d_{large}) is much higher than for small size-ratios. Furthermore, the highest packing density in mixtures with larger size-ratios occurs at lower volume percentages of the 10 mm particle group.

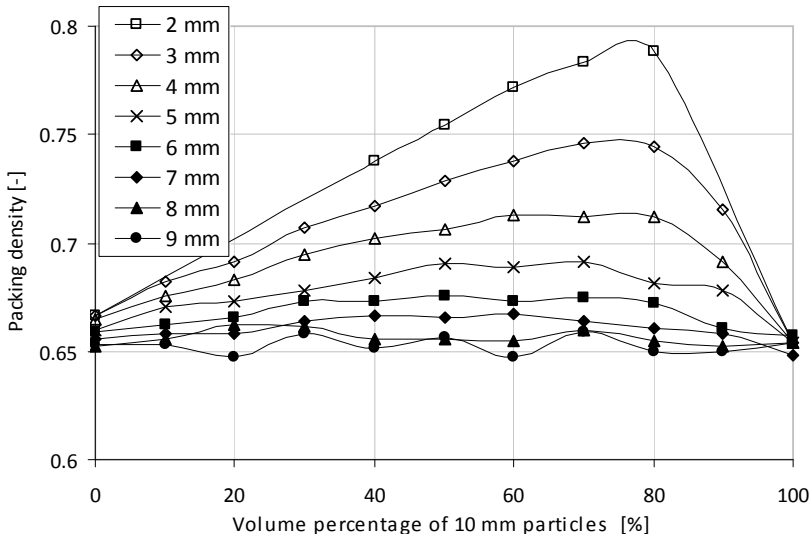

Figure 5.7 Packing density profiles of mixtures containing two particle groups.

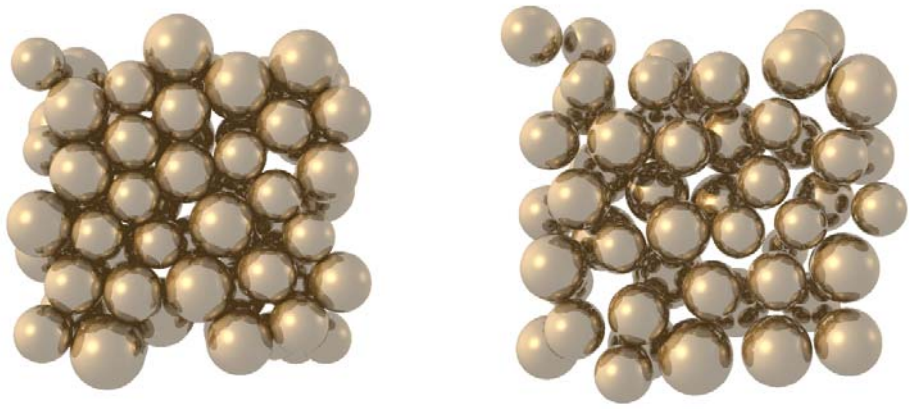

Figure 5.8 Picture of two particles layers from HADES simulations of 10 mm spheres resulting in a packing density of $\alpha_t = 0.654$ *(left hand side) and cohesive 5 µm spheres resulting in a packing density of* $\alpha_t = 0.464$ *(right hand side, scale factor 20000).*

HADES **simulations microparticles**

To investigate the influence of agglomerating particles on the packing density and particle structure of a mixture, mixtures with microparticles were simulated in *HADES*, including the new cohesive contact model. The influence of agglomerating particles on the packing density and wall effect was studied by comparing these simulations with simulations on millimeter particles. In *HADES* a 3-dimensional container was filled with spheres with an average size of $d = 5$ µm and a uniform distribution [0.8*d*, 1.2*d*]. Figure 5.8 shows the differences in the particle structure of the 5 µm spheres compared to the 10 mm spheres. The packing density in these two simulations changed from 0.654 for the 10 mm spheres to 0.464 for the agglomerating microspheres. Furthermore, 5 µm spheres were combined with 20 µm spheres to visualize the differences in wall and loosening effect. In these simulations the small spheres agglomerate with each other, but they also have a high tendency to stick to larger spheres. The effects are visualized in the schematized packing density profiles in Figure 5.9 and as schematized particle structures in Figure 5.10. The maximum packing density in the particle packing profile of the microparticles is reached at a lower volume percentage of the coarse particles when compared to the packing profile of the 10 mm particles. This is because agglomerating particles do not fit as easily between the larger particles as loose particles, see also Figure 5.10. Agglomerating of the

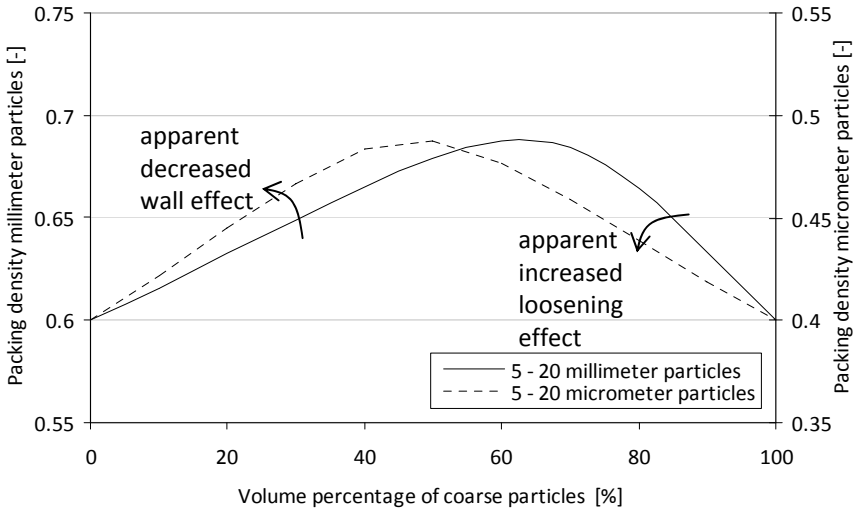

Figure 5.9 Schematized packing density profiles for millimeter particles ($\alpha_i = 0.6$, vertical axis left hand side) compared to micrometer particles ($\alpha_i = 0.4$, vertical axis right hand side) with size-ratio 0.25.

small particles therefore leads to an apparent increase in the loosening effect. Furthermore, when large particles attract smaller particles, the small particles get ordered close to the wall of the large particle. When the small particles have a low packing density due to existing agglomerates, the ordering in the particle structure will decrease the wall effect.

5.2.3 Interaction forces in the Compaction-Interaction Packing Model

For particles smaller than 125 micrometer, surface forces can exceed the gravitational forces, causing particles to agglomerate. Depending on the compaction energy and or mixing process these agglomerates might be broken or dispersed, which is further discussed in section 5.3. Analytical mathematical particle packing models assume certain randomness in the structure. Therefore local effects as adhering small particles on larger particles should be spread out to general overall interaction effects. With adhering small particles on a surface of a larger particle, the larger particle is pushed away from its neighbors to a larger extent than when these small particles are filling up the voids between the large particles. Also small particles will create agglomerates which do not fit

well in the voids between the large particles, thus increasing the loosening effect, Figure 5.10. Of course, both these additional loosening effects depend on the amount of small particles present in the mixture, in a similar way as the original size-related loosening effect.

Furthermore, the small particles are still influenced by the presence of the large particles. However, since the small particles are agglomerating this effect is less pronounced within their own bulk packing density. And adhering of the small particles leads to a high packing density close to the large particles. Both these effects cause that the original size-related wall effect is decreased.

For the implementation of these effects in the Compaction-Interaction Packing Model (CIPM), Equation 5.6 is developed into Equations 5.11 and 5.12.

$$w_{0,a} = f_{\text{int},a}\left(d_j\right) = \begin{cases} w_a * L_a & d_j < 25\mu m \\ w_a & d_j \geq 25\mu m \end{cases} \tag{5.11}$$

$$w_{0,b} = f_{\text{int},b}\left(d_i\right) = \begin{cases} w_b * L_b & d_i < 25\mu m \\ w_b & d_i \geq 25\mu m \end{cases} \tag{5.12}$$

In this equation w_a , w_b , L_a and L_b are constants which will be defined later as $w_a = w_b = 1$, $L_a = 1.5$ and $L_b = 0.2$, see section 5.4.3. This solution seems straightforward, but in combination with Equation 5.4 it already describes interaction effects depending on size-ratio in an advanced way. In Figure 5.11 the interaction function a_{ij} is presented

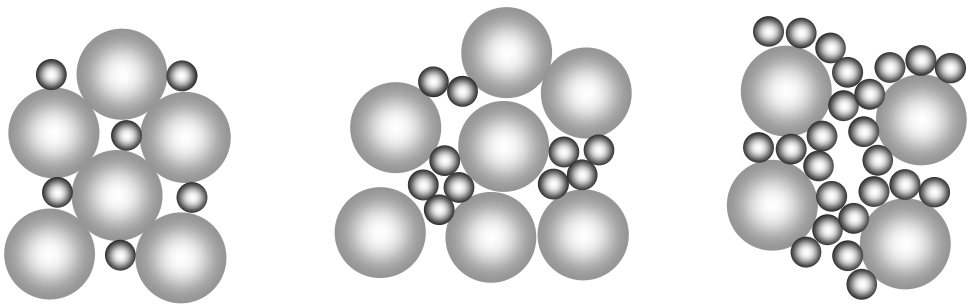

Figure 5.10 Schematization of possible agglomerating effects increasing the loosening effect. From left to right: without agglomeration, small particles agglomerating, small particles agglomerating to large particles.

for $w_0 = 1$ representing particles larger than 25 µm and for $w_0 = 1.5$ representing particles smaller than 25 µm. When two size classes with size-ratio 0.9 (for instance 18/20 µm particles or 18/20 mm particles) are compared, the additional loosening effect due to the surface forces is only slightly increased, Figure 5.11 arrow a. This is reasonable because two particle groups with a high size-ratio are very similar in size and will thus show a comparable tendency of clustering. For a 20 µm particle in combination with a 5 µm particle, the loosening effect increases much more, which is explained by the higher tendency of the smaller particles to agglomerate, Figure 5.11 arrow b. Furthermore, at low size-ratios (below 0.1) and negligible surface forces ($w_0 = 1$), adding small particles led to little or no loosening effect. But now, particles of 1 µm can adhere or agglomerate thus increasing the loosening effect exerted by them on the much larger particles of for instance 20 µm. Therefore, the increase of $w_{0,a}$ has led to an increased range of the size-ratios at which particles influence each other's packing density by a loosening effect, Figure 5.11 arrow c.

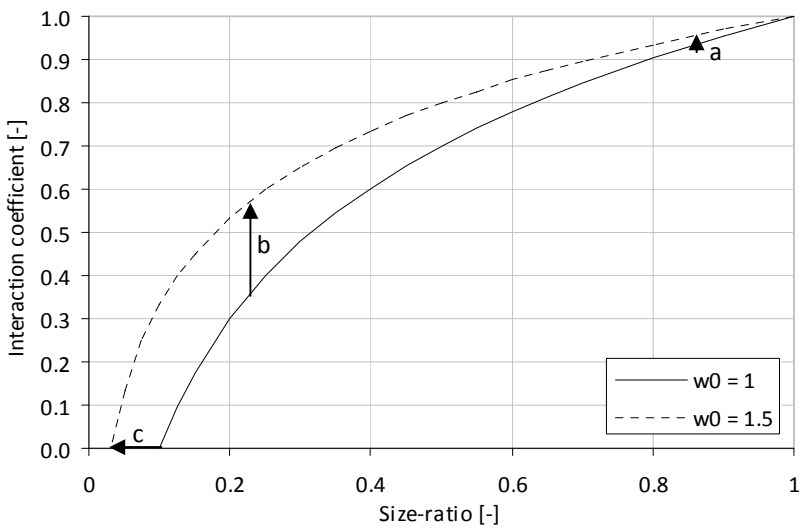

Figure 5.11 Comparison of the loosening effect a_{ij} for geometrical interaction $w_0 = 1$ and for interaction including surface forces for particles smaller than 25 µm $w_0 = 1.5$.

5.3 Compaction

5.3.1 Theory on deformation of the particle structure through compaction

Mixing and compaction are two very important parameters in relation to packing density. A good mixing process creates a well distributed particle structure. After that the applied amount of compaction energy leads to a certain packing density of this mixture. As long as surface forces are negligible these processes can be controlled to a large extent. However, as surface forces increase, also the interparticle friction within a mixture increases, causing processes such as mixing and compacting to lose effectiveness.

Interparticle friction for large particles depends on the mineral composition, texture, angularity, size, particle size distribution and packing density of the particles. Rough texture and high angularity cause particles to interlock with each other, thus reducing possible shear deformation. Angularity and size influence interparticle friction by the dilation distance *h*, where *h* represents the thickness of a layer which has to be lifted in order to overcome the interlock and to enable shear deformation. Particle size distribution influences the amount of interparticle contacts and therefore the interparticle friction. Densely graded mixtures contain more contact area per unit weight of material, which results in higher shear strength. Gap graded mixtures contain less contact area per unit weight of material, which accordingly results in lower shear strength. In the same way, a high packing density increases the interparticle friction and shear strength. Also, within mixtures with a high packing density, particles have less space to rotate and adjust their position with respect to one another, thus minimizing deformation under load.

For coarse particles, a good relation exists between loose packing density, compacted packing density and the virtual packing density. When a higher amount of energy is applied, shear deformation causes particles to pack closer to each other. Experiments on very angular particles in a narrow particle size distribution showed a small deviation from Equation 3.25, but on average the amount of compaction is well represented by the compaction index K_t as defined in the CPM. However, for mixtures containing small particles, surface forces increase the interparticle friction considerably. This means that when a certain amount of mixing or compaction energy is applied to a mixture, larger particles will move their position with respect to one another. But, this same amount of energy might not be large enough to overcome the attractive surface forces, thus resulting in particles to stay agglomerated and not compacted. This means that for small particles,

in calculations with compaction index K_t, the influence of the compaction index on the particle packing should be revised.

5.3.2 Implementation

Within the CPM, the compaction index K_t determines the relation between the real packing density α_t and the virtual packing density β_t. As K_t tends to infinity, the real packing density α_t tends to the virtual packing density β_t, following Equation 3.25. For a monosized particle class, the compaction index $K_t = K_i$ and is constant. For a combination of two size classes $K_t = K_1 + K_2$, in which K_t is constant, but K_i varies according to Equation 5.13.

$$K_t = \sum_{i=1}^{n} K_i = \sum_{i=1}^{n} \frac{r_i/\beta_i}{1/\alpha_t - 1/\beta_{ti}} \tag{5.13}$$

Though, the total compaction index K_t of a mixture remains constant, a higher compaction index is associated with a more abrupt crossover of the K_i values as shown in Figure 5.12. Generally, the compaction index has the largest influence on the dominating size class. In Figure 5.12, with a high amount of 10 mm particles (above 60-65% m^3/m^3) the compaction value K_1 belonging to this size class is always larger than K_2 (representing 4 mm particles). With higher compaction index K_t this effect becomes more pronounced, wereas for $K_t = \infty$ the compaction index for the recessive size class is 0. The total applied compaction energy has less effect on the packing density of the recessive size class compared to the dominating size class.

To implement surface force related interaction effects in combination with the compaction effect as described in section 5.3.1, similar effects as shown in Figure 5.12 should be taken into account. The compaction index K_t should be relatively less effective on the more difficultly compactable small particles and be relatively more effective in compacting the easily compactable larger particles. For a two-component packing this would mean that K_2 (compaction value small particles) has to become lower and K_1 (compaction value large particles) has to become higher. To take this effect into account, the more general form of Equation 5.13 is used as described by (Larrard F. de, 1999) and presented in Equations 5.14 and 5.15.

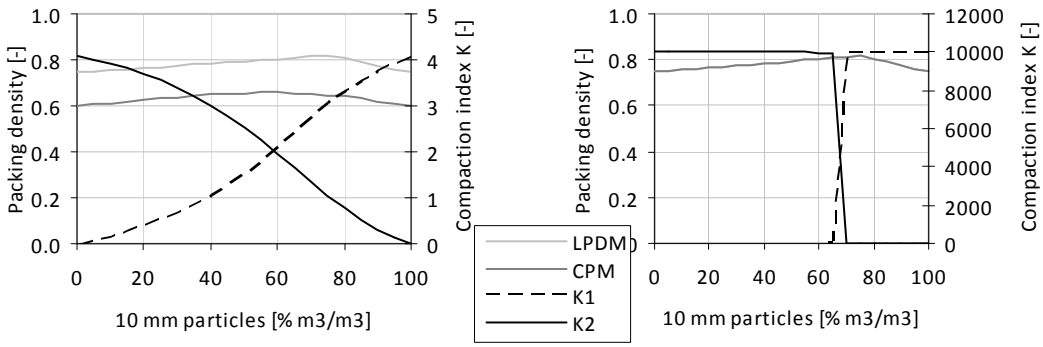

Figure 5.12 Variation of K_1 (compaction value of 10 mm particles) and K_2 (compaction value of 4 mm particles) for a total compaction index $K_t = 4.1$ (left hand side) and $K_t = 10000$ (right hand side) for a mixture consisting of two size classes 4 mm en 10 mm (each $\alpha_i = 0.6$ at $K_t = 4.1$).

$$K_t = \sum_{i=1}^{n} K_i = \sum_{i=1}^{n} \frac{\varphi_i / \varphi_i^*}{1 - \varphi_i / \varphi_i^*} \tag{5.14}$$

$$\varphi_i^* = \beta_i \left(1 - \sum_{j=1}^{i-1} \left(1 - b_{ij} \left[1 - \frac{1}{\beta_j} \right] \right) \varphi_j - \sum_{j=i+1}^{n} \frac{a_{ij}}{\beta_j} \varphi_j \right) \tag{5.15}$$

In these equations, φ_i is the actual solid volume of size class i, while φ_i^* is the maximum volume that size class i may occupy given the presence of the other size classes. By this definition φ_i is always lower than φ_i^*. In order to get a relatively lower K_2, φ_2 / φ_2^* should become lower and/or φ_1 / φ_1^* should become higher. To be able to implement this variance in compaction energy in the CIPM, Equation 5.13 is replaced by Equation 5.14 in which φ_i / φ_i^* is rewritten as Equation 5.16.

$$\frac{\varphi_i}{\varphi_i^*} = \frac{r_i \alpha_t}{\beta_i \left(1 - \sum_{j=1}^{i-1} \left(1 - b_{ij,c} \left[1 - \frac{1}{\beta_j} \right] \right) r_j \alpha_t - \sum_{j=i+1}^{n} \frac{a_{ij,c}}{\beta_j} r_j \alpha_t \right)} \tag{5.16}$$

Using Equation 5.16 instead of Equation 5.13 creates the possibility to increase the loosening effect $a_{ij,c}$ and decrease the wall effect $b_{ij,c}$ as desired according to section 5.2.3. In a mixture consisting of two size classes, a decreased $b_{ij,c}$ leads to an increased φ_i^* and thus to a decreased φ_2 / φ_2^* and lower K_2. The other way around, an increased $a_{ij,c}$

leads to a decreased φ_i^* and thus to an increased φ_1/φ_1^* and higher K_1. Therefore, $a_{ij,c}$ and $b_{ij,c}$ are defined as presented in Equations 5.17 and 5.18, where C_a and C_b are constants which will be defined in section 5.4.3 as $C_a = 1.5$ and $C_b = 0.2$. Notice that, when a varying compaction index is used in this way, the interaction coefficients a_{ij} and b_{ij} in Equations 5.1, 5.4, 5.5, 5.11 and 5.12 representing the virtual packing density do not have to be the same as $a_{ij,c}$ and $b_{ij,c}$ in Equations 5.16, 5.17, and 5.18. Furthermore, it is important to keep in mind that φ_i should always be lower than φ_i^*, so that if C_b in Equation 5.18 is chosen to be lower than 1, the minimum value for C_b is not independent of L_b and C_a. Whenever C_b is relatively too small, the eventual packing density a_t will appear to be higher than the virtual packing density, which is not possible. To prevent that this problem occurs, values of C_a lower than L_a and values of C_b lower than L_b should be chosen with care.

$$a_{ij,c} = \begin{cases} 1 - \dfrac{\log\left(d_i/d_j\right)}{w_{0,a}} & \log\left(d_i/d_j\right) < w_{0,a} \\ 0 & \log\left(d_i/d_j\right) \geq w_{0,a} \end{cases} \qquad w_{0,a} = \begin{cases} w_a * C_a & d_j < 25\mu m \\ w_a & d_j \geq 25\mu m \end{cases} \tag{5.17}$$

$$b_{ij,c} = \begin{cases} 1 - \dfrac{\log\left(d_j/d_i\right)}{w_{0,b}} & \log\left(d_j/d_i\right) < w_{0,b} \\ 0 & \log\left(d_j/d_i\right) \geq w_{0,b} \end{cases} \qquad w_{0,b} = \begin{cases} w_b * C_b & d_i < 25\mu m \\ w_b & d_i \geq 25\mu m \end{cases} \tag{5.18}$$

5.3.3 Influence of compaction values

To show the effect of varying C_a and C_b in Equations 5.17 and 5.18, some CIPM simulations were made. The simulated mixtures consist of two size classes of 4 µm and 10 µm, which each have a $\alpha_i = 0.6$ at $K_t = 4.1$. For comparative reasons w_a, w_b, L_a, L_b, C_a and C_b are all fixed at 1 to create a reference mixture. When the wall effect is decreased by decreasing C_b to 0.2 and the loosening effect is increased by increasing C_a to 1.5, this leads to an increased value of K_1 and a decreased value of K_2 as described in section 5.3.2. Figure 5.13 shows that compaction value K_2 including compaction-interaction is always equal to or smaller than K_2 without additional compaction-interaction. This effect on K_1 and K_2 becomes stronger as K_t becomes higher. Furthermore, this effect on K_2 is comparable to a change from $K_t = 16$ to $K_t = 4.1$, showing the loss of effectiveness of compaction on the smaller size class compared to the large size class.

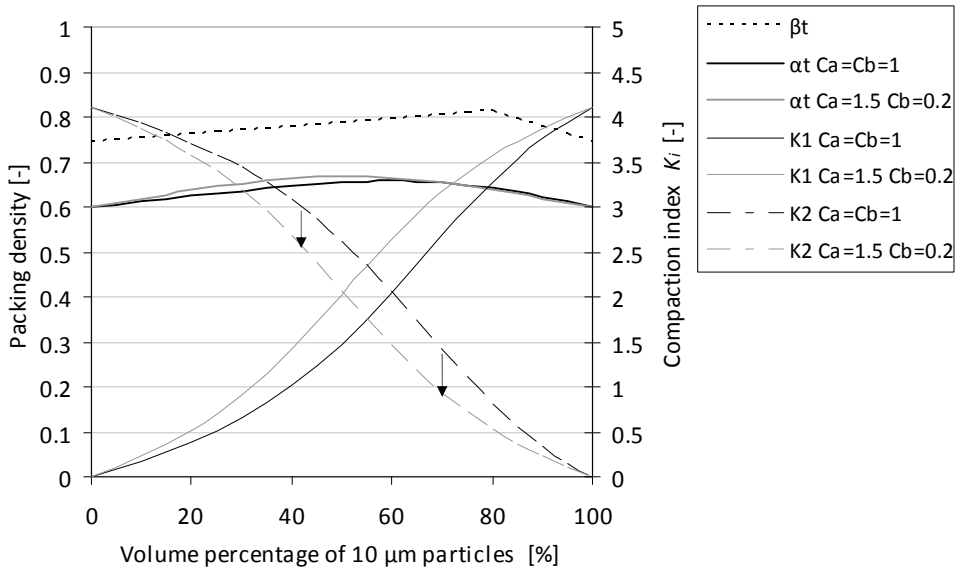

Figure 5.13 Variation of K_1 and K_2 for a compaction index $K_t = 4.1$ for a mixture consisting of two size classes of 4 µm and 10 µm (each $\alpha_i = 0.6$ at $K_t = 4.1$). In black, reference simulations with $L_a = L_b = C_a = C_b = 1$, in gray $L_a = L_b = 1$, $C_a = 1.5$ and $C_b = 0.2$.

Changing C_a and C_b as proposed in section 5.3.2 lowers the effectiveness of the compaction index K_t on the smaller particles. However, this happens independently of factors L_a and L_b, which is shown by the example presented in Figure 5.14. The reference mixture consists of two size classes of 4 µm en 10 µm ($\alpha_i = 0.6$, $K_t = 4.1$) with $L_a = L_b = C_a = C_b = 1$. Variance is made in $L_a = L_b = 0.5$ and $L_a = L_b = 1.5$ while C_a and C_b are kept constant. Figure 5.14 shows that the final packing density α_t for each simulation is the same. This example illustrates that the compaction-interaction effect is purely made in the $a_{ij,c}$ and $b_{ij,c}$ coefficients of Equation 5.16 and is not affected by the relation L_a or L_b. This could also be concluded from Equations 5.14 and 5.16, where α_t is only dependent of the mixture composition r_i, r_j, monosized packing densities β_i, β_j and compaction index K_t, and thus not of β_{ti}.

This conclusion implies that when Equation 5.16 is used, L_a and L_b might be chosen arbitrary to be any value above 0. However, for consistency, mathematical robustness and physical interpretation of the CIPM, L_a is set to be C_a ($a_{ij,c} = a_{ij}$) and L_b is set to be C_b ($b_{ij,c} = b_{ij}$). In this way the virtual packing density always remains larger than the compacted one. Furthermore, if no additional fitting or modelling is required, the usage and calculation procedure are simplified because Equation 5.13 is still valid.

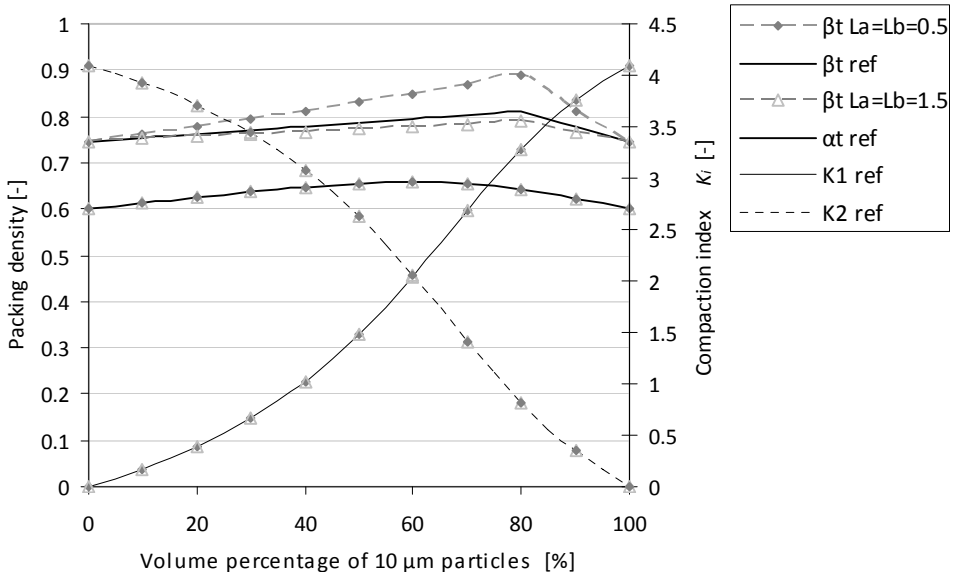

Figure 5.14 Variation of packing density, K_1 and K_2 for a compaction index $K_t = 4.1$ for a mixture consisting of two size classes of 4 µm and 10 µm (each $\alpha_i = 0.6$ at $K_t = 4.1$). In black, reference simulations with $L_a = L_b = C_a = C_b = 1$, in gray mixtures with $L_a = L_b = 0.5$ and $L_a = L_b = 1.5$.

5.4 Compaction-Interaction Packing Model: user information

5.4.1 From experiments to modelling

The Compaction-Interaction Packing Model (CIPM) as presented in the previous sections calculates the packing density of a mixture at a certain compaction index K_t. With coarse monosized particles, experimental compaction values K_{exp} comply with the K_t values in the simulation, and real mixtures can easily be compared to the calculated packing density from the model. Therefore, monosized particle classes can be directly used as input for the model. In that case the measured packing density α_{exp} is put in the model as α_i for a certain compaction index $K_{\text{exp}} = K_t$. Furthermore, Equation 5.19 can be used to recalculate packing densities if packing densities at different compaction indexes are required.

However, small particles often have a broad particle size distribution, due to which they can not be represented by a single size class. In that case the measured packing density α_{exp} of a filler complies with the total packing density α_t of this mixture. Then α_t is the total packing density as it would be calculated from that filler consisting of several size

classes. So, materials with broad particle size distributions can not directly be put into the model and should be implemented as explained below.

$$\beta_i = \left(1 + \frac{1}{K_{\exp}}\right)\alpha_i = \left(1 + \frac{1}{K_t}\right)\alpha_t \qquad \text{for monosized particles} \qquad (5.19)$$

For mixtures containing multiple size classes, Equation 5.19 is not valid. This means that the packing density $\alpha_{\exp} = \alpha_t$ at a certain compaction index $K_{\exp} = K_t$ is not constantly related anymore to α_t at a higher or lower compaction index K_t for mixtures of multiple size classes. Figure 5.15 demonstrates this for a mixture consisting of two size classes. At 0% and 100% only one monosized particle class is present, leading to a constant relation between α_t at $K_t = 4.1$ and α_t at $K_t = \infty$, as shown by arrows A and B. Arrows C and D, which have the same size as A nad B, show that within a mixture consisting of two monosized particle classes the ratio between α_t at $K_t = 4.1$ and α_t at $K_t = \infty$ varies. With higher K_t values these differences become smaller, since the CIPM tends to the virtual packing density β_t for high K_t values.

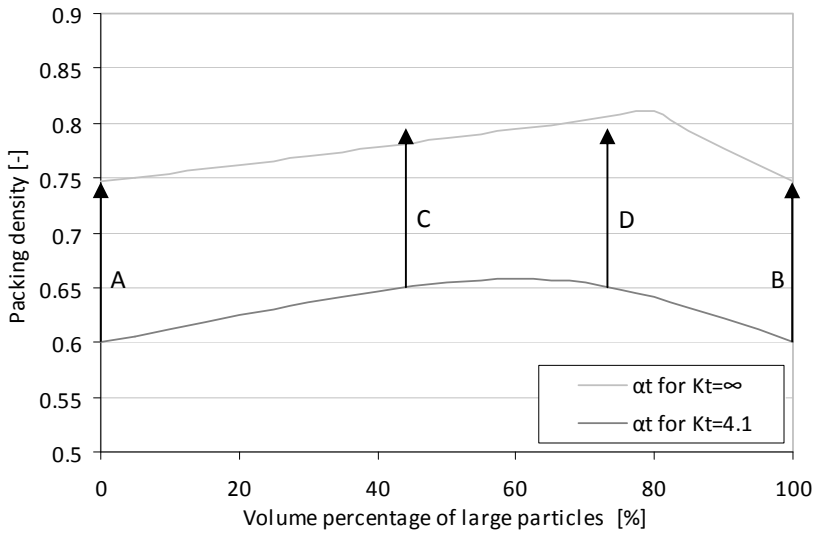

Figure 5.15 Packing density profiles of a mixture consisting of two size classes of particles for $K_t = 4.1$, $K_t = \infty$.

Materials such as cement or fillers often cover multiple size classes. Their particle size distributions easily comprehend ranges from $d_{\min}/d_{\max} = 0.01$. In most cases the experimental packing densities of these materials are determined on the material group instead of on each monosized particle class individually. This makes it impossible to use the measured packing density of the material $\alpha_{\exp}$ directly as input in the CIPM, since the CIPM requires a packing density α_i for each size class. The solution is to use the CIPM reversely, by calculating α_i from α_t instead of following the normal procedure to determine α_t from the known packing densities of the size classes. This is important in the CIPM model because of the way the interaction due to surface forces is implemented. For instance, quartz powder M600 as used in chapter 4 is not well represented by its mean diameter and should be divided into several size classes. For the size classes smaller than 25 µm the experimental compaction index $K_{\exp}$ applied to the total mixture will not densify the packing of the small particles as effectively as it compacts the larger particles. Normally this means that, with known $\alpha_i's$ for each size class, the total packing density α_t is influenced. Now that the CIPM is used reversely to determine each α_i, these α_i values will also differ from the values when determined without compaction-interaction. Table 5.1, shows the result of the reverse calculation of quartz powder M600 with a measured $\alpha_{\exp} = 0.527$ at $K_{\exp} = 12.2$. The quartz powder is first divided into 8 size classes according to the known particle size distribution. Then the CIPM is fixed to $\alpha_t = 0.527$ at $K_t = 12.2$ and the values for α_i are determined under the assumption that each size class has the same α_i value. Using the CIPM including compaction-interaction ($L_a = C_a = 1.5$, $L_b = C_b = 0.2$), a packing density $\alpha_i = 0.385$ is found. This value of $\alpha_i = 0.385$ is lower than it would have been if the mixture was simulated without compaction-interaction of the small particles ($L_a = L_b = C_a = C_b = 1$), which would give $\alpha_i = 0.419$. Therefore, in the case of a material covering multiple size classes, α_i should be seen as a comparative input parameter which depends on the model itself. Since the CIPM was developed under the assumption of representing each material by a number of size classes with a constant packing density α_i, it is very important to always use α_i in the model as described above. If α_i is not taken as a constant value for each size class of a certain material, also the compaction-interaction should be modeled in a different way.

5.4.2 Input

When using the CIPM, creating more size classes will lead to higher precision, but particle size measurements should be available. Especially for materials with overlapping particle size distributions this is very important. On the other hand, an increasing amount of size classes will slow down the calculation process, which is no problem for a single mixture but is important when mixture optimization is requested. It is suggested to divide materials into size classes with size-ratios ranging from 0.5 to 0.9, also depending on the particle size measurement data available. Furthermore, the CIPM is developed to be used with constant α_i within each material group, as presented in the input example in Table 5.1. The model determines a constant α_i (in *italics*) for each size class from the known particle size distribution, K_t and the measured packing density $\alpha_t = \alpha_{\text{exp}}$. In this way, input only depends on the experimental data and no knowledge of particle interactions is requested from the user.

Table 5.1 Example on how to revert experimental data to CIPM input by determination of α_i values.

Material		Particle size distribution		α_i by CIPM
		d [μm]	*r* [%]	
M600 size class 1	12.2	60.7	0.04	*0.385*
M600 size class 2	12.2	28.3	0.44	*0.385*
M600 size class 3	12.2	13.2	6.16	*0.385*
M600 size class 4	12.2	6.1	24.98	*0.385*
M600 size class 5	12.2	2.9	37.23	*0.385*
M600 size class 6	12.2	1.3	25.43	*0.385*
M600 size class 7	12.2	0.6	5.69	*0.385*
M600 size class 8	12.2	0.3	0.05	*0.385*
M600 total mixture	$K_{\text{exp}}=K_t=12.2$		**100**	$\alpha_{\text{exp}}=\alpha_t=0.527$

5.4.3 Compaction-interaction values

CIPM should be seen as an additional module to the Compressible Packing Model (Larrard, 1999). It is developed based on interaction and friction effects as numerically simulated with *HADES*. The final values for the interaction coefficients in Equations 5.17 and 5.18 were determined from the experimental data in chapter 4, leading to the values $w_a = w_b = 1$, $L_a = C_a = 1.5$ and $L_b = C_b = 0.2$. For aggregates these values of $w_a = w_b = 1$ were checked with theexperimental data presented in (Larrard, 1999, section 1.2.2). Compared to the Compressible Packing Model, the new Compaction-Interaction Packing Model performs slightly better for the crushed aggregates and slightly worse for the rounded aggregates. Comparing the CIPM to the experimental data resulted in an average error of 1.1%.

The results of the packing density calculations for various combinations of quartz powders are presented in Figure 5.16 and Appendix E. Figure 5.16 clearly shows the increase of the model performance by the implementation of the compaction-interaction module for $w_a = w_b = 1$, $L_a = C_a = 1.5$ and $L_b = C_b = 0.2$. It demonstrates an improvement of the average error from 3.8% to 1% and maximum error from 6.4% to 1.8%.

$$w_{0,a} = \begin{cases} w_a + C_8\left(\dfrac{d_{ci} - d_j}{d_{ci}}\right) & 0 < d_j < d_{ci}\ ,\ C_8 > -w_a \\ w_a & d_j \geq d_{ci} \end{cases} \tag{5.20}$$

In the CIPM, packing density, particle size distribution, compaction and interaction by surface forces are taken into account. This means that material properties such as particle shape and texture are only taken into account indirectly within the measured packing density. Large variations between materials in texture and shape, especially high aspect ratios, will decrease the accuracy of the CIPM as presented in this chapter. However, the open structure of Equations 5.4-5.6 creates possibilities for further extensions of the model. For instance, the effect of different types of superplasticizer was not investigated in this research. It is recognized that with different materials and different types of superplasticizer, interaction constants as well as the cut-off value d_j and d_i in Equations 5.17 and 5.18 for the size of still agglomerating particles, might vary. For instance, with lignosulfonate based plasticizers, the dispersion is based on an entirely different

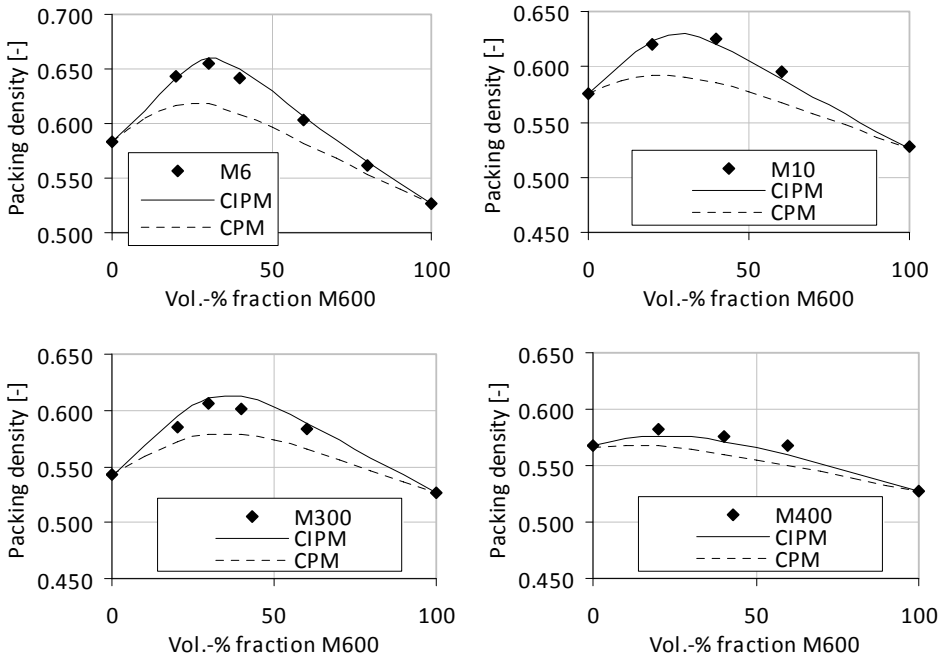

Figure 5.16 Experimental wet particle packing densities at $K_e = 12.2$ compared to calculated packing densities from the original CPM and the new CIPM at $K_t = 12.2$.

mechanism than with the polycarboxylate ether as used in this research. This could lead to a possible implementation of an equation such as 5.20 instead of Equations 5.17 and 5.18, with d_{ci} as cut-off diameter below which compaction-interaction is taken into account. Therefore, it is recommended to further investigate the influence of particle shape and superplasticizers on packing density of small particles to see whether it should be implemented in the CIPM.

5.5 Concluding remarks

In this chapter a particle packing model including compaction and interaction is presented. First the interaction formulas were adjusted in such a way that scaling of the interaction was made possible. This way also the influence of varying particle shapes might be implemented in the future.

The interaction due to the surface forces of the small particles was evaluated with the help of the discrete element model *HADES*. It was found that due to agglomeration the loosening effect increases. At the same time the wall effect of larger particles on small agglomerating particles decreases when the small particles start to stick to these larger particles. These effects were implemented in the interaction formulas. Because these additional interaction effects also influence the distribution of the compaction energy over the various size classes, the effect of varying compaction values in the model was studied. Combining the compaction and interaction has eventually led to the Compaction-Interaction Packing Model as presented by Equations 5.1, 5.13, 5.17-5.19.

The model can be used on any number of size classes, but it is recommended to select the size-ratio between two succeeding size classes between 0.5 and 0.9. Furthermore, when α_{exp} is not determined on a material with monosized particles ($\alpha_i \neq \alpha_{\text{exp}}$), the CIPM should be used first to determine an α_i value for all size classes of that material. The CIPM was developed under the assumption of representing each material by a number of size classes with a constant packing density α_i, so it should be used correspondingly. Furthermore, the values of $L_a = C_a = 1.5$ and $L_b = C_b = 0.2$ were determined with mixtures including superplasticizer Glenium 51, so for other types of superplasticizer these values should be checked first. For the mixtures with particles smaller than 125 µm (Appendix D) using the CIPM improved the average error in the packing density calculations from 2.2% to 0.6% and the maximum error from 6.4% to 1.8%.

6 Cement paste and mortar experiments

Chapter 6 presents the results of the experimental investigations on particle packing, water demand and strength of ecological mixtures. Based on the results of chapter 4, main factors in the design of ecological concrete are implemented in the setup for the experimental program in section 6.1. The packing densities of mixtures containing various amounts of cement and/or filler are presented in section 6.2 and compared to calculations from the CIPM (chapter 5). The packing densities are related to flowability and water demand in section 6.3. Relations between packing density and cement reaction are determined on the basis of isothermal conduction calorimetry measurements in section 6.4. Furthermore, section 6.4 investigates the packing density, water demand and cement reaction and their influence on strength. In section 6.5 the relations found in previous sections are assessed to be used in chapter 7 for the design method for ecological concrete.

6.1 Experiments

6.1.1 Introduction

The water demand and water/cement ratio of ecological concrete mixtures are dominating parameters with regard to workability and strength. In chapter 4 it is concluded that strength can be the general design parameter for the mechanical properties of ecological concrete. However, water demand, the use of superplasticizers and the requested workability determine whether the ecological concrete mixtures can be designed and cast with the desired water/cement ratio. Ecological concrete mixtures with a very low powder content are more sensitive with regard to water demand, because of the low amount of paste in these mixtures. Furthermore, when the cement content is very low, small changes in the applied amount of water can lead to large changes in the water/cement or water/binder ratio. Therefore, it is important to be able to predict the necessary amount of water in ecological concrete mixtures. For this reason, the influence of water demand in relation to packing density and strength was investigated.

The mixtures with their design parameters and their measured properties are presented in subsections 6.1.2 and 6.1.3. In the mixture compositions and the evaluation of these mixtures, the influence of water absorption and air content is neglected. The mixture compositions and the properties resulting from direct measurements can be found in Appendix E. The mixtures and their properties are first evaluated based on the direct measurements and subsequently analyzed in relation to theoretical packing density characteristics. The experimental results of the cement pastes and mortars are related to packing density in section 6.2. In section 6.3 the packing density is analyzed in relation to flowability of the mixtures and in section 6.4 in relation to strength measurements.

6.1.2 Mortar mixtures with cement

The first aim of the experiments presented in this chapter was to find relations between packing density, water demand and flowability. To eliminate as much variables as possible it was chosen to design test series with a constant water/cement ratio in combination with various amounts of different sizes of sand. Rounded river sand was used in five different size fractions; 0.125-0.25, 0.25-0.5, 0.5-1, 1-2, 2-4 mm (Appendix A). From each size fraction of sand, the packing density was determined experimentally. Then it was calculated how much cement paste was required to fill the voids between the sand

particles. Mixtures were composed of 2 kg of sand plus the amount of cement paste to fill the voids plus an additional amount of excess paste to allow the mixture to flow. The amount of excess paste was varied as 150, 200, 250, 300, 350 or 500 grams depending on the size fraction of sand and the stability of the mixtures. Some mixtures were too fluid or did not flow enough, but for each sand fraction at least three different amounts of excess pastes were used. The mixtures were composed with cement paste with a water/cement ratio of 0.5. They are presented as mixtures F1-F18 in Appendix E. The mixtures in series G were designed in the same way as series F, but with a water/cement ratio of 0.4.

Furthermore, mixtures were designed with a combination of two sizes fractions of sand. The same design concept was used, in which part of the cement paste fills the voids and part of it acts as excess cement paste to allow flowability. By combining sand of size 0.25-0.5 mm with 1-2 mm, mortar mixtures were created with the same packing density of the aggregates but with a varying particle size distribution. Excess cement paste was added as 200 gram (mixture F19-F23, G13-G17) or 350 gram (mixtures F24-F27, G18-G20) to 2 kilogram of sand.

Series F and G were especially designed to determine the influence of the packing density and of the sand size on the flowability of concrete. Because of the difference in water/cement ratio between the two series also differences in the amount of water could be investigated. Furthermore, series H was designed including three different water/cement ratios and varying amounts of cement paste (Appendix E). This series was added because the particle size distribution of the sand was similar to CEN reference sand used for standard mortar tests, so that also strength could be related to water/cement ratio and packing density.

6.1.3 Mixtures including quartz powder

A second aim of the experiments was to investigate the influence of packing density on strength. In chapter 4 it was concluded that the influence of the packing density and particles size distribution of the aggregates on the strength was much lower than the influence of the cement paste and filler composition. Therefore, in these series, fillers were used to find out whether differences in strength can be explained by packing density and water demand of the mixtures. At this point it was already concluded from a first evaluation of the cement paste mixtures of series F, G and H that all the particles in a mixture, including the small sized particles such as cement, should be taken into account

in the packing density. To be able to create mixtures with similar compositions with regard to water/cement ratio and cement/filler ratio, it was decided to use one type of filler in various size fractions. Furthermore, since very small reactive fillers or binders are known to react faster than coarser binders, an inert filler was chosen instead of a binder. The quartz powder in this investigation is regarded as inert and it is commercially available in various ground size fractions originating from the same quartz sand.

All the test series were based on cement replacements of 10, 20, 30 and 40% [kg/kg] by quartz powder. The quartz powders M6, M300 and M600 were selected based on experience from chapter 4 and their particle size distribution. M6 is slightly coarser than the cement, M300 is slightly smaller than the cement particles and M600 particles are much smaller than cement. Each series consisted of at least thirteen mixtures; one reference mixture and four mixtures with varying quartz powder contents for three size fractions of quartz powder.

Series C consisted of only pastes, so no aggregate was included (see Appendix E). This made it possible to test these mixtures on water demand or packing density by the mixing energy method. Furthermore, the pastes were tested on viscosity by a small scale coaxial cylinder viscometer. The heat generation of these cement pastes was determined by isothermal calorimetry measurements. The results were used to determine relations between packing density and viscosity and between packing density and thermal energy. Additionally, the thermal power and thermal energy could be compared to the strength tests from series E. Mixtures C2-C13 had a constant water/powder ratio which led to a varying water/cement ratio. Therefore, for evaluation purposes, mixtures C14-C17 were designed with the same water/cement ratios as mixtures C2-C13.

In series D and E, the pastes of series C were tested in standardized mortar tests on slump, slump flow, flow value and strength (NEN-EN 196-1:2005). Series D was performed according to the standards with a water/powder ratio of 0.5 without superplasticizer. However, it was expected that, especially with these fine quartz powders, packing density would be negatively influenced by the lack of superplasticizer. Therefore, series E was tested, including 1.2% Glenium 51 per kg of powder. To create stable, non-segregating mixtures, the water/powder ratio was lowered to 0.37. Compositions and measurements are presented in Appendix E.

6.2 Packing density

6.2.1 Packing density measurements

The maximum packing densities of sixteen pastes were tested by the mixing energy method. The procedure is described in section 4.2.3. The mixtures consisted of cement (CEM I 42.5 N ENCI Maastricht), quartz powder (M6, M300, M600 Sibelco) or a combination of both (see also Appendices A and E). The cement replacement by quartz powder was 10, 20, 30 or 40% [kg/kg] of the total powder weight. All mixtures consisted of 1500 grams of dry powder to which the water and superplasticizer (Glenium 51 BASF con.35%) were added in order to measure the packing density. For mixture compositions and results, see Table 6.1 and Appendix E, Table E.1.

Table 6.1 Mixture compositions and averaged results of mixing energy tests.

		Quartz powder				
Mixture	CEM I 42.5 N	M6	M300	M600	Glenium 51	α_{exp}
	[g]	[g]	[g]	[g]	[g]	[-]
C1	1500				18	0.604
C2	1350	150			18	0.606
C3	1200	300			18	0.610
C4	1050	450			18	0.616
C5	900	600			18	0.614
C6	1350		150		18	0.602
C7	1200		300		18	0.605
C8	1050		450		18	0.601
C9	900		600		18	0.603
C10	1350			150	18	0.649
C11	1200			300	18	0.669
C12	1050			450	18	0.669
C13	900			600	18	0.666
C18		1500			18	0.583
C19			1500		18	0.542
C20				1500	18	0.527*

**Due to required high mixing energy, one measurement only*

As shown in Table 6.1 and Figure 6.1, only the very fine quartz powder M600, which is much finer than cement, has a very large influence on the packing density α_e of the cement paste. An increase in packing density from 0.604 to 0.669 complies with, in terms of water demand, a decrease in the water/powder ratio from 0.21 to 0.16.

6.2.2 *Packing density evaluation CIPM*

The measured packing densities of the cement pastes from series C are compared to the calculated packing densities by the CIPM in Figure 6.1. For the mixtures presented, the prediction of the CIPM is consequently too low, with an average error of 2.4% and a maximum error of 4.6%.

Furthermore, the various cement pastes with 10, 20, 30 and 40% [kg/kg] quartz powder as used in series C were used to prepare mortar mixtures. Figure 6.2 shows the predicted packing densities by the CIPM of mortar mixtures consisting of sand, and the various cement pastes. The mixture compositions are presented in Appendix E as series E. The packing densities of the mortar mixtures containing M6 and M300 only show small differences, while the packing density of mixtures containing M600 are considerably

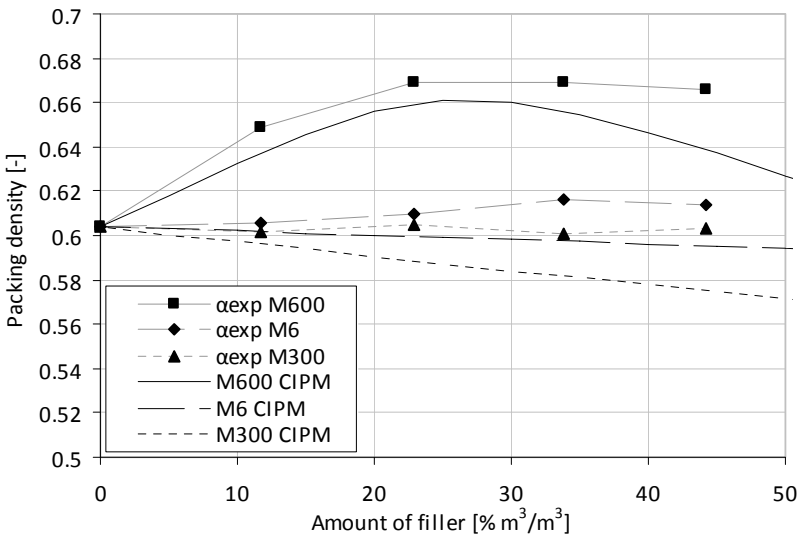

Figure 6.1 Measured packing densities of cement and quartz powder M6, M300 and M600, compared to theoretical packing densities calculated by the CIPM (K_t = 12.2).

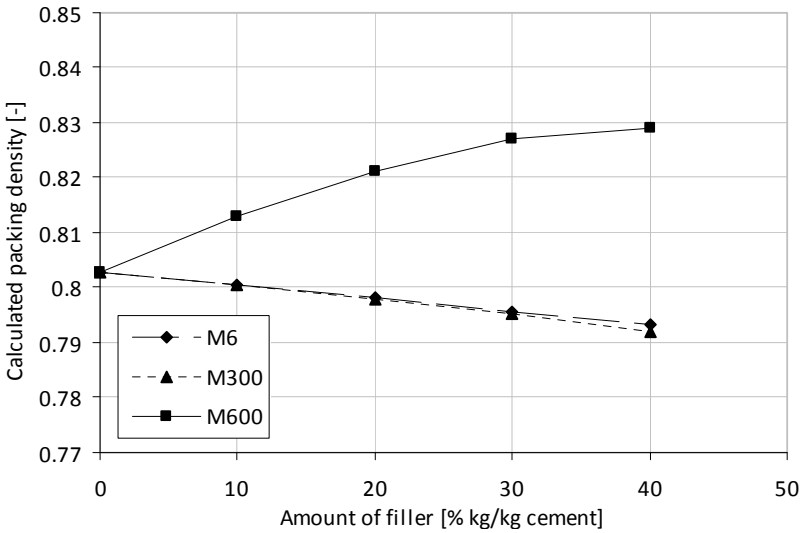

Figure 6.2 Packing densities calculated by the CIPM of mortar mixtures series E (K_t = 9).

higher. This is consistent with the particle packing measurements of the cement pastes only. The packing densities as presented in Figure 6.2 are used for further evaluation in the next sections.

6.2.3 Suitability analysis of fillers

The suitability of a filler to be used in ecological concrete can be evaluated on the basis of the measured or calculated packing density. For this evaluation a unit volume is filled with a stable particle structure in which the voids are exactly filled with water. A stable particle structure is defined as a structure of particles in which all particles are in contact with one or more particles in such a way that the particle structure is stable under the influence of gravity. A stable particle structure can exist with a loose packing density or a densely vibrated packing density and thus its packing depends on the measurement or calculation method and its accompanying K value.

The basis for evaluating the filler is a stable particle structure consisting of 100% cement particles with a packing density α_t (at $K_t = 12.2$). In a unit volume, the voids between the cement particles will be exactly filled with water when a volume of water $V_w = 1 - \alpha_t$ is added. For this 'mixture' the water/cement ratio can be determined according to Equation 6.1.

$$wcr = \frac{m_w}{m_c} = \frac{\rho_w V_w}{\rho_c V_c} = \frac{\rho_w (1-\alpha_t)}{\rho_c \alpha_t} \tag{6.1}$$

When replacing some of the cement particles by a filler, the packing density of the stable particle structure (at $K_t = 12.2$) will change. When the packing density α_t increases, the volume of water necessary to fill the voids decreases, thus having a positive effect on the wcr. However, at the same time the percentage of the cement particles in the packing structure decreases. Therefore, a decreasing volume fraction of the cement particles r_c, will increase the water/cement ratio.

Replacing cement by an inert filler is beneficial, when the packing density increases so much that the water/cement ratio can remain constant at increasing replacement levels. To determine the water/cement ratio of a stable particle structure consisting of cement and filler Equation 6.2 can be used. α_t is the packing density of a mixture and r_c the volume fraction of the cement particles. In that case the volume fraction of the filler is $r_f = 1 - r_c$.

$$wcr = \frac{\rho_w V_w}{\rho_c V_c} = \frac{\rho_w (1-\alpha_t)}{\rho_c r_c \alpha_t} \tag{6.2}$$

Equation 6.2 can be used to determine whether the water/cement ratio of the mixture including the filler is higher or lower than the original mixture consisting of 100% of cement. The other way around it can be used to create design graphs which can directly be used to evaluate the suitability of the filler. In Figure 6.3 the solid black line $\alpha_{wcr=c}$ represents the packing density at which the wcr remains constant for increasing amounts of filler. $\alpha_{wcr=c}$ is determined by Equation 6.3, which is derived from Equation 6.1 and 6.2 for the water/cement ratio of a stable particle structure of 100% cement particles with packing density α_c.

$$\alpha_{wcr=c} = \frac{\rho_w}{\frac{\rho_w (1-\alpha_c)}{\rho_c \alpha_c} \rho_c r_c + \rho_w} \tag{6.3}$$

When mixtures consisting of cement and fillers have a higher packing density than $\alpha_{wcr=c}$, the high packing density causes the *wcr* to decrease. Inert fillers with this capacity are very useful when designing ecological concrete. However, powders can also behave as binders and contribute to the hydration process of the concrete mixture. Therefore another design rule is fixed by $\alpha_{wbr=c}$, Equation 6.4. Binders with packing densities above this line in Figure 6.3 are suitable to use in ecological mixture design. Fillers or binders complying with these design rules are suitable for the design of ecological concrete mixtures. However, if a filler or binder does not comply with the design rules it can still be suitable to use, because of other beneficial effects such as the ball-bearing effect of fly ash. In that case, further research on real concrete or mortar mixtures is required.

$$\alpha_{wbr=c} = \frac{\rho_w}{\frac{\rho_w(1-\alpha_c)}{\rho_c\alpha_c}(\rho_c r_c + k\rho_b r_b) + \rho_w} \tag{6.4}$$

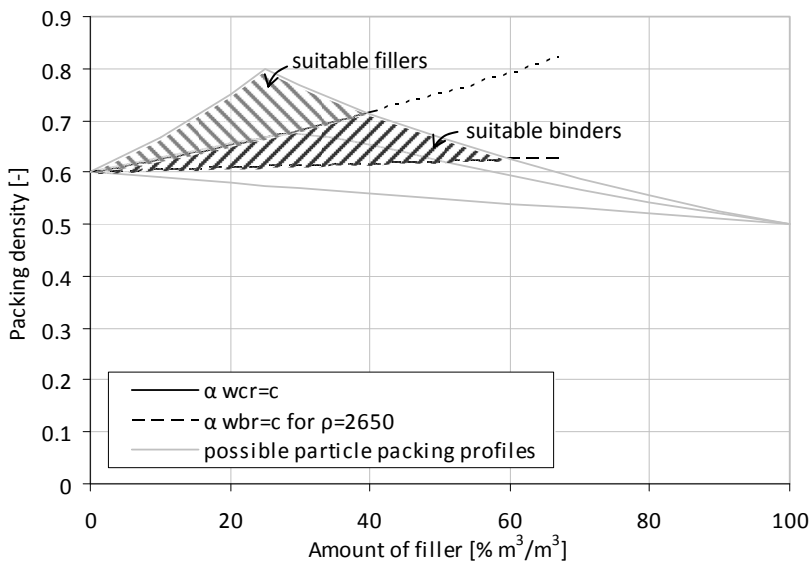

Figure 6.3 Design graph for evaluating the suitability of fillers (cement $\alpha_c = 0.6$, $\rho_c = 3150$, *binder* $\rho_b = 2650$*).*

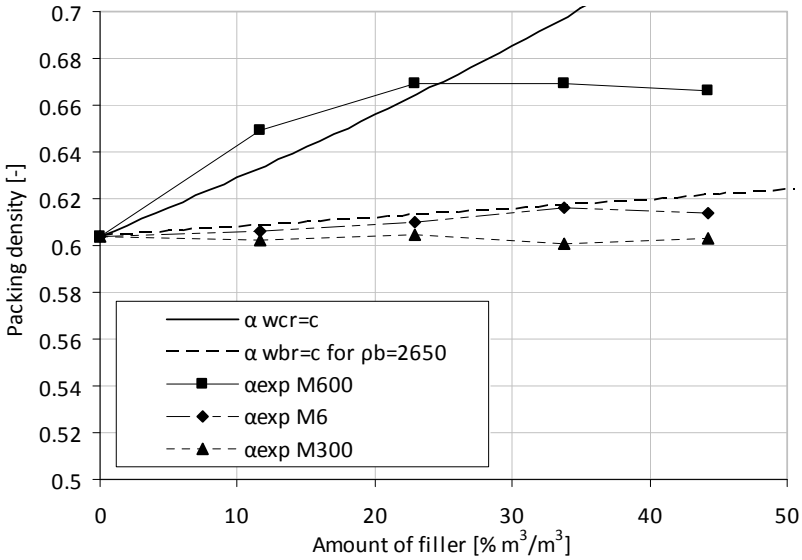

Figure 6.4 Measured packing densities of cement combined with quartz powder M6, M300, M600 in relation to the design rules for $\alpha_{wcr=c}$ *and* $\alpha_{wbr=c}$ *.*

Combining the design rules for $\alpha_{wcr=c}$ and $\alpha_{wbr=c}$ with the measured packing densities from Table 6.1 leads to Figure 6.4. As can be concluded from this figure only quartz powder M600 up to 24% [m^3/m^3] cement replacement can increase the packing density to such an extent that the water/cement ratio can be kept constant. Mixtures E1, E14 and E15 in Table 6.2 were composed with a constant water/cement ratio. Since the packing density of the 'cement pastes' of these mixtures is close to $\alpha_{wcr=c}$ these three mixtures had almost the same workability. Mixture E15 with 20% [kg/kg] M600 shows a 14% strength increase compared to the reference mixture. The water/cement ratio was constant, so this strength increase might be explained by the improved packing density combined with possible pozzolanic activity. The mixtures show clearly the suitability of filler M600 and the advantage of the increased particle packing density to replace cement while retaining a constant water/cement ratio.

Table 6.2 Mixture compositions, flow value and 28-day cube compressive strength.

	CEM I 42.5 N [g]	M600 [g]	sand [g]	water [g]	Glenium51 [g]	*wcr* [-]	$\alpha_{t,CIPM}$ [-]	flow value [mm]	strength [N/mm^2]
E1	900	-	2700	326	10.8	0.37	0.803	95	65.5
E14	810	90	2700	293	10.8	0.37	0.813	96	68.0
E15	720	180	2700	259	10.8	0.37	0.821	94	74.4

6.3 Packing density and water demand

6.3.1 Viscosity measurements of pastes

For the viscosity measurements, the cement pastes from series C were produced in a three-liter Hobart mixer. The mixtures had a constant water/powder ratio of 0.26, which led to water/cement ratios of 0.289, 0.325, 0.371 and 0.433 for cement replacements of 10, 20, 30 and 40% kg/kg respectively. First, the dry powders were mixed for ten seconds

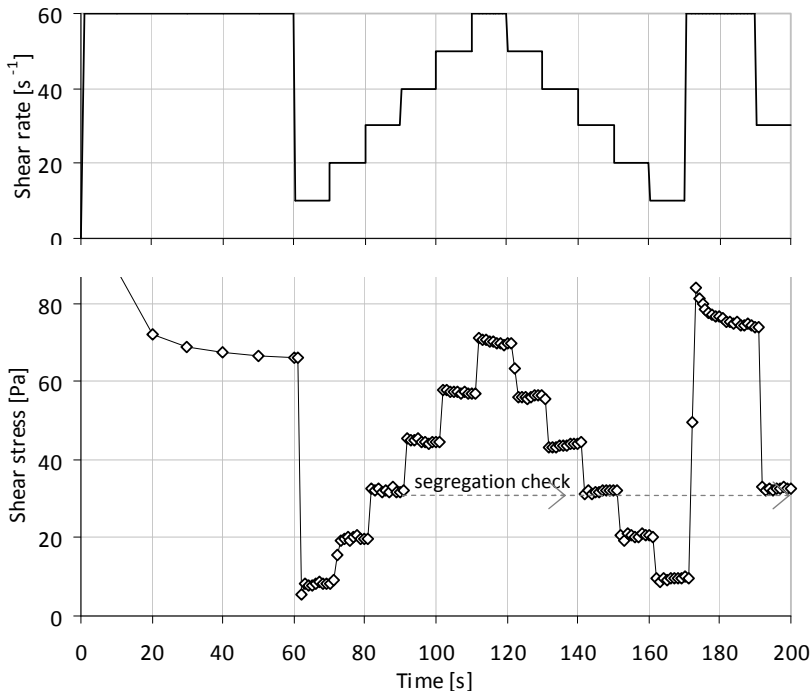

Figure 6.5 Measuring sequence, viscometer PAAR Physica MC1.

after which the water and superplasticizer were added. Mixing was continued for one minute after which the paste rested for two minutes. Paste adhering to the wall was scraped from the bowl. After this, mixing was continued for one more minute. A coaxial cylinder viscometer, PAAR Physica MC1, was used to determine the viscosity of the paste. To avoid slippage, a sandblasted cylinder with a diameter of 25 mm (standardized geometry: Z3) was used. The measurement was started 5 minutes after the beginning of the mixing procedure. The applied measuring sequence is shown in Figure 6.5. The upward curve is used for the test results and further compared to the downward curve. The final part of the measuring sequence is used to determine whether segregation occurred during testing.

In Figure 6.6 the results of the viscosity measurements are presented. Each mixture was tested two to three times. The segregation potential of the mixtures was always very low, which led to repeatable results. Only mixture C16 and C17 had such a low viscosity that it was outside the measuring range of the viscometer. This is probably also the cause of the

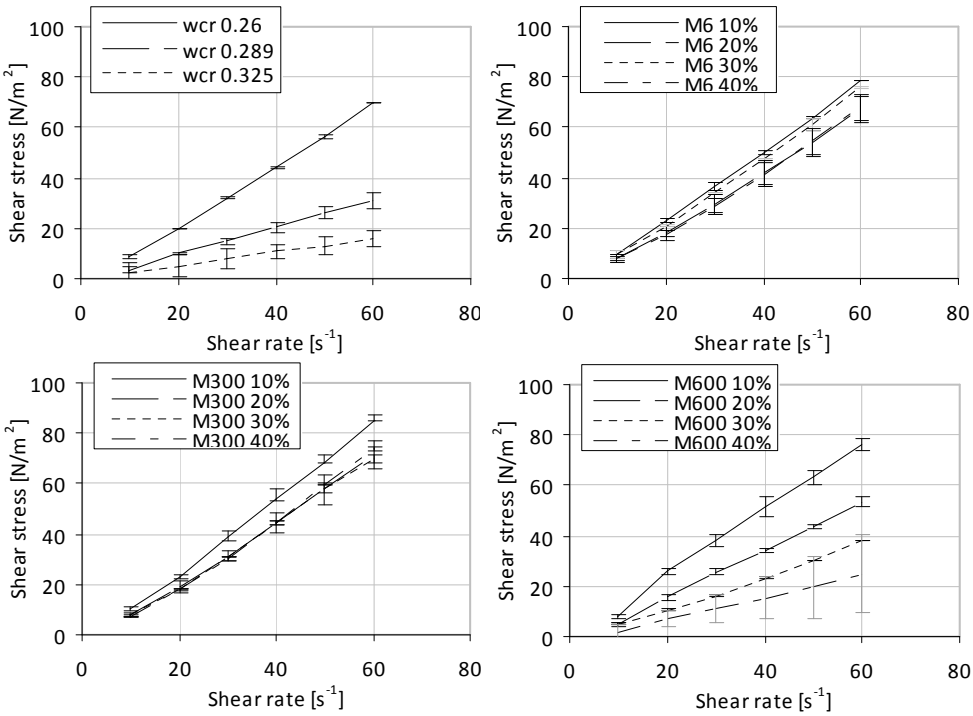

Figure 6.6 Viscosity measurements on cement pastes series C.

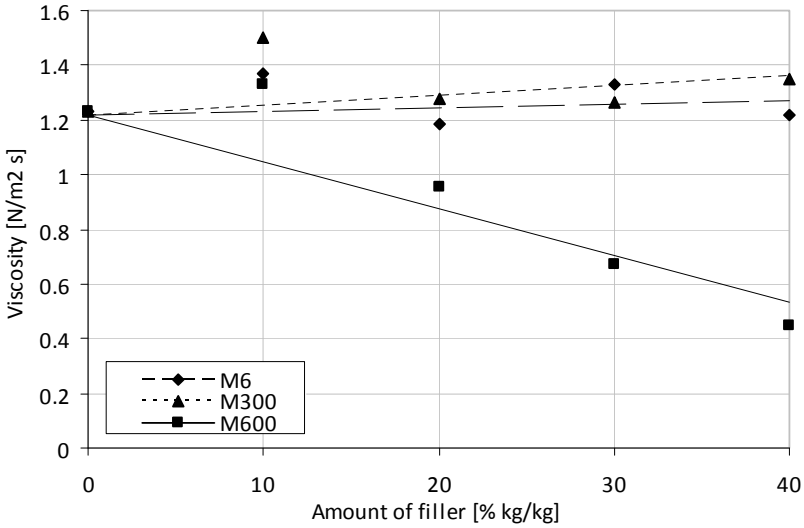

Figure 6.7 Viscosity as a function of the amount of quartz powder for M6, M300 and M600 in cement pastes series C.

larger scatter in the viscosity of mixture C13 containing 40% M600. The viscosity measurements on cement pastes containing quartz powder M6 and M300 show only minor differences when the cement is replaced, see Figures 6.6 and 6.7. This applies especially, when the changes in viscosity are compared with the reference mixtures with the same water/cement ratios or with the mixtures where cement is replaced by quartz powder M600. When cement is replaced by increasing amounts of M600 the viscosity is reduced; however, this effect is lower than the viscosity reduction due to the change in water/cement ratio. No direct relations between packing density of the mixtures and the viscosity were found. On the other hand, it seems that fillers which have a larger influence on the packing density also have a larger influence on the viscosity when they replace cement.

6.3.2 Flow value measurements of mortars

Several mortar mixtures were tested on workability by measuring the flow value from the slump test. This was done by a mini cone test (diameter 38-90 mm and height 75 mm) on a 300 mm diameter glass plate flow table (Tonindustrie). The flow value is measured after ten drops with 10 mm free falling height. Two series of 13 mixtures (Series D and E, Appendix E) including various amounts of quartz powder M6, M300 and M600 were tested as well as over 50 mixtures just containing varying amounts of cement and sand (series F, G, H in Appendix E). In Figure 6.8, mixtures with quartz powder M6 and M300 show similar flowing behavior, while mixtures containing increasing amounts of M600 have a decreasing workability without superplasticizer and increased workability with superplasticizer. Even though no direct relations between packing density of the mixtures and the flow value were found, similar trends as with the viscosity measurements were found. M600 with a larger influence on the packing density also has a larger influence on the flow value when it replaces cement.

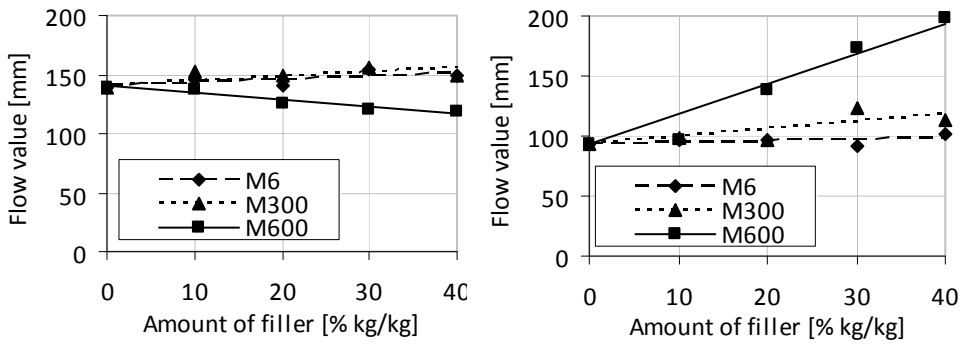

Figure 6.8 Flow values of mortar mixtures containing quartz powder, left hand side without superplasticizer wpr=0.5, right hand side with 1.2% Glenium 51 wpr=0.37.

6.3.3 Water layer analysis

To predict the necessary amount of water within an ecological mixture from its packing density, first two theories were investigated; the excess paste layer theory and the excess water layer theory. Basically, the excess paste layer theory is coming from the design of self-compacting concrete. In these types of mixtures an excess amount of paste is necessary to lubricate all the aggregates and allow flowability. The theory has proven its

usefulness in self-compacting concrete (Fraaij and Rooij, 2008; Grünewald, 2004). The mixtures of series F and G (Appendix E) were especially designed to comply with this theory. The measured packing density of the sand is used to determine the amount of cement paste necessary to fill the voids in-between the sand. Then, an additional amount of paste is added to allow flowability. The excess amount of paste is varied for each type of sand, to find relations between flowability and paste layer thickness (section 6.1.2). The volume of excess paste is calculated according to Equation 6.5.

$$V_{ep} = V_{cp} - V_{aggregate}\left(\frac{1-\alpha_{aggregate}}{\alpha_{aggregate}}\right) \tag{6.5}$$

In this equation the maximum packing density of the aggregate $\alpha_{aggregate}$ can either be the experimentally determined packing density or the theoretical packing density from the CIPM. For the evaluation of the excess paste layer theory in this section the experimentally determined packing densities are used. The volume of excess paste from Equation 6.5 is used to calculate the paste layer thickness t_{ep} according to Equation 6.6 (Midorikawa, et al., 2001). Particles in each size group are assumed to be spherical and t_{ep} is assumed to be constant for different sizes of particles.

$$V_{ep} = \sum_{i=1}^{n}\left(\frac{1}{6}\pi\left\{\left(d_i + 2t_{ep}\right)^3 - d_i^{\,3}\right\}\frac{V_i}{\frac{1}{6}\pi d_i^{\,3}}\right) \tag{6.6}$$

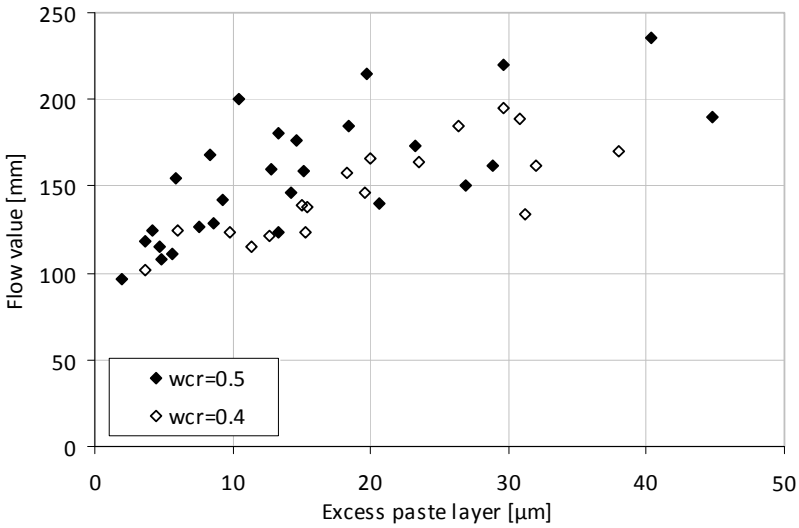

Figure 6.9 Excess paste layer thicknesses in relation to the flow value.

Figure 6.9 shows the results of the excess paste layer theory applied to the mortar mixtures of series F, G and H (Appendix E). Correlation between the flow value and excess paste layer thickness was low, even though the cement pastes in the tested series had a constant consistency due to the constant water/cement ratio. It might be explained by the fact that, due to interaction, the cement paste and cement particles exert a larger influence on the packing density of fine sand than on the packing density of coarse sand. Therefore, with fine sand, the amount of paste necessary to fill the voids between the sand becomes higher and the excess paste becomes lower. Implemented in Equation 6.6, this means that the packing density $\alpha_{aggregate}$ used to calculate the amount of excess paste should be adjusted because of the cement paste present in the mixture. In fact, it is an argument to always use the packing density of the total particle structure instead of the packing density of the aggregate structure. In that case, flowability arises from the excess amount of water present in particle mixture as in the excess water layer theory.

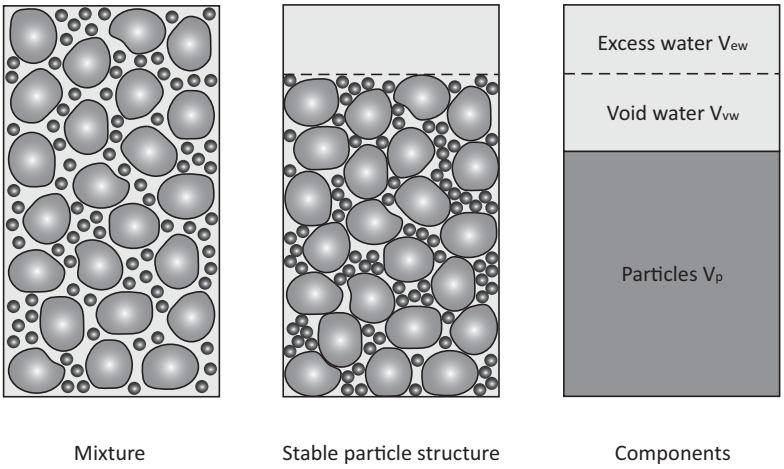

Figure 6.10 Volume of water, divided into excess water and void filling water, within a concrete mixture in a unit volume. After (Midorikawa, et al., 2001).

In the excess water layer theory, a part of the water is used to fill the voids in the particle structure, while the rest of the water forms a water layer of thickness t_{ew} , see also Figure 6.10. Following Krell (1985), this excess water layer thickness can be determined according to Equation 6.7.

$$t_{ew} = \frac{V_{ew}}{A_p m_p} = \frac{V_w - V_p\left(\frac{1-\alpha_t}{\alpha_t}\right)}{A_p m_p} \tag{6.7}$$

Originally, Equation 6.7 was used to determine the water layer thickness within cement pastes and to relate this parameter to the flowing behavior of the cement paste. A good relation between viscosity measurements and excess water layer thickness was found by Teichmann (2008). For evaluation of the measurements of this thesis, α_t was replaced by the experimental packing density when available and for A_p the Blaine value as reported by the material producers was used (Appendix A). Figure 6.11 shows that the viscosity measurements of series C did not have a clear relation with the excess water layer thickness t_{ew} . However, applying the excess water layer theory to the mortar mixtures of series F, G and H with water/cement ratios of 0.4 and 0.5 has resulted in the relations as presented in Figure 6.12. This figure shows that relations between t_{ew} and the flowability

of mortar mixtures exist, but they depend on the water/cement ratio. The correlation coefficient R^2 is 0.94 for mixtures with $wcr = 0.4$ and 0.83 for mixtures with $wcr = 0.5$. The correlation coefficient for all the mixtures together is $R^2 = 0.67$.

Before superplasticizers were commonly used in concrete mixtures, fine fillers were regarded as 'water consuming'. Adding them to a mixture increased the internal surface area and also increased the water demand. This also complies with Equation 6.7. Increasing the surface area at a constant packing density decreases t_{ew}. This will lead to either a higher viscosity or a lower flow value. So increasing the surface area of a mixture, without increasing the packing density is not beneficial with regard to the water demand.

Closer evaluation, however, shows that packing density is in this case the controlling parameter determining the water demand. The minimum amount of water necessary in a mixture consists of the water to fill the voids between the particles plus some additional water to lubricate all the particles, depending on their surface area. This last part is the part of the water which is physically bound to the particles, due to the chemical composition. According to Opitz et al. (2007) a particle is surrounded by a double layer of water molecules and an additional layer of water molecules which are not able to move freely. The total thickness of the bonded water layer is measured as 2.6±0.2 nanometer. For the mixtures used in this research, containing powders with a maximum Blaine value of 1300 m^2/kg, this leads to maximum of 1.1% lubricating water in relation to the void filling water. This means that at the minimum water content, when a mixture does

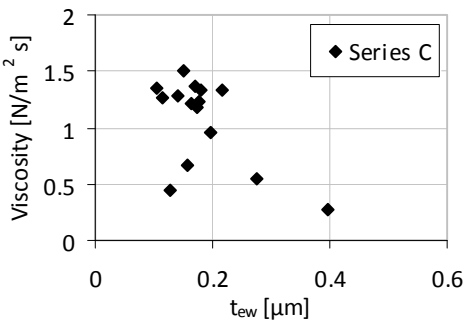

Figure 6.11 Excess water layer thickness t_{ew} in relation to the measured viscosity for cement pastes series C.

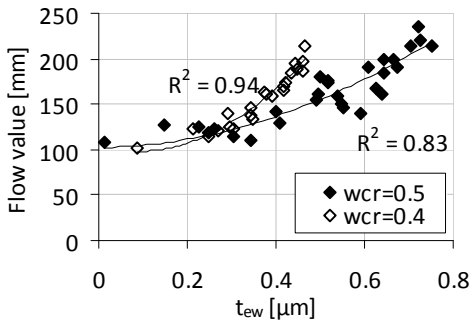

Figure 6.12 Excess water layer thickness t_{ew} in relation to the flow value for mortar mixtures series F, G and H.

not flow yet, the total amount of water is used for about 99% to fill voids and 1% to lubricate particles. Even when very fine micro-fillers such as M600 are used, the influence of increasing the surface area on the water demand of the mixture is very small compared to increasing the packing density. For that reason, each micro-filler increasing the packing density of a mixture is a suitable addition to decrease the water demand of that mixture.

However, to make a mixture flow, just lubricating the particles is not enough as can be concluded from the excess water layer thicknesses from Figure 6.12. The water layer thickness t_{ew} is 50 to 100 times thicker than the minimum lubricating water layer. This excess amount of water is necessary to enable shear deformation. To allow movement, particles have to be lifted over a dilation distance *h* in order to overcome interlock. With a higher packing density (usually also with higher surface areas and smaller particles with higher interparticle forces) it becomes harder to overcome this interlock. This means that for higher packing densities the amount of excess water in relation to the void filling water becomes higher.

Several models assigning the excess water to the particles exist, including (Midorikawa, et al., 2001; Teichmann, 2008). These models use a constant water layer thickness or variable water layer thicknesses depending on the particle size or surface area of the particles. In this thesis, one of the simplest solutions is chosen to regard the excess water only in relation to the packing density and not assume a certain distribution over the particles themselves.

$$W_{rv} = \frac{V_{ew}}{\left(V_w + V_p\right)\alpha_t} = \frac{V_w - V_p\left(\frac{1-\alpha_t}{\alpha_t}\right)}{\left(V_w + V_p\right)\alpha_t} \tag{6.8}$$

In analogy with Equations 6.5-6.7, it was chosen to divide the volume of the excess water over the particle structure. In Equation 6.8, however, the excess water is not distributed over the particles as a water layer thickness, but presented as a relative water volume W_{rv} with regard to the maximum packing density α_t.

The mortar mixtures of series E, F, G and H (Appendix E) were analyzed on the relative amount of excess water W_{rv} compared to the flow value, Figure 6.13. Further evaluation on all the mixtures (Appendix E), including two types of cement, two types of quartz powder, 5 types of sand and various water/powder ratios, show a good correlation between W_{rv} and the flow value. Only the mixtures containing quartz powder M600

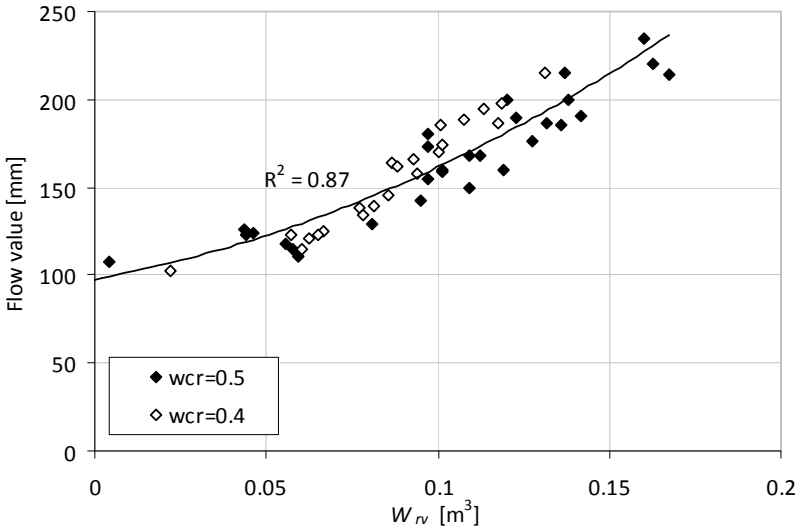

Figure 6.13 The flow value as a function of the relative amount of excess water of mortars series F, G and H.

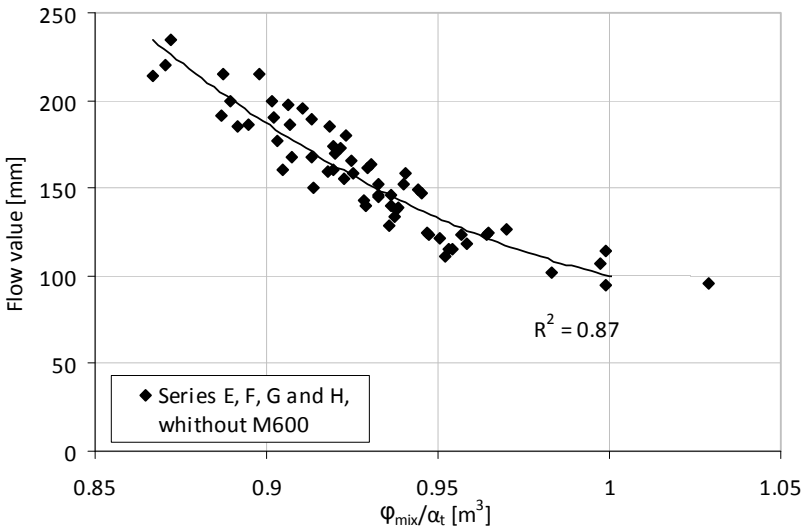

Figure 6.14 The flow value as a function of φ_{mix}/α_t *of mortars series E1-E9, F, G and H.*

showed lower flow values without superplasticizer and higher flow values with superplasticizer in relation to the relative water content. This result is probably caused by the deviation between the real maximum packing density of the mortar and the theoretical packing density as found by the CIPM (Figure 6.1).

The volume of the excess water relative to the packing density has a good relation with the flow value. Furthermore, by definition, the volume of void water is directly related to the maximum packing density α_t. Therefore, the volume of excess water in combination with the volume of void water, both relative to the maximum packing density, must also have a relation with the flow value. In a unit volume, $V_{ew} + V_{vw} = V_w$ and $V_w = 1 - \varphi_{mix}$, where φ_{mix} is the partial volume of all the particles in that mixture. By using φ_{mix}, the flow value can also be related to the total volume of water in a mixture, instead of only the excess water. This leads to Figure 6.14 in which the flow value is related to φ_{mix}/α_t and which can be used to determine the required total water content of a mixture via $V_w = 1 - \varphi_{mix}$. This concept of relating the flow value of a mixture to φ_{mix}/α_t is based on the presented relation between viscosity and packing density in (Larrard, 1999: Figure 2.13).

6.4 Packing density and strength

6.4.1 *Isothermal calorimetry measurements*

In combination with the packing density measurements and the viscosity measurements, the heat generation of the cement pastes of series C was measured on a TAM Air Isothermal Calorimeter. Furthermore, four reference mixtures with 100% cement and the same water/cement ratios as the mixtures with 10, 20, 30 and 40% [kg/kg] quartz powder, were tested. The thermal power of the cement in mixtures C1-C17 as measured during isothermal calorimetry measurements at 20°C is presented in Figure 6.15. The mixtures containing quartz powder M6 and M600 showed the same trends: replacing cement by quartz powder results in a delay in the beginning of the hydration of cement and slows down the hydration speed. These effects are larger with higher amounts of quartz powder and for larger quartz powder particles. However, the effects are smaller than for the reference mixtures C14-C17 with the same water/cement ratios. To show these effects, the time at which the thermal power is maximal is defined as the top-time in hours. Figure

6.16 shows top-time as a function of the percentage of quartz powder M6, M300 and M600 in the mixtures. Also mixtures C14-C17 are plotted as references with the same water/cement ratios as the mixtures with 10, 20, 30 and 40% [kg/kg] quartz powder. Top-time is delayed more for larger quartz powder particles but not as much as in mixtures with the same water/cement ratios without quartz powder.

Furthermore, the mixtures were evaluated on thermal energy from 1 hour until 120 hours, as it gives an indication of the hydration degree after 120 hours. The total thermal energy after 120 hours is presented in Appendix E. Compared to the reference mixture, mixtures containing quartz powder showed a higher thermal energy at higher percentages of quartz powder, while the reference mixtures with the same water/cement ratios showed comparable or lower thermal energy at 120 hours. To visualize these results, the relative thermal energy (compared to reference C1: 218 J/g = 100%) of all mixtures is plotted as a function of the percentage of quartz powder, Figure 6.17. In Figure 6.16 as well as Figure 6.17 linear averages are used to improve the clarity of the graphs and visualize trends; however, it should be noted that the amount of experiments and their accuracy was not sufficient to prove the existence of such relations.

No direct relations between packing density of the mixtures and the thermal power and thermal energy were found. Similar to the flowability measurements, only size related trends were found. Very fine fillers with a larger influence on the packing density show a smaller decrease in the thermal energy when replacing cement. See also (Kadri and Duval, 2002).

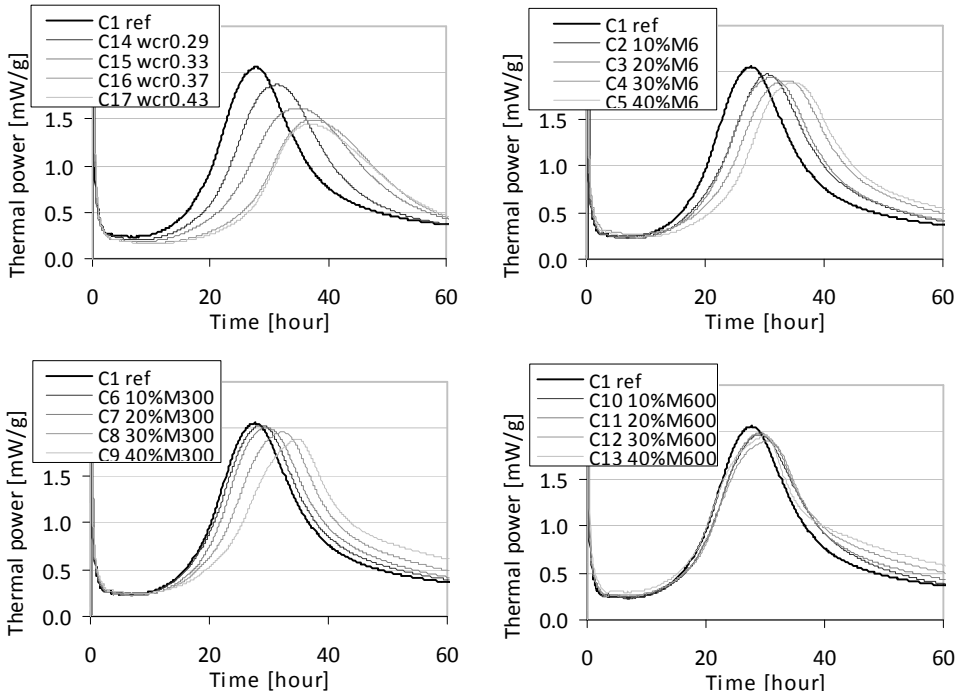

Figure 6.15 Thermal power in mW per gram cement at 20°C, where only the first 60 hours are shown for a better view.

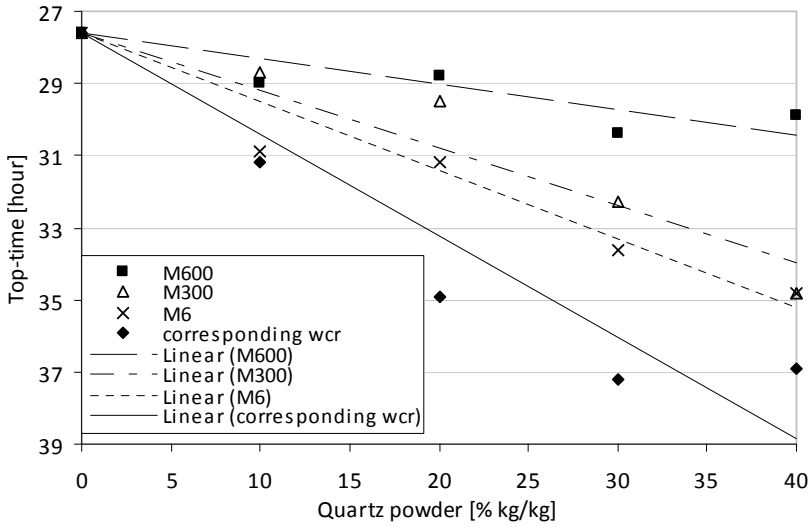

Figure 6.16 Top-time as a function of the amount of quartz powder.

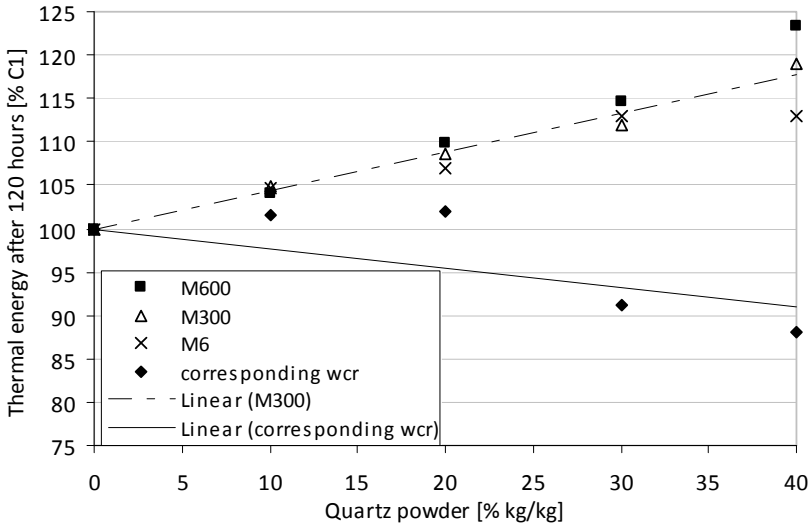

Figure 6.17 Normalized thermal energy as a function of the quartz powder content.

6.4.2 Strength measurements

The powder compositions of series C, which were tested on packing density, viscosity and heat generation, are used in strength tests of mortar beams according to NEN-EN 196-1:2005. The mixture compositions and results are presented in Appendix E as series D and E. Series D consists of mixtures composed according to NEN-EN 196-1:2005 with a water/cement ratio of 0.50. When cement is replaced by 10, 20, 30 or 40% [kg/kg] quartz powder the water content in the mixture is kept constant, thus leading to a water/powder ratio of 0.50 and water/cement ratios of 0.56, 0.63, 0.71 or 0.83 respectively. Series E contains 1.2% [kg/kg] Glenium 51 per gram of powder. The mixtures are designed with a lower water content to ensure stability. The water/cement ratio increases from 0.37 in the reference mixture up to 0.41, 0.46, 0.53 or 0.62 for increasing quartz powder contents. At 7 and 28 days, for each mixture three prisms were split in two parts and tested for cube compressive strength.

Figure 6.18 shows that the differences in cube compressive strength due to the filler size are minor when no superplasticizer is used. With superplasticizer the differences are more pronounced. Replacing cement by 40% of M600 compared to 20% of M6 or M300 results in almost the same strength. The replacement of cement by fine filler M600 is much more effective with regard to cube compressive strength, which complies with the effect of the different filler sizes on the packing density. However, no direct relation between packing density and strength was found. In fact the strength seems to decrease almost proportionally with the cement content, while especially for M600 packing density first increases and then decreases with decreasing cement contents.

Figure 6.19 shows the packing density in relation to the strength for each mortar mixture (Appendix E). Higher packing densities were expected to lead to higher strength; however, there is no clear tendency. When investigating the influence of packing density on the strength, of course the influence of the water/cement ratio can not be neglected. Therefore, in the next section it is evaluated in what way the packing density in relation to water demand or water/cement ratio influences the concrete strength.

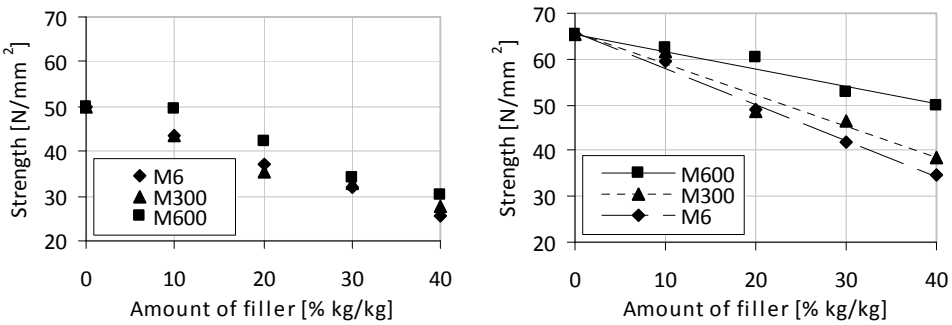

Figure 6.18 28-day cube compressive strength of mortar beams series D and E. Left hand side wpr=0.5 no superplasticizer. Right hand sides, wpr=0.37 with 1.2% Glenium 51.

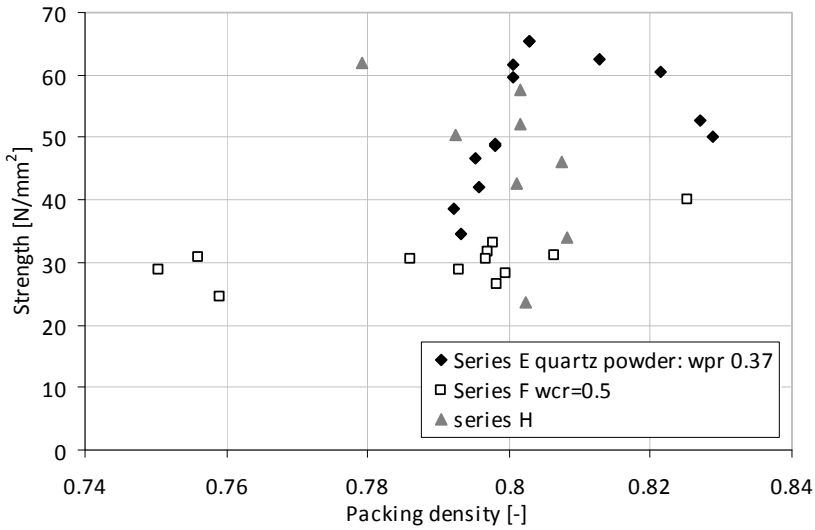

Figure 6.19 Strength as a function of packing density, not showing a clear trend for mortar mixtures series E, F, and H.

6.4.3 Particle distance analysis

Traditionally, strength of concrete is directly related to the water/cement ratio or water/binder ratio. Several equations for predicting the strength of concrete are known. Most are based on Férets law or Abrams empirical expression or derived from it, for example (Larrard, 1999; Mechling, et al., 2007; Mikulić, et al., 2008; Neville, 1995; Popovics, 1998). They are based on water/cement ratios expressed in mass or volume often in combination with the strength class of the cement. In the Netherlands Equation 6.9 (Souwerbren, 1998) is widely accepted. However, with new mixture design techniques, high amounts of fillers and different types of superplasticizer this equation often deviates from the measured strength. This is also the case with the ecological mixtures tested in this research project, Figure 6.20.

$$f_{cm(n)} = 0.8N_n + \frac{25}{wcr} - 45 \qquad (6.9)$$

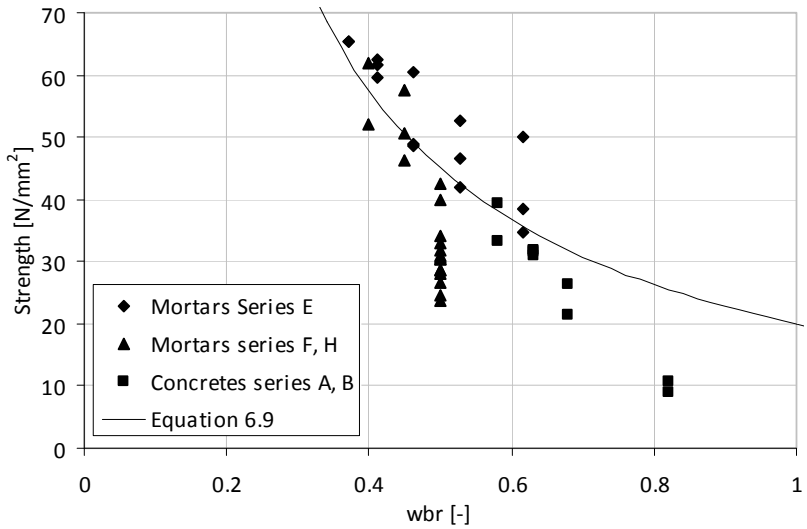

Figure 6.20 Wbr in relation to strength for mortar series E, F and H and concretes series A and B, compared to Equation 6.9 with $N_n = 50$ *[N/mm²].*

It is believed that high packing density has a positive influence on the concrete strength. However, packing density can not be the only factor responsible for strength. Imagine a filler with a higher packing density than cement and the same particle size distribution. Using this filler to replace cement will lead to a higher packing density, but it will decrease strength when the amount of water in the mixture is kept constant. So, to predict the strength of a concrete mixture, the amount of water (or water/cement ratio), the amount of cement and the packing density should all be taken into account.

Hypothetically, the distance between the cement particles should be related to the strength of the concrete or mortar mixture. With a higher amount of water and higher water/cement ratio, the cement particles are further apart. In that case, during the hydration process, the hydration products of the cement particles need to bridge a larger distance, eventually leading to a lower strength. With a high packing density in the mixture, cement particles and other particles are close to each other, making the space that needs to be filled by hydration products smaller.

As a value for the cement particle distance in a stable particle structure it is decided to use the value $\varphi_{cem}/\varphi^*_{cem}$. In this relation φ_{cem} is the volume in the mixture which is occupied by the cement. φ^*_{cem} is the maximum volume that cement may occupy given the presence of the other particles, as defined in section 5.3.2. So, φ^*_{cem} is a value for the

maximum space in which the cement particles can be present. Therefore, $\varphi_{cem}/\varphi^*_{cem}$ is a value representing the space surrounding the cement particles on a volume basis. Globally, with more cement particles present, φ_{cem} increases and with a higher fineness of fillers and higher packing density φ^*_{cem} decreases, both leading to a higher value for $\varphi_{cem}/\varphi^*_{cem}$ and thus representing closer cement spacing.

However, the factor $\varphi_{cem}/\varphi^*_{cem}$ represents a cement spacing in a stable particle structure. A stable particle structure is defined as a structure of particles in which all particles are in contact with one or more particles in such a way that the packing structure is stable under the influence of gravity for a fixed K value. In a real mixture, not only the voids between the particles are filled with water, but some excess water is always present to allow flowability (section 6.3.3.). Therefore, the available space φ^*_{cem} for the cement particles becomes larger, depending on the amount of added water. The particles forming a stable particle structure occupy a volume of α_t in a unit volume. However, when a unit volume is filled with a real mixture, the volume occupied by the particles φ_{mix} is smaller than α_t. φ_{mix} can be determined according to Equation 6.10.

$$\varphi_{mix} = \frac{V_p}{V_p + V_w} \tag{6.10}$$

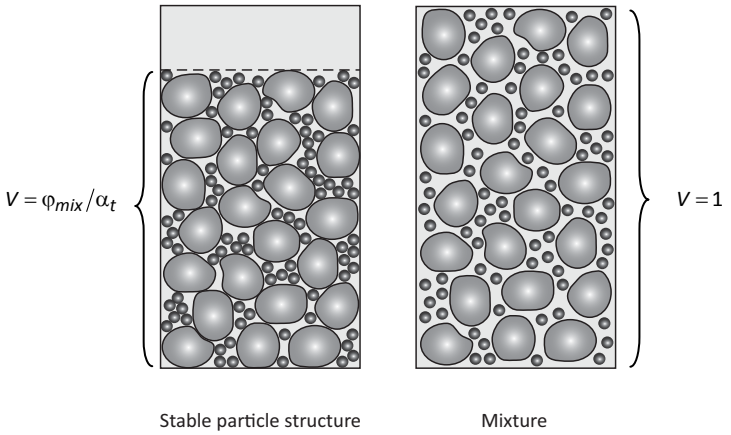

Figure 6.21 The volume of a stable particle structure compared to the volume necessary to create workability.

The particles in the mixture could form a stable particle structure as shown in Figure 6.21 on the left hand side. In that case the stable particle structure occupies a volume of φ_{mix}/α_t . So, looking at the spacing of the particles from a stable particle structure compared to a real mixture; the volume occupied by the stable particle structure is φ_{mix}/α_t within a unit volume while the real mixture occupies the entire unit volume. Therefore in the real mixture, all the particles are further away from each other, compared to the stable particle structure, by a factor $1/(\varphi_{mix}/\alpha_t) = \alpha_t/\varphi_{mix}$. For the total cement spacing this leads eventually to Equation 6.11.

$$CSF = \frac{\varphi_{cem}}{\varphi^*_{cem}\dfrac{\alpha_t}{\varphi_{mix}}} = \frac{\varphi_{cem}}{\varphi^*_{cem}}\frac{\varphi_{mix}}{\alpha_t} \tag{6.11}$$

The cement spacing factor (CSF) includes an amount of cement via φ_{cem} , the amount of water in the mixture via φ_{mix}/α_t and the influence of the packing density in φ^*_{cem} and α_t . Higher values of the cement content increase φ_{cem} and therefore the CSF. High values of the CSF represent higher strengths. This is also consistent with an increase of the amount of water in a mixture, which reduces φ_{mix} and thus the CSF and the strength.

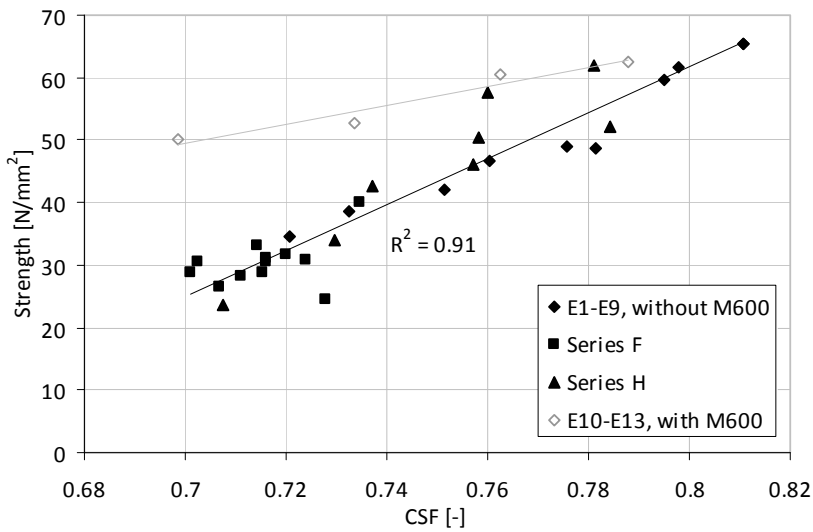

Figure 6.22 The measured cube compressive strength in relation to the cement spacing factor CSF for mixtures of series E, F and H ($K_t = 9$).

The mortar mixtures of series F and H (Appendix E) were analyzed on the CSF compared to the experimentally determined 28-day cube compressive strength, Figure 6.22. A good relation was found, proving the usefulness of the CSF with regard to the prediction of concrete strength. Furthermore, the mixtures of series E containing quartz powder were evaluated. These mixtures (Appendix E), including two types of cement, two types of quartz powder, 5 types of sand and various amounts of water, show a good correlation between CSF and the strength. Only the mixtures containing quartz powder M600 showed higher strength values. This result can not directly be explained by the expected difference between the real maximum packing density of the mortar and the theoretical packing density based on the flow value measurements. Possibly the very fine quartz powder contributes to the strength in a chemical way; however this should be further investigated.

6.5 Concluding remarks

The packing density of a powder or mixture by itself is a powerful parameter in the design of concrete mixtures. It helps to determine the suitability of fillers as cement replacing material and is related to the flowability and strength of mixtures. Very fine fillers, with high surface area can increase packing density to such an extent that the water/cement ratio can be decreased when cement is replaced by them. This shows that water demand is not only surface area related, as is often stated in water layer theories.

Furthermore, the concept that mixtures flow due to excess cement paste layers surrounding the aggregates was not in agreement with the experimental data including the particle packing of the aggregates. Small aggregates experience much more interaction from the cement particles, than large aggregates. Therefore, packing density of the aggregates can not be used without the interaction effects of cement and fillers and thus a concrete mixture should be schematized as a particle structure in water instead of an aggregate structure in cement paste.

The water demand and flow value of mixtures are related to the packing density of all the particles in that mixture via the relative water volume or the relative amount of excess water. In each mixture part of the added amount of water is used to fill voids, while the rest is used to lubricate particles and allow flowability. Maximum packing density α_t and

viscosity or α_t and flow value are not directly related. This might have been expected, since the amount of added water or water/cement ratio will influence the flowability. A good relation between the flowability and φ_{mix}/α_t was found. In a unit volume, $\varphi_{mix} = 1 - V_w$ and therefore φ_{mix}/α_t comprehends the relative amount of water present in the mixture.

In mixtures where φ_{mix} is closer to α_t relatively higher amounts of excess water in relation to the void filling water are required. This is due to the increased number of contact points between the particles within such mixtures. Relatively more water is necessary to overcome the interlock and make the mixture flow. Higher maximum packing densities α_t seem to have the same effect on the flowability. This is probably because high packing densities are often related to high amounts of fine fillers, which also increases friction and interlock due to high surface areas and higher interparticle forces of the small particles.

The relation between φ_{mix}/α_t and the flow value of mixtures as found in section 6.3.3, can be used to determine the required total water content of a mixture via $V_w = 1 - \varphi_{mix}$. In this way it can be used in chapter 7 as input within a mixture design procedure for ecological concrete.

The measured heat generation of cement and the strength of the tested mortar mixtures were not directly related to the maximum packing density α_t of the cement pastes or mortars. Also no direct relation between the heat generation and the strength was found, even though water/binder ratio or water/cement ratio in each series were kept constant. It is believed strength is related to a high packing density, but direct relations were difficult to obtain due to varying amounts of water present in the mixtures. A hypothesis was made that strength should be related to the volumetric distance between the cement particles. In that case, higher water/cement ratios and lower packing densities lead to a larger distance between the cement particles and thus eventually to a lower strength due to the fact that hydration products of the cement particles need to bridge larger distances.

A good relation between the cement spacing factor CSF and the strength was found, which shows the validity of the cement distance concept. Since the cement spacing factor can be determined directly from the mixture composition (φ_{cem} and φ_{mix}) and the theoretical particle packing model (φ^*_{cem} and α_t) the CSF can be used as a mixture design tool in chapter 7.

7 Design method for ecological concrete

In this chapter the particle packing density from chapter 5 and the water demand and strength relations from chapter 6 are linked together in a procedure for designing ecological concrete. Section 7.1 provides a global overview of the design method and the required input data. The mixture composition and cement content are the starting position for the packing density calculations in section 7.2. Section 7.3 describes how to predict the water demand and flowability from the packing density. The relative amount of water in relation to the amount of cement and the packing structure are used as parameters for concrete strength relations in section 7.4. For ecological concrete or defined performance concrete additional mixture design restriction can be implemented as proposed in section 7.5. In section 7.6 the design method is specified by using it to design an ecological concrete mixture. Finally, the concept of the cyclic design procedure for ecological concrete is summarized in section 7.7. Chapter 8 contains ecological concrete mixtures designed according to the design method as presented in this chapter.

7.1 Cyclic design procedure

To design a strong and durable ecological concrete it is important to be able to predict the material properties of the concrete. Water/binder ratio and binder type are the main factors influencing the hydration process and the resulting internal microstructure of concrete, and thus the material properties. In ecological concrete powders are used as addition or as cement replacing material. This has a direct influence on the proportion of cement to total powders and the water/cement ratio. Therefore, the design method should take the powder composition and the amount of water into account to determine the optimal composition of the ecological concrete.

Chapter 4 shows that with regard to the design of ecological concrete, strength is the governing design parameter as far as the mechanical properties of the concrete are concerned. Therefore, the strength should be a controlling parameter in the design procedure. Since packing density influences both the water demand and the strength a three step cyclic design procedure was developed as presented in Figure 7.1. The design procedure usually starts by calculating the packing density of a new mixture (top corner), but can also start with a mixture adjustment of a reference mixture based on its strength (bottom, right corner). The various steps will shortly be explained in subsection 7.1.1 and then further elaborated in the next sections.

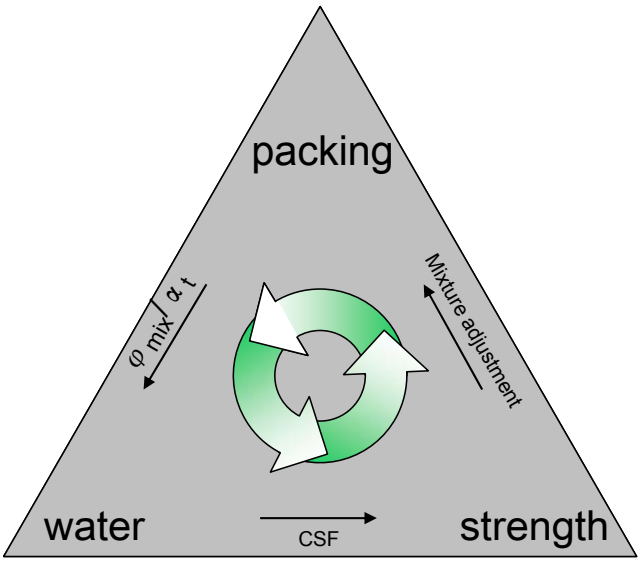

Figure 7.1 Cyclic design procedure for ecological concrete.

7.1.1 Input parameters and design steps

The cyclic design procedure starts from a mixture composition or a database of available materials for the mixture design. Table 7.1 provides the user with the required information to use the CIPM and the cyclic design procedure. The material database may already have been filled with a standardized set of materials, but can also be filled by the user. In that case, the user or concrete producer needs to provide, next to the common material properties, the packing density α_{exp} measured at a certain compaction value K_{exp}. Coarse aggregates can be measured according to (NEN-EN 1097-3:1998) with $K_{\text{exp}} = 4.1$. Fine powders can be measured with the mixing energy method presented in chapter 4 with $K_{\text{exp}} = 12.2$. Since the design method is based on the results of this research project including the superplasticizer Glenium 51, also the fine powders should be tested in combination with this superplasticizer. Furthermore, it should be noted that the design method is only valid for mixtures including Glenium 51, until the equations/coefficients of the CIPM for the use of other superplasticizers are further investigated.

Table 7.1 Input requirements for the cyclic design procedure for ecological concrete. (italic = optional(default)).

Design step	**Input by user**
Information in the database	For each material: dry density, particle size distribution, α_e in combination with K_e, *water absorption, Blaine value*
1. Particle Packing Optimization	A Existing reference mixture B Selection of materials from the database
2. Flowability requirement	Required workability: C0 dry, C1 earth moist, S2 semi plastic, S3 plastic, F4 very plastic, F5 fluid or F6 very fluid. *assumed air content (1%)*
3. Desired strength class, *additional mixture composition requirements*	Strength class C20/25, C28/35, etc or average cube compressive strength *e.g. maximum water/cement ratio, cement to binder ratio, minimum powder content, compaction index ($K_t = 9$)*

For the particle packing optimization it is convenient to start from an existing mixture and use the model to find a mixture composition with a higher packing density. Also optimization based on selected materials from the database is possible, but can require long calculation times. After optimization the particle packing of the original mixture can be compared to the optimized mixture and used in the second design step. The output of the CIPM in this step will be a mixture composition with its corresponding packing density α_t (at $K_t = 9$) and the values for φ_{cem} and φ^*_{cem}.

In the next step the water demand of the mixture is determined by using φ_{mix} / α_t. This value is directly related to the flowability of a mixture, so φ_{mix} and thus the volume of water can be adjusted to the required consistency. When water absorption of the materials and predicted air content are available, the amount of water to be dosed during the mixing process can be adjusted here.

The strength is predicted from the water available in the mixture to fill voids and surround particles (excluding the absorbed water). This is the water available for cement hydration and that is responsible for the spacing of the cement particles. By using the cement spacing factor as shown in section 6.4.3 and 7.4, the strength of the mixture can be determined.

In the last step of the cycle, the requirements of the user are taken into account to adjust the mixture composition. For the ecological concrete in this research project the requirement is fixed to be the design strength of the concrete. If the predicted strength in the previous step is higher than the desired strength, the cement content can be lowered in this step. Furthermore, additional user defined requirements can be used such as a minimum amount of powders or a fixed proportion of cement to powders. Since the mixture composition is adjusted to the requirements in this step, the particle size distribution might change again.

Cyclic design is necessary whenever one of the material amounts changes in the last design step. For instance, when the cement content is lowered due to a high predicted strength value, this changes the overall particle size distribution and thus the packing density. In that case the cyclic design procedure is repeated until the mixture composition does not change anymore in the last design step.

7.2 Particle packing

The first step in the design process is to calculate the packing density from a given mixture composition. The mixture composition can either be provided by the user or result from the optimization module in the program. The applied materials and their particle size distributions are divided into sufficient size classes. Then Equations 7.1 to 7.5 are used to determine the packing density α_t for $K_t = 9$. For background information on these equations, reference is made to chapter 5. The values $w_a = w_b = 1$, $C_a = 1.5$ and $C_b = 0.2$ are fixed for mixtures with superplasticizer Glenium 51 until further research provides values for other superplasticizers.

$$K_t = \sum_{i=1}^{n} K_i = \sum_{i=1}^{n} \frac{r_i/\beta_i}{1/\alpha_t - 1/\beta_{ti}} \tag{7.1}$$

$$\beta_i = \left(1 + \frac{1}{K_{\exp}}\right)\alpha_i \tag{7.2}$$

$$\beta_{ti} = \frac{\beta_i}{1 - \sum_{j=1}^{i-1}[1 - \beta_i + b_{ij}\beta_i\left(1 - 1/\beta_j\right)]r_j - \sum_{j=i+1}^{n}[1 - a_{ij}\beta_i/\beta_j]r_j} \tag{7.3}$$

$$a_{ij,c} = \begin{cases} 1 - \dfrac{\log\left(d_i/d_j\right)}{w_{0,a}} & \log\left(d_i/d_j\right) < w_{0,a} \\ 0 & \log\left(d_i/d_j\right) \geq w_{0,a} \end{cases} \qquad w_{0,a} = \begin{cases} w_a * C_a & d_j < 25\mu m \\ w_a & d_j \geq 25\mu m \end{cases} \tag{7.4}$$

$$b_{ij,c} = \begin{cases} 1 - \dfrac{\log\left(d_j/d_i\right)}{w_{0,b}} & \log\left(d_j/d_i\right) < w_{0,b} \\ 0 & \log\left(d_j/d_i\right) \geq w_{0,b} \end{cases} \qquad w_{0,b} = \begin{cases} w_b * C_b & d_i < 25\mu m \\ w_b & d_i \geq 25\mu m \end{cases} \tag{7.5}$$

Furthermore, the CIPM is used to calculate the values for φ_{cem} and φ^*_{cem} (see also section 7.4). In Equation 7.6 r_{cem} is the volume fraction of the cement particles relative to the total volume of particles in the mixture $\sum_{i=1}^{n} r_i = 1$. To determine the value of φ^*_{cem} Equation 7.7 is used. This makes φ^*_{cem} just as α_t a value which depends on the compaction index K_t. Therefore K_t is fixed to a value of 9 unless desired differently by the user. K_{cem} is defined as the sum of all K_i values representing the size groups of the cement. This means K_{cem} is the contribution of the cement to the total compaction index K_t. K_{cem} follows directly from the packing density calculation in the CIPM and can be used to calculate φ^*_{cem} via Equation 7.8.

$$\varphi_{cem} = r_c \alpha_t \tag{7.6}$$

$$K_t = \sum_{i=1}^{n} K_i = \sum_{i=1}^{n} \frac{\varphi_i / \varphi_i^*}{1 - \varphi_i / \varphi_i^*} \tag{7.7}$$

$$K_{cem} = \frac{\varphi_{cem} / \varphi^*_{cem}}{1 - \varphi_{cem} / \varphi^*_{cem}} \quad \text{-->} \quad \varphi^*_{cem} = \varphi_{cem} \frac{1 + K_{cem}}{K_{cem}} \tag{7.8}$$

The calculated maximum packing density α_t from the CIPM and the values for φ_{cem} and φ^*_{cem} are used in the next design steps to determine water demand and strength of the mixture.

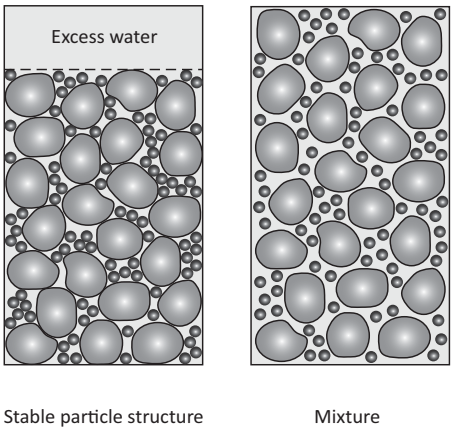

Figure 7.2 The volume occupied by a stable particle structure (left hand side) compared to the volume occupied by a flowable mixture consisting of the same particles (right hand side)

7.3 Water demand

The second design step is to determine the water demand of the mixture based upon the calculated maximum packing density. Basically, in the first design step the packing density of a stable particle structure is calculated assuming that all particles are in contact with each other. As from this second design step the maximum packing density of the particles α_t in a stable structure should be distinguished from the solid content φ_{mix} of a real concrete mixture containing that particle structure. This is shown in Figure 7.2 where the same amount of particles in a stable particle structure is packed closer than in a mixture. Therefore, the same amount of particles in a stable particle structure uses a smaller volume than in a flowable mixture. In a real mixture part of the water is used to fill the voids between the particles, while the rest of the water is regarded as excess water. This excess water provides the flowability of the mixture. Flowability increases with higher amounts of excess water in the mixture. In that case, the solid content of the mixture φ_{mix} decreases. A relation between φ_{mix}/α_t and the flow value of mortars is given in Figure 7.3.

The relation between φ_{mix}/α_t and the flow value of mixtures can be used to estimate the required amount of water in a mixture at its prescribed consistency. The necessary amount of water can be determined by calculations or from design graphs. Calculations are carried out according to Equation 7.9 based on the design values of φ_{mix}/α_t. In that case design values for φ_{mix}/α_t are required which comply with the desired workability.

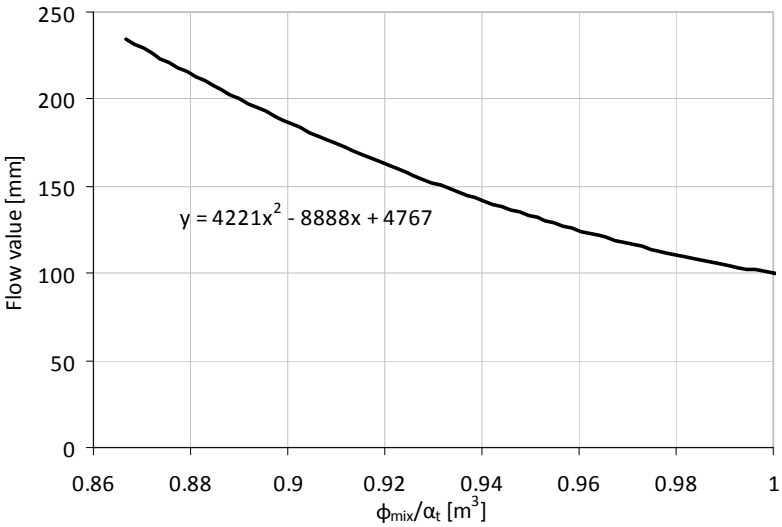

Figure 7.3 Emperical relation between φ_{mix}/α_t and the flow value of mortars (from Figure 6.14).

Suggested design values based on this research are presented in Table 7.2. If absorption of the aggregates is expected the total volume of the mixing water should be adjusted for this.

$$V_w = \left(1 - \varphi_{mix} - \frac{aircontent}{100}\right) V_{mix} \tag{7.9}$$

Table 7.2 presents design values for φ_{mix} / α_t in ecological concrete with low powder contents as found in this research. The powder content should be lower than 16% m^3/m^3 powder ≤ 250 µm. The design values were determined on ecological concrete and are based on the use of Glenium 51. Therefore, they can not yet be used on concrete containing other types of superplasticizer until proven to be valid. Furthermore, for other types of concrete, such as self-compacting concrete, the design values of φ_{mix} / α_t change, probably due to the much higher amount of powders in the mixture and the lower values of α_t.

In Figure 7.4 two design graphs are presented for ecological concrete in consistency class C1 and F4. An example is given for a mixture with a maximum packing density $\alpha_t = 0.8$. From the packing density calculated by the CIPM on the horizontal axis of the figure, the total amount of water can directly be found on the vertical axis. Although the amount of water can also be calculated by Equation 7.9, these graphs give a good overview of the change in water volume for various packing densities. Since the volume of the water necessary to fill the voids is the largest part of the total water, increasing the total packing density is always beneficial with regard to water demand. However, with higher packing densities a relatively higher percentage of excess water is necessary to make the mixture

Table 7.2 Design values for φ_{mix} / α_t for ecological concrete.

Required consistency		Slump [mm]	φ_{mix} / α_t [-]
C0	Dry	< 30	0.99
C1	Earth moist	10-40	0.98
S2	Semi plastic	50-90	0.97
S3	Plastic	100-150	0.95
F4	Very plastic	> 160	0.93

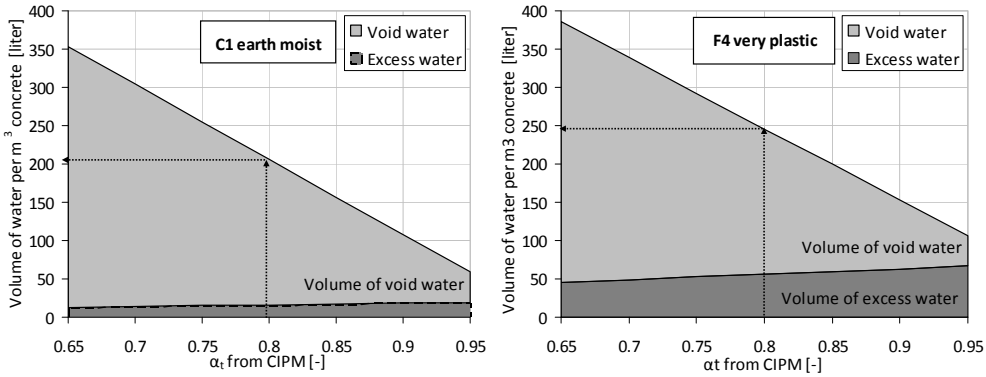

Figure 7.4 Design graphs to determine the water content in ecological concrete for consistency class C1 semi plastic on the left hand side and F4 fluid on the right hand side.

flow. This is because higher packing densities have a higher interparticle friction so that it is more difficult to overcome the interlock and to enable shear deformation. For a concrete mixture in consistency class F4 with $\alpha_t = 0.8$ the excess water makes up 23% of the total water, while at an increased packing density of $\alpha_t = 0.9$ this is already 41% of the total water. This is important to keep in mind during the mixture design of ecological concrete. Mixtures with a very high packing density will be harsher due to high internal friction and will bleed if the powder volume is not in relation to the volume of excess water.

7.4 Strength

In this design step the strength of an ecological concrete mixture is predicted from the mixture composition and the applied amount of water. The strength prediction is based on the assumption that in low strength ecological concrete all aggregates are stronger than the produced concrete. In that case the cement glues the aggregates together and the strength depends on the space to be bridged to connect all aggregates. With a high packing density in the mixture, cement particles and other particles are close to each other, reducing the space that needs to be filled by hydration products. This leads to high strengths. With higher amounts of water and higher water/cement ratios, the cement particles are more remote. Therefore, during the hydration process, the hydration products of the cement particles need to bridge a larger distance, eventually leading to lower strengths.

As a value of the space between the cement particles in a stable particle structure, it is decided to use the value $\varphi_{cem}/\varphi^*_{cem}$. In this relation φ_{cem} is the volume in the mixture which is occupied by the cement. φ^*_{cem} is the maximum volume that cement may occupy given the presence of the other particles, as defined in section 5.3.2. $\varphi_{cem}/\varphi^*_{cem}$ is a value representing the space surrounding the cement particles on a volume basis. Globally, with more cement particles present, φ_{cem} increases and with a higher fineness of fillers φ^*_{cem} decreases, both leading to a higher value for $\varphi_{cem}/\varphi^*_{cem}$ and thus representing closer cement spacing.

In a real mixture, not only the voids in the stable particle structure are filled with water, but some excess water is always present to allow flowability. A stable particle structure is defined as a structure of particles in which all particles are in contact with one or more particles in such a way that the packing structure is stable under the influence of gravity for a fixed K value. By adding the water, all particles move away from each other by the factor α_t/φ_{mix}. Therefore adding more water leads to larger distances between the cement particles and thus to lower strength. The space between the cement particles is expressed as the cement spacing factor CSF according to Equation 7.10.

$$CSF = \frac{\varphi_{cem}}{\varphi^*_{cem}} \frac{\varphi_{mix}}{\alpha_t} \tag{7.10}$$

High values of the CSF represent closer cement spacing and higher strengths. Higher values of the cement content increase φ_{cem}. At constant packing density α_t this leads to a higher CSF and thus a higher strength. The CSF is also consistent with a strength decrease due to an increased water/cement ratio. An increase of the amount of water in a mixture reduces φ_{mix} and thus the CSF and the strength. The experimentally determined strength relation from this research is presented in Figure 7.5. Within the measured range a linear relation is assumed. This linear relation is restricted by an upper and a lower boundary. The lower boundary is reached when not enough cement particles are present in order to connect the non-reacting particles and aggregates. Until further research shows at which volume of cement particles the linear relation becomes invalid, the lower boundary is fixed at $CSF = 0.7$ or a minimum strength of 25 N/mm^2. Maximum strength can be reached with very dense particle packing and low water/cement ratio. In these mixtures strength becomes dependent on the possibility to fully compact the mixture and on the availability

of water for full hydration. For that reason the upper boundary is fixed at $CSF = 0.81$, which was found in earth moist ecological concrete mixtures.

To predict the concrete strength during this design step φ_{cem}, φ^*_{cem} and α_t from the first design step are combined with the water demand expressed as φ_{mix} resulting from the second design step. In this way strength can be predicted and the mixture can be adjusted to meet the strength requirement. When the strength is higher than requested the amount of cement can be decreased. A way to decrease the cement content is to replace the cement by a filler of choice in such a way that the total volume of powders remains constant. To show the influence of the size of fillers on the cement spacing an example is given in Figure 7.6. In the reference mixture, the cement is replaced by a filler of the same size as the cement. This stable particle structure including coarse filler occupies a larger volume than a stable particle structure with fine filler. In the mixture with the very fine filler, exactly the same volume of cement is replaced by the fine particles. In this way r_{cem} is kept constant for the two mixtures. With these very fine filler particles, however, the packing density increases. Therefore, the same amount of cement particles can be present in a smaller overall volume and thus the cement particles are closer to each other. When the reference mixture is a standardized mortar mixture from which 40% of the cement is

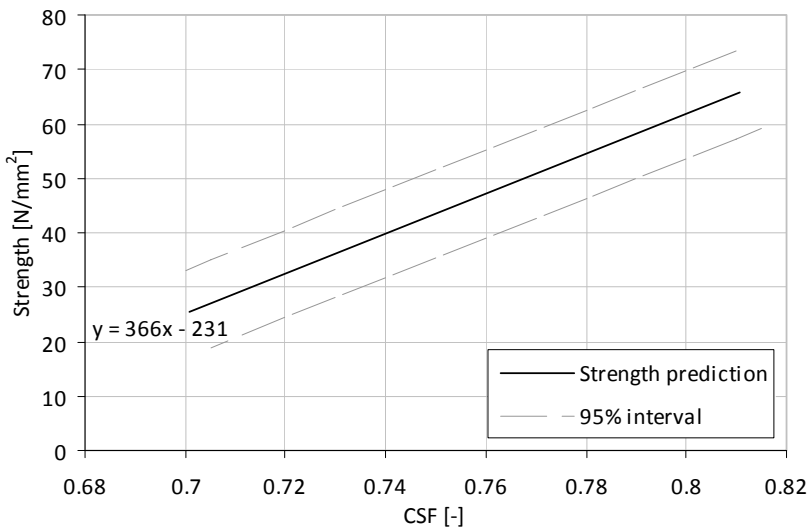

Figure 7.5 Experimental relation between the cement spacing factor CSF and the mean 28-day strength of mixtures series E, F and H ($K_t = 9$).

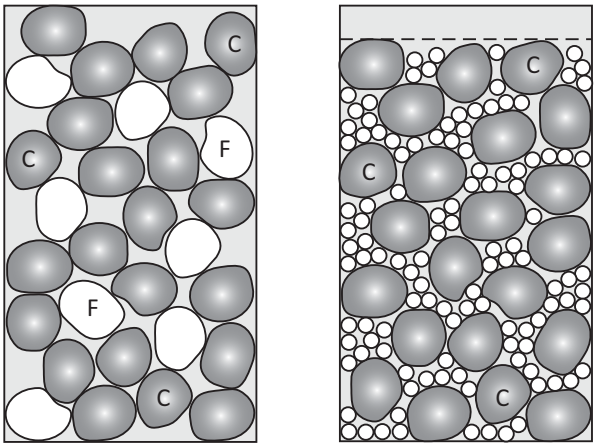

Figure 7.6 The volume occupied by a stable particle structure with coarse filler (F) compared to the volume occupied by a stable particle structure with fine filler.(C=Cement)

replaced by filler M6 ($d_{50} = 25\mu m$) the CSF is 0.721. Using a finer filler such as M300 ($d_{50} = 15\mu m$) leads to the cement particles being closer together and CSF to increase to 0.733. Decreasing the filler size in this way leads to a theoretical strength increase of 4.4 N/mm^2.

In the previous example inert fillers were used as cement replacing material. However, in ecological concrete often binders will be used to replace the cement. The binders actively contribute to the strength development of concrete and should therefore be taken into account in the design process. To predict the influence of the binders on the strength development of the concrete a proposal is made to include the binders based on the k-value concept from (NEN-EN 206-1:2001). Following Equations 2.1 and 2.2, fly ash can be taken into account with an efficiency factor of 0.4 for the amount of fly ash which is less than 33% kg/kg of the cement content. The compaction value of the binder K_b includes then the compaction value of cement K_{cem} as well as a part of the compaction value of the fly ash K_{fa} as presented in Equation 7.11. Also the volume fraction of the binder in the mixture φ_b is increased, as well as the possible space which might be used by the binder denoted as φ_b^*, Equations 7.12 and 7.13. The use of the efficiency factor of fly ash of 0.4 in the strength prediction of concrete should be validated by experiments.

$$K_b = 1.0K_{cem} + 0.4K_{fa} \tag{7.11}$$

$$\varphi_b = r_c\alpha_t + 0.4r_{fa}\alpha_t \tag{7.12}$$

$$\varphi_b^* = \varphi_b \frac{1+K_b}{K_b} \tag{7.13}$$

7.5 Mixture adjustment

In the final step of the mixture design cycle, adjustments are made to the mixture composition. For instance when the strength is still higher than required, cement can be replaced by a filler in order to create a more ecologic mixture. After changing the mixture composition, the cyclic design procedure is followed again to come from packing density, via water demand to a strength prediction. Cyclic design is repeated until the mixture meets all requirements. For this research project the only controlling parameter in the design procedure was set to be the strength requirement. However, the set-up of the cyclic procedure allows also for mixture design based on mixture composition restrictions, or mixture design based on defined performance requirements.

7.5.1 Mixture composition restrictions

For each country, several design restrictions exist, defined in national standards or coming from practice. Often they depend on the types of materials used, thus differing for each country. Examples are design grading curves, minimum amount of cement, minimum amount of powders, maximum water/cement ratio, maximum water/binder ratio, proportion of cement to total powders, maximum percentage of recycled aggregates, minimum percentage of sand compared to gravel, etc. All these mixture composition restrictions can be used directly in this design step to adjust the mixture composition. For instance, a mixture with optimal packing density can have a low amount of powders. Because of the high particle packing and the friction between the particles these mixtures tend to be a little harsh. For workability reasons, such as the required pumpability on a construction site, a minimum content of powders can be prescribed. In that case, this design step can be used to increase the total amount of powders, while keeping the amount of aggregates constant. This will lead to a mixture with a lower packing density, so that the total design cycle procedure should be run at least once more.

In general, mixtures with a high packing density are very stable. Due to the high amount of contact points and high friction the segregation potential of the particles is very low. Still, a user might desire to use additional models or mixture design software. In that case, it is suggested to use these models within this design step for mixture adjustment. Also special mixture composition requirements can be made within this step. For ecological concrete this could be a maximum amount of cement, a minimum amount of special environmental friendly cement, a minimum amount of recycled aggregates or even minimum CO_2-emissions of the mixture, during the production process or during the entire lifecycle of the ecological concrete. In the latter case also additional models should be used within this step of the cyclic design procedure.

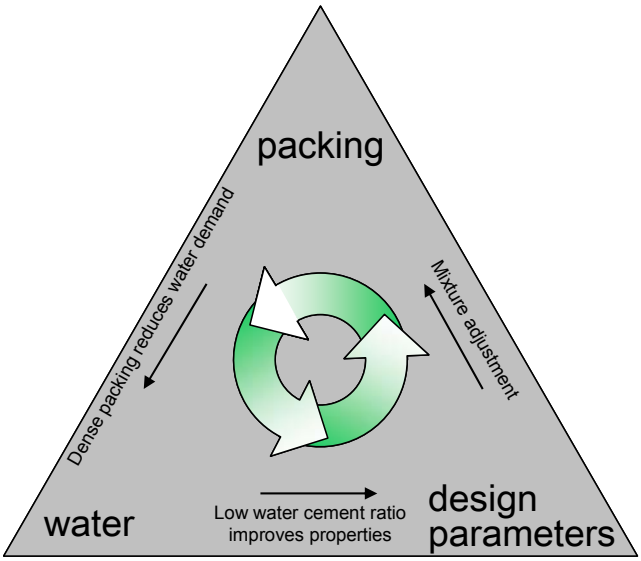

Figure 7.7 Cyclic design procedure for defined performance concrete.

7.5.2 Defined performance concrete

Ecological concrete is a special type of concrete designed for special applications in the lower strength classes. Ecological mixtures with cement contents below 260 kg/m^3 do not comply with Dutch standards. With these special types of concrete it becomes more and more important to be able to predict their material properties and design custom made mixtures for each application. Instead of using a standardized mixture which is categorized by its strength class, the demands coming from the application will define the

performance of the concrete. In case strength is not the governing criterion, mixtures could be designed on criteria such as mass, stiffness, acoustic insulation, appearances such as color, maximum crack width, maximum deformation during hardening, etc. A similar cyclic design procedure can be followed based on the required performance, Figure 7.7.

The defined performance concept is very important for ecological concrete. This is because relations between strength and other material properties change depending on the mixture. For instance, in most standards, the design value for shrinkage is directly related to the strength class. In ecological concrete, however, shrinkage is much lower than can be expected from its strength class. In an application where shrinkage or deformation in the construction phase is the governing design parameter, high strength mixtures would be selected based on the standards. Low strength ecological mixtures with a low cement content could in that case just as well have fulfilled the deformation demands. Therefore, defined performance-based mixture design leads to a more economic material use and more environmental friendly concrete.

Special applications in which defined performance concrete has high advantages are structures in which the minimum percentage of reinforcement is applied for crack width control. Since the minimum percentage of reinforcement depends on the concrete strength, applying ecological concrete with a low strength would also decrease the amount of required reinforcement. For industrial concrete floors supported on sand design regulations prescribe minimum reinforcement. With low strength concrete, the concrete will crack at lower strength thus lowering the minimum amount of reinforcement. In that case, however, crack formation is influenced by different parameters such as the modulus of elasticity of the concrete, the thickness of the floor and the stiffness of the foundation. This makes special applications in which the minimum percentage of reinforcement is required especially suitable for defined performance concrete design.

7.6 Example of ecological concrete design

As an example to show the use of the cyclic design method, this section presents the process of designing an ecological concrete mixture. The starting point of the mixture design was reference mixture A1, see Table 4.1. This mixture consists of CEM I 32.5 R and seven size fractions of aggregates ranging from 0.125 mm to 16 mm. The CIPM was used

to calculate the packing density of this mixture, based on its volumetric particle composition. The packing density $\alpha_t = 0.886$, as well as the compaction value for the cement $K_{cem} = 2.55$ follow directly from the model. In the reference mixture the particles make up 84.8% of the total volume, which leads to a value of $\varphi_{mix}/\alpha_t = 0.848/0.886 = 0.96$. This value complies with a design consistency in between S2 semi plastic and S3 plastic. Once the amount of water is fixed, the strength can be predicted with the help of the cement spacing factor CSF. The CSF is calculated to be 0.68 (Equation 7.8 and 7.10) which is a little too low for a reliable strength prediction. For concrete with a maximum particle size of 16 mm, the strength is estimated to be in strength class C20/25.

Since the reference mixture A1 was already tested on slump and strength it is a good starting point for the design procedure. The slump measured during the experiments was 12 cm, which agrees well with the predicted consistency class S3 plastic. The strength was 31.8 N/mm^2, which was a little higher than expected but it would be within the 95% interval for a cement spacing factor $CSF = 0.7$ (lower boundary).

Mix1

An ecological concrete mixture was designed based on reference mixture A1 with the same consistency and strength. As a first step the CIPM is used to optimize the particle structure of the mixture. The result is a new particle size distribution, its packing density $\alpha_t = 0.893$ and the compaction value of the cement $K_{cem} = 2.72$. The new particle composition is presented in Table 7.3. The next step in the design cycle is choosing the consistency class for the new mixture. For comparative reasons the same consistency as the reference mixture is chosen with $\varphi_{mix}/\alpha_t = 0.96$. Due to the increased packing density the new ecological mixture can be designed with less water, 0.145 m^3/m^3 instead of 0.158 m^3/m^3. This will eventually lead to a small strength increase. Furthermore, due to the higher packing density also the cement spacing factor CSF increased. In the next design step the CSF is used for the strength prediction. The CSF of the new ecological mixture is calculated to be 0.70. The increase in the CSF leads to an estimated strength increase of 7.5 N/mm^2, which is about 20% of the total strength. At this point the cyclic design could be stopped, depending on the goal of the optimization. The goal was to design a more ecologic mixture with the same strength as the reference mixture. In this first cycle, there was an increase in strength instead of a reduction in cement. Therefore, the mixture is adjusted and the design cycle is followed for a second time.

Table 7.3 Particle compositions and packing densities of ecological mixtures during the design process.

Volume fraction	**Mixtures**			
[m^3/m^3]	**Ref-A1**	**Mix1**	**Mix2**	**Mix3**
CEM I 42,5 N	0.093	0.093	0.074	0.066
Fly ash SMZ Maasvlakte	-	-	0.026	0.036
Sand 0.125-0.25 mm	0.036	0.071	0.070	0.070
Sand 0.25-0.5 mm	0.118	0.020	0.020	0.020
Sand 0.5-1 mm	0.118	0.101	0.100	0.100
Sand 1-2 mm	0.073	0.161	0.160	0.160
Sand 2-4 mm	0.045	0.030	0.030	0.030
Coarse aggregates 4-8 mm	0.181	-	-	-
Coarse aggregates 8-16 mm	0.336	0.524	0.520	0.518
Packing density α_t CIPM [-]	0.886	0.893	0.892	0.891
K_{cem} [-]	2.44	2.72	2.53	2.44
Predicted strength [n/mm^2]	31.4	39.1	34.0	31.4

Mix2

The mixture is adjusted by replacing a part of the cement by fly ash, in such a way that the cement is reduced to balance the strength increase. Since the strength of Mix1 was increased by 20% a new mixture is composed with 20% kg/kg cement replaced by fly ash. From this new mixture Mix2, the packing density and compaction value of the cement need to be recalculated. The new volume fractions and packing density are presented in Table 7.3. After that, φ_{mix}/α_t is fixed at 0.96 again in order to determine the water demand and CSF. Based on experiments with ecological mixtures including fly ash, the efficiency factor of the fly ash is fixed at 0.4 for the amount of fly ash $\leq 0.75 *$ cement [kg/kg]. During this second run through the design cycle, the K_{cem} and thus also the CSF have decreased a little. However, since the CSF and the strength of this mixture are still higher than the reference mixture, optimization is continued and the design cycle is followed for a third time.

Mix3

Before starting the third run the mixture should be changed again in such a way that some additional cement is replaced by fly ash. To increase the speed of the optimization process and gain some insight into the optimal percentage of fly ash, the CIPM was used to create Figure 7.8. In this example the design strength was fixed by the reference mixture at 31.4 N/mm^2. The new optimal ecological mixture should have the same design strength and thus it follows from the graph that 28.5% of the original cement content should be replaced by fly ash. The reference mixture contained 250 kg cement. The new optimal ecological mixture contains 71 kg fly ash and 179 kg of cement. For validation the design cycle is followed for the third time. The new ecological mixture Mix3 has a packing density $\alpha_t = 0.891$ and a compaction value of the cement of $K_{cem} = 2.44$ which is consistent with the desired strength. By using the cyclic design procedure, almost thirty percent of cement is saved in the end. The final particle composition is presented as Mix3 in Table 7.3. Even more cement could have been saved when a finer type of fly ash would have been used, so that packing density would have been increased for increasing amounts of fly ash.

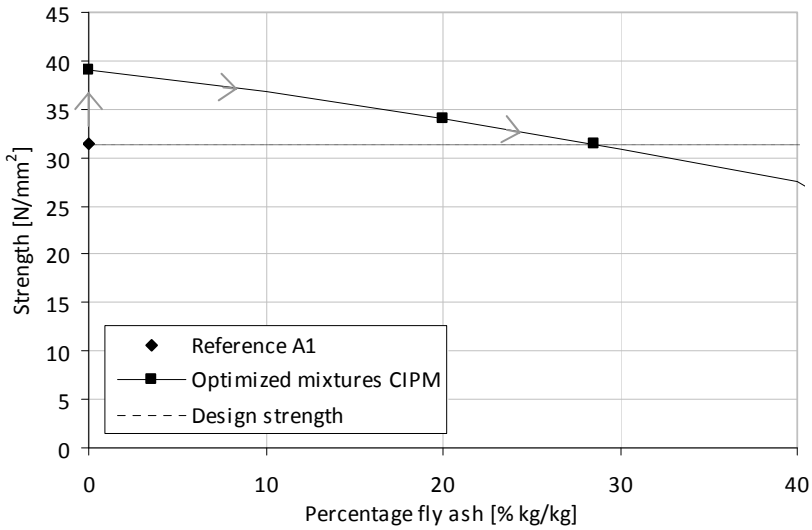

Figure 7.8 Graphical overview of CIPM optimization, used to determine the optimal fly ash percentage based on a reference mixture with a strength of 31.4 N/mm^2. The fly ash is expressed as percentage of the total amount of cement and fly ash.

7.7 Concluding remarks

In this chapter a design method for ecological concrete based on particle packing models has been presented. The design procedure is able to predict the strength of a mixture from its packing density calculations and water demand. The method is verified for mixtures containing cement and inert fillers with 28 day concrete strengths above 25 N/mm^2 and cement spacing factors between 0.7 and 0.81. It is formulated based on mixtures with low powder contents (less than 16% m^3/m^3 particles $\leq$ 250 µm), which can be regarded as a two phase system consisting of solid particles in a fluid. The fluid part is made up by water and a sufficient amount of superplasticizer Glenium 51. Other superplasticizers can only be used after further research validates the possible use of the CIPM with these superplasticizers.

From the packing density calculation the water demand of a mixture is predicted. Design graphs show that increasing the packing density is always beneficial for the total water demand of a mixture. This is because increased packing density causes a decrease in the required amount of void water which is always larger than the increase of the necessary amount of excess water. In this way, improving the packing density at constant cement content leads to lower water demands and indirectly to higher strength. However, adding a filler, replacing cement by a filler or decreasing the total water in the mixture, changes the mixture composition. An accurate strength prediction helps to determine the exact cement content to fulfill user requirements. The strength prediction is based on the assumption that during the hydration process, the hydration products of the cement particles need to bridge a certain space in order to connect the stronger aggregates to each other. Strength prediction based on the cement spacing factor is checked for mixtures including cement and inert filler but should be extended for the use of binders.

8 Application of ecological concrete mixtures

To show how the design method from chapter 7 can be applied to optimize ecological concrete mixtures, chapter 8 contains experiments on an application level. In section 8.1 three ecological concrete mixtures are optimized and evaluated with regard to CO_2-emissions. These mixtures are tested on strength development, modulus of elasticity, shrinkage and creep in section 8.2. Section 8.3 reviews which influence can be expected from the mixture design on the durability of ecological concrete. In section 8.4 industrial applications are described that were executed during this research project. Section 8.5 summarizes the conclusions coming from the experiments and industrial applications.

8.1 Ecological mixture design

8.1.1 Introduction

Ecological concrete mixtures can be designed for several reasons. Concrete producers would like to reduce the amount of cement to reduce production costs. Using less cement reduces the heat of hydration and the drying shrinkage, leading to less cracking problems. In defined performance concrete ecological concrete can reduce the minimum amount of reinforcement. In this research project the drives for designing ecological concrete were the wish to reduce the CO_2-emissions and to use residual products from concrete industry or other industries in the Netherlands. Because designers have different goals or limitations for every mixture design, a method for designing ecological mixtures was created. The method can be used to optimize mixtures, depending on the available materials and the desired performance. The value of the method is found in the computer design based on particle packing. It saves costs in the optimization process because binders and fillers can easily be qualified and less trial mixtures are required. In the next section three ecological concrete mixtures are presented to show how the design method can be used and how much cement can be saved.

8.1.2 Mixtures

In this research project ecological concrete mixtures were designed in strength class C20/25 with minimum amounts of cement. It shows how the cyclic design method for ecological concrete works. The method focused on minimizing the cement content at the desired strength. This means that CO_2-emissions were not used as a directive parameter in the design process and only reduced indirectly via the cement content. Various binders and fillers were taken into account in a qualification process. However, many of these, such as fjordstone filler or limestone filler, were not suitable for water or cement reduction, because their packing density was low in relation to the particle size distribution. In the end, three fillers were selected: fly ash because of its ball bearing effect and high packing density, quartz powder because of its fine and narrow particle size distribution, and ground incinerator bottom ash as residual product with low environmental impact.

Table 8.1 Compositions [kg/m^3] of concrete mixtures series J.

		Mixtures			
Composition		**J1**	**J2**	**J3**	**J4**
CEM I 42.5 N	[kg/m^3]	260	110	44	125
CEM III/B 42.5 N	[kg/m^3]	-	-	66	-
Fly ash SMZ Maasvlakte	[kg/m^3]	-	88	65	75
Quartz powder M600	[kg/m^3]	-	62	85	-
Ground IBA	[kg/m^3]	-	-	-	50
Aggregates 4-16	[kg/m^3]	1193	1162	1160	1157
Sand 0-4	[kg/m^3]	718	867	866	864
Glenium 51 [% kg/kg of powders]	[%]	0.8	0.8	1.2	1.2
Effective amount of water	[kg/m^3]	162	103	103	112
Water/cement ratio	[-]	0.62	0.94	0.94	0.90
Water/powder ratio	[-]	0.62	0.40	0.40	0.45
Estimated density (incl. 1% air)	[kg/m^3]	2351	2409	2408	2402
Packing density CIPM	[-]	0.886	0.897	0.898	0.890

The mixture compositions of three ecological mixtures and their reference mixture are presented in Table 8.1 as series J. The reference mixture was designed with 260 kg cement per m^3 concrete, which is the minimum cement content according to the Dutch standards. Since the mixture was designed for strength class C20/25 with design strength 33 N/mm^2, a relative high amount of water had to be dosed. Mixture J2 and J3 were optimized on packing density. Using the design cycle as presented in chapter 7 the cement content was minimized to 110 kg/m^3, in order to reach the estimated design strength of 33 N/mm^2. Mixture J2 contained a combination of fly ash and quartz powder M600. In mixture J3 also CEM III/B 42.5 N was used to increase the packing density even further and create a more ecological mixture containing less Portland clinker. In both mixtures the cement content was 110 kg/m^3 and the total powder content 260 kg/m^3 for comparative reasons. The particle size distributions are presented in Figure 8.1.

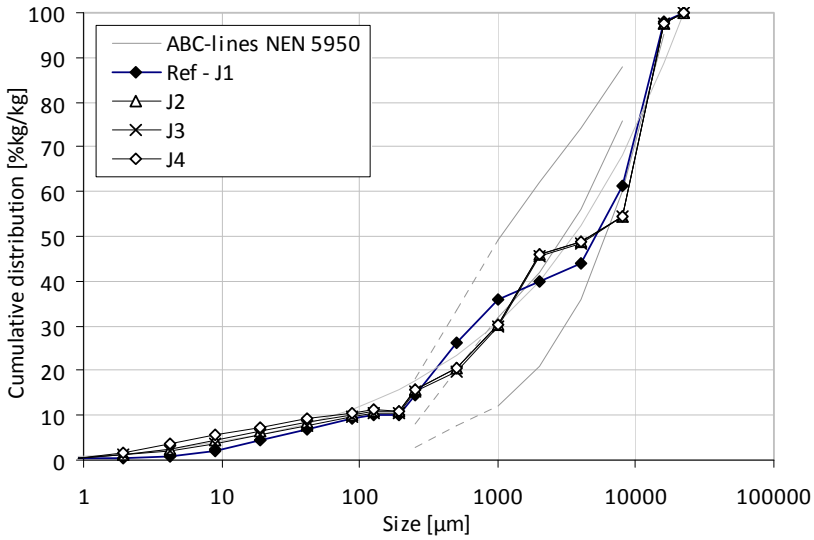

Figure 8.1 Particle size distributions of concrete mixtures series J combined with workability recommendations of (NEN 5950: 1995 nl).

Mixture J4 was designed with ground municipal solid waste incinerator bottom ash from INASHCO. The incinerator bottom ash is a waste product, which is upgraded to a filler by a wet grinding process (Bertolini, et al., 2005). In this way, the risk of entrapment of hydrogen bubbles produced by corrosion of aluminum particles in the fresh concrete is reduced. The chemical composition of the material is very similar to other binding materials such as cement and fly ash, which might lead to a positive effect of this filler on concrete strength. A point of attention for using incinerator bottom ash (IBA) in reinforced concrete structures is the high percentage of chloride of 0.38% in the IBA. This makes the ground IBA only suitable for use in unreinforced concrete products or in reinforced concrete with cement replacement levels below 20%. The chemical composition of the ground IBA is recorded in Appendix A.

To be able to evaluate the use of the ground IBA as a cement replacing material, the maximum replacement level of 20% was used. By fixing the total amount of powders to 250 kg/m^3 concrete, the performance of mixture J4 can easily be compared to reference mixtures A1, B1 and B3. The mechanical performances of the mixtures in series J are presented in section 8.2.

8.1.3 Ecological impact

In this section the CO_2-emissions of the ecological concrete mixtures are estimated. First CO_2-emissions for each material are estimated based on literature. In the next part these values are used to visualize the ecological differences between the mixtures.

In concrete production cement is responsible for a large part of the CO_2-emissions. In cement production, limestone is heated in a process called calcination. This process requires high temperatures which makes it very energy-intensive. Furthermore, when the limestone is transformed to Portland clinker CO_2 is released, as presented in Equation 8.1 (Worrell, et al., 2001).

$$\begin{array}{ccccc} CaCO_3 & \rightarrow & CaO & + & CO_2 \\ 1kg & & 0.56kg & + & 0.44kg \end{array} \tag{8.1}$$

CEM I 42.5 N contains 99% of clinker and 64% of CaO (ENCI, 2008). This means that for this type of cement the CO_2-emisions resulting from the calcination process are 0.50 kg CO_2 per kilogram of cement. Besides the calcination process other sources in the production process of cement are responsible for CO_2-emissions, including fuel burning, transportation of fuels and materials and electricity consumption. Based on data from (Cement&BetonCentrum, 2008; Worrell, et al., 2001) the CO_2-emissions per kg of cement excluding calcination are estimated to be 0.33 kg.

These emission values are used for an estimation of the CO_2-emissions of each material in a concrete mixture. For waste materials such as fly ash, ground slag and ground incinerator bottom ash no CO_2-emissions are attributed to the waste product. Just as aggregates and sand they only require process energy for extraction, grinding and transport. The results are summarized in Table 8.2. It should be noted that life cycle analyses of materials are complex calculations and depend very much on which variables are taken into account and which not. For instance the type of (bio)fuel or improvements in the production process strongly influence CO_2 impact. Furthermore, a single ecological design will differ even from producer to producer depending on the ecological impact assigned to for instance cement or superplasticizer. Therefore, Table 8.2 should be seen as an indicative overview of CO_2-emissions per kg of cement or concrete, which is merely used to visualize the differences between various ecological mixtures of this research project.

Table 8.2 Estimated CO_2-emissions in kg per kg of powder and per kg of concrete (Cement&Beton Centrum, 2008; gronbeton.dk; Worrell, et al., 2001).

CO_2-emissions / kg powder [kg]	**calcination**	**fuel for calcination**	**process energy**	**total**
CEM I 42.5 N (99% clinker)	0.50	0.22	0.11	0.83
CEM III/B 42.5 (29% clinker)	0.14	0.07	0.11	0.32
Fly ash SMZ Maasvlakte			0.11	0.11
Quartz powder M600			0.11	0.11
Ground IBA			0.11	0.11

Average CO_2-emissions / kg concrete [kg]	**calcination**	**fuel for calcination**	**process energy**	**total**
Aggregates and sand				0.02
steel				0.04
moulding				0.01
transport				0.01
cement (12%)	0.05	0.03	0.01	0.09
				0.17

The CO_2-emissions for each mixture of section 8.1.2 are calculated based on Table 8.2. The reference mixture has a CO_2-emission of 0.17 kg per kg concrete, which is about average for concrete. Ecological concrete mixtures J2 and J4 emit about 25% less CO_2 due to cement replacement by fly ash and quartz powder or ground IBA, Table 8.3. Mixture J3 in which also part of the Portland cement is replaced by blast furnace slag cement is the most environmental one saving more than 35% of CO_2. It only produces 0.11 kg CO_2-emissions per kg of concrete which is even lower than the 0.12 kg/kg a reference mixture with 260kg/m^3 blast furnace slag cement would produce.

Saving about 50% of the Portland cement in the mixtures leads eventually to an average CO_2 reduction of around 25%. This is a considerable amount especially because of the large amounts of concrete produced worldwide every year. In the Netherlands alone, already about 40 million tons of concrete are produced each year. By using ecological concrete mixtures, an amount of 2 million tons CO_2-emissions can be saved.

Table 8.3 CO_2 impact of ecological concrete mixtures series J.

	Mixtures				
CO_2-emissions / kg concrete [kg]	**J1**	**J2**	**J3**	**J4**	**J1a**
CEM I 42.5 N	0.092	0.038	0.015	0.043	-
CEM III/B 42.5	-	-	0.009	-	0.035
Fly ash SMZ Maasvlakte	-	0.004	0.003	0.003	-
Quartz powder M600	-	0.003	0.004	-	-
Ground IBA	-	-	-	0.002	-
Aggregates and sand	0.02	0.02	0.02	0.02	0.02
Steel	0.04	0.04	0.04	0.04	0.04
Formwork	0.01	0.01	0.01	0.01	0.01
Transport	0.01	0.01	0.01	0.01	0.01
Total	**0.17**	**0.12**	**0.11**	**0.13**	**0.12**

8.2 Performance of ecological mixtures

Evaluation of the fresh state of the ecological concrete mixtures showed that all mixtures in series J were homogeneous and stable. Slump measurements (NEN-EN 12350-2:2009), air content (NEN-EN 12350-7:2009) and density (NEN-EN 12350-6:2009) are presented in Table 8.4. All the mixtures had sufficient workability for casting and vibration. Mixture J3 was judged as harsh compared to the other mixtures, which was especially noted when filling the moulds. To increase the ability to cast in practice, it is recommended to increase the total powder content. This will also improve the cohesion of the mixtures which was evaluated as low for mixtures J3 and J4 leading to easy collapse of the slump. These two mixtures had similar workability as mixture J2, consistency class C1 earth moist. Nevertheless, very low segregation and little bleeding of the mixtures was observed, by virtue of the dense particle structure.

Table 8.4 Mixture compositions [kg/m^3] and the measured material properties of series J.

		Mixtures			
Composition		**J1**	**J2**	**J3**	**J4**
CEM I 42.5 N	[kg/m^3]	260	110	44	125
CEM III/B 42.5	[kg/m^3]	-	-	66	-
Fly ash SMZ Maasvlakte	[kg/m^3]	-	88	65	75
Quartz powder M600	[kg/m^3]	-	62	85	-
Ground IBA	[kg/m^3]	-	-	-	50
Aggregates 4-16	[kg/m^3]	1193	1162	1160	1157
Sand 0-4	[kg/m^3]	718	867	866	864
Glenium 51 [% kg/kg of powders]	[%]	0.8	0.8	1.2	1.2
Effective amount of water	[kg/m^3]	162	103	103	112
Water/cement ratio	[-]	0.62	0.94	0.94	0.90
Water/powder ratio	[-]	0.62	0.40	0.40	0.45
Estimated density (1% air)	[kg/m^3]	2351	2409	2408	2402
Packing density CIPM	[-]	0.886	0.897	0.898	0.890
Rheological properties					
Slump	[cm]	20	3	*12*	*14*
Air content	[%]	0.9	1.8	0.9	0.9
Density	[kg/m^3]	2366	2406	2424	2456
Mechanical properties					
2-day cube compressive strength	[N/mm^2]	13.9	15.2	7.2	12.9
7-day cube compressive strength	[N/mm^2]	24.2	25.2	17.6	22.9
28-day cube compressive strength	[N/mm^2]	32.1	39.6	33.5	37.9
56-day cube compressive strength	[N/mm^2]	36.4	39.9	35.3	48.0
90-day cube compressive strength	[N/mm^2]	36.4	53.1	39.1	55.1
7-day tensile splitting strength	[N/mm^2]	2.0	2.1	1.4	2.0
28-day tensile splitting strength	[N/mm^2]	2.5	2.7	2.5	3.0
56-day tensile splitting strength	[N/mm^2]	2.6	2.7	3.0	3.3
90-day tensile splitting strength	[N/mm^2]	2.7	3.7	2.6	4.0
28-day prism compressive strength	[N/mm^2]	29.5	26.6	20.0	29.1
28-day modulus of elasticity	[N/mm^2]	30500	32500	30500	30500

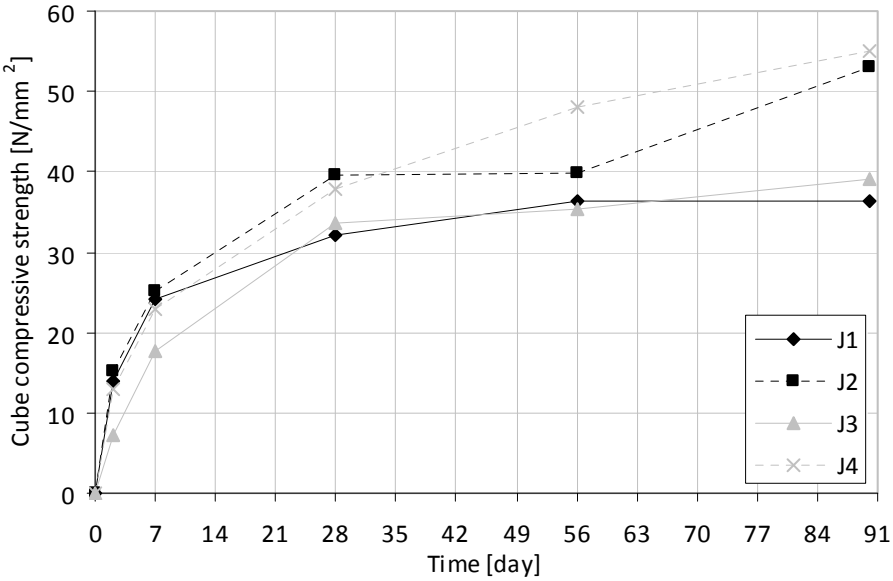

Figure 8.2 Cube compressive strength development of series J during the first 90 days.

The cube compressive strength development of series J is presented in Table 8.4 and Figure 8.2. All mixtures reach the design strength of 33 N/mm^2 for strength class C20/25 within 28 days. The contribution of the fly ash and quartz powder to decrease the water demand is substantial. However, neither the conventional water/cement ratio nor the water/binder ratio of mixtures J2 and J3 can explain the strengths attained by these mixtures. Mixture J2 has a water/cement ratio of 0.94 and a water/binder ratio of 0.83 (NEN-EN 206-1:2001). Mixture J3 has a water/cement ratio of 0.94 and a water/binder ratio of 0.89. Based on the water/binder ratio the 28-day strength of these mixtures should have been between 20 and 25 N/mm^2. The additional strength gain up to 39.6 N/mm^2 for mixture J2 and up to 33.5 N/mm^2 for mixture J3 is explained by the high particle packing density of the powders and possible additional pozzolanic effects of the fly ash and quartz powder both improving the microstructure of the concrete. This is also confirmed by the electrical resistance measurements as presented in section 8.3. Mixture J2 and J3 show similar strength development after 56 days as mixture B3 and B4 (section 4.1). This can be explained by an additional pozzolanic reaction of the fly ash, depending on the amount of calcium hydroxide (which is proportional to the amount of Portland clinker) present in the mixtures.

Mixture J4 contained ground IBA as cement replacing material. The mixture reaches a 28-day cube compressive strength of 37.9 N/mm^2. When this result is compared to mixtures B1 and B3, the ground IBA is qualified as a binder with a higher strength development potential than ordinary fly ash. This is probably due to the chemical composition and the much higher fineness of the material (Appendix A), creating a much denser micropacking in the concrete. Furthermore, the fineness and high surface area of the IBA improves the possible chemical contribution to the strength development.

The relationship between the average cube compressive strength and the tensile splitting strength of the ecological mixtures is the same as for normal concrete, Equations 4.1-4.3 (CUR Rapport 94-12, 1994; NEN-EN 1992-1-1:2005). Also the measured moduli of elasticity of the ecological mixtures comply with the relation for compressive strength versus modulus of elasticity as described in Eurocode 2 for normal concrete. Only mixture J4 has a relatively low modulus of elasticity compared to its strength. The correspondence of the ecological mixtures to the standard relations was expected based on the preliminary investigations of chapter 4. Confirmation of these relations by test series J proves the possibility to design for cube compressive strength and therefore improves the introduction of ecological concrete in the market.

The drying shrinkage and creep of the ecological mixtures were measured on six 100×100×400 mm concrete prisms in the longitudinal direction over a distance of 200 mm. Shrinkage testing started after 7 days of hardening at 20°C, 95% RH. Creep measurement started after 28 days of hardening, of which 7 days at 20°C, 95% RH and 21 days at 20°C, 50% RH. For the creep measurement a force of 0.33 times the prism compressive strength was applied. The prism compressive strength was determined on specimens of the same size, which hardened under the same conditions as the creep specimens. All shrinkage and creep tests were conducted for 90 days at 20°C and 50% RH.

The measured drying shrinkage and creep of the ecological mixtures J2 and J3 were relatively low compared to normal concrete. The results can be explained by the relatively low cement content, the normal modulus of elasticity and the high density of the particle structure, which provides resistance against deformation of the cement matrix. In Figures 8.3 and 8.4 the shrinkage and creep are compared with corresponding formulations in Eurocode 2 (NEN-EN 1992-1-1:2005) for concrete in strength class C20/25, Equations 4.4-

4.6. Mixture J4 has a relatively higher shrinkage than mixtures J2, J3, B1 and B3, suggesting that the ground IBA contributes to shrinkage in the same way as cement. In the first 77 days this shrinkage is even larger than the shrinkage of the reference mixture J1. The shrinkage of both reference mixture J1 and mixture J4 is still lower than the shrinkage estimation according to Eurocode 2. The creep of reference mixture J1 is larger than was expected based on its strength class and Eurocode 2.

The variation in the shrinkage and creep measurements of the different mixtures shows that shrinkage and creep very much depend on the types of fillers and binders which are used in the ecological concrete. When for a certain application shrinkage or creep is the most important mixture design criterion, performance-based design will lead to optimal ecological concrete.

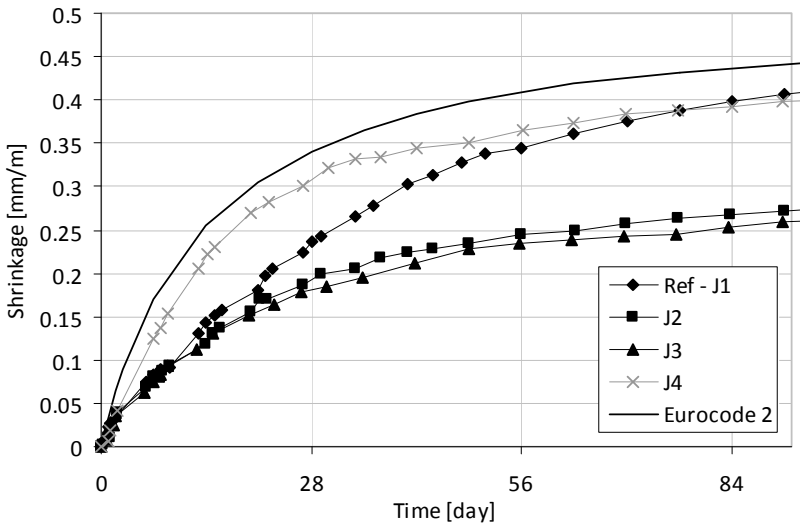

Figure 8.3 Shrinkage measurements of mixtures series J compared to Eurocode 2.

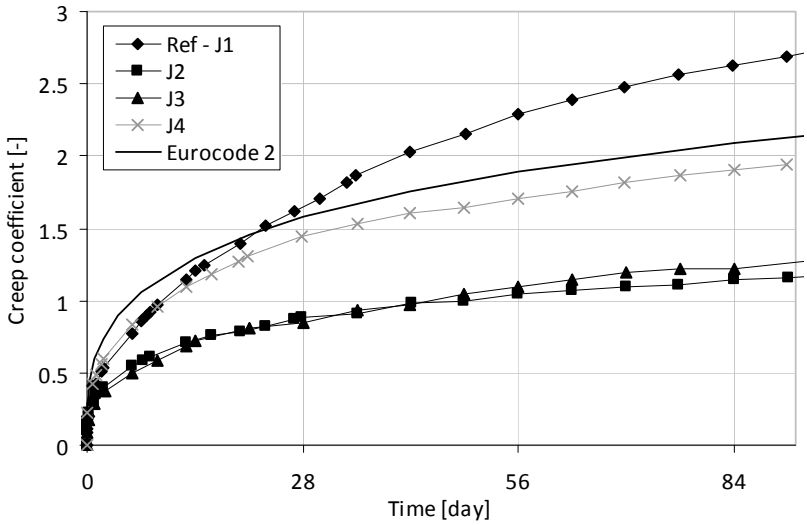

Figure 8.4 Creep measurements of mixtures series J compared to Eurocode 2.

8.3 Durability aspects

Traditionally, the durability of concrete is guaranteed by fulfilling requirements with regard to the minimum cement content and maximum water/cement ratio. Durability investigations were not the goal of this research project; however, the ecological concrete mixtures do have a very low cement content and high water/cement ratio, indicating the need for extensive durability testing. Furthermore, the use of new types of binders might also lead to new deterioration mechanisms in concrete, which makes further investigations inevitable.

To make a first prediction on the performance of ecological concrete with regard to durability, some experiments were performed to gain knowledge on the density of the microstructure of ecological concrete. A permeable microstructure is undesirable, because water easily gets out and harmful substances easily get inside the concrete. If the concrete dries out too fast, no water is left for hydration of the cement. Especially when cement is replaced by slowly reacting binders it is important to hold the water inside the concrete to enable further chemical reactions. Furthermore, dry concrete is subject to carbonation. Carbonation causes a reduction of the pH of the concrete and thus removes the protection against corrosion of the reinforcement. A less dense microstructure is more sensitive to freeze-thaw attack and more permeable for chemicals. This makes concrete

with a high permeability susceptible to chloride ingress and sulfate attack. For that reasons in this section experiments are presented which improve the understanding of the permeability of the microstructure of ecological concrete.

8.3.1 Drying out during hardening process

To determine the susceptibility of ecological concrete to dry out during the hardening process, weight loss and compressive strength of concrete specimens have been determined for different hardening conditions. Concrete cubes of 150×150×150 mm hardened for 1, 3, 7 and 28 days at 20°C, 95% RH. After that, they were stored in 20°C, 50% RH to measure their weight loss. The specimens were tested on cube compressive strength after 21 days of storage at 50% RH.

The tests were performed on ecological concrete mixture B3 containing 125 kg/m^3 cement and 125 kg/m^3 fly ash. This mixture is taken as a representative mixture with a low cement content in relation to the minimum cement content of 260 kg/m^3 prescribed by the Dutch standards (NEN-EN 206-1:2001). The mixture contains 135 liter water per m^3 concrete. Calculated from the mixture composition each cube contains about 450 grams of water

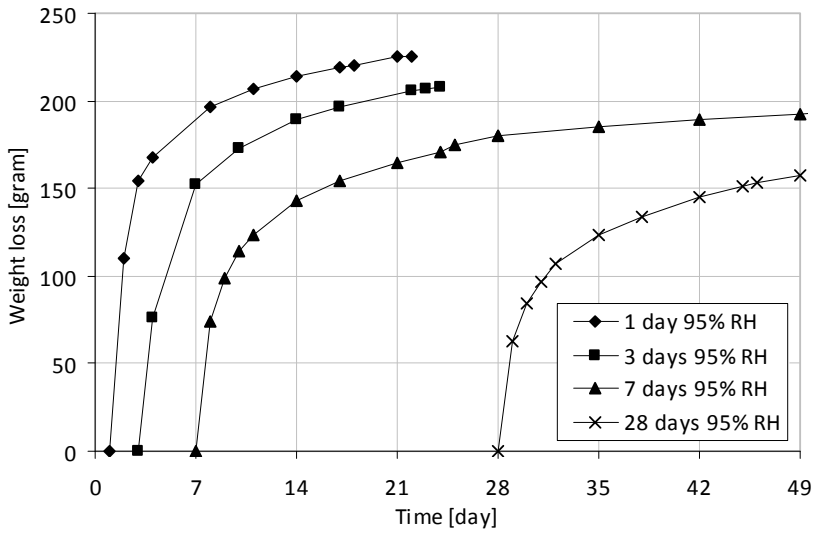

Figure 8.5 Weight loss of specimens during storage at 50% RH after a hardening period of 1, 3, 7 and 28 days at 95% RH.

and 420 grams of cement. This amount of cement can bind about 170 grams of water. The remaining amount of water of 450-170=280 gram could evaporate from the specimens over time. The measurements show that the specimens which did not get the time to harden properly, lost more water and at a faster rate than the specimens which remained longer at 95% RH, Figure 8.5. The specimen which hardened for 1 day at 95% RH lost 155 grams of water over the next 2 days, compared to the 84 grams of weight loss found in the specimen which hardened 28 days at 95% RH. Clearly, these mixtures did not have a chance yet to build a close and less permeable microstructure to prevent drying out. This is also found in the results of the cube compressive strength tests as presented in Figure 8.6. The reductions of the strength of specimens with 1 day and 3 days of hardening at 95% RH compared to the 28 day reference strength were estimated to be 20% and 10% respectively. The differences in the 28 days cube compressive strength of the specimens with 7 and 28 days of hardening at 95% RH were not significant.

These experiments show the need for good curing when ecological concrete is going to be used in practice. The relatively less dense microstructure and the slow hydration at early ages due to the lower cement content and increased water/cement ratio, make ecological concrete more susceptible to drying out. A recommendation is made to cure and protect concrete structures according to (NEN-EN 13670:2009) for slow or very slow concrete strength development.

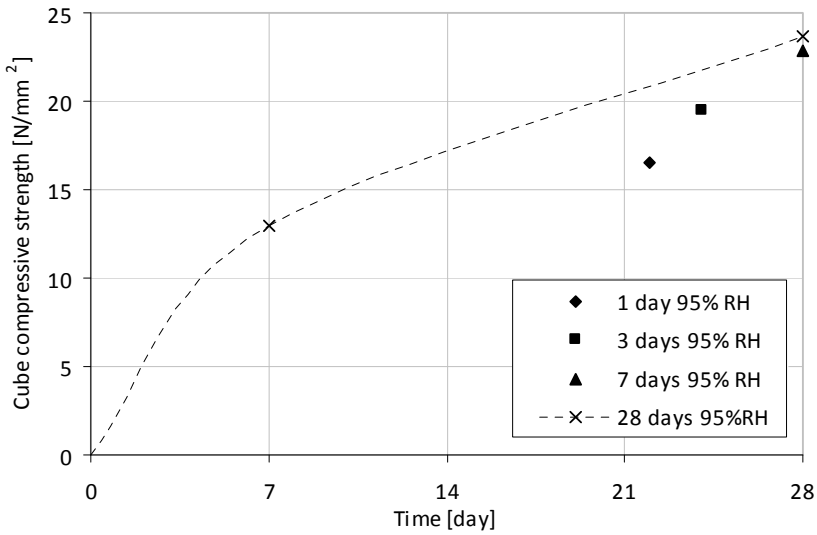

Figure 8.6 Cube compressive strength of specimens hardened for 1, 3, 7 and 28 days at 95% RH.

8.3.2 Electrical resistance

An indication of the durability of ecological concrete can be provided by measuring the permeability of concrete, since concrete with lower permeability is less sensitive for transport mechanisms such as chloride ingress. The two electrode method (TEM) is used to determine the electrical resistance of concrete and provides an indirect measurement of the amount of uninterrupted water in a fully saturated specimen. This amount of water is related to the quantity of continuous pores in the concrete and thus also to the permeability of the concrete. From theoretical and experimental work there appears to be a relationship between resistivity of and chloride diffusion in a particular concrete composition (Andrade, et al., 1993; DuraCrete, 2000; Polder, 1997; Polder, 2000). Furthermore, Smith (2006) reports that electrical resistance measurements are related to chloride penetration resistance as measured by the rapid chloride permeability test.

The electrical resistance is measured at a frequency of 120 Hz on a saturated 150×150×150 mm concrete cube tightened between two steel plates. Measurements were taken on saturated cubes at 20 ± 2°C and 65 ± 5% relative humidity.

The resistivity of all the ecological mixtures is higher than the resistivity of reference mixture J1, Figure 8.7 and Table 8.5. Only mixture B3 (section 4.1) has a lower initial resistivity, but after 90 days the resistivity is higher than that of the reference. Mixtures

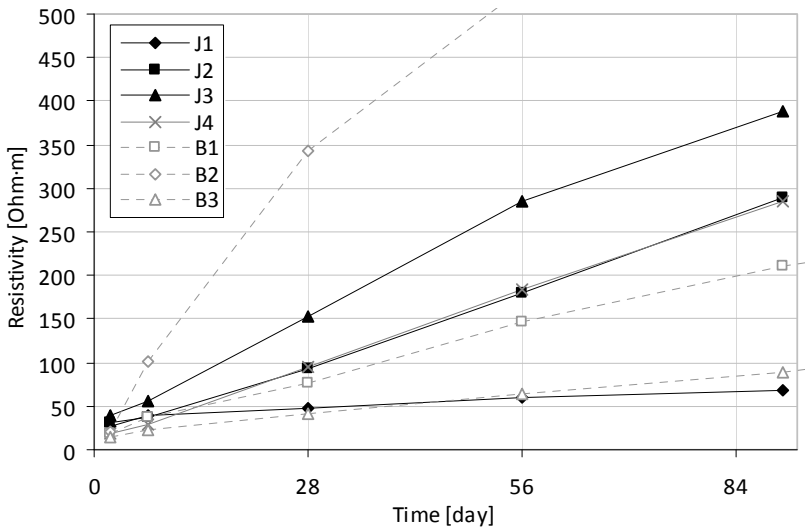

Figure 8.7 Resistivity measurements of series J and mixtures B1-B3.

Table 8.5 Resistivity measured by TEM of ecological concrete mixtures B1-B3 and J1-J4.

Resistivity	**Mixtures**						
[Ohm·m]	**B1**	**B2**	**B3**	**J1**	**J2**	**J3**	**J4**
2-day	19	21	14	27	31	38	18
7-day	37	101	23	40	38	55	29
28-day	77	344	41	47	94	154	94
56-day	147	530	65	59	180	286	184
90-day	210	707	89	69	290	389	286
365-day	573	1421	397	-	-	-	-

containing blast furnace slag cement often show high resistivities, caused by differences in microstructure and pore solution conductivity. This explains the differences in the resistivity of B1 compared to B2 and J2 compared to J3. The resistivity was not related to the water/cement ratio or water/binder ratio. In fact, mixture J2 with a water/cement

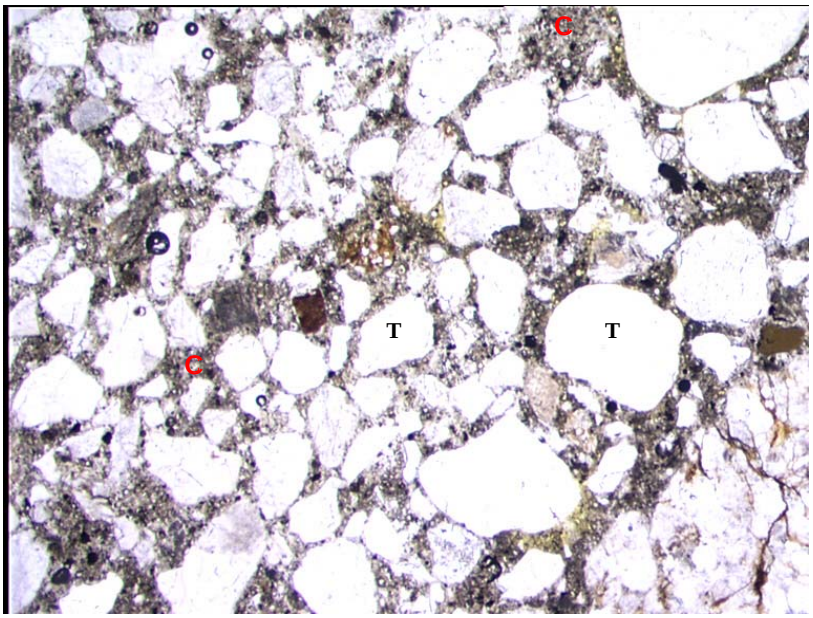

Figure 8.8 Micropicture overview of PFM_B1. It shows a very close packing of the sand particles (T), with a small amount of hardened cement paste (C) in between the particles. (Image size 5.4 x 3.5 mm, parallel polarized light).

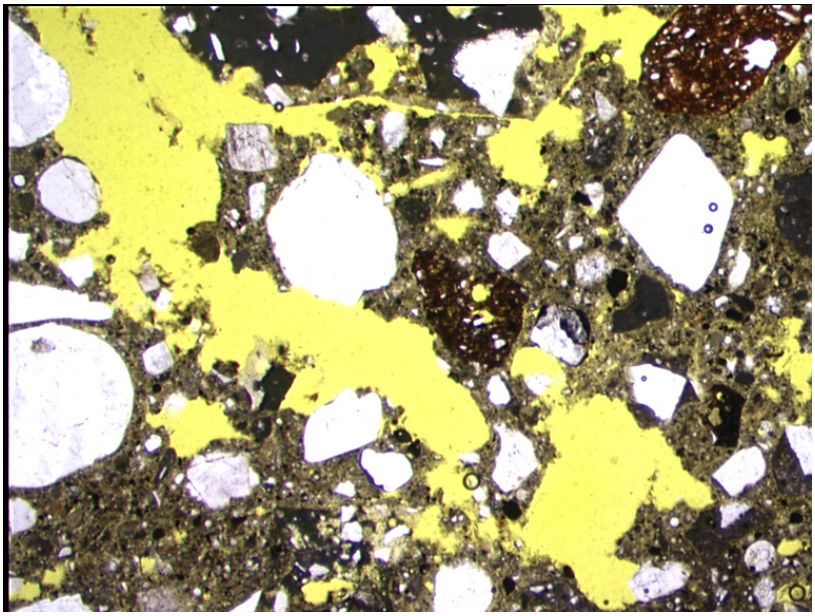

Figure 8.9 Micropicture showing the bad compaction of PFM_B2. All yellow areas are voids. (Image size 5.4 x 3.5 mm, parallel polarized light).

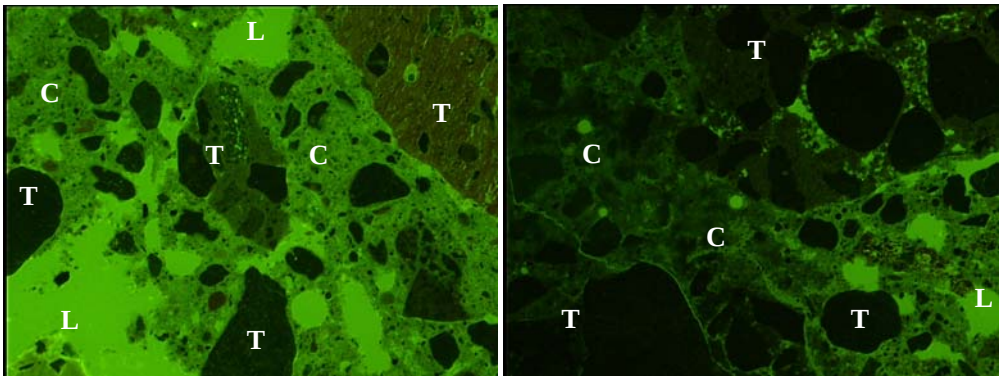

Figure 8.10 Micropictures of PFM_B2, UV-fluorescent light. Increased brightness corresponds to increased capillary porosity and thus the water/binder ratio of the hardened cement paste. In the picture on the right hand side water/binder ratio is substantially lower than in the picture on the left hand side coming from the same specimen. (Image size 5.4 x 3.5 mm, C= hardened cement paste, L=air voids, T=aggregates).

ratio of 0.94 and a water/binder ratio of 0.83 has a much better resistivity than J1 with a water/cement ratio of 0.62 and B1 with a water/cement ratio of 0.68 and water/binder ratio of 0.60.

The electrical resistance measurements show that predicting concrete properties related to durability by using the water/cement ratio, the water/binder ratio and/or the cement content is not reliable. To evaluate the durability, the total composition of the mixture specified by the particle size distribution, water content, cement content and water/powder ratio, should be taken into account. For durability aspects, extensive research on performance-based design is recommended.

8.3.3 Polarizing and fluorescent microscopy

Polarizing and fluorescent microscopy (PFM) is a type of optical microscopy in which thin sections are studied under polarized light as well as fluorescent light. By using polarized light concrete can be judged on mineralogical composition of various particles, their mutual relations and possible changes or deterioration in the material. UV-fluorescent light is used to observe cavities, micro-cracks and porosity. To produce the thin sections, a specimen was first dried at 40°C. Next, this specimen was impregnated with UV-fluorescent resin under a vacuum. After hardening of the resin, the specimen was sawn, after which the sawn surface was polished and glued onto a glass plate. Subsequently, the specimen was sawn parallel to the glass plate, resulting in a 1 mm thick block. This block was ground and polished until it was circa 25 µm thick. Finally, the thin section was covered with a cover glass.

The microstructures of mixtures B1, B2 and B3 were evaluated by polarizing and fluorescent microscopy (PFM) after 56 days of hardening at 20°C, 95% RH. Specimen PFM_B1 with 175 kg/m^3 Portland cement and 75 kg/m^3 fly ash has a homogeneous microstructure. The bond between cement and sand and between cement and coarse aggregates is strong. No large voids or areas without bond were found. Only small amounts of hardened cement paste are present between the sand particles, indicating a high packing density, Figure 8.8. Along the coarse aggregates some carbonation is observed, indicating that this part of the hardened cement paste has an increased CO_2

permeability, see also Figure 8.12. The water/binder ratio is uniformly distributed across the specimen.

Specimen PFM_B2 with 175 kg/m^3 blast furnace slag cement and 75 kg/m^3 fly ash was poorly compacted at the microlevel, Figure 8.9. The amount of air voids strongly varies over the sample, resulting in parts with a local air content above 10%. The average air content across the specimen is estimated to be 6-7% m^3/m^3. These voids also negatively influence the bond between hardened cement paste and aggregates. The water/binder ratio varies for different parts of the specimen, ranging from 0.5 to 0.6, as shown by Figure 8.10. The average water/binder ratio is estimated to be 0.55. Areas which are compacted well at the microlevel show good bond between hardened cement paste and sand and coarse aggregates, Figure 8.11.

Specimen PFM_B3 with 125 kg/m^3 Portland cement and 125 kg/m^3 fly ash has a homogeneous microstructure and a very close packing. Especially the space in between the sand particles is small but well filled with cement paste, Figure 8.13. The bond between the hardened cement paste and the aggregates is strong. Along the coarse aggregates some carbonation is observed, indicating that this part of the hardened cement paste has an increased CO_2 permeability, Figure 8.12. No large voids or areas without bond were found. Some local variations occur in the proportion of cement to fly ash, Figure 8.14. The fly ash particles present in the specimen hardly show any hydration. The water/binder ratio in this specimen was uniformly distributed.

Evaluation of the microstructures of specimens PFM_B1 and PFM_B3 showed that these mixtures are homogeneous, have close packing and good internal bond. No direct evidence was found to suspect a decreased durability. Specimen PFM_B2 is poorly compacted and has a considerable variation in the water/binder ratio, which both unfavorably influence the durability. When ecological concrete mixtures are designed special attention should be given to the ease to mix and compact the mixtures, especially for the mixtures with very low powder contents (< 0.09 m^3 particles smaller than 125µm per m^3 concrete). To improve durability it is suggested to include more fine powders in the mixture to increase the cement spacing factor as well as the workability. For further information on the durability of concrete containing high amounts of fly ash as cement replacing material reference is made to (Leegwater, et al., 2007).

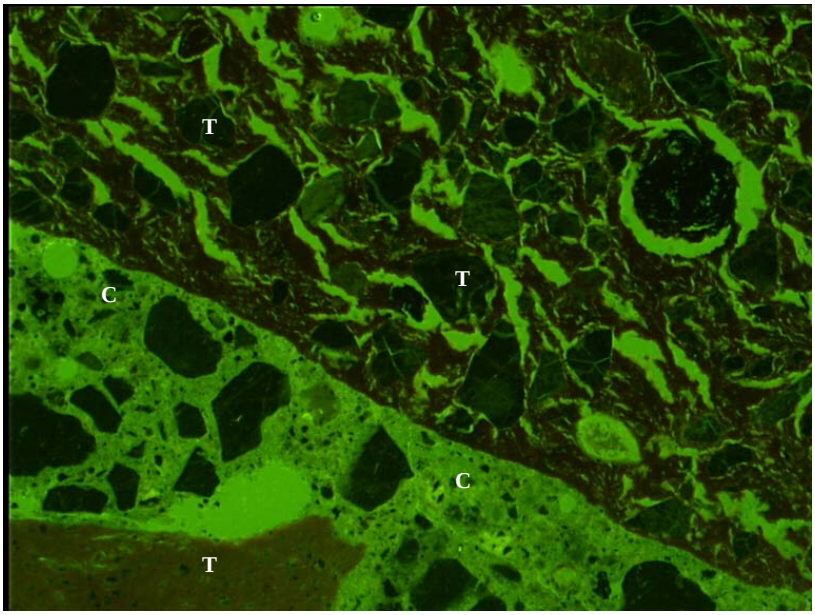

Figure 8.11 Micropicture of PFM_B2, UV-fluorescent light. In well compacted areas at the microlevel, the bond between hardened cement paste (C) and aggregates is strong. (Image size 5.4 x 3.5 mm)

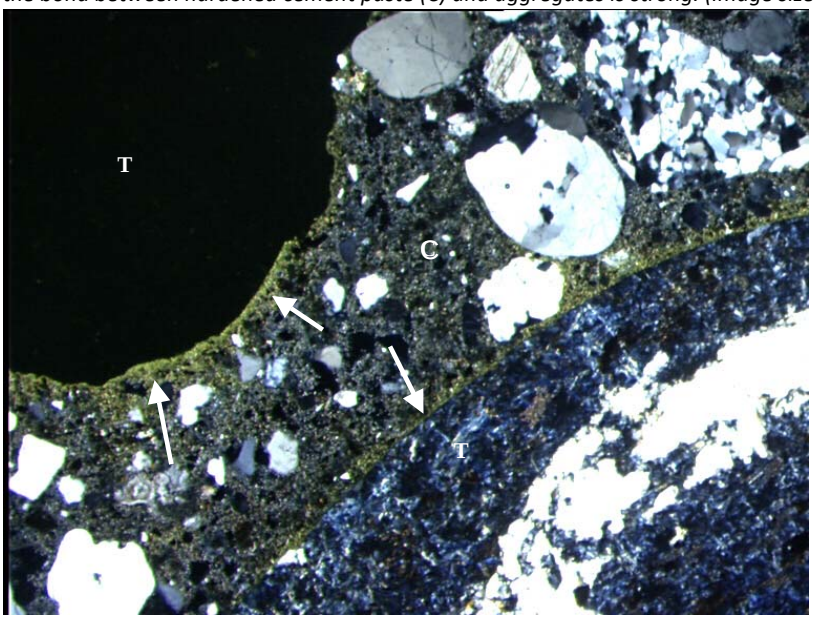

Figure 8.12 Micropicture overview of PFM_B3, polarized light with crossed nicols. Along the coarse aggregates (T) carbonation of the hardened cement paste (C) is observed. Carbonated parts are indicated by arrows and can be recognized by their yellowish color in relation to the beige color of the non-carbonated hardened cement paste. (Image size 5.4 x 3.5 mm)

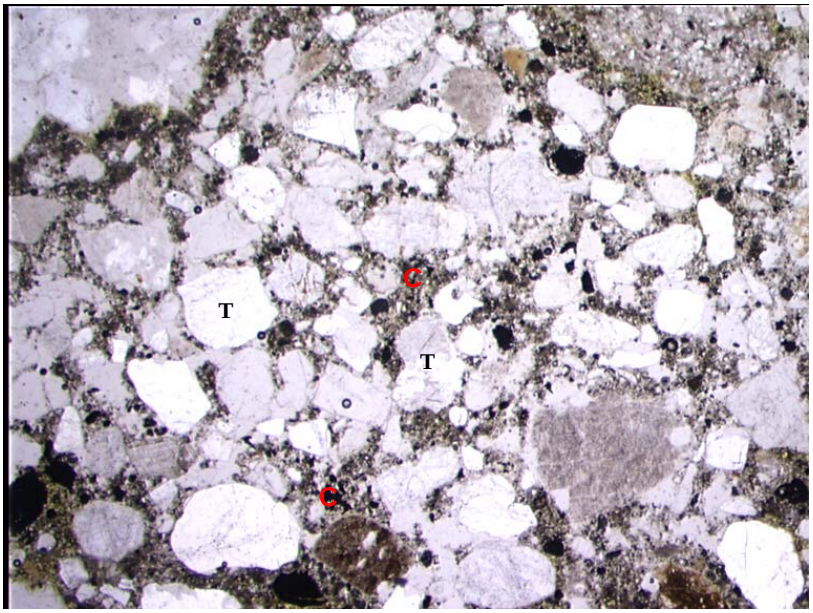

Figure 8.13 Micropicture of PFM_B3, showing a very close packing of the sand (T), with only little cement paste (C) in between the particles. (Image size 5.4 x 3.5 mm, parallel polarized light.)

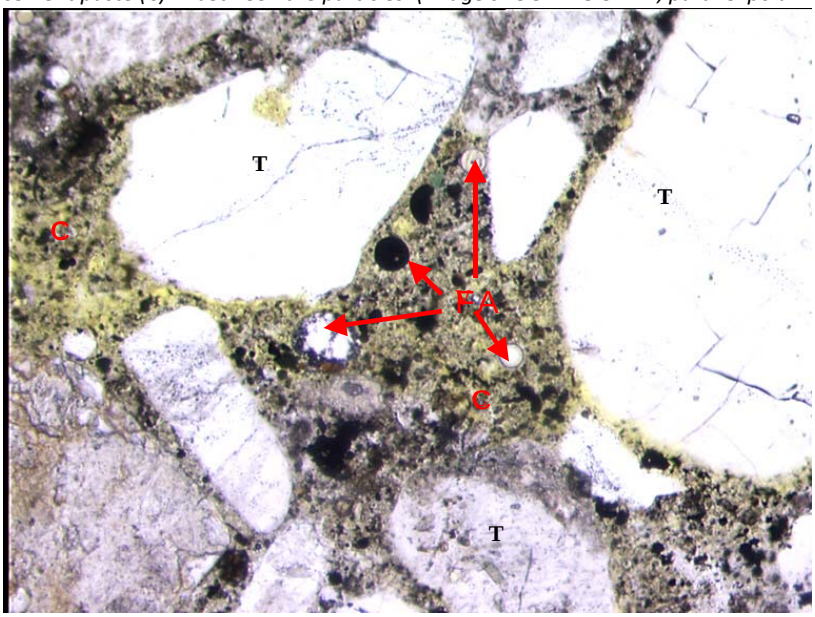

Figure 8.14 Micropicture showing a detail of PFM_B3. In the hardened cement paste (C) fly ash particles (FA) are present which hardly show any hydration. (Image size 1.4 x 0.9 mm, parallel polarized light, T=aggregates.)

8.4 Demonstration projects

After the first preliminary test series A and B it was decided to execute further experiments on ecological concrete in some demonstration projects. The demonstration projects were carried out during the development of the design method in this study, so the mixtures being used in these projects were only semi optimized. The execution of the demo projects served two purposes. With a full scale test the feasibility of casting with ecological concrete was investigated and practical experience was gained. Secondly, the demo projects were an excellent opportunity to compare the in situ performance of the ecological concrete with laboratory test results.

8.4.1 *Industrial pavement Werf Heijmans Rosmalen*

At the Werf Heijmans in Rosmalen, the Netherlands, a pavement was cast, which serves now as an industrial floor for the building firm itself. For durability reasons and because of the transport of heavy equipment over this part of the pavement, the design strength was fixed at C30/C37. To make sure that the mixtures reached the desired concrete strength the reference mixture was designed with 350 kg/m^3 fly ash cement CEM II/B-V 32.5 R (ENCI Maastricht). The ecological mixture was designed to contain 50% kg/kg fly ash and 50% Portland cement clinker, which leads to a mixture containing 240 kg/m^3 CEM II/B-V 32.5 R and 110 kg of fly ash as additional filler. The sand (0-4 mm) and gravel (4-16 mm) are standard river aggregates as used by mixing plants in the Netherlands. The mixture compositions are presented in Table 8.6. During construction specimens were cast for laboratory testing and the mixture composition was checked. Furthermore, the density of the fresh concrete was determined on a cube specimen according to (NEN-EN 12350-6:2009) for production control testing. The degree of compactability was determined according to (NEN-EN 12350-4:2009). The results of the in situ testing of the fresh concrete mixtures are presented in Table 8.6.

At the construction site two areas of about 20 m by 5 m were reserved for the reference mixture and ecological mixture for fixed-form paving. In both test areas a plain concrete pavement of 200 mm thickness was constructed, with doweled joints every 4.2 m. The concrete was mixed at the mixing plant and then delivered to the construction site by a truck mixer. At the site the concrete was cast in the test area and vibrated, Figure 8.15.

Table 8.6 Mixture compositions [kg/m^3] and the measured rheological and mechanical properties of the industrial pavement Werf Heijmans Rosmalen.

		Mixtures	
Composition		**Ref**	**Eco**
CEM II/B-V 32.5 R	[kg/m^3]	350	240
Fly ash	[kg/m^3]	-	110
Sand 0-4	[kg/m^3]	705	880
Aggregates 4-16	[kg/m^3]	1150	975
Water/powder ratio	[-]	0.52	0.51
Rheological properties			
Degree of compactability	[-]	1.06	1.05
Mixture temperature	[°C]	23.1	21.8
Density	[kg/m^3]	2348	2310
Mechanical properties			
7-day cube compressive strength	[N/mm^2]	34.3	17.5
28-day cube compressive strength	[N/mm^2]	49.9	31.4
56-day cube compressive strength	[N/mm^2]	54.7	38.3
90-day cube compressive strength	[N/mm^2]	61.6	43.8
28-day tensile splitting strength	[N/mm^2]	3.5	2.9
28-day modulus of elasticity	[N/mm^2]	31500	30500
56-day cylinder compressive strength	[N/mm^2]	54.7	45.3

The ecological concrete had about the same workability as the reference concrete which made both mixtures easy to process. The surface of the pavements was finished between the fixed forms by two hand-operated vibratory screeds. After this, irregularities were flattened out by hand with steel floats, Figure 8.16. Then a broomed surface texture was made in the transverse direction and curing compound was sprayed to prevent drying out, Figure 8.17. Finally, the transverse joints were sawn to control the cracking of the concrete due to drying shrinkage.

Figure 8.15 Casting and vibrating of the ecological mixture.

Figure 8.16 The surface of the pavements was finished between the fixed forms by two hand-operated vibratory screeds. After this, irregularities were flattened out by hand with steel floats.

Figure 8.17 Finishing the top surface of the reference mixture.

Figure 8.18 Additional specimens for laboratory testing were cast simultaneously with the same mixtures.

To determine the material properties of the ecological concrete and to be able to compare them to the reference concrete, additional specimens were made for testing strength, modulus of elasticity and freeze-thaw resistance. For both mixtures thirty 150×150×150 mm cubes and nine 100×100×400 mm prisms were cast directly at the construction site (Figure 8.18) and vibrated on a vibrating table. The next day these specimens were transported to the laboratory for demoulding and curing according to (NEN-EN 12390-2:2009). Furthermore, three cores with 100 mm diameter and 100 mm height were taken from the pavement at 56 days to compare the compressive strength of the pavement (outside conditions) to the compressive strength of the laboratory cured specimens.

The results from the compressive strength testing and the tensile splitting strength testing are presented in Table 8.6. On average the ecological concrete only reached 60-70% of the compressive strength of the reference mixture. However, the cores taken directly from the pavement show a relatively higher strength of the ecological concrete compared to the reference mixture. At 56 days the ecological mixture reached 83% of the reference strength. These differences can be caused by variance in the casting method, vibration method, curing procedure and long-term hardening conditions.

Furthermore, the freeze-thaw resistance was tested according to (NPR-CEN/TS 12390-9:2006). The loss of mass by scaling during the freeze-thaw resistance test was compared to the loss of mass of the reference mixture. For each mixture from four specimens the amount of scaled material in kg/m^2 was determined. The amount of scaling of the reference concrete was 2.86 kg/m^2 compared to 3.98 kg/m^2 for the ecological concrete mixture. Even though the ecological mixture scored worse in the scaling test, visual evaluation of the pavement did not show any signs of deterioration up to now.

8.4.2 Cycling path Hemaalpad Rosmalen

After the successful casting of the pavement at the Werf Rosmalen, a similar ecological mixture was used to build a cycling path. The mixture had to be adjusted for the production by slipform paver. Therefore, the water/cement ratio was lowered to have a lower degree of compactability and to reach the design strength of C30/37. The mixture was designed with 175 kg/m^3 Portland cement CEM I 32.5 R and 175 kg/m^3 of fly ash. Furthermore, aggregates with a maximum diameter of 32 mm were used. The cycle path has a length of 300 meter and is 3 meter wide, with a thickness of 160 mm. The concrete was prepared at the mixing plant and then delivered to the construction site by a truck

mixer. At the site the concrete was processed by the slipform paver, Figures 8.19 and 8.20. A broomed surface texture was made in transverse direction to minimize the chance of slippage for the users, Figure 8.21. Special attention was paid to spraying the curing compound, Figure 8.22, because of earlier experiences with drying out and slow strength increase. Finally, transverse joints were sawn to control the cracking of the concrete due to temperature and time dependent deformations.

To avoid differences in the material properties due to casting, vibration, curing and long-term hardening conditions, tests were performed on cores drilled from the cycle path. PFM analysis showed that the concrete was well compacted and had a homogeneous distribution of the aggregate. In the specimens some small areas without fine aggregate were found, indicating minor segregation. The Portland clinker showed good hydration, but a major part of the fly ash did not react and acted as a filler, even after 467 days. The bond between hardened cement paste and aggregate was good and the amount of microcracks was low. The effective water/binder ratio (*wbr*) varied across the specimens, with microbleeding channels with high *wbr* intersecting low *wbr* domains. Carbonation depth of the exposed surface of the specimen was less than 1 mm. Visual inspection of the cycle path did not show any evidence of freeze-thaw damage. (Leegwater, et al., 2007).

8.4.3 Self-compacting concrete Heembeton

This demonstration project aimed at reducing the cement content in one of the self compacting concrete mixtures of Heembeton. Mixture optimization was performed following the procedure as prescribed in chapter 7. For the ecological mixtures the same materials are used as in the reference mixture. In this way no changes have to be taken in the production process at Heembeton, Lelystad, to be able to cast the mixtures. Mixture requirements were self-compacting concrete with a slump flow between 600 and 800 mm and a V-funnel flow-time between 5 and 15 seconds, a 7-hour strength at elevated temperature hardening at 40°C of at least 15 N/mm^{2} and a strength class C35/45 after 28 days.

Figure 8.19 Production of cycling path Rosmalen by slipform paver.

Figure 8.20 Concrete delivered by truck mixer is processed to create a 16 cm thick cycling path.

Figure 8.21 The surface is broomed in the transverse direction to create texture and minimize chance of slippage for the users.

Figure 8.22 Spraying of the curing compound to prevent drying out at early age.

The mixtures were tested in the laboratory on slump flow (Abraham's cone, diameter 100-200 mm and height 300 mm) and V-funnel flow-time (V-funnel opening at top 515×75 mm, at bottom 65×75 mm). The reference mixture K1 had a slump flow of 640 mm and a V-funnel flow-time of 5.4 seconds, Table 8.7. Mixtures K2 and K3 were both evaluated as stable SCC mixtures; however, mixture K3 does not comply with the requested slump flow of 600-800 mm. The strength development over time of the mixtures is evaluated on the basis of 7 and 28-days cube compressive strength tests and maturity measurements. The

Table 8.7 Mixture compositions and rheological and mechanical properties of series K.

		Mixtures		
Composition		**Ref K1**	**K2**	**K3**
CEM I 52,5 R	[kg/m^3]	320	310	304
fly ash	[kg/m^3]	80	80	89
sand 0-4	[kg/m^3]	900	840	840
lime stone 2-14	[kg/m^3]	700	804	804
recycled concrete aggregates	[kg/m^3]	200	183	183
water	[kg/m^3]	164	158	156
Admixture 1	[%]	2	2	2
Admixture 2	[%]	0.8	0.8	0.8
Admixture 3	[%]	0.8	0.8	0.8
predicted air content [%]	[%]	2	2	2
water/cement ratio [-]	[-]	0.51	0.51	0.51
Water/binder ratio ($k_{fly\ ash}$=0.4) [-]	[-]	0.47	0.46	0.46
calculated packing density aggregate structure	[-]	0.695	0.705	0.705
calculated packing density particle structure	[-]	0.830	0.839	0.841
Rheological properties				
Slump flow	[mm]	640	650	580
V-funnel flow-time	[s]	5.4	7.3	7.2
Mechanical properties				
7-day cube compressive strength	[N/mm^2]	25.0	28.6	29.0
28-day cube compressive strength	[N/mm^2]	43.3	48.0	47.2

strength tests show a 7-days strength of 25 MPa and a 28-days strength of 43.3 MPa for the reference mixture. The optimized mixtures have higher strengths at 7 and 28 days. Other fillers might be considered in the optimization process. Especially fillers with a particle size smaller than cement can lead to higher packing densities and thus higher cement reductions.

8.5 Concluding remarks

In this chapter experiments were discussed that have been conducted to show the performance of ecological concrete on laboratory scale and in practice. Mixtures with different types of fillers and binders have been designed according to the cyclic design procedure of chapter 7. However, not all tested fillers and binders were suitable to be used in ecological concrete. This is because they were not able to increase the packing density and thus reduce the water demand of the mixtures. Fly ash, quartz powder and ground incinerator bottom ash were used in ecological mixtures, thereby saving up to 57% of cement. By virtue of the design method no trial testing was required and all ecological mixtures reached at least their predicted design strength of 33 N/mm^2. These high strengths compared to the applied low cement contents were achieved despite the high water/cement ratios and high water/binder ratios. Possibly the applied cement replacing materials contributed to the strength by pozzolanic reaction or because they were acting as nucleation cores in between the cement particles. This also depends on the chemical composition of the particles. It is important to take this mineralogical composition into account when designing based on the performance of concrete. For instance, shrinkage and creep results did vary for the different types of fillers used in series J. On the other hand, the relationship between the average cube compressive strength and the tensile splitting strength and the relationship between compressive strength and modulus of elasticity for ecological mixtures correspond to those for normal concrete. Confirmation of these relations proves the possibility to design for cube compressive strength and therefore improves the introduction of ecological concrete in the market.

The environmental impact of the ecological mixtures was evaluated based on the CO_2-emissions of their components. Saving about 50% of the Portland cement in the mixtures led eventually to an average CO_2 reduction of around 25%.

The demonstration projects and durability testing showed that attention should be paid to the slower strength increase in the beginning of the hardening process. This is for instance important when high strengths are requested at early ages for demoulding. However, it is especially important for durability, since the slow strength increase at early ages indicates a slower development of the density of the microstructure. With slow cement hydration in the early ages, the concrete more easily dries out and less water remains available for a long-term development of the microstructure. In the end this will lead to lower strengths but even more important lower durability. For that reason it is very important to apply good curing and protection of ecological concrete structures at early ages.

After 28 days the electrical resistances of all the ecological mixtures are higher than the resistance of reference mixture J1. The electrical resistance tests showed that the durability does not only depend on the water/cement ratio or water/binder ratio. To evaluate the durability, the total composition of the mixture specified by the particle size distribution, water content, cement content and water/powder ratio, should be taken into account. Furthermore, microstructural analysis has proven that poor mixing and compacting of these ecological mixtures can lead to very low durability. Therefore, it is important that the ecological mixtures contain sufficient amounts of fine filler. With increased powder contents, workability is improved and also better durability performance can be expected. For durability aspects, extensive research on performance-based design is recommended, for which packing density and the cement spacing factor CSF could eventually prove to be important parameters predicting the durability.

The demonstration projects were carried out during the development of the design method in this study, so the mixtures being used in these projects were only semi optimized. Series J was composed at the end of this study after selecting optimal cement replacing materials. In these mixtures fine fillers are applied in such a way that the packing density increases. Mechanical and electrical resistance test showed that ecological mixtures in series J perform much better than mixtures B3-B4, despite the lower cement contents. Especially, a great improvement was found in the early strength gain, which is important for preventing drying out and developing a dense microstructure. Furthermore, this shows that cyclic design of ecological concrete and applying fillers which improve packing density can greatly improve concrete performance.

9 Conclusions and recommendations

This chapter contains the conclusions and the recommendations for market introduction and further research. After the main conclusions section 9.1 deals with topics on replacing cement, measuring particle packing density, particle packing optimization, packing density relations, design by particle packing models and ecological concrete. Section 9.2 contains recommendations with regard to the possibilities to design and use ecological concrete according to the standards

9.1 Conclusions

Particle packing models can be used to predict the mechanical properties of ecological concrete from its basic components by using the cyclic design method developed during this project. In this cyclic design method the mixture composition of ecological concrete is readjusted according to the compressive strength which is predicted based on packing density and water demand. Designing ecological concrete based on strength is possible because relationships between cube compressive strength, tensile splitting strength and modulus of elasticity correspond to those for normal concrete. At the same time shrinkage and creep are low compared to normal concrete, which makes compressive strength the governing design parameter.

Using the cyclic design method has led to a cement reduction from 260 kg/m^3 to 110 kg/m^3. Thus up to 57% of Portland cement can be saved, while at the same time the concrete still satisfies the demands for appropriate use. In this way an average CO_2 reduction per cubic meter of cast concrete of around 25% is achieved.

Replacing cement

In this research project ecological concrete was defined as mixtures containing a cement content below 260 kg/m^3 and lying within strength class C20/25. Literature research on ecological concrete showed large variations, probably caused by varying research objectives such as testing of cement paste, mortar or concrete or adding various types and amounts of fillers and superplasticizers. In general, the literature study showed that adding fillers or binders that are able to decrease water demand improve the workability of concrete. On the other hand, agglomerating particles lead to bad workability and high water demands. Adding small fillers contributes to the interparticle friction of the mixture, which is good for the concrete properties in the hardened state. Also when the water/cement ratio is decreased fast hydration, dense microstructure, higher strength and good durability are reported, for concrete including fillers as well as for binders. However, when cement is replaced by fillers the higher water/cement ratio makes the cement matrix less dense. Therefore, high packing density is important to reduce the cement paste and water content.

The preliminary investigations showed that it is possible to optimize the concrete composition with packing density models in order to lower the cement content while

retaining satisfactory mechanical properties. The relationship between the average cube compressive strength, the tensile splitting strength and the modulus of elasticity of the ecological mixtures is the same as for normal concrete, while shrinkage and creep are lower than in normal concrete. Therefore, compressive strength can be used as the governing design criterion for the mechanical properties.

Control of the water demand of ecological mixtures is very important. Because of the low cement contents, small increases in the water demand may lead to very high water/cement ratios. Selecting the right type and amount of filler as cement replacing material is therefore very important. Size, shape and texture are important parameters for water demand, workability and strength. For that reason fine fillers should be included in the packing density model for ecological concrete mixtures.

Measuring particle packing density

The packing density of dry particles can be determined according to NEN-EN 1097-3:1998 for loose bulk density. The method can be extended to determine the maximum packing density at a certain compaction level, by applying external loads such as vibration or top-weight. To determine the maximum packing density of wet particles (<125 µm) no single method is generally accepted and therefore various test methods are used to determine packing density or water demand of fine particles. The mixing energy test is a fast and direct measurement of the water demand. Determining water demand by measuring the mixing energy was found to have the highest reproducibility and was chosen as comparative packing density measurement for this research.

With fine particles, the interparticle forces become increasingly important. These interparticle forces can cause, for instance, agglomeration of particles, thus lowering the packing density. Since the interparticle forces depend on the conditions (dry, wet) of the packing structure, also packing density is influenced by this. Therefore it is important that the maximum packing density of the particles is measured under the same conditions as under which the particles would be used in concrete and in the model. The conditions for this research project were fixed for packing densities in water including a sufficient amount of superplasticizer Glenium 51. Other superplasticizers can only be used after further research validates the possible use of the particle packing optimization method with these superplasticizers.

Particle packing optimization

The ideal particle size distribution depends on the particle shape and packing density of the various size fractions. Therefore, the ideal particle size distribution varies for each type of concrete. For instance, when rounded sand is combined with coarse recycled aggregates, the optimal particle size distribution differs from one of a mixture with angular sand and rounded coarse aggregates. Therefore, an ideal optimization curve does not inevitably lead to the mixture with the highest packing density. Analytical particle packing models and discrete element models are suitable to calculate the maximum packing density of concrete mixtures. However, discrete element models are not yet suitable for concrete mixture optimization due to limitations in computational speed. Therefore, at this moment analytical particle packing models provide the best solution for particle packing optimization of ecological concrete mixtures.

The particle packing models evaluated in this thesis have proven to be able to predict the packing density of randomly ordered particle structures consisting of coarse particles. They take into account the most important material factors for coarse particles such as size distribution and shape. However, in ecological concrete not only the packing density of the coarse particles is important, but especially the packing of the fine fillers replacing the cement itself. These small particles (<125 µm) have a different packing structure and increased particle interaction compared to coarse particles. For small particles surface forces become increasingly important compared to gravitation and shear forces. Therefore, one of the models had to be extended to include additional interactions. The Compressible Packing Model was judged to be the most accurate model, having the highest potential for modification to include these additional interactions. It can take into account wet and dry packing densities. *HADES* simulations including Van der Waals forces and electrostatic forces showed that small particles may agglomerate with each other, but also stick to larger particles. The increased loosening effect and decreased wall effect for particles smaller than 25 µm were implemented in the new Compaction-Interaction Packing Model (CIPM) by combining interaction with compaction. By using the adjusted interaction formulas, scaling of the interaction is made possible. In this way, also the influence of varying particle shapes might be implemented in the future. For mixtures with particles smaller than 125 µm using the CIPM reduced the average error in the packing density calculations from 2.2% to 0.6% and the maximum error from 6.4% to 1.8%.

Packing density relations

The packing density of a powder or mixture in itself is a powerful parameter in the design of concrete mixtures. It helps to determine the suitability of fillers as cement replacing material and is related to the flowability and strength of mixtures. Very fine fillers, with high surface area can increase packing density to such an extent that the water/cement ratio can be decreased when cement is replaced by them. This shows water demand is not just surface area related as often stated in water layer theories.

Furthermore, the concept that mixtures flow due to excess cement paste layers surrounding the aggregates was not in agreement with the experimental data including the particle packing of the aggregates. Small aggregates experience much more interaction from the cement particles than large aggregates. Therefore, the packing density of aggregates can not be used without the interaction effects of cement and fillers and thus a concrete mixture should be schematized as a particle structure in water instead of an aggregate structure in cement paste.

The maximum packing density of the tested mixtures was not directly related to their viscosity, flow value, heat generation or compressive strength. However, in each mixture part of the added amount of water is used to fill voids, while the rest is used to lubricate particles and allow flowability. In this way maximum packing density is directly related to the water demand of the mixture. The relative water volume and relative amount of excess water, which both depend on the packing density, are directly related to the flow value of the tested mixtures. Furthermore, the relative amount of excess water pushes the cement particles further away from each other, thus increasing the volumetric distance between the cement particles. In that case, higher water/cement ratios and lower packing densities lead to a larger distance between the cement particles and thus eventually to a lower strength due to the fact that the hydration products of the cement particles need to bridge larger distances. The distance between the cement particles is expressed as the cement spacing factor, which depends on the maximum packing density, the amount of water and the volume fraction of the cement particles. Mortar tests showed a good relation between the cement spacing factor and the compressive strength of a mixture.

Design based on particle packing models

The cyclic design procedure is able to predict the strength of a mixture from its packing density calculations and water demand. Starting from the (optimized) particle size distribution of a concrete mixture, the necessary amount of water is predicted from the required workability and calculated packing density. After that, the strength of the new mixture is predicted from packing density calculations and the amount of water in the mixture via the cement spacing factor. Subsequently, the mixture composition might be adjusted to comply with the desired performance or strength class. After this mixture adjustment the design cycle can be used again for a new strength prediction. The method is verified for mixtures containing cement and inert fillers with 28-day concrete strengths above 25 N/mm^2 and cement spacing factors between 0.7 and 0.81. It is formulated based on mixtures with low powder contents, which can be regarded as a two phase system consisting of solid particles in a fluid. The fluid part is made up by water and a sufficient amount of superplasticizer Glenium 51.

Design graphs show that increasing the packing density is always beneficial for the total water demand of a mixture. This is because increased packing density causes a decrease in the required amount of void water which is always larger than the increase of the necessary amount of excess water. In this way, improving the packing density at constant cement content leads to lower water demands and indirectly to higher strength. However, with higher packing densities also relatively higher amounts of excess water in relation to the void filling water are required. This is due to the increased number of contact points between the particles within such mixtures. The high packing density and high amounts of fillers increase friction and interlock due to high surface areas and higher interparticle forces of the small particles. In that case relatively more water is necessary to overcome the interlock and make the mixture flow.

Within the cyclic design procedure, strength can be predicted from the calculated packing densities by the CIPM and the mixture composition. The prediction is based on the relation between strength and volumetric distance between the cement particles expressed as cement spacing factor. It is checked for mixtures including cement and inert filler but should be extended for the use of binders. An accurate strength prediction helps to adjust the mixtures to fulfill user requirements. For ecological concrete such a requirement can be a minimum cement content for a certain strength class. In that case the mixture composition is changed by adding a filler, replacing cement by a filler or decreasing the total water content of the mixture. The cyclic design procedure enables

mixture composition adjustments based on concrete property requirements, which makes the method also suitable for defined performance concrete design.

Ecological concrete

Ecological concrete mixtures were designed containing fly ash, quartz powder and ground incinerator bottom ash, thereby saving up to 57% of cement. Other fillers were tested, but were not suitable to be used in ecological concrete because they were not able to increase the packing density. By making use of the cyclic design method no trial testing was required and all ecological mixtures reached at least their predicted design strength of 33 N/mm^2. The mixtures were tested on compressive strength, tensile strength, modulus of elasticity, shrinkage and creep. Good material properties were achieved despite the low cement contents and the high water/cement ratios. In performance based design of concrete it is important to take the mineralogical composition of the filler and binders into account. For most applications strength can be used as the governing design parameter for ecological concrete. The relationship between the average cube compressive strength and the tensile splitting strength and the relationship between compressive strength and modulus of elasticity for ecological mixtures correspond to those for normal concrete. Confirmation of these relations proves the possibility to design for cube compressive strength and therefore improves the introduction of ecological concrete in the market.

Electrical resistance tests indicated that durability does not depend on the water/ cement ratio or water/binder ratio. To evaluate the durability, the total composition of the mixture specified by the particle size distribution, water content, cement content and water/powder ratio, should be taken into account. Furthermore, durability testing showed that attention should be paid to the slower strength increase in the beginning of the hardening process. With slow hydration in the early ages, the concrete more easily dries out and less water remains available for long-term development of the microstructure. Also poor mixing and compacting of ecological mixtures can lead to increased porosity of the microstructure. Less dense microstructures will lead to lower strengths but, even more important, to lower durability. For that reason it is very important to apply good curing and protection of ecological concrete structures at early ages. Furthermore, it is important that ecological mixtures contain sufficient amounts of fine filler. With increased powder contents, workability is improved and also better durability performance is

expected. With regard to durability aspects, extensive research on performance-based design is recommended, for which packing density and the cement spacing factor CSF could eventually prove to be important parameters predicting durability.

Application of fine fillers which improve the packing density in ecological concrete has proven that the use of the cyclic design procedure can greatly improve concrete performance.

9.2 Recommendations

Mixture design of ecological concrete agrees well with design based on performance criteria. However, European standards for absolute performance testing of concrete do not exist yet, because of different long-term experience. Therefore, requirements to resist environmental actions are given in the standards by the minimum strength class and limiting values for the concrete composition. This means that concrete mixtures in the Netherlands should comply with a minimum cement content of 260 kg/m^3 and a water/cement ratio below 0.65 (for exposure class XC1). It is only allowed to disregard these requirements, when equivalent performance of the concrete mixture is proven. For ecological concrete mixtures such as the ones presented in chapter 4 and 8, not fulfilling these composition requirements, this means that extensive testing is required. This includes mechanical tests for cube compressive strength, tensile splitting strength, modulus of elasticity, long-term compressive strength, (4-point) tensile bending strength, shrinkage and creep. Also, the suitability of all components and properties such as workability, density and air content should be checked. Furthermore, durability tests which are relevant for the required exposure class should be performed. Depending on the exposure class and the application, tests might be required to determine carbonation, chloride ingress, sulphate resistance, freeze-thaw resistance, permeability, alkali-silica reaction, abrasion or other deterioration mechanisms. In this way it shall be proven that an ecological concrete mixture has an equivalent performance with respect to its reaction to environmental actions and to its durability when compared with a reference concrete which fulfills the requirements for the relevant exposure class.

Proving equivalent performance for each concrete mixture is expensive and time consuming. It was shown that the relationship between the average cube compressive strength and the tensile splitting strength and the relationship between compressive

strength and modulus of elasticity for ecological mixtures correspond to those for normal concrete. Although these mechanical relations remain valid, durability performance should still be investigated. In the future it would be beneficial to have standards which are based on performance-related design methods, so no minimum cement content has to be prescribed anymore. In that case also the variability of ecological concrete mixtures is important, because high scatter in the mechanical properties of ecological concrete would also lead to the need for increased safety factors. At this point, however, with the use of the cyclic design method based on packing density to determine the water demand of ecological concrete mixtures, no indication was found for an increased scatter in the mechanical properties. With the help of the cyclic design procedure strength based design is possible, which improves the market introduction of ecological concrete until the standards are based on absolute performance testing.

The cyclic design method as presented in this thesis can be used to design ecological concrete mixtures based on their strength and workability requirements. Since the method can also be used in a general way for performance-based design of concrete (see also subsection 7.5.2), it can help to design different types of concrete, but it can also be of significance for creating performance-based design regulations. In that case it is recommended to perform additional research on real packing structures of powders (<125µm) first.

The real particle structure of the powders should be measured to verify the cement spacing and local packing density effects. In this research project polarizing and fluorescent microscopy was used to investigate packing structures of samples compacted by centrifugal consolidation (Fennis, et al., 2008). It was found that it is difficult to create suitable thin sections of non-hydrated specimens. On the other hand, after hydration it is hard to determine the position of the original particles, due to variations in mineralogical composition. A good non-destructive measuring method for powder structures should be developed. Possibly this method could be based on nuclear magnetic resonance. Nuclear magnetic resonance can be used to detect hydrogen. So far it has successfully been used on concrete to detect quantities of water. When the resolution is high enough the entire water or pore structure could be mapped, thus providing a negative image of the particle structure.

With such a non-destructive test method, real particle structures can be checked on packing density and distances between the cement particles. This would provide valuable

input for durability predictions, but it will also create possibilities to investigate the influence of fillers and different types of superplasticizers on the particle distance and agglomeration. In this research project the effect of the superplasticizer was only measured indirectly by measuring the packing density of particle structures. With a direct measurement of the particle structure, it can be shown to what extent particles are agglomerating, when combined with different amounts and different types of superplasticizers. Information on the dispersing effects of the different types of superplasticizer can be used to validate and improve the CIPM. The same approach might be used to investigate the influence of other properties on the packing density, such as particle shape. Implementing the influences of superplasticizers and particle shape in the CIPM would be a valuable contribution.

Furthermore, research should be conducted on binder efficiency. Until further research is carried out, the requirements given by the standards on using cement replacing materials should be fulfilled. The sum of cement and filler should be at least equal to the minimum cement content requirement and the water/(cement + $k \cdot$ filler) ratio should not be greater than the water/cement ratio requirement for the relevant exposure class. Until now only fly ash and silica fume are allowed to be regarded as a binder for a maximum proportion of that binder. However, other materials now used as filler, such as limestone powder and ground incinerator bottom ash, also contribute to strength development and durability of concrete mixtures. When fillers contribute to the hydration process they should be taken into account as a binder with a certain efficiency factor k within the cyclic design method for ecological concrete. A first concept to implement binder efficiency in the cement spacing factor was given by Equations 7.11-7.13. This concept was not tested yet on ecological concrete mixtures, due to the lack of knowledge on efficiency factors for the various types of powders used. When the efficiency of binders can be implemented in the cement spacing factor, far less trial and error mixing is required due to improved predictions of strength and durability.

References

Abdel-Jawad, Y.A. and Salman Abdullah, W. (2002) Design of maximum density aggregate grading. *Construction and Building Materials*, Vol. 16, pp. 495-508.

Adaska, W.S. (1997) Controlled Low-Strength Materials. *Concrete International*, Vol. April.

Andrade, C., Sanjuan, M.A. and Alonso, M.C. (1993) Measurement of chloride diffusion coefficient from migration tests. *NACE Corrosion '93*, paper 319.

Andreasen, A.H.M. and Andersen, J. (1930) Über die Beziehung zwischen Kornabstufung und Zwischenraum in Produkten aus losen Körnern (mit einigen Experimenten). *Colloid & Polymer Science*, Vol. 50 (3), pp. 217-228.

Bakker, R. (1999) Application and advantages of blended cement concretes.

Ball, D. (1998) Selecting Aggregates for maximum packing density in low permeability concretes. *Concrete (London)*, Vol. 32 (5), pp. 9-10.

Barret, P.J. (1980) The shape of rock particles, a critical review. *Sedimentology*, Vol. 27 (1), pp. 15-22.

Ben Aïm, R. and Le Goff, P. (1967) Effet de paroi dans les empilements désordonnés de sphères et application à la porosité de mélanges binaires *Powder Technology*, Vol. 1 (5), pp. 281-290.

Bentz, D.P. (2005) Replacement of "coarse" cement particles by inert fillers in low w/c ratio concretes; II. Experimental validation. *Cement and Concrete Research*, Vol. 35, pp. 185-188.

Bertolini, L., Carsana, M., Cassago, D., Collepardi, M. and Quadrio Curzio, A. (2005) Bottom ash of municipal solid wastes from incineration plant as mineral additions in concrete. *Special Publication, American Concrete Institute*, Vol. 229, pp. 467-476.

Bigas, J.P. and Gallias, J.L. (2002) Effect of fine mineral additions on granular packing of cement mixtures. *Magazine of Concrete Research*, Vol. 54 (3), pp. 155-164.

Bilodeau, A. and Malhotra, V.M. (2000) High-volume fly ash system: Concrete solution for sustainable development *ACI Structural Journal*, Vol. 97 (1), pp. 41-48.

Bilodeau, A., Malhotra, V.M. and Seabrook, P.T. (2001) Use of high-volume fly ash concrete at the Liu Centre. Materials of technolgy laboratory, pp. 21.

Boden, T.A., G. Marland, R.J. Andres. (2009) Global, Regional, and National Fossil-Fuel CO2 Emissions. Carbon Dioxide Information Analysis Center, Oak Ridge National Laboratory, U.S. Department of Energy, Oak Ridge, Tenn., U.S.A..

Bonneau, O., Vernet, C., Moranville, M. and Aïtcin, P.C. (2000) Characterization of the granular packing and percolation threshold of reactive powder concrete. *Cement and Concrete Research*, Vol. 30 (12), pp. 1861-1867.

Bornemann, R. (2005) Untersuchungen zur Modellierung des Frisch- und Festbetonverhaltens erdfeuchter Betone. *PhD Thesis. K*assel: Universität Kassel.

Bouzoubaâ, N. and Fournier, B. (2002) Optimization of Fly Ash Content in Concrete. Materials Technology laboratory.

Brendle, S., Erfurt, S. and Rooij, M.R.d. (2008) Simulation of the particle size distribution during the early hydration of Portland cement. In: Schlangen, E. and De Schutter, G. (eds). *Proceedings of the International Rilem Symposium on Concrete Modelling - CONMOD'08*. Delft, The Netherlands.

Brouwers, H.J.H. and Radix, H.J. (2005) Self-Compacting Concrete: Theoretical and experimental study. *Cement and Concrete Research*, Vol. 35, pp. 2116-2136.

Brouwers, H.J.H. (2006) Particle-size distribution and packing fraction of geometric random packings. *Physical Review E - Statistical, Nonlinear, and Soft Matter Physics.* Vol. 74 (3), pp. 031309- 031309-14.

Cement&BetonCentrum. (2008) Cement, beton en CO2; Feiten en trends.

Chu, H. and Machida, A. (1998) Experimental evaluation and theoretical simulation of self compacting concrete by the modified distinct element method (MDEM). In Malhotra, V.M. (eds). *Proceedings of the fourth canmet/ACI/JCI international symposium Advances in Concrete Technology.* pp. 691-714.

Creegan, P.J. and Monismith, C.L. (1996) Asphalt-concrete water barriers for embankment dams. New York: ASCE, 169.

Crouch, L.K., Hewitt, R. and Byard, B. (2007) High Volume Fly Ash Concrete. *2007 World of Coal Ash (WOCA), May7-10*. Covington, Kentucky, USA.

CUR Rapport 94-12. (1994) Beoordeling van de constructieve consequenties van het toepassen van grindvervangende toeslagmaterialen. Gouda.

Cyr, M., Lawrence, P. and Ringot, E. (2005) Mineral admixtures in mortars. Quantification of the physical effects of inert materials on short-therm hydration *Cement and Concrete Research*, Vol. 35, pp. 719-730.

Derjaguin, B. and Landau, L. (1941) Theory of the stability of strongly charged lyophobic sols and of the adhesion of strongly charged particles in solutions of electrolytes. *Acta Physico chemica URSS*, Vol. 14:633.

Dewar, J.D. (1999) Computer Modelling of Concrete Mixtures. London: E & FN Spon.

Dhir, R.K., McCarthy, M.J. and Paine, K.A. (2002) Dry fly ash. Abridged version of Use of Fly Ash to BS EN 450 in Structural Concrete, Technology Digest 1. Crowthorne: The Concrete Society.

Dhir, R.K., McCarthy, M.J. and Paine, K.A. (2005) Engineering property and structural design relationships for new and developing concretes. *Materials and Structures*, Vol. 38 (275), pp. 1-9.

DuraCrete (2000) DuraCrete Final Technical Report R17, BE95-1347/R17. TheEuropean Union - Brite EuRam III, DuraCrete - Probabilistic Performance based Durability Design of Concrete Structures, CUR, Gouda.

EBA, Engineering Consultants Ltd. (2004) Fly Ash Concrete Trials; Government of Canada Building; Yellowknife NT.

ENCI (2008) Portlandcement CEM I 42.5 N Prod.blad.

Erdoğdu, K. and Türker, P. (1998) Effects of fly ash particle size on strength of portland cement fly ash mortars. *Cement and Concrete Research*, Vol. 28 (9), pp. 1217-1222.

Fedors, R.F. and Landel, R.F. (1979) An Empirical Method of Estimating the Void Fraction in Mixtures of Uniform Particles of Different Size. *Powder Technology*, Vol. 23, pp. 225-231.

Fennis, S.A.A.M., Walraven, J.C., Nijland, T. (2008) Measuring the packing density to lower the cement content in concrete. In J.C. Walraven & D. Stoelhorst (Eds.); Tailor made concrete structures: new solutions for our society. London UK: Taylor & Francis Group. pp. 419-424.

Feret, R. (1892) Sur la compacité des mortiers hydrauliques. *Annales des Ponts et Chaussees.* Vol. 4 (2e semestre), pp. 5-16.

Flatt, R.J. (2004) Dispersion forces in cement suspensions. *Cement and Concrete Research*, Vol. 34, pp. 399-408.

Fraaij, A.L.A. and Rooij, M.R. de (2008) The workability of concrete: is there an easy way to produce self-compacting concrete? In: Dhir, R.K., Hewlett, P.C., Csetenyi, L.J. and Newlands, M.D. (eds). *Role for concrete in global development*. Dundee, Scotland, UK, pp. 387-396.

Fu, G. and Dekelbab, W. (2003) 3-D random packing of polydisperse particles and concrete aggregate grading. *Powder Technology*, Vol. 133, pp. 147-155.

Fuller, W.B. and Thompson, S.E. (1907) The laws of proportioning concrete. *ASCE J. Transport.*, Vol. 59, pp. 67-143.

Funk, J.E. and Dinger, D.R. (1994) Predictive Process Control of Crowded Particulate Suspensions - Applied to Ceramic Manufacturing. Boston: Kluwer Academic Publishers.

Funk, J.E., Dinger, D.R. and Funk, J.E.J. (1980) Caol Grinding and Particle Size Distribution Studies for Coal-Water Slurries at High Solids Content. *Final Report, Empire State Electric Energy Research Corporation (ESEERCO)*. New York.

Furnas, C.C. (1929) Flow of gasses through beds of broken solids. *Bureau of Mines Bulletin 307*.

Furnas, C.C. (1931) Grading Aggregates; Mathematical Relations for Beds of Broken Solids of Maximum Density. *Industrial and Engineering Chemistry.* Vol. 23 (9), pp. 1052-1058.

Garas, V.Y. and Kurtis, K.E. (2008) Assessment of methods for optimising ternary blended concrete containing metakaolin. *Magazine of Concrete Research*, Vol. 60 (7), pp. 499-510.

Geisenhanslüke, C. (2008) Einfluss der Granulometrie von Feinstoffen auf die Rheologie von Feinstoffleimen. Influence of the granulometry of fine particles on the rheology of pastes. *Fachbereich Bauingenieurwesen*. PhD Thesis. Kassel: Universität Kassel.

German, R.M. (1989) Particle packing characteristics Princeton: Metal Powder Industries Federation.

Glavind, M. and Munch-Petersen, C. (2002) Green Concrete - a life cycle approach. *Challenges of Concrete Construction*. University of Dundee.

Glavind, M., Olsen, G.S. and Munch-Petersen, C. (1999) Packing Calculations and concrete mix design. *Danish Technological Institute*.

Goltermann, P., Johansen, V. and Palbøl, L. (1997) Packing of Aggregates: An Alternative Tool to Determine the Optimal Aggregate Mix. *ACI Materials Journal*, Vol. 94 (5), pp. 435-443.

Gopalan, M.K. (1993) Nucleation and Pozzolanic Factors in Strength Development of Class F Fly Ash Concrete. *ACI Materials Journal*, Vol. 90 (2), pp. 5.

Gram, A. and Silfwerbrand, J. (2007) Computer simulation of SCC flow. *Betonwerk und Fertigteil-Technil/Concrete Plant and Precast Technology*, Vol. 73 (8), pp. 40-48.

Gray, W.A. (1968) The packing of solid particles London: Chapman and Hall.

Grünewald, S. (2004) Performance-based design of self-compacting fibre reinforced concrete. PhD Thesis. Delft: Delft University of Technology.

He, H. (2010) Computational modelling of particle packing in concrete. PhD Thesis. Delft: Delft University of Technology.

Hoffmann, A.C. and Finkers, H.J. (1995) A relation for the void fraction of randomly packed particle beds. *Powder Technology*. Vol. 82, pp. 197-203.

Hunger, M. (2010) An integral Design Concept for Ecological Self-Compacting Concrete. *Bouwkunde*. PhD Thesis. Eindhoven: Eindhoven University of Technology.

Hunger, M. and Brouwers, H.J.H. (2009) Flow analysis of water-powder mixtures: Application to specific surface area and shape factor. *Cement & Concrete Composites*, Vol. 31, pp. 39-59.

Hwang, C.L. and Tsai, C.T. (2005) The effect of aggregate packing types on engineering properties of self-consolidating concrete. *First International Symposium on Design, Performance and Use of Self-Consolidating Concrete SCC'2005*. Changsha, Hunan, China.

Idorn, G.M. (1995) Europack V1.1 User Manual Europack (G.M. Idorn Consult A/S, Denmark).

Jepsen, M.T., Mathiesen, D. and Munch-Petersen, C. (2001) Durability of Resource Saving "Green" Types of Concrete. *FIB-symposium "Concrete and environment"*. Berlin, Germany.

Jiao, Y., Stillinger, F.H. and Torquato, S. (2008) Optimal Packings of Superdisks and the Role of Symmetry. *Physical Review Letters, Vol.* 100, art. 245504.

Johansen, V. and Andersen, P.J. (1991) Particle Packing and Concrete Properties. In: Skalny, J. and Mindess, S. (eds). *Materials science of concrete 2*. Westerville: American Ceramic Society.

Jones, M.R., Zheng, L. and Newland, M.D. (2002) Comparison of particle packing models for proportioning concrete constituents for minimum voids ratio. *Materials and structures*, Vol. 35, pp. 301-309.

Joshi, R.C. and Lohtia, R.P. (1997) Fly ash in concrete: production, properties and uses. Amsterdam: Gordon and Breach.

Kadri, E.H., Aggoun, S., Schutter, G.d. and Ezianne, K. (2009) Combined effect of chemical nature and fineness of mineral powders on Portland cement hydration *Materials and Structures/Materiaux et Constructions*, Vol., pp. 9.

Kadri, E.H. and Duval, R. (2002) Effect of Ultrafine Particles on Heat of Hydration of Cement Mortars. *ACI Materials Journal*, Vol. 99, pp. 138-142.

Kaufmann, J. and Winnefeld, F. (2002) Influence of addition of ultrafine cement on the rheological properties and strength of portlandcement paste. In: Dhir, R.K., Hewlett, P.C. and Csetenyi, L.J. (eds). *Innovations and developments in concrete materials and construction*. University of Dundee, Scotland, UK.

Kjeldsen, A.M. (2007) Consolidation behavior of cement-based systems. Influence of inter-particle forces. *Department of Civil Engineering*: Technical University of Denmark.

Kolonko, M., Raschdorf, S. and Wäsch, D. (2008) A Hierarchical Approach to Estimate the Space Filling of Particle Mixtures with Broad Size Distributions. pp. 28.

Kordts, S. (2005) Herstellung und Steuerung der Verarbeitbarkeitseigenschaften selbstverdichtender Betone. *Bauingenierwesen and angewandte Geowissenschaften*. Berlin: Technischen Universität Berlin.

Krell, J. (1985) Die Konsistenz von Zementleim, Mörtel, und Beton und ihre zeitliche Veränderung. *Faculty of Civilengineering*. Aachen, Germany: Rheinisch-Westfälische Technische Hochschule Aachen.

Kronlöf, A. (1997) Filler effect of inert mineral powder in concrete. *VTT Technical research centre of Finland*. Espoo, Finland.

Kumar, S.V. and Santhanam, M. (2003) Particle packing theories and their application in concrete mixture proportioning: A review. *The Indian Concrete Journal*, Vol. 77 (9), pp. 1324-1331.

Kwan, A.K.H. and Mora, C.F. (2001) Effects of various shape parameters on packing of aggregate particles. *Magazine of Concrete Research*, Vol. 53 (2), pp. 91-100.

Lagerblad, B. and Vogt, C. (2004) Ultrafine particles to save cement and improve concrete properties. *summary of CBI report 1:2004*.

Lange, F., Mörtel, H. and Rudert, V. (1997) Dense packing of cement pastes and resulting consequences on mortar properties. *Cement and Concrete Research*, Vol. 27 (10), pp. 1481-1488.

Larrard, F. de (1999) Concrete mixture proportioning: a scientific approach. London: E & FN Spon.

Larrard, F. de, Lédée, V., Sedran, T. Brochu, F. and Ducassou, J. (2003) New test for measuring the compactness of granular fractions on the shock table. *Bulletin des Laboratoires des Ponts et Chaussées* 246-247, réf 4492. pp. 101-115.

Lee, D.I. (1970) Packing of spheres and its effect on the viscosity of suspensions. *Journal of Paint Technology*, Vol. 42, pp. 579-587.

Leegwater, G.A., Polder, R.B., Visser, J.H.M. and Nijland, T.G. (2007) Durability study High Filler concrete. TNO report, Delft, the Netherlands.

Lees, G. (1970) The rational design of aggregate gradings for dense asphaltic compositions. *Asphalt Paving Technologies*. Kansas City, USA.

Liu, B. and Xie, Y. (2005) Influence of fly ash on properties of cement-based materials. *First International Symposium on Design, Performance and Use of Self-Consolidating Concrete (SCC'2005)*, 26-28 may 2005, Changsha, Hunan, China.

Maeyama, A., Maruyama, K., Midorakawa, T. and Sakata, N. (1998) Characterization of Powder for Self-Compacting Concrete. In: Ouchi, O.a. (ed). *Second Int. Workshop on SCC*. Kochi: Concrete Engineering Series, Japan Society of Civil Engineers, pp. 191-200.

Mahmoodi Baram, R. (2005) Polydisperse granular packings and bearings. *Institute of Computational Physics, Faculty of Mathematics and Physics*. Stuttgart, Germany: Universität Stuttgart.

Mansoutre, S., Colombet, P. and Van Damme, H. (1999) Water retention and granular rheological behavior of fresh C3S paste as a function of concentration. . *Cement and Concrete Research*, Vol. 29, pp. 1441-1453.

Marquardt, I. (2002) Ein Misschungskonzept für selbstverdichtenden Beton auf der Basis der Volumenkenngrössen und Wasseransprüche der Ausgangsstoffe. Rostock, Germany.

McGeary, R.K. (1961) Mechanical packing of spherical particles. *Journal of the American Ceramic Society*, Vol. 44 (10), pp. 513-522.

Mechling, J., Lecomte, A. and Diliberto, C. (2007) The influence of the clinker composition on concrete compressive strength. *Concrete under Severe Conditions: Environment & Loading CONSEC 2007*. Tours, France.

Mechtcherine, V. and Shyshko, S. (2007) Virtual concrete laboratory - Continuous numerical modelling of concrete from fresh to the hardened state. *In Advances in Construction Materials, Part VI*, pp. 479-488.

Mehta, P.K. (2001) Reducing the environmental impact of concrete. *Concrete International*, Vol. (october 2001), pp. 61-66.

Midorikawa, T., Pelova, G.I. and Walraven, J.C. (2001) Application of ''the water layer model'' to self-compacting mortar with different size distribution of fine aggregate. In: Ozawa, K. and Ouchi, M. (eds). *The Second International Symposium on Self-Compacting Concrete*. Tokyo, Japan, pp. 237-246.

Mikulić, D., Gabrijel, I. and Milovanović, B. (2008) Prediction of concrete compressive strength. *International RILEM Symposium on Concrete Modelling - CONMOD'08*. Delft, the Netherlands.

Miller, K.T., Melant, R.M. and Zukoski, C.F. (1996) Comparison of the compressive yield response of aggregated suspensions: Pressure filtration, Centrifugation, and osmotic consolidation. *Journal of the American Ceramic Society*, Vol. 79 (10), pp. 2545-2556.

Miyajima, T., Yamamotot, K. and Sugimoto, M. (2001) Effect of particle shape on packing properties during tapping. Advanced Powder Technology, Vol. 12 (1), pp. 117-134.

Moosberg-Bustnes, H., Lagerblad, B. and Forssberg, E. (2004) The function of fillers in concrete. *Materials and Structures/Materiaux et Constructions*, Vol. 37 (266), pp. 74-81.

Müller, A. and Reinhold, M. (2002) The measurement of important granulometric chacteristics of aggregates on the basis of photo-optical image analysis systems. In: Dhir, R.K. and Dyer, T.D. (eds). *Modern concrete materials: binders, additions and admixtures*. Dundee, Scotland: London: Telford.

Naik, H.K., Mishra, M.K. and Rao Karanam, U.M. (2009) Rheological Characteristics of Fly Ash Slurry at Varying Temperature Environment with and without Additive. *2009 World of Coal Ash (WOCA) Conference - May 4-7*. Lexington, KY, USA.

Nehdi, M. (2000) Why some carbonate fillers cause rapid increases of viscosity in dispersed cement-based materials. *Cement and Concrete Research*, Vol. 30 pp. 1663-1669.

Neville, A.M. (1995) Properties of Concrete. Harlow: Longman.

Nijland, T.G., Larbi, J.A., Rooij, M.R. de and Polder, R.B. (2007) Use of Rhenish trass in marine concrete: A microscopic and durability perspective. *Heron*, Vol. 52 (4), pp. 269-288.

Okamura, H. and Ozawa, K. (1995) Mix design for self-compacting concrete. *Concrete library of the JSCE, No 25, pp 107-120 (Translation from Proc. Of ISCE, no 496/v-24, 1994.8)*.

Opitz, A., Scherge, M., Ahmed, S.I.-U. and Schaefer, J.A. (2007) A comparative investigation of thickness measurements of ultra-thin water films by scanning probe techniques. *Journal of Applied Physics*, Vol. 101 (6), pp. 064310-064311 - 064310-064315.

Palm, S. and Wolter, A. (2009) Determining and optimizing the void filling of dry particle systems. *Cement international*, Vol. 7 (1/2009), pp. 1-8.

Peronius, N. and Sweeting, T.J. (1985) On the correlation of minimum porosity with particle size distribution. *Powder Technology*, Vol. 42 pp. 113-121.

Polder, R.B. (1995) Chloride diffusion and resistivity testing of five concrete mixes for marine environment, In Nilsson, L.-O. and Ollivier, P. (eds). *Proc. RILEM. International Workshop on Chloride Penetration into Concrete*, St-Remy-les-Chevreuses, France, pp 225-233.

Polder, R. B. (2000) Test methods for on site measurement of resistivity of concrete (Draft Technical Recommendation RILEM TC 154-EMC). *Materials and Structures*, Vol. 33, pp. 603-611

Popovics, S. (1998) History of mathematical model for strength development of Portland cement concrete. *ACI Materials Journal*, Vol. 95 (5), pp. 593-600.

Poppe, A. and Schutter, G. de (2005) Cement hydration in the presence of high filler contents. *Cement and Concrete Research*, Vol. 35, pp. 2290-2299.

Pouliot, N., Sedran, T., Larrard, F. de and Marchand, J. (2001) Prediction of the compactness of roller-compacted concrete using a granular packing model. *Bulletin de Laboratoires des Ponts et Chaussées*, Vol. 233 (Réf. 4370), pp. 23-36.

Powers, T.C. (1968) The Properties of Fresh Concrete. New York: Wiley.

Puntke, W. (2002) Wasseranspruch von feinen Kornhauf-werken. *Beton*, Vol. 52 (H.5), pp. 242-248.

Puri, U.C. and Uomoto, T. (1999) Properties of Shotcrete (11); A Proposal to Characterize the DEM Parameters for Fresh Concrete Modeling. *Seisan-Kenkyu,* Vol 51 (4), pp. 13-16.

Reinhardt, H.W. (2002) Betonkunde. *Collegedictaat TUDelft*. Delft.

Reschke, T. (2000) Der Einfluss der Granulometrie der Feinstoffe auf die gefügeentwicklung und die Festigkeit von Beton *VBT Verlag Bau+Technik GmbH*. Düsseldorf.

Roussel, N., Geiker, M.R., Dufour, F., L.N., T. and Szabo, P. (2007) Computational modelling of concrete flow: General overview. *Cement and Concrete Research*, Vol. 37, pp. 1298-1307.

Schaafsma, S.H., Vonk, P., Segers, P. and Kossen, N. (1998) Description of agglomerate growth. *Powder Technology*, Vol. 97, pp. 183-190.

Schuitemaker, E.J. (2002) Geëxpandeerd glas als toeslagmateriaal in beton. *CiTG - concrete structures*. Delft: Technische Universiteit Delft.

Schwanda, F. (1966) Das rechnerische Verfahren zur Bestimmung des Hohlraumes und Zementleimanspruches von Zuschlägen und seine Bedeutung für Spannbetonbau. *Zement und Beton*, Vol. 37, pp. 8-17.

Sedran, T. and Larrard, F. de. (2000) Manuel d'utilisation de René-LCPC, version 6.1d, Logiciel d'optimisation granulaire.

Slanička, S. (1991) The influence of fly ash fineness on the strength of concrete. *Cement and Concrete Research*, Vol. 21, pp. 285-296.

Smith, D. (2006) The Development of a Rapid Test for Determining the Transport Properties of Concrete University of New Brunswick,

Snoeijer, J.H. and Hecke M. van, S.E., Saarloos W. van. (2003) Force and weight distributions in granular media: Effects of contact geometry. *Physical review E 67, 030302®*.

Snoeijer, J.H., Hecke, M.v., Somfai, E. and Saarloos, W.v. (2003) Packing geometry and statistics of force networks in granular media. *Physical Review E - Statistical, Nonlinear, and Soft Matter Physics*, Vol. 70 (1 1), pp. 15.

Souwerbren, C. (1998) Betontechnologie, stichting Betonprisma.-III, tiende druk, ‘s-Hertogenbosch.

Stark, U. and Müller, A. (2008) Optimization of packing density of aggregates. In: Fehling, E., Schmidt, M. and Stürwald, S. (eds). *Second International Symposium on Ultra High Performance Concrete*. Kassel, pp. 121-127.

Stephan, D., Schmidt, M. and Krelaus, R. (2008) Direct measurement of particle-particle interactions of fines for UHPC using AFM technology. In: Fehling, E., Schmidt, M. and Stürwald, S. (eds). *Second International Symposium on Ultra High Performance Concrete*. Kassel, pp. 375-381.

Stovall, T., Larrard, F. de and Buil, M. (1986) Lineair Packing Density Model of Grain Mixtures. *Powder Technology*, Vol. 48, pp. 1-12.

Stroeven, P. and Stroeven, M. (1999) Assessment of packing characteristics by computer simulation. *Cement and Concrete Research*, Vol. 29, pp. 1201-1206.

Stroeven, P., Stroeven, M. and Bui, D.D. (2003) On optimum packing density. In: Shu Yuan, Y., Shah, S.P. and Lin Lü, H. (eds). *Proceedings of International Conference on Advances in Concrete and Structures, Rilem Publications SARL*, pp. 793-800.

Stroeven, P., Sluys, L.J., Guo, Z. and Stroeven, M. (2006) Virtual reality studies of concrete. *FORMA*, Vol 21 (3), pp. 227-242.

Talbot, A.N. and Richart, F.E. (1923) The strength of concrete in relation to the cement, aggregates and water. *University of Illinois Engineering Experiment Station, Bulletin No. 137*.

Tange Hasholt, M. and Mathiesen, D. (2002) Beton med alternativ flyveaske. Center for Grön Beton, Teknologisk institut.

Tattersall, G.H. and Banfill, P.F.G. (1983) The Rheology of Fresh Concrete. Boston: Pitman.

Teichmann, T. (2008) Einfluss der Granulometrie und des Wassergehaltes auf die Festigkeit und Gefügedichtigkeit von Zementstein (Influence of the granulometrie and the water content on the strength and density of cement stone). *Fachbereich Bauingenieurwesen*. PhD Thesis. Kassel: Universität Kassel.

Toufar, W., Born, M. and Klose, E. (1976) Beitrag zur Optimierung der Packungsdichte Polydisperser körniger Systeme. *Freiberger Forschungsheft A 558, VEB Deutscher Verlag für Grundstoffindustrie*, pp. 29-44.

Trejo, D., Folliard, K.J. and Du, L. (2004) Sustainable Development Using Controlled Low-Strength Material David Trejo, Kevin J. Folliard, and Lianxiang Du. *International Workshop on Sustainable Development and Concrete Technology*. Beijing, China, May 20–21, 2004.

Verwey, E.J.W. and Overbeek, J.T.G. (1948) Theory of the stability of lyophobic colloids. Amsterdam: Elsevier.

Vogt, C. (2010) Ultrafine particles in concrete; Influence of ultrafine particles on concrete properties and application to concrete mix design. *School of Architecture and the Built Environment, Division of Concrete Structures*. Stockholm: Royal Institute of Technology.

Vogt, C. and Lagerblad, B. (2006) Ultrafine particles to save cement and improve concrete properties. *Advances in cement and concrete X*. July 2-7, Davos, Switzerland.

Vries, W. de (2008) The Use of Micronized Sand as Cement Replacement. An exploring study into the new use of a material. Delft: TU Delft.

Vries, W. de and Ye, G. (2010) Sustainability starts from the building material study of micronized sand as a cement replacement (Nachhaltigkeit beginnt beim baustoff untersuchung von hoch aufgemahlenem sand als zementersatz) Betonwerk und Fertigteil-Technik/Concrete Plant and Precast Technology, 76 (5), pp. 14-20.

Walker, W.J. (2003) Persistence of Granular Structure during Compaction Processes. *KONA*, Vol. 21, pp. 133-142.

Weng, Y. and Vipulanandan, C. (1999) A Study on Controlled Low Strength Material (CLSM).

Westerholm, M., Lagerblad, B., Silfwerbrand, J. and Forssberg, E. (2008) Influence of fine aggregate characteristics on the rheological properties of mortars. *Cement & Concrete Composites*, Vol. 30, pp. 274-282.

Westman, A.E.R. and Hugill, H.R. (1930) The packing of particles. *Journal of the American Ceramic Society*, Vol. 13 (10), pp. 767-779.

Wong, H.C. and Kwan, K.H. (2008a) Packing density of cementitious materials: part 1 - measurement using a wet packing method. *Materials and structures*, Vol. 41, pp. 689-701.

Wong, H.H.C. and Kwan, A.K.H. (2008b) Packing density of cementitious materials: measurement and modelling. *Magazine of Concrete Research*, Vol. 60 (3), pp. 165-175.

Worrell, E., Price, L., Martin, N., Hendriks, C. and Ozawa Meida, L. (2001) Carbon Dioxide Emissions from the Global Cement Industry. *Annual Review of Energy and the Environment*, Vol. 26, pp. 303-329.

Wouterse, A. (2008) Random packing of colloids and granular matter. PhD thesis. Utrecht: Universiteit Utrecht.

Yu, A.B., Feng, C.L. and Yang, R.Y. (2003) On the relationship between porosity and interparticle forces. *Powder Technology*, Vol. 130, pp. 70-76.

Yu, A.B. and Standish, N. (1987) Porosity calculations of multi-component mixtures of spherical particles. *Powder Technology*, Vol. 52, pp. 233-241.

Yu, A.B. and Standish, N. (1988) An analytical-parametric theory of the random packing of particles. *Powder Technology*, Vol. 55 pp. 171-186.

Yu, A.B. and Standish, N. (1991) Estimation of the Porosity of Particle Mixtures by Linear-Mixture Packing Model. *Ind. Eng. Chem. Res.*, Vol. 30, pp. 1372-1385.

Yu, A.B. and Standish, N. (1993) Limitation of Proposed Mathematical Models for the Porosity Estimation of Nonspherical Particle Mixtures. *Ind. Eng. Chem. Res.*, Vol. 32, pp. 2179-2182.

Yu, A.B., Zou, R.P. and Standish, N. (1996) Modifying the Linear Packing Model for Predicting the Porosity of Nonspherical Particle Mixtures. *Ind. Eng. Chem. Res.*, Vol. 35 pp. 3730-3741.

Zheng, J., Johnson, P.F. and Reed, J.S. (1990) Improved Equation of the Continuous Particle Size Distribution for Dense Packing. *Journal of the American Ceramic Society*, Vol. 73 (5), pp. 1392-1398.

Zheng, J. and Stroeven, P. (1999) Computer-simulation of particle section patterns from sieve curve for spherical aggregate. In: Dhir, R.K. and Dyer, T.D. (eds). *Modern concrete materials: binders, additions and admixtures: proceedings of the international Conference held at the University of Dundee, Scotland, UK on 8-10 September.*

Standards

NEN-EN 196-1:2005. Methods of testing cement - Part 1: Determination of strength.

NEN-EN 206-1:2001. Concrete - Part 1:Specification, performance, production and conformity.

NEN-EN 1097-3:1998. Tests for mechanical and physical properties of aggregates - Part 3: Determination of loose bulk density and voids.

NEN-EN 1097-6:2000. Tests for mechanical and physical properties of aggregates - Part 6: Determination of particle density and water absorption.

NEN-EN 1992-1-1:2005. Eurocode 2: Design of concrete structures - Part 1-1: General rules and rules for buildings.

NEN-EN 12350-2:2009. Testing fresh concrete - Part 2: Slump-test.

NEN-EN 12350-4:2009. Testing fresh concrete - Part 4: Degree of compactability.

NEN-EN 12350-6:2009. Testing fresh concrete - Part 6: Density.

NEN-EN 12350-7:2009. Testing fresh concrete - Part 7: Air content - Pressure methods.

NEN-EN 12390-2:2009. Testing hardened concrete - Part 2: Making and curing specimens for strength tests.

NEN-EN 13286-2:2004. Unbound and hydraulically bound mixtures - Part 2: Test methods for the determination of the laboratory reference density and water content - Proctor compaction.

NEN-EN 13670:2009. Execution of concrete structures.

NEN 5950:1995 nl. Voorschriften Beton Technologie (VBT 1995). Eisen, vervaardiging en keuring. withdrawn.

NPR-CEN/TS 12390-9:2006. Testing hardened concrete - Part 9: Freezethaw resistance - Scaling.

Websites

www.builditgreen.org. Fly ash concrete, http://www.builditgreen.org/files/uploads/Resources/Build%20It%20Green%20fact%20sheets/Fly-Ash-Concrete.pdf.

www.citg.tudelft.nl. Hymostruc free download, http://www.citg.tudelft.nl/live/pagina.jsp?id=7ca184c6-0b87-4be4-81fa-f8597f85ff13&lang=en.

www.concrete.elkem.com. Software EMMA, http://www.concrete.elkem.com/eway/default.aspx?pid=245&trg=Main_7244&Main_7244=7270:0:4,4564:1:0:0:::0:0.

www.dti.dk. 4C-Packing, http://www.dti.dk/2783.

www.fhwa.dot.gov. Fly Ash, http://www.fhwa.dot.gov/infrastructure/materialsgrp/flyash.htm.

www.flyash.com. Fly ash for concrete, http://www.flyash.com/data/upimages/press/HWR_brochure_flyash.pdf.

www.greenconcrete.dundee.ac.uk. Use of Recycled Materials and Industrial By-Products in Concrete, www.greenconcrete.dundee.ac.uk.

www.gronbeton.dk. Articles. www.gronbeton.dk.

www.lcpc.fr. RENÉ-LCPC, http://www.lcpc.fr/fr/produits/rene/index.dml.

www.mixsim.net. Software MixSim, http://www.mixsim.net/.

www.wikipedia.org Information on discrete element methods, http://en.wikipedia.org/wiki/Discrete_element_method.

Appendix A Material properties

The sand and natural aggregates consist of rounded river sand and gravel originating from the Maas river and supplied by fa. Filcom Papendrecht, the Netherlands. Particle shape was measured by U. Stark (Müller and Reinhold, 2002). The particles in all size fractions were evaluated as round; however, microscopic analysis showed that the sand particles in size class 0.125-0.25 were more angular. The properties are summarized in Table A.1.

Table A.1 Cumulative size distribution and properties of the aggregates in % kg/kg.

	aggregates						
Sieves	**0.125 - 0.25**	**0.25 - 0.5**	**0.5 - 1**	**1 - 2**	**2 - 4**	**4 - 8**	**8 - 16**
C 31.5	0	0	0	0	0	0	0
C 22.4	0	0	0	0	0	0	0
C 16	0	0	0	0	0	0	4.5
C 8	0	0	0	0	0	10.29	88.25
C 4	0	0	0	0	2.15	97.79	99.25
2 mm	0	0	0	1.45	98.29	98.77	99.25
1 mm	0	0	2.06	98.17	99.56	99.75	99.25
500 µm	0.03	4.38	97.26	99.9	99.83	99.75	99.25
250 µm	37.55	97.76	99.95	99.97	99.96	99.75	99.25
125 µm	98.95	99.92	99.99	99.97	99.96	99.75	99.25
Rest	100	100	100	100	100	100	100

	aggregates						
	0.125 - 0.25	**0.25 - 0.5**	**0.5 - 1**	**1 - 2**	**2 - 4**	**4 - 8**	**8 - 16**
density [kg/m3]	2610	2610	2610	2610	2580	2580	2580
water absorption [%]	0.3	0.3	0.3	0.3	1.1	1.1	1.1
α_{exp} loose $K_t = 4.1$ [-]	0.524	0.560	0.578	0.574	0.570	0.563	0.564
sphericity	1.06	1.06	1.07	1.09	1.12	1.10	1.09
length/width	1.43	1.39	1.36	1.43	1.52	1.47	1.46

The quartz powder originated from Sibelco, Belgium is a grinded quartz sand consisting of at least 99% SiO_2. The particle size distribution was determined by Delft Solid Solutions on a Malvern Mastersizer 2000 in a configuration from 0.02 to 2000 µm with Lorentz-Mie as optical model. The samples were dispersed in 1 liter ethanol with an ultrasonic transducer. Circularity and aspectratio were measured by digital image analysis on an Ankersmid Eyetech, ACM104A flow cell, in water and after 10 minutes of ultrasonic treatment. Furthermore, shape was analysed based on the ESEM pictures by W. de Vries (Vries, 2008; Vries and Ye, 2010), Figures A.1-A.4. The properties are summarized in Table A.2. Chemical compositions are presented in Table A.4.

Table A.2 Cumulative size distribution and properties of the quartz powders in % m^3/m^3.

	powders						
Size [µm]	**M3**	**M4**	**M6**	**M10**	**M300**	**M400**	**M600**
0.20	0	0	0	0	0	0	0
0.42	0.01	0.02	0.02	0.03	0.02	0	0.05
0.91	1.06	1.39	1.52	2.13	1.66	2.88	5.73
1.95	5.22	6.80	7.26	10.19	8.05	15.52	31.16
4.19	11.96	15.33	16.18	22.62	18.60	34.53	68.38
9.00	20.71	25.67	27.60	37.42	34.78	56.95	93.36
19.3	32.82	39.02	43.43	56.75	60.51	83.54	99.52
41.4	50.40	58.01	66.67	82.13	90.21	98.64	99.96
88.9	71.95	82.06	91.43	98.32	100	100	100
191	91.66	98.25	99.90	100	100	100	100
409	100	100	100	100	100	100	100
879	100	100	100	100	100	100	100
	powders						
	M3	**M4**	**M6**	**M10**	**M300**	**M400**	**M600**
density [kg/m3]	2650	2650	2650	2650	2650	2650	2650
Blaine [cm^2/g]	1500	1900	2500	3600	4000	6500	13000
α_{exp} loose bulk [-]	0.47	0.43	0.38	0.34	0.32	0.26	0.23
α_{exp} wet $K_t = 12.2$ [-]	0.625	0.618	0.583	0.576	0.542	0.567	0.527
Circularity (std)	0.63(0.15)	-	0.67(0.13)	0.71(0.10)	0.73(0.10)	0.68(0.12)	0.70(0.11)
Aspectratio (std)	0.64(0.15)	-	0.65(0.14)	0.67(0.14)	0.67(0.14)	0.64(0.15)	0.63(0.16)

The cement originated from ENCI, HeidelbergCementGroup, the Netherlands. The fly ash came from Vliegasunie, SMZ Maasvlakte, the Netherlands. The IBA was delivered by INASHCO. The particle size distributions were determined by Delft Solid Solutions on a Malvern Mastersizer 2000 in a configuration from 0.02 to 2000 µm with Lorentz-Mie as optical model. The samples were dispersed in 1 liter ethanol with an ultrasonic transducer. The properties are summarized in Table A.3. Chemical compositions are presented in Table A.4.

Table A.3 Cumulative size distribution and properties of the cement and binders in % m^3/m^3.

	powders					
	CEM I	**CEM I**	**CEM I**	**CEM III/B**	**Fly ash**	**IBA**
Size [µm]	**32.5 R**	**42.5 N**	**52.5 R**	**42.5 N LH HS**		**dried**
0.20	0	0	0	0	0.02	0
0.42	0.58	0.88	1.41	0.75	0.54	2.15
0.91	2.26	3.55	5.64	3.86	2.19	18.53
1.95	4.37	7.53	13.15	9.32	5.08	37.12
4.19	8.84	15.88	28.80	19.55	10.60	63.25
9.00	22.09	32.55	54.07	38.60	24.24	82.58
19.3	43.92	54.72	83.21	65.96	46.09	92.10
41.4	69.82	79.32	98.15	91.97	69.91	97.45
88.9	92.37	95.66	98.99	99.84	90.67	98.50
191	99.79	99.45	99.17	100	99.72	99.51
409	100	100	100	100	100	100
879	100	100	100	100	100	100

	powders					
	CEM I	**CEM I**	**CEM I**	**CEM III/B**	**Fly ash**	**IBA**
	32.5 R	**42.5 N**	**52.5 R**	**42.5 N LH HS**		**dried**
density [kg/m3]	3150	3160	3130	2960	2290	2750
Blaine [cm^2/g]	2850	2950	5330	4720	-	-
α_{exp} loose bulk [-]	0.413	0.427	0.319	0.338	-	-
α_{exp} wet $K_t = 12.2$ [-]	0.584	0.604	0.596	0.605.	0.593	*0.433*

Table A.4 Chemical compositions (XRF) of the powders in % m^3/m^3.

	powders								
Size	**M3, M4, M6, M10**	**M300, M400**	**M600**	**CEM I 32.5 R**	**CEM I 42.5 N**	**CEM I 52.5 R**	**CEM III/B 42.5 N**	**Fly ash**	**IBA dried**
SiO_2	99.4	99.5	99.2		20	19	30	53.68	43.20
Fe_2O_3	0.03	0.03	0.05		3	3	1	5.11	15.92
Al_2O_3	0.1	0.2	0.4	5	5	5	9	27.67	8.87
TiO_2	0.07	0.03	0.03					1.84	1.01
K_2O		0.05	0.05					1.14	1.03
CaO		0.02	0.02		64	64	47	6.76	19.54
C_3A				8	-	-	-		
SO_3					2.4-3.5	3.3-4.0	3.2-4.0	0.41	
Cl				0.04	0.03-0.10	0.04-0.10	0.05-0.10	0.01	0.35
Na_2O				0.7	0.7	0.68	0.54	0.6	
MgO								1.15	
P_2O_5								2.01	0.82

The superplasticizers used in this project were: CUGLA® CRETOPLAST SL-01 (http://www.cugla.nl/producten/hulpstoffen/Cretoplast%20SL-01%20con35%20SPL%20-%20februari%202009.pdf) and Glenium 51 con 35 from BASF (http://www.basf-cc.nl/nl/Producten/Hulpstoffen/Hulpstoffenvoorbeton/Superplastificeerders/GLENIUM51CON35/Documents/PN_GLENIUM%2051%20CON%2035.pdf).

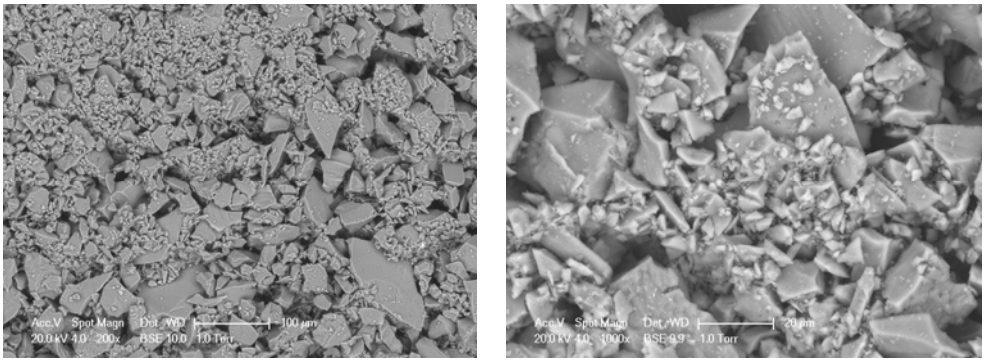

Figure A.1 Pictures of quartz powder M6 by Environmental scanning electron microscope (ESEM).

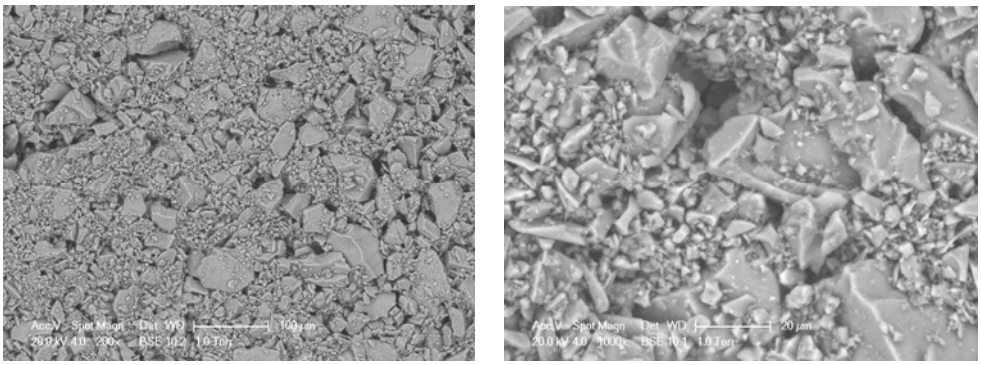

Figure A.2 ESEM pictures of quartz powder M10.

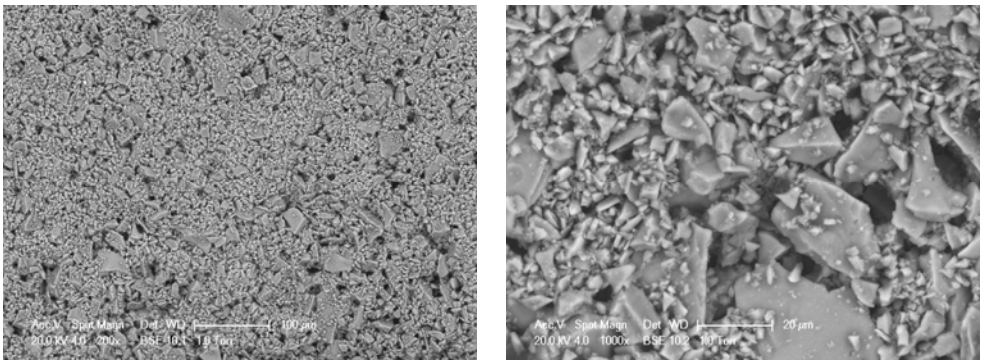

Figure A.3 ESEM pictures of quartz powder M300.

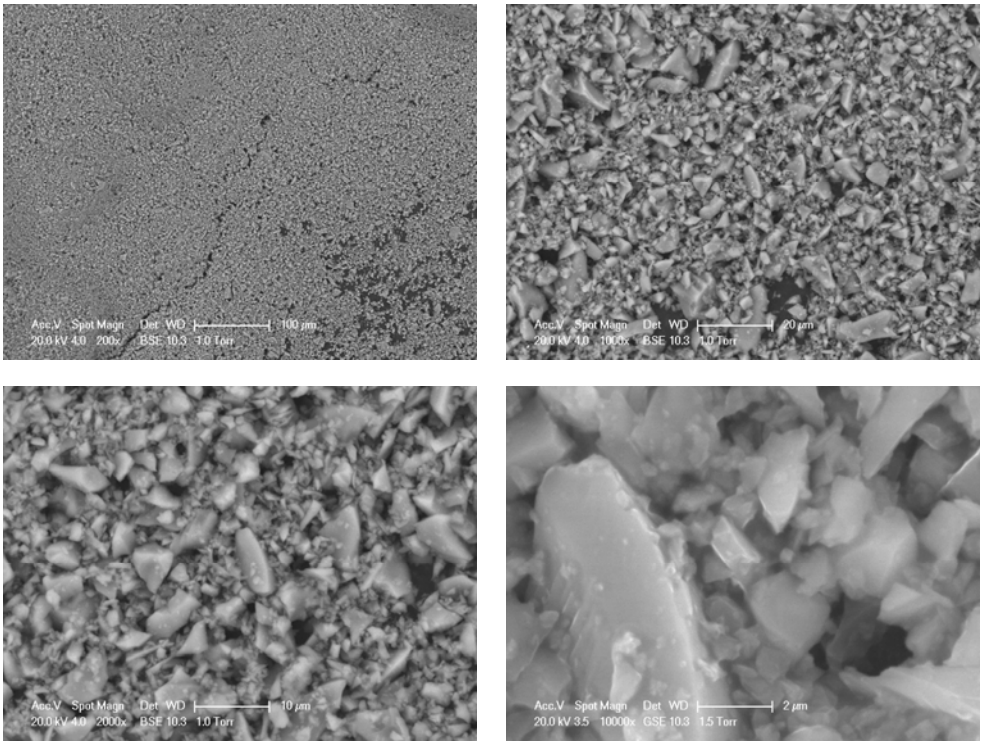

Figure A.4 ESEM pictures of quartz powder M600.

Measuring water demand or packing density of micro powders - comparison of methods

This article was originally published by Fennis, S.A.A.M. in 2008 at http://repository.tudelft.nl/search/ir/?q=fennis&w=Publications&faculty=&department=&type=&year=

Introduction

The particle packing models and optimisation techniques nowadays used in the design of concrete have resulted in new mixture compositions with very high compressive strengths. These new methods and theories can also be used to investigate the effects of cement replacing materials and fine fillers. This way the particle packing theories would not serve an increase of strength, but a reduction of the cement content, thus creating a more ecological concrete. However, the existing particle packing models do not yet include the particle packing of fine particles (< 100 micrometer) in a sound way. One of the reasons for this might be caused by the difficulty measuring the maximum packing density of fine powders.

With particle packing measurements of particles > 1 mm gravitational force and shear forces are dominant. However, with fine particles, the inter-particle forces become increasingly important. These inter-particle forces can cause, for instance, agglomeration of particles, thus lowering the packing density. Since the inter-particle forces depend on the conditions (dry, wet) of the packing structure, also packing density is influenced by this. Therefore it is important that the maximum packing density of the particles is measured under the same conditions as under which the particles would be used in concrete and in the model.

The maximum packing density of dry particles, can be determined according to NEN-EN 1097-3 for loose bulk density. The method can be extended to determine the maximum packing density at a certain compaction level, by applying external loads such as vibration or top-weight. To determine the maximum packing density of wet particles no single method is generally accepted and therefore different countries use their own test methods to determine packing density and/or water demand of fine particles. In this paper a comparison between a number of these techniques is made to evaluate them on number of tests, accuracy, repeatability, reproducibility and suitability to use for cementitious materials.

Methods

The methods to determine packing density and/or water demand of fine particles evaluated in this paper are:

- Water demand France [de Larrard]
- Water demand Germany [Puntke]
- Water demand - mixing energy [Marquardt]
- Proctor test [NEN-EN 13286-2]
- Centrifugal consolidation [Miller]
- Water demand Japan [Okamura,]
- Rheology - Krieger and Dougherty [Mansoutre,]

A description of each method is presented in the next subsections. Most methods determine the minimum amount of water necessary to fill the voids between particles in a packing. In this basic principle maximum packing density is achieved when all voids are filled with water, but no excess amount of water is available to surround the particles.
Some of the methods determine this minimum water demand directly by mixing a paste with a very low water powder ratio (water, powder superplasticizer) and then slowly adding water until the point were all voids are filled is reached. Other methods calculate the minimum water demand from a relation found by mixing and testing pastes with a water powder ratio higher than the water demand. Figure 1.

Methods to determine packing density and/or water demand of fine particles not evaluated in this paper:

- Vicat test [Hunger]
- (Gas) pressure filtration [Mansoutre]
- Shearcompacter [Tattersall ; Palm]
- ...

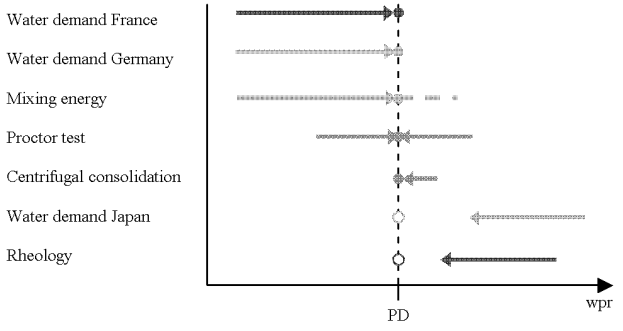

Figure 1 Direct (●) and indirect (○) determination of the minimum water demand depending on the water powder ratio of the paste(s) during the test.

Water demand France

This method aims at finding the minimum water dosages to produce a thick paste. A slightly lower amount of water should give a humid powder [Larrard]. Since the water demand measurement is influences by the type and amount of superplasticizer, it should be dosed as a percentage of the powder dosage. A mass of 350 gram of powder is mixed with water according to the next procedure: The amount of water at minimum water demand is estimated (Equation 1) and mixed with the superplasticizer. First the water (including SP) is added to the mixing bowl, then the powder. The paste is mixed for 1 minute at low speed, then rested/ scraped and subsequently mixed for one minute at high speed. During the mixing at high speed an extra amount of water is added using a pipette to adjust the workability of the paste. The test is repeated with a slightly lower amount of water than in the first test. The packing density of the powder is calculated by Equation 1, as average of two tests, in which the amount of water in the pipette was lower than 5 grams.

$$PD = \frac{1000}{1000 + \rho \frac{M_w}{M_p}} \qquad (1)$$

PD = packing density

M_w = mass of the water

M_p = mass of the powder

ρ = density of the powder in kg/m3

The difficulty of the method is recognizing the transition from a humid powder to a thick homogeneous paste, especially when the humid powder forms a sticky non-homogeneous 'paste'.

Water demand Germany

The method is based on the idea that a fine, low-cohesion particle packing without a load, then and only then can be compacted to a powder specific value, when the water content is sufficient to fill all the voids in that packing. With humid but not yet saturated particle packings of fine powders, the surface tension (capillary forces) will block the water from surrounding the particles. At the saturation point the capillary forces will disappear and the particles can easily be packed to the characteristic highest packing density. Not the compaction energy is important, but the compactability. The transition from 'not yet compactable' to 'compactable' can occur by adding just 0.1 grams of water to a sample containing 100 gram of powder. An excess amount of water will also lead to possible compaction, but it will result in a lower packing density or possible bleeding. For this reason it is very important to approach the saturation point by carefully adding water according to the next procedure: Place 50 grams of powder in a plastic or metal container with a flat bottom. Water is added slowly by making use of a siphon/pipette while the humid powder is mixed with a steel blade or rod. The saturation point is reached when after repeatedly tapping against the container the powder surface levels off and starts to shine. The test should be repeated at least two times with a slightly lower amount of water. The final water demand is calculated according to Equation 1 from the smallest amount of water of three tests.

A disadvantage of the test is that the method can only confidently be used when the the existence of air voids in the 'saturated paste' can be ruled out.

Water demand - mixing energy

When water is added to a powder it condenses on the particles to form capillary bridges (pedular bonds) localized at the particle contacts. In this way, agglomerates of particles are formed. The strength of the pendular bond increases with the liquid-vapor surface energy and depends inversely on the square of the particle diameter. At less than total saturation, the strength of the agglomerates increases with the amount of liquid and the surface energy of the liquid. The absence of internal liquid-vapor surfaces at 100 % saturation causes the strength to suddenly decrease at this point. [German]
The method described by [Marquardt] is based on the idea that the differences in internal pendular bond strength can be measured by measuring the mixing energy according to the following procedure: A powder volume of about 200 cm^3 is mixed in a mortar mixer (DIN EN 196, Teil 1), with a constant water supply of 1.5 ml/s during the entire mixing time, at a mixing speed of 140 rounds/minute. During mixing, the voltage, electricity consumption and the phase shift between the voltage and the electricity consumption of the mixer are registered to determine power use. The water demand of the mix is recorded as the water to powder ratio at which maximum power use is measured.

Proctortest

The proctortest is normally used to determine maximum mixture density of unbound and hydraulically bound mixtures used in road construction and civil engineering work; however, it can also be used on fine powders. In that case a powder is mixed thoroughly with a certain amount of water. The moist mixture is placed in a mould (diameter 100 mm, height 120 mm) in three layers, such that after compaction the sample is higher than the mould body. After placing each layer it is compacted by applying 25 blows of a 2.5 kg rammer dropped from a height of 305 mm above the mixture in such way that the blows are uniformly distributed over the surface of the sample. The extension of the mould is removed and the surface of the compacted mixture is carefully leveled off. After determining the mass of the sample (moist mixture) by weighing, the water content w is determined by drying according to EN 1097-5. The compacted dry density of the mixture is calculated for each compacted sample by Equation 2.

$$\rho_d = \frac{100\rho}{100+w} \qquad (2)$$

ρ_d = dry density [Mg/m^3]
ρ = bulk density of the sample after proctor compaction [Mg/m^3]
w = water content of the mixture [%]

The dry densities obtained from at least five determinations with different water content are plotted against the corresponding water contents. A curve of best fit is drawn to the plotted points to identify the position of the maximum on this curve. The dry density at the maximum of the curve is considered to correspond to the maximum achievable packing density of the moist mixture. Unfortunately, because of the necessary drying of the powder after testing to determine the water content, this method is not suitable do determine the packing density of cement very accurately.

Centrifugal consolidation

The particle packing density of a powder can be determined by centrifugal consolidation according to the following procedure: A paste, with a known composition, is mixed in a three-litre Hobart mixer. First, the dry powders are mixed for ten seconds after which the water and superplasticizer are added. The paste is mixed for 1 minute at low speed, then rested/ scraped for one minute and subsequently mixed for another minute at low speed. The paste is poured into 90 mm long test-tubes with an internal diameter of 22 mm. By determining the mass of the paste in the test-tube, the amounts of powder and water in the test-tube at the beginning of the test are known. The test-tube is then centrifuged for ten minutes at 4000 rounds per minute in a Dumee Jouan E82N Centrifuge with an internal diameter of ± 300 mm. By centrifuging the test-tubes, the particles in the paste are compacted and less amount of water is necessary to fill the voids in between the compacted particle matrix.

Therefore, the total sample will possess an excess amount of water, which will occur as a water layer on top of the (compacted) paste. This water layer can be removed with a pipette, after centrifuging. By determining the amount of removed water, the amount of water and particles in the compacted sample are known and thus the packing density of the powder can be calculated at the applied compaction energy.

Water demand Japan

This method is based on the idea that the water demand of a mixture can be determined indirectly from a linear relationship between the relative flow area R_p, Equation 3, and the water by powder ratio by volume V_w/V_p [Okamura 1995].

$$R_p = \frac{D^2 - D_0^2}{D_0^2} \qquad (3)$$

D = the average spread diameter in a slump flow test

D_0 = the base diameter of the cone in a slump flow test.

When R_p would be zero, $D = D_0$ and no flow is initiated. This state is considered to be achieved when the amount of water in the paste is just sufficient to adsorb on the particle surfaces and fill all the voids in the particle system (saturation point). This saturation point which corresponds to a certain V_w/V_p is called the retained water ratio θ_p (or water demand). Since it is not possible to perform a slump flow test on mixtures with a water powder ratio close to the saturation point a number of mixtures with higher water powder ratios are tested and θ_p is calculated from the linear relation between V_w/V_p and R_p as the interception point at R_p is zero.

For this method, measurements were performed according to the following procedure:
A paste, with a known composition, is mixed in a three-litre Hobart mixer. First, the dry powders are mixed for ten seconds after which the water and superplasticizer are added. The paste is mixed for 1 minute at low speed, then rested/ scraped for one minute and subsequently mixed for another minute at low speed.The slump flow was determined by a mini cone test (upper/lower diameter 20/37 mm and height 57 mm) on a flow table (Tonindustrie) with a 300 mm diameter glass plate. The slump flow is taken as the average spread diameter, calculated in four directions.

Rheology – Krieger and Dougherty

In this method maximum packing density (ϕ_M) is determined indirectly by fitting the results of viscosity measurements of pastes to the Krieger-Dougherty Equation (4)

$$\eta_r = \eta/\eta_c = \left(1 - \frac{\phi_s}{\phi_M}\right)^{-[\eta]\phi_M} \qquad (4)$$

In which η_r is the relative viscosity, η is the apparent shear viscosity of the cement paste, η_c is the apparent viscosity of the liquid phase, ϕ_s is the volume fraction of the solids, $[\eta]$ is the intrinsic viscosity of the particles, and ϕ_M is the maximum packing volume fraction of the cement particles. η_c is assumed to be the viscosity of water at 20 °C, 0.001 Pa·s.

For this method, measurements were performed according to the following procedure: A paste, with a known composition, is mixed in a three-litre Hobart mixer. First, the dry powders are mixed for ten seconds after which the water and superplasticizer are added. The paste is mixed for 1 minute at low speed, then rested/ scraped for one minute and subsequently mixed for another minute at low speed. A coaxial cylinder viscometer, PAAR Physica MC1, is used to determine the apparent viscosity of a paste. To avoid slippage, a sandblasted cylinder with a diameter of 25 mm (standardized geometry: Z3) is used. The measurement is started 5 minutes after the beginning of the mixing procedure. The applied measuring sequence was adopted from [Weerdt] and is shown in Figure 2. The solid contents and their apparent viscosities at a shear rate of 30 s^{-1} were fitted to the Krieger-Dougherty equation.

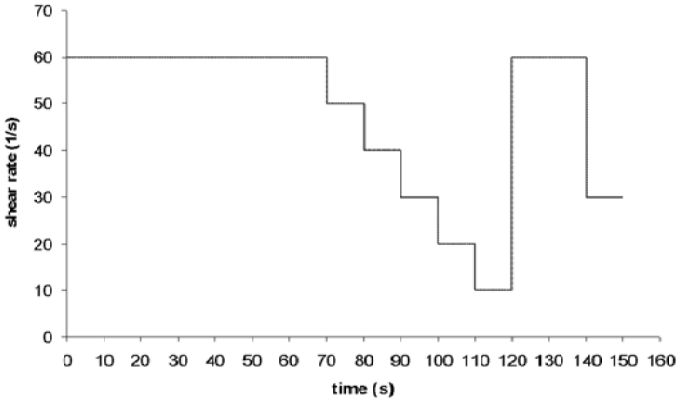

Figure 2 Measuring sequence, viscometer PAAR Physica MC1.

Results

In the section all measurements are presented for each method described in the previous section. When the measurement procedure differed from the standard procedure as described in the previous section, changes are reported. Furthermore, some comments on the estimated precision are presented for each method.

Water demand France

Changes to the method:

- Mixing procedure: Mixing of dry material + water and superplasticizer for 1 minute at low speed, 1 minute resting, ± 1 minute mixing at low speed while adding the last ± 5 gram of water.
- Amount of powder

Table 1 Results from determining the water demand by the French method.

CEM I 42.5 N [g]	Water [g]	Glenium 51 [g]	WCR [-]	Packing density [-]
1500	266.68	18	0.186	0.631
1500	268.39	18	0.187	0.630
1500	269.3	18	0.187	0.629
1500	268.93	18	0.187	0.629
1500	267.52	18	0.186	0.630
300	60.99	3.6	0.211	0.601
Technician 2				
1500	304.54	18	0.211	0.601

Estimated accuracy one mixing method, one technician: ± 0.002.
Measured water demand depends on the technician and on the mixing procedure (in this case: amount of material mixed).

Water demand Germany

Changes to the method:

- Mixing procedure – hand mixing is replaced by mixing in a Hobart mixer for homogeneity of the mixture.
- Amount of powder – in relation to bowl size, same amount as other methods.

Table 2 Results from determining the water demand by the German method.

Material	Powder [g]	Water [g]	Glenium 51 [g]	Hobart mixer	WCR [-]	Packing density [-]
CEM I 42.5 N	416.4	114.3		No	0.274	0.536
CEM I 42.5 N	1500	263.55	18	Yes	0.184	0.634
CEM I 42.5 N	1500	236.51	18	Yes	0.165	0.657
Quartz p. M10	1500	438.45	18	Yes	0.300	0.557

Estimated accuracy one mixing method, one technician: ± 0.02.
Measured water demand depends on the technician, the mixing procedure and the amount of tapping.

Water demand - mixing energy

Changes to the method:

- Amount of powder - in accordance to other methods
- Adding the water / mixing procedure: First 264 grams of water and the superplasticizer (according to the French method) are added. After one minute of mixing and one minute of resting the remaining water is added in drops.

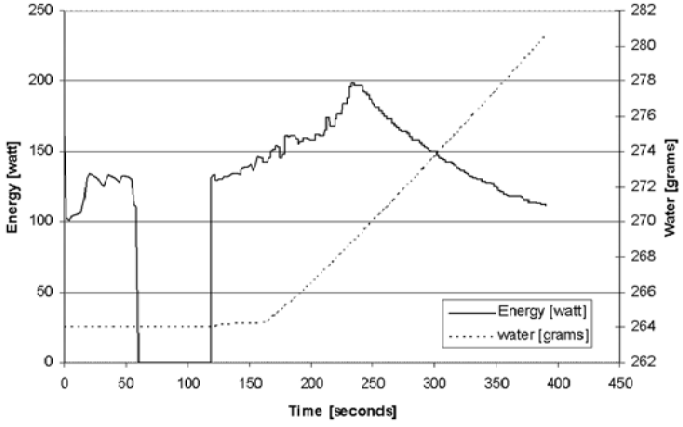

Figure 3 Results from 'mixing energy' test 1.

Table 3 Results from determining the water demand by measuring mixing energy.

Material	Powder [g]	Water [g]	Glenium 51 [g]	WCR [-]	Packing density [-]
CEM I 42.5 N	1500	268.93	18	0.187	0.629
CEM I 42.5 N	1500	267.51	18	0.186	0.630
CEM I 42.5 N	300	74.84	3.6	0.257	0.552
Quartz p. M10	1500	412.34	18	0.283	0.572

Estimated accuracy one mixing method, one technician: ±0.001
Measured water demand depends on the amount of material mixed (300 gram powder is assumed to be below the capacity of the mixer).

Proctortest

Table 4 Amount of sand and water in the Proctor mould after the test and the corresponding water cement ratio and packing density.

	Sand 0.125-0.25 [g]	Water [g]	WCR [-]	Packing density [-]	Maximum packing density [-]
Series 1	1400	309	0.221	0.576	0.587
	1433	302	0.210	0.587	
Series 2	1406	246	0.175	0.580	0.585
	1414	281	0.199	0.584	
	1424	287	0.202	0.585	
	1379	291	0.211	0.584	
	1400	310	0.221	0.577	

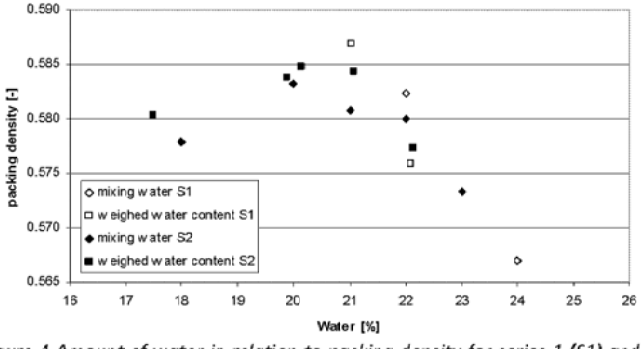

Figure 4 Amount of water in relation to packing density for series 1 (S1) and 2 (S2).

Estimated accuracy for one series, when drying the materials after the test: ± 0.002.When this method would be used on powders which react with water, such as cement, the accuracy is estimated to be ± 0.004, without drying the materials (Packing density is calculated from the initial water content of the mix).

Centrifugal consolidation

In all mixtures Glenium 51 was added as 1.2% by mass of the cement content.

Table 5 Results from determining the water demand by centrifugal consolidation.

Material	Powder [g]	WPR [-]	Packing density [-]
CEM I 32.5 R	1500	0.24	0.604
CEM I 32.5 R	1500	0.24	0.610
CEM I 32.5 R	1500	0.27	0.586
CEM I 32.5 R	1500	0.27	0.581
CEM I 32.5 R	1500	0.27	0.584
CEM I 32.5 R	1500	0.3	0.573
CEM I 32.5 R	1500	0.35	0.544
CEM I 32.5 R	1500	0.35	0.546
CEM I 42.5 N	1500	0.24	0.605
CEM I 42.5 N	1500	0.26	0.591
CEM I 42.5 N	300	0.27	0.586
CEM I 42.5 N	1500	0.28	0.582
CEM I 52.5 R	1500	0.24	0.599
32.5 R / 52.5 R	750 / 750	0.24	0.604
Quartz powder M10	1500	0.30	0.576
Quartz powder M10	1500	0.34	0.555
Quartz powder M10	1500	0.36	0.551
Sand 0.125-0.25	-	-	0.596

Estimated accuracy for one measurement: ± 0.004
Measured packing density depends on the water cement ratio of the mixture.

Water demand Japan

In all mixtures Glenium 51 was added as 1.2% by mass of the cement content.

Table 6 Results from determining the water demand of CEM I 32.5 R by the Japanese method.

CEM I 32.5 R [g]	Water powder ratio [-]	Flow value [mm]	Rp [-]	Packing density [-]	Estimated precision [-]
1500	0.24	177	21.8	0.685	± 0.15
1500	0.25	180	22.5		
1500	0.27	169	19.9		
1500	0.29	177	21.8		
1500	0.30	161	18.0		
1500	0.32	180	22.6		
1500	0.34	180	22.6		
1500	0.35	186	24.2		

Table 7 Results from determining the water demand of CEM I 52.5 R by the Japanese method.

CEM I 52.5 R [g]	Water powder ratio [-]	Flow value [mm]	Rp [-]	Packing density [-]	Estimated precision [-]
1500	0.24	170	20.1	0.726	± 0.03
1500	0.26	187	24.3		
1500	0.28	201	28.5		
1500	0.3	207	30.2		
1500	0.32	219	34.0		
1500	0.34	224	35.4		

Table 8 Results from determining the water demand of a mixture of 50% CEM I 32.5 R and 50% CEM I 52.5 R by the Japanese method.

CEM I 32.5 R [g]	CEM I 52.5 R [g]	WPR [-]	Rp [-]	Packing density [-]	Estimated precision [-]
750	750	0.24	21.0	0.713	± 0.05
750	750	0.26	28.1		
750	750	0.28	29.8		
750	750	0.3	30.3		
750	750	0.32	32.0		
750	750	0.34	39.8		

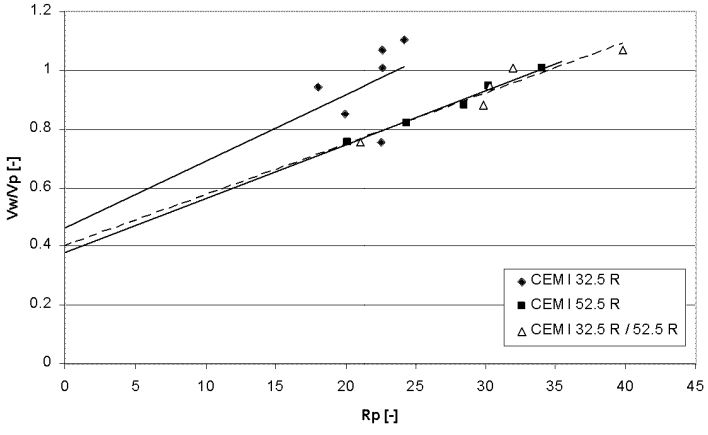

Rheology – Krieger and Dougherty

All mixtures were composed with 18 grams of Glenium 51.
The presented estimated precision is the possible error when fitting the results to the Krieger-Dougherty function.

Table 9 Results from determining the packing density of CEM I 32.5 R by rheology measurements according to Krieger and Dougherty.

CEM I 32.5 R [g]	Water powder ratio [-]	Apparent viscosity [Pa.s]	Packing density [-]	Estimated precision [-]
1500	0.24	1.217	0.63	± 0.03
1500	0.30	0.647		
1500	0.32	0.403		
1500	0.34	0.295		
1500	0.35	0.182	segregation	

Table 10 Results from determining the packing density of CEM I 52.5 R by rheology measurements according to Krieger and Dougherty.

CEM I 52.5 R [g]	Water powder ratio [-]	Apparent viscosity [Pa.s]	Packing density [-]	Estimated precision [-]
1500	0.26	0.806	1.3	± 0.7
1500	0.28	0.674		
1500	0.30	0.408		
1500	0.32	0.379		

Table 11 Results from determining the packing density of a mixture of 50% CEM I 32.5 R and 50% CEM I 52.5 R by rheology measurements according to Krieger and Dougherty.

CEM I 32.5 R [g]	CEM I 52.5 R[g]	WPR [-]	Apparent viscosity [Pa.s]	Packing density [-]	Estimated precision [-]
750	750	0.26	0.747	1.01	± 0.14
750	750	0.28	0.493		
750	750	0.30	0.427		
750	750	0.32	0.309		
750	750	0.34	0.221		

The tests presented in Table 12 are performed according to the measuring sequence in Figure 6:

Table 12 Results from determining the packing density of CEM I 42.5 N by rheology measurements according to Krieger and Dougherty.

CEM I 42.5 N [g]	Water powder ratio [-]	Apparent viscosit [Pa.s]	Packing density [-]	Estimated precision [-]
1500	0.24	0.765	1.11	± 0.5?
1500	0.26	0.557		
1500	0.28	0.493		
1500	0.30	0.315		
1500	0.32	0.181		

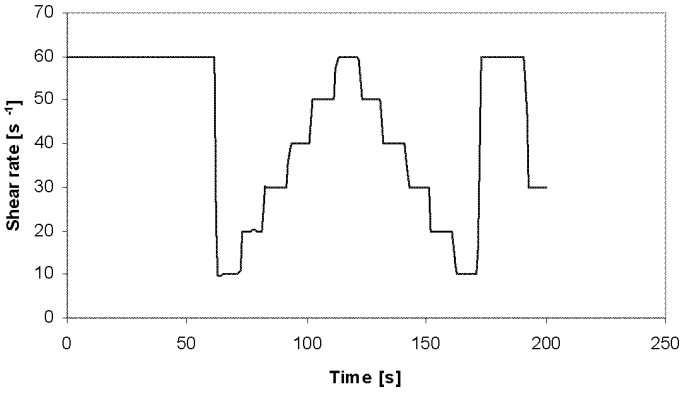

Figure 6 Alternative measuring sequence.

The following seven tests were performed with a parallel plate rheometer (Paar physica). Glenium 51 was added as 1.2% by mass of the cement content.

Table 13 Results from determining the packing density of CEM I 42.5 N by rheology measurements (parallel plate rheometer) according to Krieger and Dougherty.

CEM I 42.5 N [g]	Water powder ratio [-]	Viscosity [Pa.s]	Packing density [-]	Estimated precision [-]
567.00	0.219	1.26	0.687	± 0.03?
562.28	0.224	1.10		
557.55	0.228	0.937		
552.83	0.233	0.735		
548.10	0.238	0.596		
538.65	0.247	0.467		
519.75	0.268	0.162	segregated	

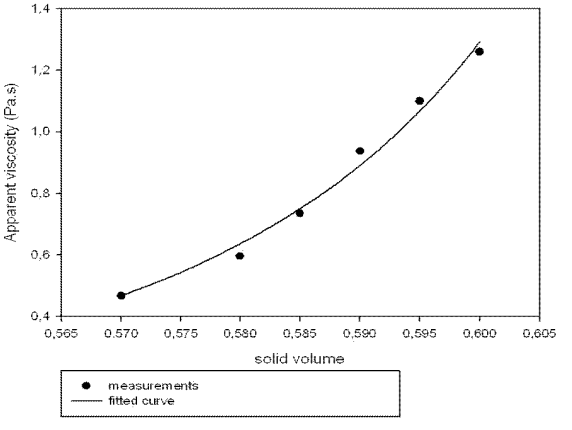

Figure 7 Fitting measurements by Krieger Dougherty equation for a shear rate 30 s^{-1}.

Table 14 Comparison of the packing density measured by different methods and the estimated measuring accuracy.

CEM I 42.5 N	Packing density [-]	Accuracy [-]
Water demand France	0.630	± 0.002
Water demand Germany	0.64	± 0.02
Water demand - mixing energy	0.630	± 0.001
Centrifugal consolidation (wcr=0.24)	0.605	± 0.004
Water demand – Japan	0.69	± 0.15
Rheology - Krieger and Dougherty	0.63	± 0.03
	0.69	± 0.03
Sand	Packing density [-]	Accuracy [-]
Centrifugal consolidation	0.596	± 0.002
Proctor test	0.585	± 0.002

Discussion

The Japanese method to determine water demand has the highest inaccuracy, Table 14. This is caused by the extrapolation towards much lower water powder ratios than the ones that can be used during the measurements. Low water powder ratios can not be used during the measurement, because of the large variation in slump flow of these measurements.

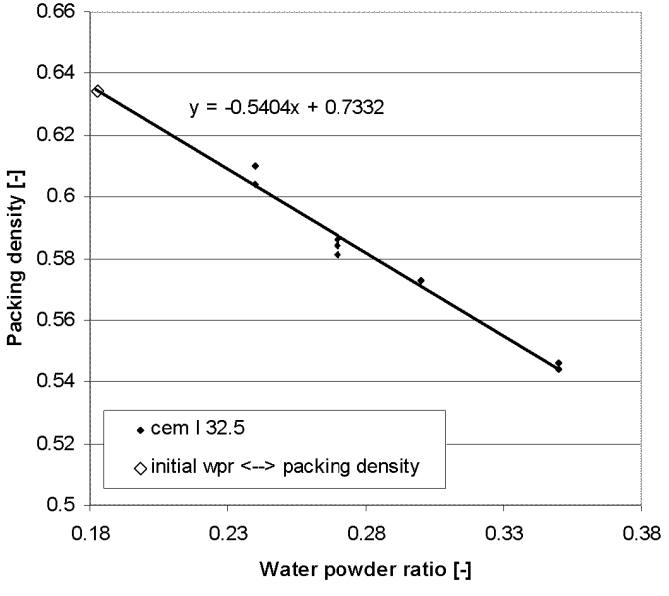

Figure 8 Extrapolation of centrifugal consolidation results to predict the minimum water content corresponding to the maximum packing density.

The other methods all give a reasonably accurate prediction of the water demand; however, they do not all comply with each other. Water demand measurements according to the French method and determining the mixing energy are in good agreement, predicting a packing density of 0.630 for CEM I 42.5 N. Centrifugal consolidation shows a lower packing density, which can be explained in terms of effective compaction energy. With a higher initial water powder ratio, the result of the packing density measurement is lower. In other words, the high amount of water in mixtures with a high water powder ratio is not completely pushed out of the sample during the 10 minutes of the centrifugal consolidation test. Analysis according to Figure 8 shows that the maximum possible packing density would be 0.634 if the test could be performed with a correspondingly low water powder ratio of 0.183. This method then is also in compliance with the French method and the determination of mixing energy.

Determining packing density by rheology measurements and fitting to the Krieger Dougherty equation was not as accurate as expected from literature. Since the method is not based on the same physical relations as the other methods (The equation is an extrapolation of a fluid with a low amount of particles to a fluid containing crowding particles, instead of the concept where the fluid is only filling the voids in between a particle skeleton), this method will not be taken into account any more.

The final two methods, the Proctor test and water demand Germany, seem to be less accurate because of the same physical problem. In the Proctor test a curve is found, which shows the highest packing density at the 'optimal' water content. However, the state of total saturation is not achieved. At the highest measured packing density the voids of the powder skeleton are not completely filled with water and some air voids are left. For a ternary system containing powder, water and air, maximum packing density depends on the amount of compaction energy. Since the amount of compaction energy in the Proctor test is exactly prescribed, the test can be used to measure a comparative packing density (at a certain compaction level) for different types of powders; however, it can not be used to determine the maximum packing density. The German water demand test as described by Puntke suffers from the same problem. At the 'maximum packing density' and its corresponding amount of water, still some air voids can be present in the mixture (with fine powders, mixing

becomes harder and achieving a homogeneous mixture without air voids becomes difficult). Because of the air voids present in the mixture, the differences in the amount of the applied compaction energy will result in differences in the reached packing density. Since the volume of the paste at the highest packing density is not taken into account in this method, the predicted amount of water is too low (extra water should be added to fill the air voids) and the packing density is too high.

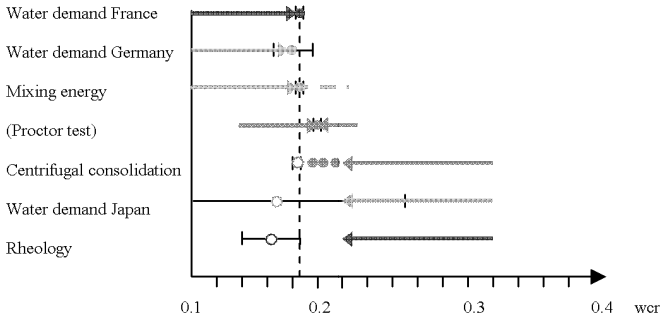

Figure 9 Schematic comparison of test methods to determine the water demand of cement.

Conclusions

In Figure 9 all test methods are compared to each other and for each method the water cement ratio corresponding to the measured packing density is presented. The only method which is certainly not able to predict the maximum packing density of a powder is the Proctor test. From its results it can be concluded that mixtures containing powder, water and voids are not suitable for predicting the maximum packing density. For this reason it is believed that the water demand test from Germany [Puntke] is also not able to predict the maximum packing density accurately. Though the existence of air voids in the water demand test from France and the mixing energy test can not completely ruled out, the results from these tests seem very good and also comply with the centrifugal consolidation test. The centrifugal consolidation test was believed to be a direct test; however, it proved not to be able to measure the maximum packing density. In order to determine the maximum packing density of a powder with this test at least three measurements and an indirect analysis of the packing density are necessary. With enough measurements the method is quite accurate and complies with the water demand from France and the mixing energy test.

Water demand testing from Japan and determining the water demand by rheology measurements (Krieger-Dougherty equation) are inaccurate methods and not suitable to make a precise estimation of the maximum packing density of a powder.

To determine the packing density of powders, two methods can be recommended: Determining water demand by mixing energy and centrifugal consolidation. The mixing energy method is preferred above the French method, because it does not depend on the technician performing the test.
For both methods it is very important that mixing will result in a homogeneous paste. This is because no air voids or clumps should be present in the mixing energy method and for the centrifugal consolidation it is important to know exactly how much water and powder is put in the container. For both methods it should be taken into account that there could be differences in compaction level. With the centrifugal consolidation test, the compaction level depends on the water powder ratio. By doing several tests with various water powder ratios the maximum packing density at 'infinite' compaction energy can be estimated. Also the water demand test by determining mixing energy might result in different compaction levels for different powders, for instance, because of totally different mixing behavior of powders. While adding water, some mixtures transform from dry sandy mixtures, via a state with paste 'balls', to a paste, while other mixtures do not have this intermediate stage and transform directly in a 'clump'.
An advantage of the centrifuge test is that the mixture can directly be used for other tests such as viscosity measurements or strength measurements. An advantage of determining water demand by measuring mixing energy is that the test method is fast and accurate.

References

German R.M. 1989. Particle packing characteristics, Metal Powder Industries Federation, Princeton

Hunger M., Brouwers H.J.H. 2006. Development of Self-Compacting Eco-Concrete. In proceedings of the internationale Baustofftagung, Ibausil; 16., Weimar, Germany: Bauhaus Universitat. 2006. pp. 1-1313 - 1-1320

Larrard F. de, 1999. Concrete mixture proportioning, A scientific approach, EF & Spon, London

Mansoutre S., Colombet P., Van Damme H. 1999. Water retention and granular rheological behavior of fresh C_3S paste as a function of concentration. Cement and Concrete Research Vol. 29, pp. 1441-1453

Marquardt I., Ein Misschungskonzept für selbstverdichtenden Beton auf der Basis der Volumenkenngrössen und Wasseransprüche der Ausgangsstoffe. Rostock, Germany: Univ., Fak. für Ingenieurswissenschaften, Fachbereich Bauingenieurswesen, Fachgebiet Baustoffe, 2002. 190 pages

Miller K.T., Melant R.M., Zukoski C.F. 1996. Comparison of the compressive yield response of aggregated suspensions: Pressure filtration, Centrifugation, and osmotic consolidation. Journal of the American Ceramic Society, Vol. 79, No. 10, pp. 2545-2556

Okamura H., Ozawa K., 1995. "Mix design for self-compacting concrete", Concrete library of the JSCE, No 25, pp 107-120 (Translation from Proc. Of ISCE, no 496/v-24, 1994.8)

Palm S., Wolter A., 2009. Determining and optimizing the void filling of dry particle systems. Cement international, Vol 7 1/2009, pp 1-8.

Puntke W., 2002. Wasseranspruch von feinen Kornhauf-werken. Beton 52 H. 5, pp. 242-248.

Tattersall G.H., Banfill, P.F.G., 1983. The rheology of fresh concrete. Pitman, Boston.

Weerdt K. de, 2007. Course report Rheology of cement-based materials, DTU-RILEM Doctoral Course, Technical University of Denmark, Lyngby, August 19-24.

NEN-EN 1097-3 Beproevingsmethoden voor de bepaling van mechanische en fysische eigenschappen van toeslagmaterialen - Deel 3: Bepaling van de dichtheid van onverdicht materiaal en het gehalte aan holle ruimten.

NEN-EN 13286-2 (en) Unbound and hydraulically bound mixtures – Part 2: Test methods for the determination of the laboratory reference density and water content – Proctor compaction.

Appendix C Packing profiles CPM

Single fractions: Loose packing density

Fraction [mm]	Packing density [-]
8-16	0.564
4-8	0.563
2-4	0.570
1-2	0.574
0.5 -1	0.578
0.25-0.5	0.560
0.125-0.25	0.524

Packing profiles: Loose packing density *K* =4.1

Fraction 4-8 mm combined with 1-2 mm

Vol.% coarse	Packing [-]	CPM [-]	Error [%]
100	0.563	0.563	-
90	0.588	0.588	0.00
80	0.618	0.611	1.16
70	0.636	0.630	0.96
60	0.635	0.639	0.53
50	0.632	0.637	0.82
40	0.622	0.629	1.12
30	0.614	0.617	0.38
20	0.603	0.603	0.06
10	0.594	0.588	0.91
0	0.574	0.574	-
	Mean Error		0.66
	Maximum Error		1.16

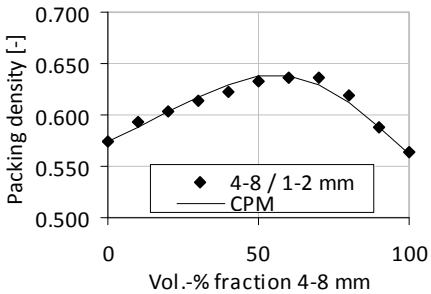

Fraction 2-4 mm combined with 1-2 mm

Vol.% coarse	Packing [-]	CPM [-]	Error [%]
100	0.570	0.570	-
90	0.583	0.581	0.20
80	0.591	0.591	0.00
70	0.599	0.598	0.11
60	0.603	0.602	0.17
50	0.602	0.602	0.09
40	0.600	0.600	0.02
30	0.592	0.595	0.48
20	0.587	0.589	0.23
10	0.584	0.582	0.35
0	0.574	0.574	-
	Mean Error		0.18
	Maximum Error		0.48

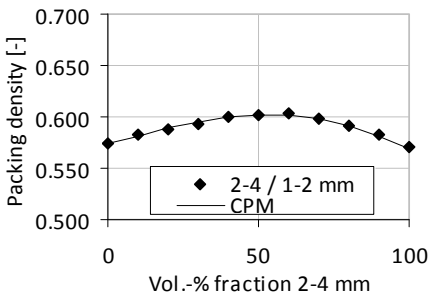

Fraction 1-2 mm combined with 0.5-1 mm

Vol.% coarse	Packing [-]	CPM [-]	Error [%]
100	0.574	0.574	-
90	0.593	0.585	1.22
80	0.602	0.595	1.12
70	0.611	0.602	1.34
60	0.610	0.606	0.66
50	0.608	0.606	0.24
40	0.603	0.604	0.15
30	0.598	0.599	0.18
20	0.591	0.593	0.26
10	0.586	0.586	0.02
0	0.578	0.578	-
	Mean Error		0.58
	Maximum Error		1.34

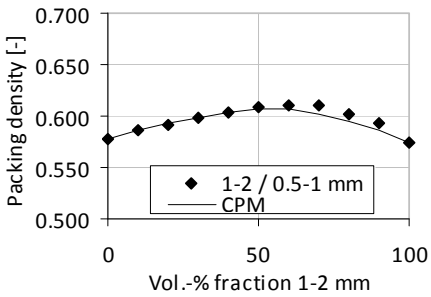

Fraction 1-2 mm combined with 0.25-0.5 mm

Vol.% coarse	Packing [-]	CPM [-]	Error [%]
100	0.574	0.574	-
85	0.597	0.609	1.92
70	0.620	0.634	2.17
48	0.630	0.632	0.20
31	0.596	0.609	2.22
20	0.579	0.592	2.30
0	0.560	0.560	-
	Mean Error		1.76
	Maximum Error		2.30

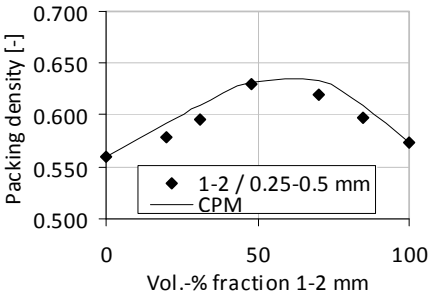

Single fractions fine particles: Wet packing density

Fraction	Packing density [-]
M3	0.625
M4	0.618
M6	0.583
M10	0.576
M300	0.542
M400	0.567
M600	0.527

Packing profiles: Wet packing density *K* =12.2

M6 combined with M300

Vol.% coarse	Packing [-]	CPM [-]	Error [%]
100	0.583	0.583	-
80	0.577	0.578	0.09
60	0.570	0.570	0.03
40	0.561	0.561	0.05
20	0.551	0.552	0.06
0	0.542	0.542	-
	Mean Error		0.06
	Maximum Error		0.09

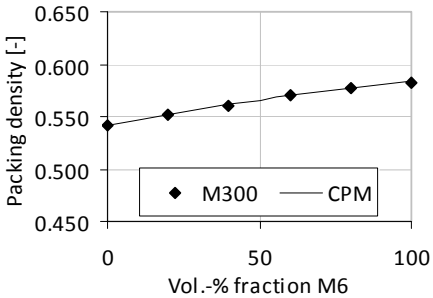

M6 combined with M400

Vol.% coarse	Packing [-]	CPM [-]	Error [%]
100	0.583	0.583	-
80	0.595	0.594	0.13
60	0.598	0.595	0.43
40	0.594	0.589	0.82
20	0.579	0.579	0.10
0	0.567	0.567	-
	Mean Error		0.37
	Maximum Error		0.82

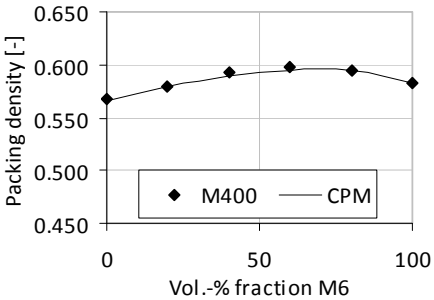

M6 combined with M600

Vol.% coarse	Packing [-]	CPM [-]	Error [%]
100	0.583	0.583	-
80	0.644	0.617	4.15
70	0.655	0.618	5.65
60	0.642	0.609	5.14
40	0.603	0.582	3.42
20	0.562	0.554	1.47
0	0.527	0.527	-
	Mean Error		3.97
	Maximum Error		5.65

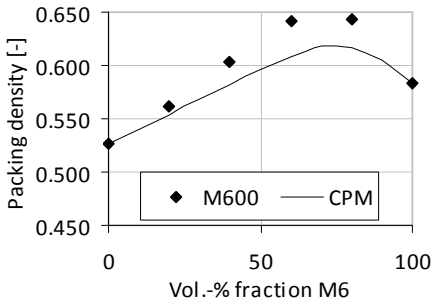

M10 combined with M400

Vol.% coarse	Packing [-]	CPM [-]	Error [%]
100	0.576	0.576	-
80	0.577	0.579	0.28
60	0.580	0.579	0.15
40	0.578	0.576	0.28
20	0.572	0.572	0.05
0	0.567	0.567	-
	Mean Error		0.19
	Maximum Error		0.28

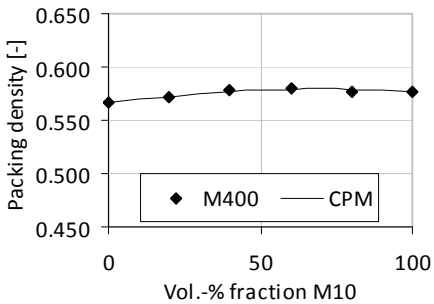

M10 combined with M600

Vol.% coarse	Packing [-]	CPM [-]	Error [%]
100	0.576	0.576	-
80	0.620	0.593	4.43
60	0.625	0.585	6.37
40	0.595	0.567	4.68
0	0.527	0.527	-
	Mean Error		5.16
	Maximum Error		6.37

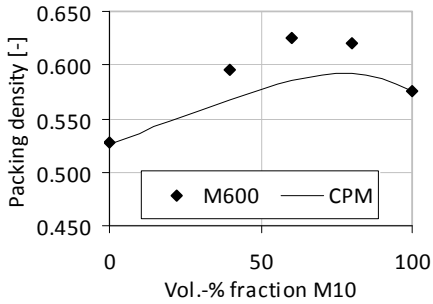

M300 combined with M400

Vol.% coarse	Packing [-]	CPM [-]	Error [%]
100	0.542	0.542	-
80	0.553	0.552	0.09
60	0.559	0.560	0.30
40	0.563	0.565	0.37
20	0.566	0.567	0.20
0	0.567	0.567	-
	Mean Error		0.24
	Maximum Error		0.37

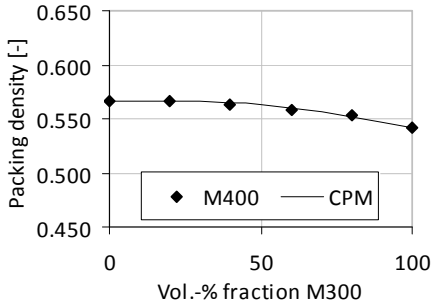

M300 combined with M600

Vol.% coarse	Packing [-]	CPM [-]	Error [%]
100	0.542	0.542	-
80	0.585	0.572	2.19
70	0.606	0.578	4.63
60	0.601	0.578	3.79
40	0.583	0.565	2.96
0	0.527	0.527	-
	Mean Error		3.39
	Maximum Error		4.63

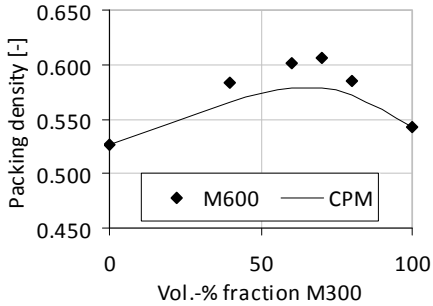

M400 combined with M600

Vol.% coarse	Packing [-]	CPM [-]	Error [%]
100	0.567	0.567	-
80	0.583	0.567	2.72
60	0.577	0.560	2.80
40	0.568	0.550	3.21
0	0.527	0.527	-
	Mean Error		2.91
	Maximum Error		3.21

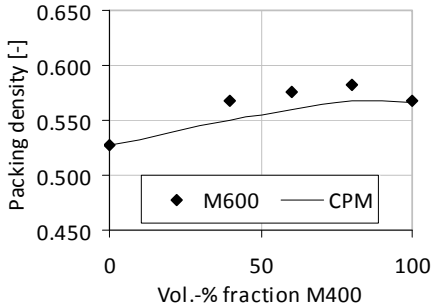

M6	M300	M600	Packing [-]	CPM [-]	Error [%]
100	0	0	0.583	0.583	-
80	20	0	0.577	0.578	0.09
80	0	20	0.644	0.617	4.15
60	40	0	0.570	0.570	0.03
60	20	20	0.633	0.606	4.17
60	0	40	0.642	0.609	5.14
40	60	0	0.561	0.561	0.05
40	40	20	0.617	0.595	3.57
40	20	40	0.631	0.599	5.04
40	0	60	0.603	0.582	3.42
20	80	0	0.551	0.552	0.06
20	60	20	0.606	0.583	3.71
20	40	40	0.620	0.589	5.07
20	20	60	-	0.574	-
20	0	80	0.562	0.554	1.47
0	100	0	0.542	0.542	-
0	80	20	0.585	0.572	2.19
0	60	40	0.601	0.578	3.79
0	40	60	0.583	0.565	3.02
0	20	80	-	0.547	-
0	0	100	0.527	0.527	-
			Mean Error		2.81
			Maximum Error		5.14

Appendix D Packing profiles CIPM

Single fractions: Loose packing density

Fraction [mm]	Packing density [-]
8-16	0.564
4-8	0.563
2-4	0.570
1-2	0.574
0.5 -1	0.578
0.25-0.5	0.560
0.125-0.25	0.524

Packing profiles: Loose packing density at K_e=4.1

Fraction 4-8 mm combined with 1-2 mm

Vol.% coarse	Packing [-]	CIPM [-]	Error [%]
100	0.563	0.563	-
90	0.588	0.592	0.80
80	0.618	0.619	0.08
70	0.636	0.637	0.20
60	0.635	0.643	1.14
50	0.632	0.638	0.92
40	0.622	0.628	0.96
30	0.614	0.615	0.16
20	0.603	0.602	0.24
10	0.594	0.588	0.99
0	0.574	0.574	-
	Mean Error		0.61
	Maximum Error		1.14

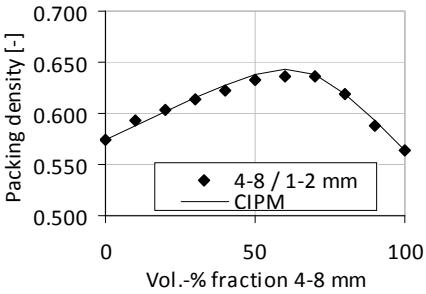

Fraction 2-4 mm combined with 1-2 mm

Vol.% coarse	Packing [-]	CIPM [-]	Error [%]
100	0.570	0.570	-
90	0.583	0.582	0.13
80	0.591	0.591	0.02
70	0.599	0.598	0.20
60	0.603	0.601	0.38
50	0.602	0.601	0.20
40	0.600	0.598	0.30
30	0.592	0.593	0.20
20	0.587	0.588	0.09
10	0.584	0.581	0.43
0	0.574	0.574	-
	Mean Error		0.21
	Maximum Error		0.43

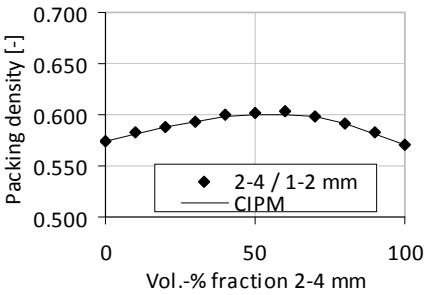

Fraction 1-2 mm combined with 0.5-1 mm

Vol.% coarse	Packing [-]	CIPM [-]	Error [%]
100	0.574	0.574	-
90	0.593	0.586	1.16
80	0.602	0.595	1.13
70	0.611	0.602	1.45
60	0.610	0.605	0.88
50	0.608	0.605	0.53
40	0.603	0.602	0.17
30	0.598	0.597	0.10
20	0.591	0.592	0.05
10	0.586	0.585	0.07
0	0.578	0.578	-
	Mean Error		0.62
	Maximum Error		1.45

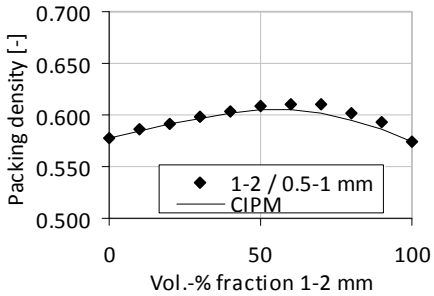

Fraction 1-2 mm combined with 0.25-0.5 mm

Vol.% coarse	Packing [-]	CIPM [-]	Error [%]
100	0.574	0.574	-
85	0.597	0.615	2.97
70	0.620	0.640	3.22
48	0.630	0.632	0.20
31	0.596	0.607	1.87
20	0.579	0.590	2.02
0	0.560	0.560	-
	Mean Error		2.06
	Maximum Error		3.22

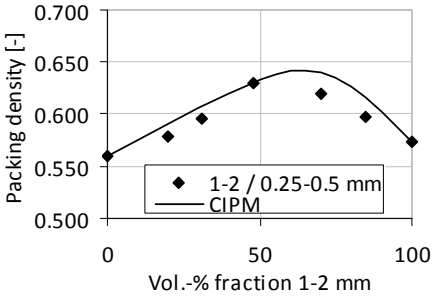

Single fractions fine particles: Wet packing density

Fraction	Packing density [-]
M3	0.625
M4	0.618
M6	0.583
M10	0.576
M300	0.542
M400	0.567
M600	0.527

Packing profiles: Wet packing density at K_e=12.2

M6 combined with M300

Vol.% coarse	Packing [-]	CIPM [-]	Error [%]
100	0.583	0.583	-
80	0.577	0.575	0.43
60	0.570	0.566	0.67
40	0.561	0.558	0.50
20	0.551	0.550	0.28
0	0.542	0.542	-
	Mean Error		0.47
	Maximum Error		0.67

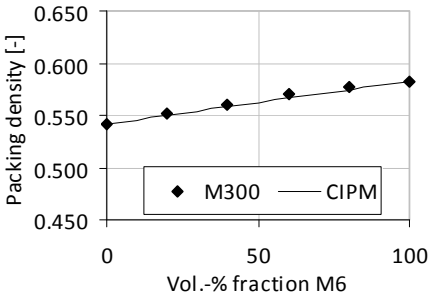

M6 combined with M400

Vol.% coarse	Packing [-]	CIPM [-]	Error [%]
100	0.583	0.583	-
80	0.595	0.595	0.01
60	0.598	0.600	0.39
40	0.594	0.593	0.06
20	0.579	0.582	0.42
0	0.567	0.567	-
	Mean Error		0.22
	Maximum Error		0.42

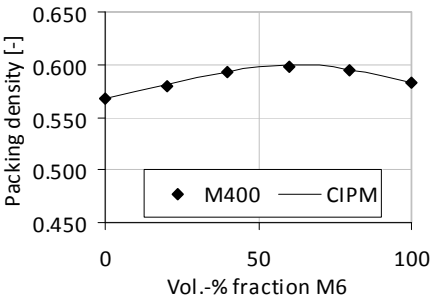

M6 combined with M600

Vol.% coarse	Packing [-]	CIPM [-]	Error [%]
100	0.583	0.583	-
80	0.644	0.642	0.33
70	0.655	0.660	0.80
60	0.642	0.650	1.22
40	0.603	0.607	0.67
20	0.562	0.565	0.45
0	0.527	0.527	-
	Mean Error		0.70
	Maximum Error		1.22

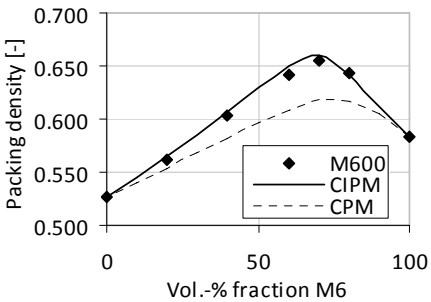

M10 combined with M400

Vol.% coarse	Packing [-]	CIPM [-]	Error [%]
100	0.576	0.576	-
80	0.577	0.579	0.38
60	0.580	0.580	0.01
40	0.578	0.577	0.05
20	0.572	0.573	0.22
0	0.567	0.567	-
	Mean Error		0.17
	Maximum Error		0.38

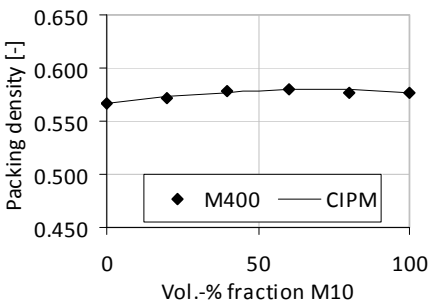

M10 combined with M600

Vol.% coarse	Packing [-]	CIPM [-]	Error [%]
100	0.576	0.576	-
80	0.620	0.624	0.67
60	0.625	0.620	0.82
40	0.595	0.589	0.97
0	0.527	0.527	-
	Mean Error		0.82
	Maximum Error		0.97

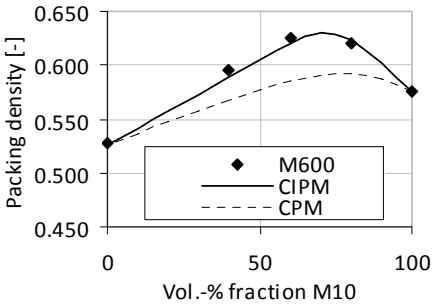

M300 combined with M400

Vol.% coarse	Packing [-]	CIPM [-]	Error [%]
100	0.542	0.542	-
80	0.553	0.549	0.68
60	0.559	0.555	0.55
40	0.563	0.561	0.32
20	0.566	0.566	0.06
0	0.567	0.567	-
	Mean Error		0.40
	Maximum Error		0.68

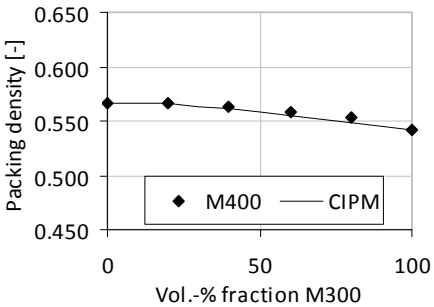

M300 combined with M600

Vol.% coarse	Packing [-]	CIPM [-]	Error [%]
100	0.542	0.542	-
80	0.585	0.595	1.73
70	0.606	0.611	0.82
60	0.601	0.612	1.83
40	0.583	0.589	1.02
0	0.527	0.527	-
	Mean Error		1.35
	Maximum Error		1.83

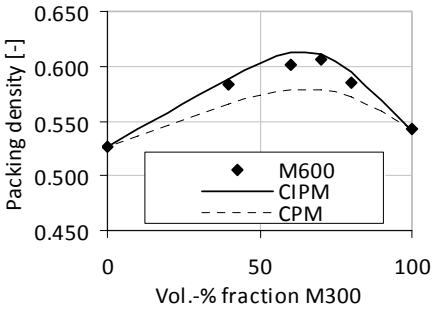

M400 combined with M600

Vol.% coarse	Packing [-]	CIPM [-]	Error [%]
100	0.567	0.567	-
80	0.583	0.577	1.11
60	0.577	0.572	0.86
40	0.568	0.559	1.63
0	0.527	0.527	-
	Mean Error		1.20
	Maximum Error		1.63

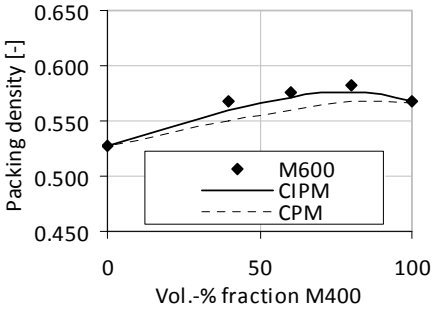

M6	M300	M600	Packing [-]	CIPM [-]	Error [%]
100	0	0	0.583	0.583	-
80	20	0	0.577	0.575	0.33
80	0	20	0.644	0.642	0.31
60	40	0	0.570	0.567	0.57
60	20	20	0.633	0.631	0.31
60	0	40	0.642	0.649	1.05
40	60	0	0.561	0.559	0.40
40	40	20	0.617	0.619	0.37
40	20	40	0.631	0.637	1.03
40	0	60	0.603	0.606	0.57
20	80	0	0.551	0.550	0.19
20	60	20	0.606	0.607	0.24
20	40	40	0.620	0.625	0.79
20	20	60	-	0.598	-
20	0	80	0.562	0.564	0.41
0	100	0	0.542	0.542	-
0	80	20	0.585	0.595	1.73
0	60	40	0.601	0.612	1.83
0	40	60	0.583	0.589	1.02
0	20	80	-	0.558	-
0	0	100	0.527	0.527	-
			Mean Error		0.70
			Maximum Error		1.83

Appendix E Cement pastes and mortar mixtures

Table E.1 Mixture compositions and test results of cement pastes series C.

		CEM I 42.5 N	M6	M300	M600	Water	Glenium 51	WCR	WPR	α_e	$\alpha_{t\ CIPM}$ K_t=12.2	Viscosity	Calorimetry top-time	Thermal energy 120 hours
		[g]	[g]	[g]	[g]	[g]	[g]	[-]	[-]	[-]	[-]	[Ns/m^2]	[hour]	[J/g cem]
C1	CP100_W026	1500	-	-	-	378.3	18.0	0.26	0.26	0.604	0.604	1.23	27.6	218
C2	CP90-M6	1350	150	-	-	378.3	18.0	0.29	0.26	0.606	0.602	1.37	30.9	228
C3	CP80-M6	1200	300	-	-	378.3	18.0	0.33	0.26	0.61	0.600	1.19	31.2	233
C4	CP70-M6	1050	450	-	-	378.3	18.0	0.37	0.26	0.616	0.598	1.33	33.6	246
C5	CP60-M6	900	600	-	-	378.3	18.0	0.43	0.26	0.614	0.596	1.22	34.8	246
C6	CP90-M300	1350	-	150	-	378.3	18.0	0.29	0.26	0.602	0.597	1.50	28.7	229
C7	CP80-M300	1200	-	300	-	378.3	18.0	0.33	0.26	0.605	0.589	1.28	29.5	236
C8	CP70-M300	1050	-	450	-	378.3	18.0	0.37	0.26	0.601	0.582	1.27	32.3	244
C8	CP60-M300	900	-	600	-	378.3	18.0	0.43	0.26	0.603	0.575	1.35	34.8	259
C10	CP90-M600	1350	-	-	150	378.3	18.0	0.29	0.26	0.649	0.637	1.33	29	227
C11	CP80-M600	1200	-	-	300	378.3	18.0	0.33	0.26	0.669	0.660	0.95	28.8	239
C12	CP70-M600	1050	-	-	450	378.3	18.0	0.37	0.26	0.669	0.656	0.67	30.4	250
C13	CP60-M600	900	-	-	600	378.3	18.0	0.43	0.26	0.666	0.639	0.45	29.9	269
C14	CP100_W029	1500	-	-	-	421.8	18.0	0.29	0.29	0.604	0.604	0.55	31.2	221
C15	CP100_W033	1500	-	-	-	475.8	18.0	0.33	0.33	0.604	0.604	0.27	34.9	222
C16	CP100_W037	1500	-	-	-	545.4	18.0	0.37	0.37	0.604	0.604	**	37.2	199
C17	CP100_W043	1500	-	-	-	637.8	18.0	0.43	0.43	0.604	0.604	**	36.9	192
C18	M6	-	1500	-	-	393.2	-	-	-	0.583	0.583	-	-	-
C19	M300	-	-	1500	-	466.3	-	-	-	0.542	0.542	-	-	-
C20	M600	-	-	-	1500	496.4	-	-	-	0.527*	0.527	-	-	-

* Due to required high mixing energy, one measurement only

** below measuring range

Table E.2 Mixture compositions and test results of mortars series D.

		CEM I 42.5 N	M6	M300	M600	Sand	Water	WCR	WPR	Slump	Slump flow	Flow value	Tensile strength		Comp. strength	
													7-day	28 day	7-day	28 day
		[g]	[g]	[g]	[g]	[g]	[g]	[-]	[-]	[mm]	[mm]	[mm]	[N/mm^2]	[N/mm^2]	[N/mm^2]	[N/mm^2]
D1	C100_W050	900	-	-	-	2700	450	0.50	0.50	15	92	140	7.1	8.8	33.3	50.0
D2	C90-M6	810	90	-	-	2700	450	0.56	0.50	22	93	146	5.6	8.5	27.9	43.3
D3	C80-M6	720	180	-	-	2700	450	0.63	0.50	10	90	140	6.1	8.0	25.0	37.1
D4	C70-M6	630	270	-	-	2700	450	0.71	0.50	12	91	152	5.2	7.0	22.2	32.0
D5	C60-M6	540	360	-	-	2700	450	0.83	0.50	14	91	149	4.4	6.2	16.9	25.7
D6	C90-M300	810	-	90	-	2700	450	0.56	0.50	21	92	152	6.8	8.0	30.8	43.6
D7	C80-M300	720	-	180	-	2700	450	0.63	0.50	18	92	147	6.4	8.2	26.9	35.5
D8	C70-M300	630	-	270	-	2700	450	0.71	0.50	17	93	158	5.5	7.1	23.3	32.9
D9	C60-M300	540	-	360	-	2700	450	0.83	0.50	17	92	148	4.3	6.2	18.9	27.8
D10	C90-M600	810	-	-	90	2700	450	0.56	0.50	14	90	139	7.0	9.0	35.1	49.4
D11	C80-M600	720	-	-	180	2700	450	0.63	0.50	11	90	125	6.5	7.8	31.3	42.1
D12	C70-M600	630	-	-	270	2700	450	0.71	0.50	9	90	120	6.7	7.4	26.3	34.1
D13	C60-M600	540	-	-	360	2700	450	0.83	0.50	9	90	119	5.0	7.3	22.0	30.3

Table E.3 Mixture compositions and test results of mortars series E.

		CEM I 42.5 N	M6	M300	M600	Sand	Water	Glenium 51	WCR	WPR	$\alpha_{t\ CPM}$ K_t=9	Slump	Slump flow	Flow value	Comp. strength 7-day	Comp. strength 28 day
		[g]	[g]	[g]	[g]	[g]	[g]	[g]	[-]	[-]	[-]	[mm]	[mm]	[mm]	[N/mm^2]	[N/mm^2]
E1	C100_W037	900	-	-	-	2700	326	10.8	0.37	0.37	0.803	2	83	95	49.6	65.5
E2	C90-M6	810	90	-	-	2700	326	10.8	0.41	0.37	0.801	5	91	95	42.8	59.6
E3	C80-M6	720	180	-	-	2700	326	10.8	0.46	0.37	0.798	5	83	95	36.8	49.0
E4	C70-M6	630	270	-	-	2700	326	10.8	0.53	0.37	0.796	2	84	91	33.6	42.0
E5	C60-M6	540	360	-	-	2700	326	10.8	0.62	0.37	0.793	12	89	102	24.1	34.7
E6	C90-M300	810	-	90	-	2700	326	10.8	0.41	0.37	0.801	3	86	98	47.6	61.6
E7	C80-M300	720	-	180	-	2700	326	10.8	0.46	0.37	0.798	3	87	97	37.7	48.6
E8	C70-M300	630	-	270	-	2700	326	10.8	0.53	0.37	0.795	13	92	124	35.6	46.6
E9	C60-M300	540	-	360	-	2700	326	10.8	0.62	0.37	0.792	16	93	113	27.8	38.5
E10	C90-M600	810	-	-	90	2700	326	10.8	0.41	0.37	0.813	15	90	97	47.8	62.6
E11	C80-M600	720	-	-	180	2700	326	10.8	0.46	0.37	0.821	27	92	140	47	60.4
E12	C70-M600	630	-	-	270	2700	326	10.8	0.53	0.37	0.827	39	134	177	38.9	52.6
E13	C60-M600	540	-	-	360	2700	326	10.8	0.62	0.37	0.829	48	159	202	35.9	50.0
E14	C90-M600	810	-	-	90	2700	293	10.8	0.37	0.33	0.813	4	86	96	54.9	68.0
E15	C80-M600	720	-	-	180	2700	259	10.8	0.37	0.30	0.821	2	85	94	57.6	74.4

Table E.4 Mixture compositions and test results of mortars series F.

		CEM I 32.5 R	Sand (mm)					Water	WCR	$\alpha_{t\,CIPM}$	Slump	Slump	Flow	Comp. strength	
			0.125-0.25	0.25-0.5	0.5-1	1-2	2-4			K_t=9		flow	value	7-day	28 day
		[g]	[g]	[g]	[g]	[g]	[g]	[g]	[-]	[-]	[mm]	[mm]	[mm]	[N/mm^2]	[N/mm^2]
F1	A1_W050	604	1320	-	-	-	-	302	0.50	0.678	0	90	96	-	-
F2	A2_W050	636	1252	-	-	-	-	318	0.50	0.684	4	90	108	-	-
F3	A3_W050	665	1192	-	-	-	-	333	0.50	0.688	10	91	127	-	-
F4	B1_W050	562	-	1412	-	-	-	281	0.50	0.750	6	92	118	24.2	28.7
F5	B2_W050	596	-	1338	-	-	-	298	0.50	0.756	12	95	143	23.5	30.7
F6	B3_W050	628	-	1270	-	-	-	314	0.50	0.759	27	97	177	23.2	24.6
F7	C1_W050	536	-	-	1465	-	-	268	0.50	0.793	22	94	155	21.3	28.7
F8	C2_W050	577	-	-	1378	-	-	289	0.50	0.798	40	105	185	23.3	33.1
F9	C3_W050	612	-	-	1303	-	-	306	0.50	0.797	50	140	220	22.0	31.8
F10	D1_W050	545	-	-	-	1447	-	272	0.50	0.797	19	92	147	20.6	30.5
F11	D2_W050	556	-	-	-	1424	-	278	0.50	0.798	20	93	141	18.5	26.6
F12	D3_W050	569	-	-	-	1396	-	284	0.50	0.800	21	96	162	18.8	28.2
F13	E1_W050	537	-	-	-	-	1447	269	0.50	0.793	20	113	180	20.7	28.9
F14	E2_W050	548	-	-	-	-	1424	274	0.50	0.795	6	91	150	22.1	28.0
F15	E3_W050	563	-	-	-	-	1394	281	0.50	0.797	25	129	190	19.9	29.1
F16	E4_W050	580	-	-	-	-	1357	290	0.50	0.798	35	135	200	19.5	28.8
F17	E5_W050	584	-	-	-	-	1349	292	0.50	0.798	32	132	191	19.9	28.2
F18	E6_W050	618	-	-	-	-	1276	309	0.50	0.797	42	158	214	20.9	26.5
F19	BD41_W050	523	-	1270	-	224	-	262	0.50	0.766	4	90	124	-	-
F20	BD42_W050	499	-	1066	-	479	-	250	0.50	0.786	5	90	115	22.4	30.4
F21	BD43_W050	464	-	843	-	778	-	232	0.50	0.807	3	91	111	21.6	31.0
F22	BD44_W050	502	-	461	-	1077	-	251	0.50	0.825	22	94	168	28.4	39.9
F23	BD45_W050	524	-	224	-	1269	-	262	0.50	0.819	40	116	200	-	-
F24	BD52_W050	546	-	998	-	448	-	273	0.50	0.791	19	91	160	-	-
F25	BD53_W050	514	-	787	-	727	-	257	0.50	0.810	19	92	159	-	-
F26	BD54_W050	544	-	435	-	1015	-	272	0.50	0.821	46	135	215	-	-
F27	BD55_W050	523	-	1032	-	464	-	261	0.50	0.789	9	92	129	-	-

Table E.5 Mixture compositions and test results of mortars series G.

		CEM I 32.5 R	Sand (mm)					Water	WCR	$\alpha_{t\ CPM}$	Slump	Slump flow	Flow value
			0.125-0.25	0.25-0.5	0.5-1	1-2	2-4			K_t=9			
		[g]	[g]	[g]	[g]	[g]	[g]	1000	[-]	[-]	[mm]	[mm]	[mm]
G1	B1_W040	640	-	1412	-	-	-	256	0.40	0.757	2	90	102
G2	B2_W040	683	-	1331	-	-	-	273	0.40	0.760	9	92	123
G3	B3_W040	718	-	1265	-	-	-	287	0.40	0.759	11	92	139
G4	C1_W040	612	-	-	1465	-	-	245	0.40	0.798	8	91	125
G5	C2_W040	657	-	-	1379	-	-	263	0.40	0.797	19	94	158
G6	C3_W040	698	-	-	1303	-	-	279	0.40	0.792	35	102	195
G7	D1_W040	623	-	-	-	1443	-	249	0.40	0.800	14	93	138
G8	D2_W040	665	-	-	-	1365	-	266	0.40	0.798	30	97	170
G9	D3_W040	704	-	-	-	1292	-	282	0.40	0.792	46	110	186
G10	E1_W040	628	-	-	-	-	1417	251	0.40	0.799	7	90	134
G11	E2_W040	669	-	-	-	-	1341	268	0.40	0.796	30	98	174
G12	E3_W040	708	-	-	-	-	1269	283	0.40	0.791	45	122	198
G13	BD41_W040	643	-	1125	-	281	-	257	0.40	0.780	3	90	115
G14	BD42_W040	621	-	999	-	449	-	248	0.40	0.791	2	90	121
G15	BD43_W040	586	-	786	-	726	-	234	0.40	0.808	8	90	123
G16	BD44_W040	620	-	435	-	1014	-	248	0.40	0.813	33	97	166
G17	BD45_W040	644	-	211	-	1193	-	258	0.40	0.808	35	160	185
G18	BD52_W040	664	-	943	-	424	-	266	0.40	0.788	15	90	146
G19	BD53_W040	633	-	741	-	684	-	253	0.40	0.803	23	97	164
G20	BD54_W040	663	-	410	-	957	-	265	0.40	0.804	35	107	189

Table E.6 Mixture compositions and test results of mortars series H.

	CEM I 32.5 R		Sand (mm)					Water	WCR	$\alpha_{t\ CIPM}$	Slump	Slump	Flow	Comp. strength	
			0.125-0.25	0.25-0.5	0.5-1	1-2	2-4			K_t=9		flow	value	7-day	28 day
	[kg/m^3]	[g]	[g]	[g]	[g]	[g]	[g]	1000	[-]	[-]	[mm]	[mm]	[mm]	[N/mm^2]	[N/mm^2]
H1	BE1_W040	751	-	578	313	144	167	300	0.40	0.779	45	128	215	46.4	61.9
H2	BE3_W040	638	-	680	368	170	196	255	0.40	0.802	18	92	162	37.0	52.1
H3	BE1_W045	668	-	610	331	153	176	301	0.45	0.792	47	143	227	32.6	50.5
H4	BE2_W045	618	-	658	356	165	190	278	0.45	0.802	42	111	210	39.4	57.5
H5	BE3_W045	566	-	708	384	177	204	255	0.45	0.807	6	92	128	30.4	46.2
H6	BE1_W050	603	-	635	344	159	183	301	0.50	0.801	49	147	235	25.8	42.6
H7	BE3_W050	511	-	730	395	182	210	255	0.50	0.808	21	94	173	26.6	34.0
H8	BE4_W050	452	-	790	428	197	228	226	0.50	0.802	4	91	123	12.7	23.6

Acknowledgements

The research reported in this thesis was performed at Delft University of Technology, Faculty of Civil Engineering and Geosciences, section of Structural Engineering. The financial support of the Dutch Technology Foundation STW, applied science division of NWO and the Technology Program of the Ministry of Economic Affairs under grant 06922 is gratefully acknowledged. The realization of this thesis has been a great learning process for me, which I could not have done without the help of many persons. For that reason I would like to point out the similarities between their contributions to this work and the necessary contributions to create ecological concrete.

Of course, it is impossible to create ecological concrete without some very special ingredients. The first component has to be the cement. The cement component glues everything together, so without cement there would be no concrete. I would like to think of my supervisors as the cement component in my project. Joost Walraven and Joop den Uijl, you made the project possible, by initiating the project and bringing the right people together. During the project you kept track of the process and stimulated me to continue and improve my work. I would like to thank you both for all your input, discussions, valuable advice and never ending optimism.

Of course, without water, the cement will never harden and will fall apart as loose particles. I would like to think of all the technicians in our laboratory as the water. The technicians are needed to really cast the concrete and their practical experience is priceless. Without them, all the technical ideas would not have become reality and therefore I would like to thank them all very much, especially, Ron Mulder, Edwin Scharp, Fred Schilperoort and Ger Nagtegaal.

At this point, one could create a hardened cement paste, but we are far off from a real ecological concrete mixture. Therefore, we need to add some sand. The sand particles in my project were my co-workers. They were a big part of the joy of coming to work every day. The people joining me for lunches and coffee breaks know how much I appreciate that half hour during the day thinking of other things than concrete. Thank you for all the laughs and crazy conversations. A special thanks to my roommates during the project, Lena Lappa and Yuguang Yang and to my fellow PhD-students Herbert van der Ham and Ilse Mes-Vegt.

For me, cement, water and sand makes a mortar, although I know some of my co-workers will gladly dispute on the size of the aggregate needed for 'real' concrete. So I would like to think of all my acquaintances in the field of concrete technology as the coarse aggregates. They discussed with me about ways of creating concrete and stimulated me to deliver good work. A special thanks to everyone who joined me in all those nice discussions and for all the help, especially to Steffen Grünewald, Walter de Vries, Jeannette Bouwmeester, Mario de Rooij, Sonja Scher, Martin Hunger, Götz Hüsken, Jos Brouwers, Mette Geiker, Klaartje de Weerdt, Annika Gram, Carsten Vogt, Dimitri Feys and Gert Baert.

Fillers are the main component to make a concrete more ecological. The people joining my project filled my head with ideas, therefore I would like to think of them as the fillers. These were the people supporting me and collaborating with me, or even providing me with real fillers (or concrete). A warm thanks to all the people in the STW-committee, the people from Heijmans, TNO and Heembeton and especially Martijn Stroeven, Mark van Kempen, Erik de Vries, Patrick van Beers, Ursula Stark, Anette Müller, Timo Nijland, Jeanette Visser and Agnieszka Bigaj-van Vliet.

The last component to make the ecological mixture flow is the admixture. This thesis is the final result of my PhD study and in this comparison I consider it as the admixture. The research presented in this thesis can help to create good ecological concrete. Use it wisely, because just as admixtures in practice; some are beneficial for your concrete mixture but others still have to be further developed.

At this point we have all the key-ingredients for an ecological concrete mixture. However, I would like to remind you all that once you put on enough pressure, eventually concrete will always crack. This is one of the reasons to use reinforcement in a concrete structure. In my case, my family and friends can be regarded as the reinforcement. They were there for me whenever I needed to release some pressure. Special thanks of course to my husband Erwin Fennis, but also to my parents who have always stimulated me to continue studying. Furthermore, thanks to Lydia Kwast, for putting things in perspective.

Finally, I would like to say thanks to all the people I did not mention by name. Thank you for contributing to the project or helping me to finish this thesis. A last thanks to two special people who supported me, but are not here today to celebrate with me. Eric Horeweg and Joe Larbi, I will always remember you.

Sonja Fennis-Huijben
November 26, 2010

Curriculum vitae

Name: Sebastiana Antonia Adriana Maria Fennis-Huijben
Date of birth: January 8, 1980
Place of birth: Amersfoort, the Netherlands

1992-1998	High school: Laar & Berg, Laren (NH), the Netherlands. VWO Diploma, 1998.
1998-2003	Civil Engineering, Delft University of Technology, the Netherlands. Main disciplines: Structural mechanics, materials and concrete structures. Thesis on structural properties of a new concrete floor element. Diploma Master of Science, 2003, with Honours.
2004-2005	Heijmans Infratech B.V. 's Hertogenbosch, the Netherlands. Research and advice on economical and ecological concrete at Delft University of Technology, the Netherlands.
2005-2010	Concrete structures, Faculty of Civil Engineering and Geosciences, Delft University of Technology, the Netherlands. PhD-study on ecological concrete.

Publications related to this research project

Fennis, S.A.A.M. (2004) Ecobeton. Oriënterend onderzoek naar beton met alternatieve grondstoffen. TU Delft, CiTG, Structural and Building Engineering report 25.5-04-10

Fennis, S.A.A.M. (2005) Materiaaleigenschappen van Ecobeton. TU Delft, CiTG, Structural and Building Engineering report 25.5-04-22

Fennis, S.A.A.M., Walraven, J.C., Uijl, J.A. den. (2006) Minimizing the cement content in ecological concrete by improving particle packing. In Advances in cement and concrete X – sustainability, conference Davos, Switzerland: Engineering conferences international ECI, Brooklyn, NY, USA. pp. 185-189.

Fennis, S.A.A.M. (2006) Mechanical properties and durability aspects of low cement content concrete. In Proceedings of the 6th international PhD symposium in Civil Engineering, Zurich, Switzerland: ETH Zurich, IBK.

Fennis, S.A.A.M., Walraven, J.C., Uijl, J.A. den. (2006) Optimizing the particle packing for the design of ecological concrete. In proceedings of the internationale Baustofftagung, Ibausil; 16., Weimar, Germany: Bauhaus Universitat. pp. 1-1313 - 1-1320.

Fennis, S.A.A.M., Walraven, J.C., Uijl, J.A. den. (2007) The use of particle packing models to reduce the water demand of concrete. CONSEC'07 Concrete under Severe Conditions, Environment and Loading. Tours, France. pp. 937-942

Fennis, S.A.A.M. (2008) Measuring water demand or packing density of micro powders: comparison of methods. http://repository.tudelft.nl/search/ir/?q=fennis&w=Publications&faculty=&department=&type=&year=

Fennis S.A.A.M., Walraven J.C., Nijland T. (2008) Measuring the packing density to lower the cement content in concrete. In J.C. Walraven & D. Stoelhorst (Eds.); Tailor made concrete structures: new solutions for our society. London UK: Taylor & Francis Group. pp. 419-424.

Fennis S.A.A.M., Walraven J.C., Uijl J.A. den. (2008) The use of geometry-based particle packing models with fine particles. In E. Schlangen & G. de Schutter (Eds.), Concrete modelling; CONMOD '08. Bagneux, France: RILEM Publications. pp. 471-478.

Fennis, S.A.A.M., Walraven, J.C., Uijl, J.A. den. (2008) Optimising particle packing to reduce the cement content in concrete. In R.K. Dhir, PC Hewlett, L.J. Csetenyi & M.D. Newlands (Eds.); Role for concrete in global development. Watford, UK: IHS BRE Press. pp. 407-418.

Fennis S.A.A.M., Walraven J.C. (2008) Experimenteren met korrelpakkingmodellen. Cement, Vol. 4. pp. 74-77.

Fennis S.A.A.M., Walraven J.C., Uijl J.A. den. (2009) The use of particle packing models to design ecological concrete. Heron, Vol. 54, NO. 2/3. pp. 185-204.

Fennis S.A.A.M., Walraven J.C., Uijl J.A. den. (2009) Influence of particle size distribution and particle packing on the heat evolution of cement In proceedings of the internationale Baustofftagung, Ibausil; 17., Weimar, Germany: Bauhaus Universitat. pp. 1-0247 - 1-0252.

Fennis, S.A.A.M. (2009) Design of self compacting concrete by particle packing optimization. http://repository.tudelft.nl/search/ir/?q=fennis&w=Publications&faculty=&department=&type=&year=